

AD-A115 883

BATTELLE COLUMBUS LABS OH

F/6 9/5

WORKSHOP ON DIFFUSE DISCHARGE OPENING SWITCHES (JANUARY 13-15, --ETC(U))

APR 82 M KRISTIANSEN, K H SCHOENBACH

DAA629-81-D-0100

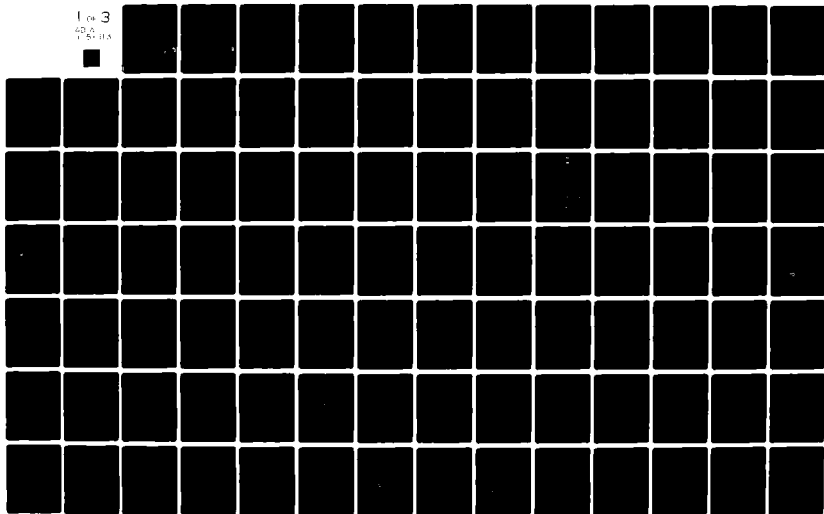
NL

UNCLASSIFIED

1 of 3

40.0

15.0



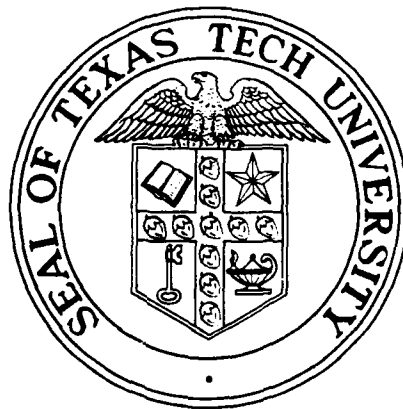
AD A115883

DTIC FILE COPY

# WORKSHOP ON DIFFUSE DISCHARGE OPENING SWITCHES

(January 13-15, 1982)

M. Kristiansen and K. Schoenbach  
Workshop Co-Chairmen



Sponsored by  
Battelle Columbus Laboratories  
April 23, 1982

DTIC  
ELECTE  
JUN 22 1982  
H

PLASMA AND SWITCHING LABORATORY  
LASER LABORATORY  
Department of Electrical Engineering  
TEXAS TECH UNIVERSITY

Lubbock, Texas 79409

82 06 21 126

2

Scientific Services Program

U.S. Army Research Office

Final Report on

WORKSHOP ON DIFFUSE DISCHARGE OPENING SWITCHES

Sponsored by

Battelle Columbus Laboratories  
Contract DAAG29-81-D-0100  
Delivery Order No. 0056  
200 Park Drive  
P.O. Box 12297  
Research Triangle Park, NC 27709

Conducted by

Plasma and Switching Laboratory  
Department of Electrical Engineering  
Texas Tech University, Lubbock, Texas 79409

at

Tamarron, Colorado

on

January 13-15, 1982

Submitted by

M. Kristiansen

R.H. Schoenbach

Workshop Co-Chairman

Workshop Co-Chairman

April 23, 1982

The views, opinions, and/or findings contained in this report are those of the author(s) and should not be construed as an official Department of the Army position, policy, or decision, unless so designated by other documentation.

DTIC  
ELECTE  
JUN 22 1982  
S D H

## TABLE OF CONTENTS

I.	Workshop Advisory Committee	iii
II.	Abstract	1
III.	Working Groups	2
IV.	Introduction	5
V.	Workshop Summary	10
VI.	Invited Overview Papers	17
1.	Opening Switches: Scenarios for Their Use (M.F. Rose and A.K. Hyder, Jr.)	18
2.	Inductive Switching Principles (P.J. Turchi)	43
3.	Fundamental Processes in Diffuse Discharges (M.A. Biondi)	60
4.	Fundamental Processes in Diffuse Discharges for Opening Switches (A.V. Phelps)	71
5.	Arcs vs Diffuse Discharges (A. Garscadden)	91
6.	E-Beam Experiments: Interpretations and Extrapolations (P. Bletzinger)	112
7.	Optical Control of Diffuse Discharge Opening Switches (K.H. Schoenbach, G. Schaefer, M. Kristiansen, L.L. Hatfield, and A.H. Guenther)	134
8.	Modeling of Diffuse Discharges (L.E. Kline)	152
VII.	Group Reports	
1.	Repetitive Opening Switches (I.M. Vitkovitsky)	159
2.	Diffuse Discharge Production [Electron Beam Discharge Switch] (D.H. Douglas-Hamilton)	169



3.	Gases - Basic Data and Experimental Methods - - - - -	184
	(L.G. Christophorou and L.L. Hatfield)	
4.	Optically Induced Processes - - - - -	190
	(A.H. Guenther)	
5.	Modeling of Diffuse Discharge Opening Switches - - - - -	226
	(W.H. Long, Jr.)	
VIII.	Appendices - - - - -	235
A.	Gases for Possible Use in Diffuse Discharge Switches - - - - -	236
	(L.G. Christophorou, S.R. Hunter, J.G. Carter and S.M. Spyrou)	
B.	Summary of Meeting on "Diffuse Discharge Opening Switches" in Lubbock, September 23-24, 1981 - - - - -	252
C.	List of Participants - - - - -	255



Accession For	
NTIS GRA&I	<input checked="" type="checkbox"/>
DTIC TAB	<input type="checkbox"/>
Unannounced	<input type="checkbox"/>
Justification	<i>for 50 on</i>
By	<i>fcc</i>
Distribution/	
Availability Codes	
Dist	Avail and/or Special
<i>A</i>	

# WORKSHOP ADVISORY BOARD

M. Kristiansen	Texas Tech University (Co-Chairman)
K. Schoenbach	Texas Tech University (Co-Chairman)
F. Biondi	University of Pittsburgh
L. Christophorou	Oak Ridge National Laboratory
A. Garscadden	Air Force Wright Aeronautical Laboratory
A. Guenther	Air Force Weapons Laboratory
L. Kline	Westinghouse R&D Center
A. Phelps	Joint Institute for Laboratory Astrophysics

## EX-OFFICIO MEMBER OF ADVISORY BOARD

B. Guenther	Army Research Office
A. Hyder	Air Force Office of Scientific Research
B. Junker	Office of Naval Research
F. Rose	Naval Surface Weapons Center

## ABSTRACT

A workshop on Diffuse Discharge Opening Switches was conducted by Texas Tech University for the U.S. Army Research Office. The workshop was a result of recommendations from an earlier workshop on Repetitive Opening Switches. A group of invited papers set the tone for the discussions in the various working groups. These papers along with the summaries of the working group discussions and recommendations are included in this report. A summary of the workshop and of the suggested research topics is also presented.

## WORKING GROUPS

1. Repetitive Opening Switches

Ihor Vitkovitsky (Chairman)	Naval Research Laboratory
Rudy Buser	U.S. Army Night Vision & Electro Optics Laboratory
Bob Guenther	Army Research Office
Larry Luessen	Naval Surface Weapons Center
Michael Mando	U.S. Army Mobility Equipment Research and Development Command
Marshall Molen	Old Dominion University
R.M. Patrick	AVCO Everett Research Laboratory
Karl Schoenbach	Texas Tech University
Peter Turchi	R & D Associates
Bill Wright	U.S. Army Electronics Technology and Device Laboratory

2) Diffuse Discharge Production

D.H. Douglas-Hamilton (Chairman)	AVCO Everett Reserach Laboratory
Peter Bletzinger	Air Force Wright Aeronautical Laboratory
Frank DeLucia	Duke University
Albert Engelhardt	Los Alamos National Laboratory
J.J. Ewing	Mathematical Sciences N.W., Inc.
M. Kristiansen	Texas Tech University
Bill Moeny	Tetra Corporation
Joe Proud	GTE Laboratories, Inc.
Frank Rose	Naval Surface Weapons Center
Jim Thompson	University of South Carolina

3) Gases - Basic Data and Experimental Methods

Lucas Christophorou (Chairman)	Oak Ridge National Laboratory
Fred Biondi	University of Pittsburgh
Ara Chutjian	Jet Propulsion Laboratory
Alan Garscadden	Air Force Wright Aeronautical Laboratory
Lynn Hatfield	Texas Tech University
Tony Hyder	Air Force Office of Scientific Research
Don Lorents	SRI International
Art Phelps	Joint Institute for Laboratory Astrophysics
Wolfgang Seelig	Institut für Angewandte Physik, Technische Hochschule Darmstadt, FRG

4) Optically Induced Processes

Art Guenther (Chairman)	Air Force Weapons Laboratory
Norman Bardsley	University of Pittsburgh
Peter Chantry	Westinghouse R&D Center
Charles Frost	Sandia National Laboratories
Martin Gundersen	University of Southern California
Jim Lawler	University of Wisconsin
Jacob Leventhal	University of Missouri/ St. Louis
Gerhard Schaefer	Texas Tech University
Santosh Srivastava	Jet Propulsion Laboratory

5) Modeling of Diffuse Discharge Opening Switches

Bill Long  
(Chairman)

Northrop Research & Technology  
Center

Richard Fernsler

Naval Research Laboratory

Bob Junker

Office of Naval Research

Larry Kline

Westinghouse R&D Center

Erich Kunhardt

Texas Tech University

Leanne Pitchford

Sandia National Laboratories

Larry Rapagnani

Air Force Weapons Laboratory

## INTRODUCTION

A workshop on "Diffuse Discharge Opening Switches" was sponsored by the U.S. Army Research Office and conducted by Texas Tech University at Tamarron, Colorado on January 13-15, 1982. This workshop was held as a result of the recommendations from an earlier workshop on "Repetitive Opening Switches" on January 28-29, 1981.

Some basic information about inductive energy storage, its potential, and limitations, as well as many specific opening switch ideas, can be found in the proceedings of the first workshop. (DTIC AD-A110770). As a result of the deliberations at the earlier workshop, it appears that diffuse discharges have the highest promise for leading to the development of a successful, fast, repetitive opening switch. Most ideas for utilizing arc discharges appear either too slow or too energy inefficient. The earlier workshop also showed that solving the problem of developing a practical switch requires an extremely wide range of expertise. Researchers with backgrounds in circuit analysis, materials properties, fundamental discharge theory, basic gas data determination, plasma chemistry, etc. are needed. The main goal of the second workshop was, therefore, to bring researchers with these varied backgrounds together in an environment conducive to free discussions. At the same time it seemed important to bring in representatives from the various government agencies with potential interest in this R & D area to contribute realistic background scenarios

to some of the discussions and to assess the future potential and important issues of this research area.

The 45 invited attendees came from universities, industry, national laboratories, and government agencies. A series of invited papers presented the first day served to provide background information and set the tone for the subsequent working group discussions. Each working group had an appointed discussion leader and each group's conclusions and recommendations were presented in a general meeting on the last day. The Advisory Committee then met the following day to further refine some of these conclusions. A preliminary meeting, involving some 20 of the workshop participants, was held at Texas Tech University in September of 1981. This meeting helped to define many of the workshop goals and to determine some of the expertise areas needed, as well as to identify some of the people with backgrounds appropriate for contributing to the successful achievement of these goals.

We, the workshop coordinators, feel that the workshop was very successful. The unusual amount of intense, scientific discussion resulted in significant information exchange. The participants seemed genuinely interested in the problems posed and many (certainly we) learned a great deal about an exciting problem and generated many new ideas for future work.

The primary goals for the workshop were given as:

- 1) To identify the limitations, in a broad sense, of diffuse discharge switches with regard to possible applications.



- 2) To identify relevant (in the workshop context) unresolved research problems and define the research areas that must be supported to solve these problems.
- 3) To determine ways to promote exchange of information between scientists working on fields or research which are relevant to diffuse discharge opening switches.
- 4) To establish research goals and priorities.

The first of these points was addressed mainly by the working groups on Repetitive Switch Applications and on Diffuse Discharge Production. Both groups carried out "strawman" calculations and the results came out quite favorable. Although these calculations were admittedly crude, they gave considerable confidence that the basic problem issue was not totally ridiculous or impractical. Some possible application ranges of interest to the DoD were also summarized by the Repetitive Opening Switch working group in Table I in their report. This table provides an update of a similar one in the first Workshop Proceedings.

The second goal of the workshop was addressed in various degrees by all the five working groups. Most of the discussions were concerned with two basic approaches to discharge initiation, maintenance, and turn-off. These approaches were the e-beam controlled diffuse discharge and the optically controlled or modified diffuse discharge. The e-beam controlled discharge is the better understood of the two processes and has been investigated earlier to a certain extent in both the U.S. and the USSR. Also, there is a large body of potentially

relevant information available from high-power, electron beam pumped laser development. The optically controlled or modified discharge approach is a relatively new research area for this application (although the "optogalvanic effect" has been known for a long time but never considered in this vain). These two approaches are not necessarily mutually exclusive and one can certainly consider an "optically assisted, e-beam controlled opening switch". Many of the basic data needed, such as recombination coefficients, drift velocities, plasma chemistry reactions, etc. are equally important to both approaches.

The third workshop goal is, as evidenced by the discussions at this workshop and at the earlier meeting at TTU, extremely important, since so many different disciplines have an impact on this research area. A principal problem is the limited availability of travel funds. To alleviate this situation, efforts have been made to organize special sessions at national meetings and to utilize, as much as possible, these meetings as a way to bring interested parties together. Some of the research sponsors have also encouraged the use of contract funds for such interactions and, in some cases, provided supplementary travel support for this purpose.

The fourth and last workshop goal is an extremely difficult one to reach complete agreement on. The research topics listed in the next section are primarily due to the workshop Co-Directors with some suggestions from the Advisory Board members. Because of time limitations, we were not able to

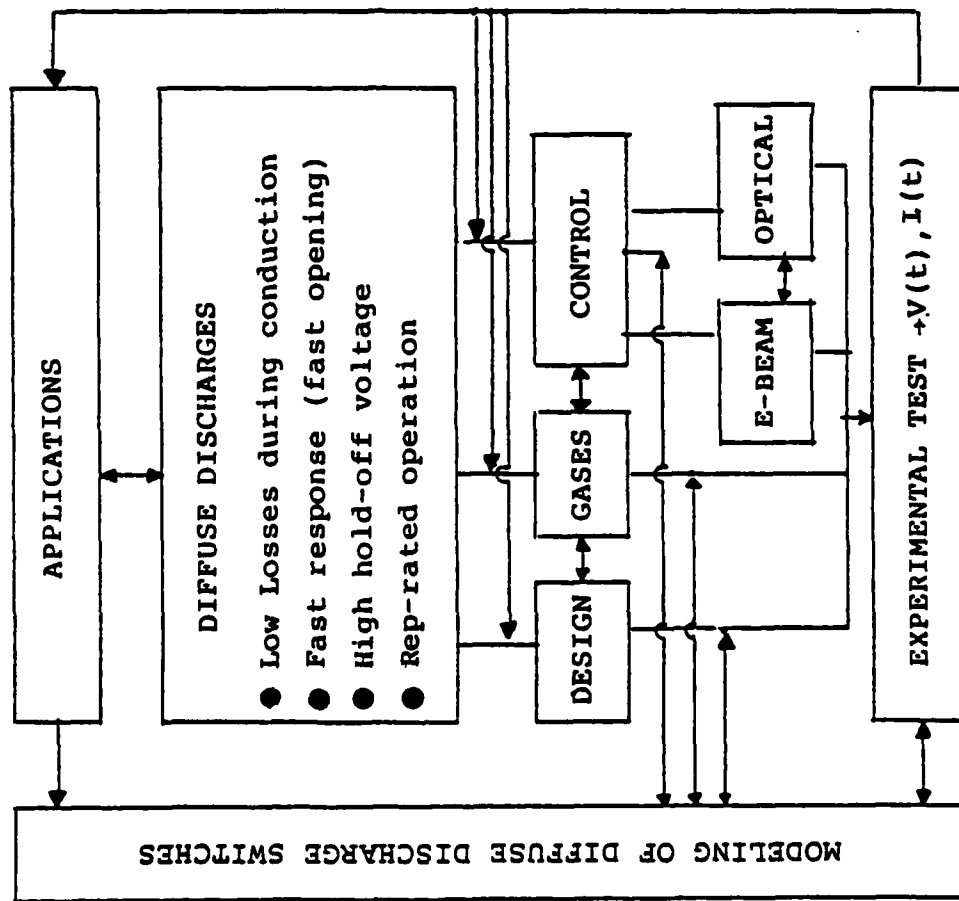
give each Advisory Board member time for careful comments and rebuttals to our draft, although a copy was sent to each of them before we went to print, with request for verbal comments in cases of violent disagreements.

## SUMMARY

The basic results of the workshop deliberations are summarized in Fig. 1. It was generally agreed that a screening of candidate gases should be performed in existing e-beam facilities (or facilities already under construction). The key information needed is the attachment coefficient,  $k_a$ , the recombination coefficient,  $\alpha$ , and the electron mobility,  $\mu$ , vs the reduced electric field ( $E/N$ ) for various gas mixtures. These gases should also have high voltage hold-off strength and be resistant to streamer formation. In repetitive operation there is concern about information on thermal, acoustic, and attachment instabilities which may prevent the generation of repetitive diffuse discharges. The acoustic disturbances in the system when, for instance, the e-beam is turned on and off, may set up density gradients which lead to arc formation. When the attachment coefficient increases rapidly with increasing electric field, an instability may occur, as described in the group report on diffuse discharge production. Other instabilities may also be significant.

The "strawman" calculations performed by the working groups are summarized in their individual reports. The main conclusion was, however, that an approach, such as the e-beam controlled opening switch, did not seem unreasonable in size or efficiency. Several of the workshop participants expressed encouragement by these calculations. Some of the limitations set on these switches are due to the current density and allowable temperature rise before instabilities (filamentations) set in (e.g. an assumed maximum temperature rise of  $\Delta T = 500^\circ K$ ).

Fig. 1 DIFFUSE DISCHARGE OPENING SWITCHES



NEEDED:

- SYSTEM STUDIES
  - DEVELOPMENT OF MODELING CODES
  - INVESTIGATIONS OF
    - GAS DYNAMICS
    - ELECTRODE EFFECTS
    - INSTABILITIES
    - GAS CHEMISTRY
  - INFORMATION ON ATOMIC AND MOLECULAR DATA OF FILLGAS COMPONENTS
  - MEASUREMENT OF RATE-CONSTANTS AND TRANSPORT COEFFICIENTS IN GAS MIXTURES (Attachment, recombination, mobility, etc.)
  - INVESTIGATION OF RESONANT PHOTON PROCESSES
  - FAST ELECTRICAL AND OPTICAL DIAGNOSTICS
- WHICH TO BENCHMARK ANALYTICAL MODELS, PARTICULARLY IN THE E-BEAM AND OPTICALLY CONTROLLED SWITCH OPERATIONS

Considerable performance improvements could be expected if some of these values (which were conservatively based on empirical results with electron beam excited gas lasers) could be increased.

Additional basic data relating to recombination coefficients, electron impact cross-sections for higher vibrational levels, etc. are needed. The properties of the sheath region during turn-off are also poorly understood. The limiting factors on current density in diffuse discharges need to be studied for the gases of interest, considering their unique properties, in order to determine if they are basically the same as for gas laser discharges.

User oriented computer codes which couple the discharge system to a circuit analysis code are needed. This approach may not be practical, except on very large computers, but a possible compromise, as a first step, is to develop a two-step code and let the first one calculate various rate constants as a function of  $E/N$  and then let the second use the output from the first code in a circuit analysis code. The second code would allow changes in circuit parameters as well as perturbations in the gas discharge parameters. It is important to use this code to determine the sensitivity of the system performance to various parameter changes and thus help to decide on the crucial research issues. The code must, of course, be checked against reliable experiments to determine its validity and applicability.

For the optically controlled switch systems there is a need for the knowledge of various transition probabilities.

The possible production, by lasers, of radicals with strong electron attachment should be investigated. One needs gases in which the attachment coefficient increases for vibrationally or electronically excited states without too much shift in the peak of the absorption coefficient towards lower energies. One should also determine the feasibility of rearranging and forming new molecules with strong  $k_a$ . The disassociation of certain molecules may also lead to fragments with high  $k_a$ .

It was also pointed out, as mentioned in the introduction, that it is extremely important to maintain the information exchange that has been started among various interested parties with widely different areas of expertise. This objective can, of course, be achieved in part by normal travel, correspondence, telephone calls, meetings at national conferences, etc. In addition, however, it will be necessary to hold a few informal meetings and workshops, as during the last 18 months. It is hoped that the sponsoring agencies will be able to help implement this objective. If another workshop similar to the two held so far should be organized, it has been suggested that the near term goals (switch parameters) of interest should be specified more firmly next time. The various working groups would then have the same parameters and goals in mind during their deliberations so that results, concerns, and recommendations could be more easily compared. Also, it was noted that the area of low pressure, diffuse discharges (~ the thyatron regime) deserve more attention than it received at this workshop.

The area of plasma chemistry and possible catalytic effects of nearby insulators received insufficient attention. The workshop organizers had great difficulty in finding experts in this field. Two days before the conference the only such person located called and cancelled for personal reasons. This subject should, therefore, also be given special attention at any future workshop.

A general research plan was suggested, as shown in Fig. 2. The point was raised, however, that perhaps one should keep a close watch on the screening results (of candidate gas mixtures) in view of going directly from these to the switch design.

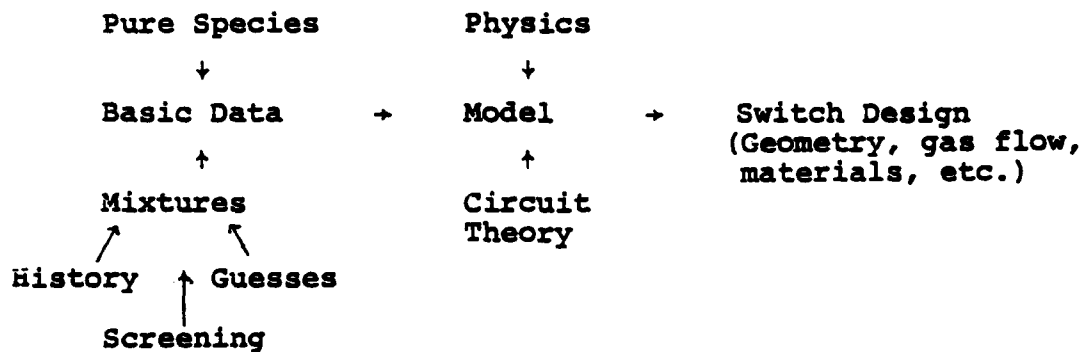


Fig. 2 General Research Program Outline

Several research topics were recommended by the various working groups, as stated in their individual reports. Many of the topics were similar in nature and there was no great disagreement as to the importance of most of these topics. It is difficult to prioritize all these topics, however, and we have instead chosen simply to list in Table I, the ones we consider to be most important.



Table I. MAIN RESEARCH AREAS1. Basic Data and Processes

- a) Atomic and Molecular Data on Candidate Gas Components
- b) Rate Constants and Transport Coefficients in Gas Mixtures
- c) Gas Chemistry
- d) Resonant Photon Processes

2. Code Development

- a) Plasma Kinetics (Positive Column and Sheaths)
- b) Parameter Sensitivity Analysis  
(Coupling of Discharge Effects and Circuit Behavior)

3. Experimental Investigations of Switch Systems

- a) Screening of Candidate Mixtures
- b) Bench Mark Experiments for Code Verifications
- c) Diagnostic Development
- d) High Pressure Discharge Stability Analysis and Understanding of Channel Formation in Repetitive and/or Long Pulse Systems
- e) Gas Dynamics in Repetitive and/or Long Pulse System
- f) Electrode and Insulator Effects (Sheath and Geometry Effects)

INVITED OVERVIEW PAPERS

OPENING SWITCHES  
Scenarios for Their Use

M. F. Rose  
Naval Surface Weapons Center

and

A. K. Hyder, Jr.  
Air Force Office of Scientific Research

INTRODUCTION

There are many ways in which energy can be stored and made to do useful work. For the purpose of pulsed power, energy is usually stored at a slow rate in some suitable media and subsequently released on demand by the experimenter at whatever rate is suitable.

Obviously the use of storage mechanisms allows a time compression in the delivery of energy to a load. It is advantageous to do this because most of the phenomena studied using pulsed-power techniques demand power levels in excess of gigawatts and energy levels in excess of a megajoule. The time scales for delivery range from milliseconds to nanoseconds. It is neither practical nor possible to build continuous power supplies which can provide the requisite amount of energy on the appropriate time scale.

The most demanding technical applications for pulsed-power technology are in inertial-confinement fusion and the military-oriented programs such as nuclear-weapons effects simulation

and directed-energy weapons concepts. Invariably, the time scales and energy densities sought after for these applications make energy storage and pulse compression a necessity rather than an experimental nicety.

The range of applications of pulsed power is enormous. The following list, by no means exhaustive, represents some of the more interesting applications currently underway:

- Inertial confinement fusion
- Electrical discharge lasers
- Directed energy weapons concepts
- Nuclear weapons effects simulators
- X-ray generators
- Magneforming
- Particle accelerators
- Radar
- Acoustic ranging
- Electromagnetic mass drivers
- Micromachining
- Toys
- Shock testers
- Strobe photography

Applications of particular interest to the DOD are indicated in Fig. 1, and the pulsed-power chain from prime power to the load is shown in Fig. 2. There are several routes by which power levels of interest can be delivered. Each of these routes

involve different storage mechanisms with a broad range of energy densities, switching requirements, and operating time scales. Because of this, it does not follow that a given experiment can be powered by the most compact store without several critical intermediate stages in the power-flow train.

Table 1 illustrates approximate energy storage densities which are currently available for a number of storage techniques. It is obvious from Table 1 that not only is there a wide range of storage densities available to the user, but the time scale for delivery of the energy to the load also varies over several orders of magnitude.

Table 1 Comparison of Energy Storage Techniques

<u>Storage Mode/ Device Type</u>	<u>Energy/ Volume <math>\text{J/m}^3 \times 10^6</math></u>	<u>Energy/ Weight <math>\text{J/kg}</math></u>	<u>Time Scale to Deliver to Load</u>
o Electrostatic Capacitors	.01-1	300-500	$\mu\text{s}$
o Magnetic/Inductors			
Conventional	3-5	$10^2$ - $10^3$	ms to $\mu\text{s}$
Cryogenic	10-30		
Superconducting	20-40		
o Chemical			
Batteries	2000	$10^6$	minutes
Explosives	6000	$5 \times 10^6$	$\mu\text{s}$
o Inertial			
Flywheel	400	$10^4$ - $10^5$	seconds

In Table 2 we present several typical large pulsed energy sources employing storage techniques characterized in Table 1.

Table 2 Large Pulsed Energy Sources

<u>Source</u>	<u>Largest Existing Installation (MJ)</u>	<u>Potential Discharge Times (ms)</u>	<u>System Cost (\$/J)</u>
Inductive	100 (Frascati)	0.1 - 10	0.25 - 0.3
Capacitive	10 (Los Alamos) (Fast Bank) 25 (Lawrence Livermore) (Slow Bank)	$10^{-3}$ - 10	0.25 - 1.0
Inertial (Motor-Flywheel-Alternator)	1400 (Garching)	$10^3+$	0.015 - 0.04
Inertial (Homopolar)	500 (Canberra)	$1 - 10^3$	.001 - .01
Chemical (Batteries)	100 (Frascati)	$10^3+$	.03 - 3.0
Chemical (MHD)	~ 300 (USSR)	$3 \times 10^4$	---

The nature of the energy store and conversion scheme employed in a particular pulsed power experiment is governed by such factors as the nature of the load, cost, portability (weight and volume) and reliability. If cost and reliability were the only governing factors, inertial stores would be the obvious choice. Unfortunately, many of the experiments demand terawatts of power delivered in the submicrosecond time scale. Hence there

are some experimental loads where time constraints dictate the choice of the storage medium to be used. Even then, several stages of energy compression may be necessary to shape the pulse for optimum transfer to the experimental load. While inertial-inductive systems possess the attractiveness of high-energy density they also demand a repetitive opening switch -- the device fundamental to this workshop.

### Inductive Storage

Inductive storage offers the possibility of achieving higher energy densities, resulting in a smaller weight and cost, than, for example, a capacitive system of equal energy. The energy density in an inductor is given by  $B^2/2\mu_0$  and in a capacitor by  $\epsilon_0 E^2/2$ . Taking "reasonable" upper limits of  $B = 20$  Tesla,  $k = 80$ , and  $E = 10^8$  V/m, we find the energy density for the inductor to be  $1.6 \times 10^8$  J/m<sup>3</sup> and for the capacitor  $2.8 \times 10^6$  J/m<sup>3</sup>. The magnetic field energy density is about 50 times greater than the electrostatic energy density.

Unfortunately, this simplistic reasoning is incomplete, since the complete pulsed system must be considered, not the inductor alone. Figure 3 shows schematically a simple inductive pulser system. A charging source (needed in capacitive systems also) must first cause the current to build up in the inductor while  $S_1$  is closed. A transfer mechanism must then deliver the energy to the load in the form of a pulse. This is accomplished by opening  $S_1$  and closing  $S_2$ . In practice, the

greatest problem is in designing an opening switch, which must divert the inductor current from the charging path to the load as  $S_2$  closes. Two or more switches opening sequentially may be required (for example, mechanical plus crossed-field tube or mechanical plus vacuum tube). The switching apparatus may be so large and complex that the advantages of the small size of the inductor is negated. In order to be efficient, charging must be done quickly to minimize joule heating of the windings. Therefore, for a large store of energy, high input powers are required. The charge restrictions apply only to room temperature and cryogenic storage inductors. Superconducting storage systems also suffer from switch technology and must have complicated dewar systems with special feedthrough bushings.

The high energy density of inductive storage systems make them likely candidates for further study. Inductive energy storage becomes of primary interest at high energy (nominally 50 kJ). While the most interesting approach which minimizes the charging problems is to use superconducting coils, they cannot be discharged rapidly with today's technology. The overriding technical problem limiting magnetic storage is the requisite switch technology. Since many applications demand high repetition rate, high voltage, and high current, the development of opening switch technology must start with basic research to define switch concepts capable of high rep-rate, terawatt performance.



## APPLICATIONS

The advanced microwave devices, particle beam weapons concepts, particle beam fusion devices, the free electron lasers, and some nuclear weapons effects simulators share common load characteristics in that they require electron/particle beam generators.

For example, in the case of an electron accelerator the major power and load requirements are those imposed by the required particle energy and the impedance of the electron source. The design of source diodes is reasonably straightforward. For space charge limited flow, the diode impedance is given by

$$Z = \frac{137 d^2}{\sqrt{V} A}$$

where  $V$  is the diode voltage in megavolts,  $A$  is the beam area/emitter area, and  $d$  is the anode-cathode gap spacing. Setting the particle energy fixes  $V$ , which allows calculation of diode impedance in terms of the gap spacing and beam diameter. Once the beam current is fixed,  $Z$  becomes established, and the  $A/d$  ratio for the diode is calculable. Knowing  $Z$  allows the calculation of the remainder of the parameters in the pulse power train. There may be several more stages of pulsed power associated with acceleration of the electron beam to higher energies. These are usually accomplished by Blumlein transmission/pulser systems which are matched to accelerator cavities of the same impedance. The beam is inductively coupled to these

pulse sources. The length of the pulse produced in the energy storage system is chosen to match the particle pulse which is to be accelerated. Systems of this type can transfer over 90 percent of their energy from the store to the beam.

Regardless of the method used to fire the accelerator, either directly from the inductive store or through some intermediate store (e.g., inductive/Blumlein pulse shaping network), the critical opening switch must appear between the store and the load.

Figures 4 and 5 are simplified schematic diagrams of typical Soviet pulsed inductive accelerators. The Soviets have for sometime been active in the area of inductively driven accelerators. Figure 4 represents a case where the energy store is transformer coupled to the accelerator load, thus allowing for some pulse conditioning. These two examples are selected from a rather large body of Soviet literature in this area. To the best of our knowledge, no comparable level of effort exists in the United States.

Free electron lasers employ a "true" accelerator in the conventional sense. Electric discharge lasers, however, tend to be hybrids: some cases (Fig. 6,a) employ an accelerator for initial excitation of the lasing medium, but the main energy pulse is provided by a sustainer power supply which 'sees' a plasma as a load (Fig. 6, a,b,c). In a pulsed chemical laser (Fig. 6c) the power supply delivers its pulse to a flash lamp to initiate the laser action. All of these do 'see' a plasma as a load,

be it in the laser medium or in a flash lamp. Incidentally, this plasma behavior in a pulsed laser may be quite similar to the operation of a low rep-rate opening switch in that excited products must be cleared between pulses.

A plasma is usually considered a purely resistive load. It is true that the current and voltage relationships in a plasma load show no inductive or capacitive components once the plasma is established, but the power supply is often called upon to compensate for strongly nonlinear early-time behavior in the load. Power is introduced to the plasma through electrodes and the electrode-plasma interface is a very nonlinear region. Many of the loads must be pulsed and true steady state operation is never achieved. In addition, the plasma geometry dictated by the load physics or output requirements can give rise to a number of instabilities that may place severe requirements on the power system. In a typical electron beam initiated laser for instance, the load is initially a capacitor. When the electron beam is turned on, the dielectric strength of the inter-electrode space is reduced to a point where current starts to flow. A relatively high voltage is usually impressed on the electrodes prior to the initiation of current flow, but the resistance in the gas very rapidly drops to a low value and the plasma becomes a high-current, low-voltage resistor whose actual value of geometry dependent. If the early-time behavior of the plasma is important, two pulse sources are usually used, one to bring the plasma to the "steady state" and a second "working" pulse which sees a nearly constant impedance.

A final interesting application is the electromagnetic mass drivers which have broad applications in such areas as electromagnetic guns, shock testing, as a means of launching lunar raw materials into precise orbits for space manufacturing, and to resupply passing starships. Mass drivers in general represent nonlinear loads to the pulser.

The most highly developed and simplest accelerators are the classic rail guns shown schematically in Figure 7. A set of rigid rails is provided with a projectile in the form of a movable short. When the pulser is discharged through the rails,  $\underline{J} \times \underline{B}$  due to the current and resultant magnetic field produces a force which accelerates the projectile down the rails. For the purposes of this discussion, assume that the pulser has a constant voltage for the interval of interest. Typical pulsers might be battery banks, fuel cells, MHD generator, large homopolar generators, or L-C pulse forming networks. In any event, the internal characteristics of the source  $R_s$ ,  $L_s$ , and  $V$  can be specified. It is easy to design a set of rails with a given inductance ( $L_r$ ) and resistance ( $R_r$ ) per unit length. These variables constitute the load insofar as the pulser is concerned.

Existing rail gun experiments employ homopolar generators and inductive stores (Fig. 8), with an attendant opening switch ( $S_2$ ). The requirements on  $S_2$  in this application are much less severe than those for lasers and accelerators for two reasons:

1)  $S_2$  may be needed only at the start of a burst and, 2) the payload is an initial short across  $S_2$ .

For any of these applications there are several practical problems which must pace the opening-switch research and development:

- The on-state impedance must be near zero to prevent losses in the switch.
- The off-state impedance must be much larger than the load impedance.
- $\int I^2 R dt$  limitations will require either cryogenics or impulse charging.
- The switch must eventually work reliably outside of the laboratory.
- The energy involved in maintaining the on-state must be minimal in comparison to the total energy stored or switched.

An attempt to generalize parameters governing the range of applications discussed above is presented below:

<u>Application</u>	<u>V<sub>so</sub></u>	<u>I<sub>max</sub></u>	<u>Rep Rate</u>	<u>Duty</u>
CPB	100 kV	10'skA	kHz	10%
Microwave Source	1 MV	kA's	10 Hz-1 kHz	10%
Laser Driver	kV's	100 kA	kHz	?

$V_{so}$  is the minimum stand-off voltage,  $I_{max}$  is the maximum current flow in the on-state, and the duty cycle is defined as on-time/total time.

Only ranges and order of magnitude estimates are given since the actual figures are system/circuit specific.

Within the framework of this generalized parameter space, we examined in slightly more detail the interaction of the circuit with the switch operation using the Net II computer code. These represent preliminary results, and more refined calculations will be done as more details of the switch model evolve. Figure 9 is a schematic of the simple circuit used; the opening switch is represented by a purely resistive, non-linear element. The inductive store,  $L$ , is driven by a power source characterized by  $V_B$ ,  $R_B$ ;  $R_L$  is the purely resistive load.

Figures 10 through 13 summarize the calculations. A typical time history of the switch impedance is given in Figure 10. The transition time from the conducting to the non-conducting state was varied between one and two microseconds, while the high-impedance (non-conducting) state was maintained for 20 microseconds. In all cases the impedance collapse from 100 ohms to one micro-ohm occurred in one microsecond.

Figures 11 and 12 are typical results of these calculations. For the case shown:

$$V_B = 500 \text{ volts}$$

$$L = 10^{-6} \text{ Henry}$$

$$R_B = 0.001 \text{ ohm}$$

$$R_L = 10 \text{ ohms}$$

It is interesting to note that more energy was deposited in the switch than in the load in this case.

Several additional cases are summarised in Table 3. Clearly, and not surprisingly, dramatic improvements in the switch losses can be made by increasing the ratio of the switch non-conducting impedance to the load impedance, and by decreasing the transition time from conducting to non-conducting states.

Table 3

L H	V <sub>s</sub> V	R <sub>L</sub>	$\tau_s$ $\mu s$	$\tau_p$ $\mu s$	$\tau_f$ $\mu s$	E <sub>I</sub> kJ	E <sub>L</sub> kJ	E <sub>s</sub> kJ	V <sub>L</sub> kV	Z <sub>s</sub>	E <sub>s</sub> /E (% loss)
10 <sup>-6</sup>	500	10	2	20	1	27.45	11.84	15.61	894	10	57
10 <sup>-6</sup>	500	10	1	20	1	27.45	19.2	8.25	1171	10	30.0
10 <sup>-5</sup>	5000	1	2	20	1	3308	3153	255	769	100	8.0
10 <sup>-5</sup>	5000	10	2	20	1	3308	2700	608	5700	10	18.4
10 <sup>-5</sup>	5000	10	1	20	1	3308	2860	448	5800	10	13.5
10 <sup>-5</sup>	5000	1	1	20	1	3308	3232	72	780	100	2.3

Military systems, of necessity, are weight and volume constrained. The availability of credible opening-switch technology would allow use of inertial/inductive stores with their attendant energy-density advantages. This could conceivably result in power trains that are simpler, more reliable, and perhaps an order-of-magnitude smaller when compared to existing pulser designs.

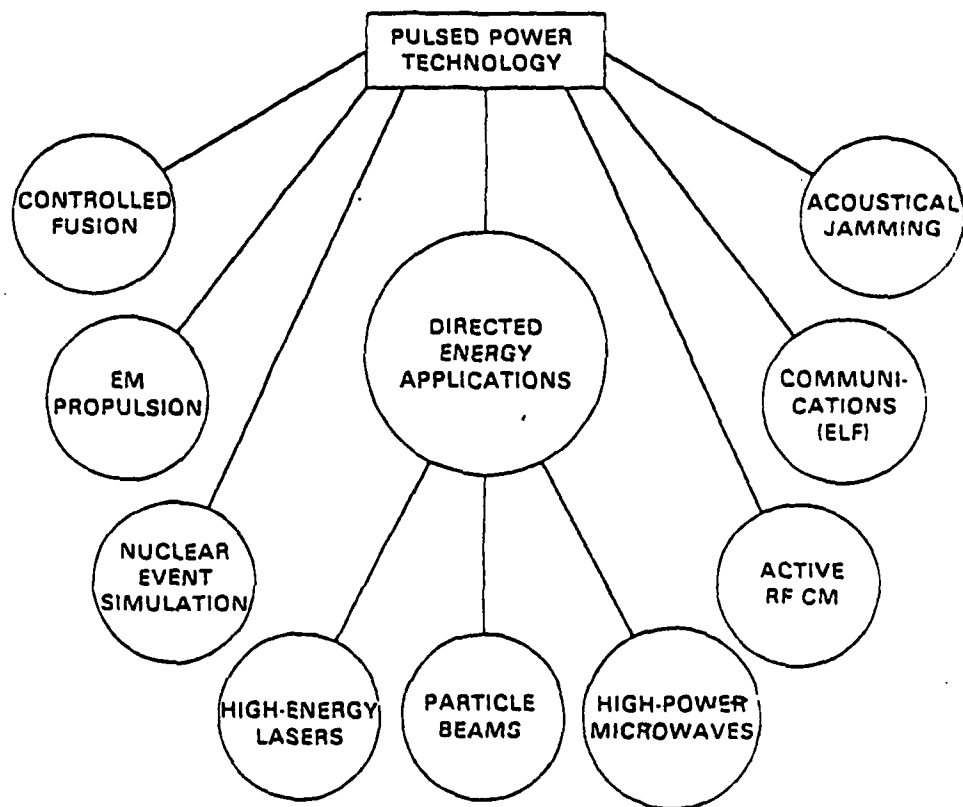


FIGURE 1. Applications of pulsed power which are of particular interest to the Department of Defense.



# PULSED POWER TECHNOLOGY CHAIN

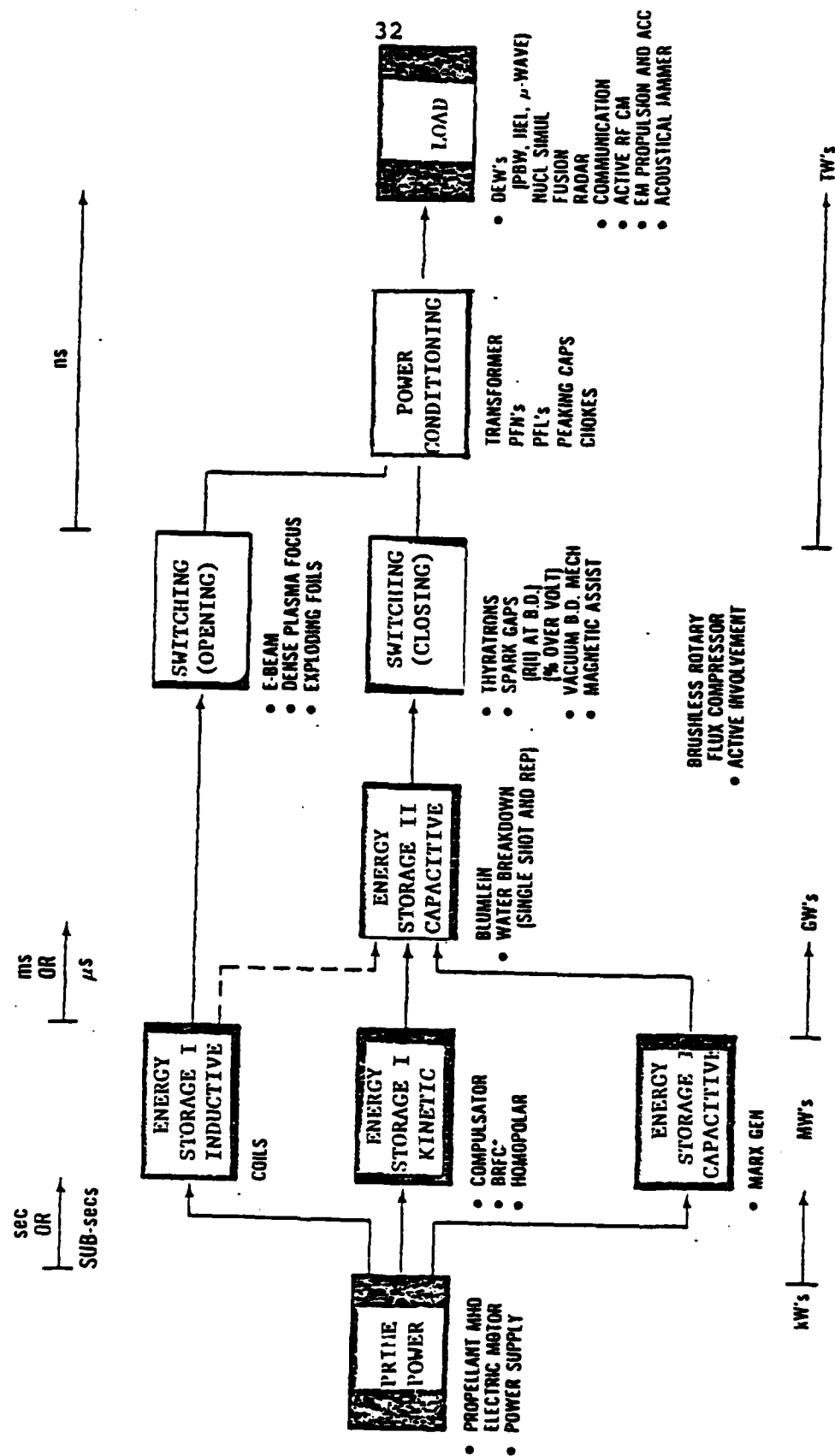


FIGURE 2. The pulsed-power technology train.

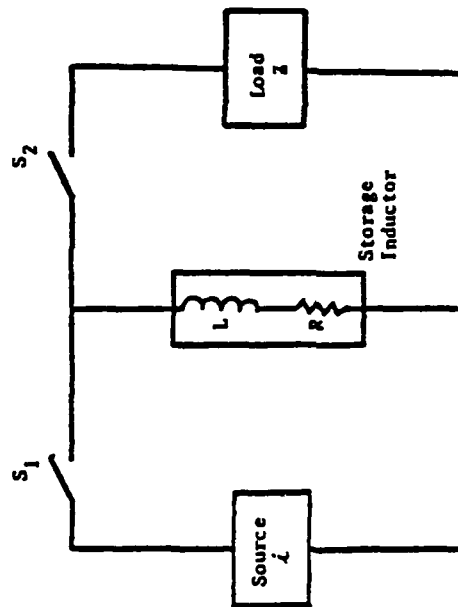


FIGURE 3. Simple diagram of an inductive storage unit.

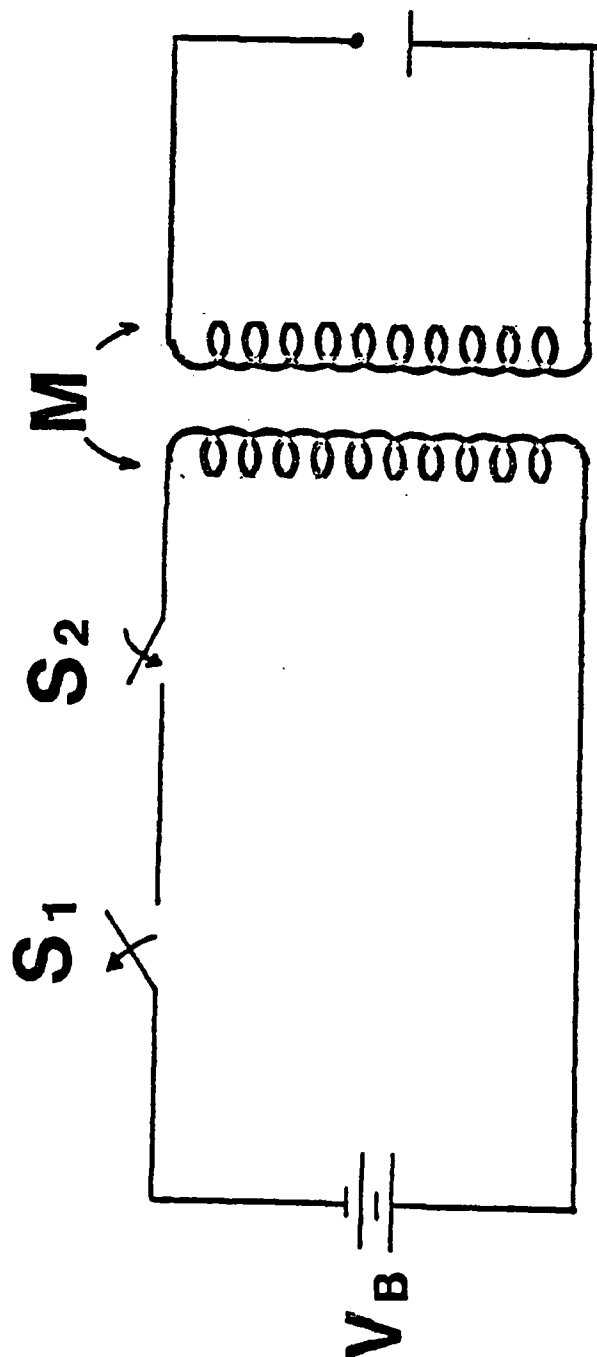
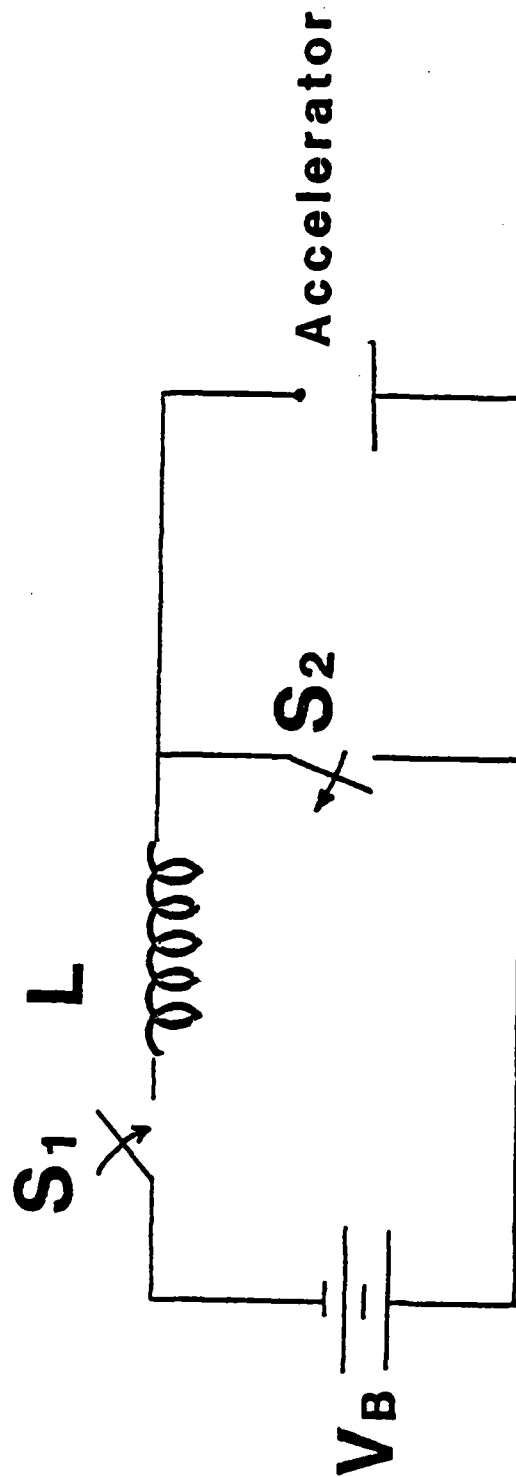


FIGURE 4. Simplified schematic of a typical Soviet pulsed inductive accelerator - after Dubovoi, et al.

L. V. DUBOVOI, et al.  
Atomnaya Energiya 38, 87 (1975)



V. I. MIKHAILOV, et al.  
Sov Phys Tech Phys 22, 703 (1977)

FIGURE 5. Simplified schematic of a typical Soviet pulsed inductive accelerator—after Mikhailov, et al.

# TYPICAL ELECTRICAL EXCITATION/INITIATION SCHEMES FOR HIGH ENERGY LASER

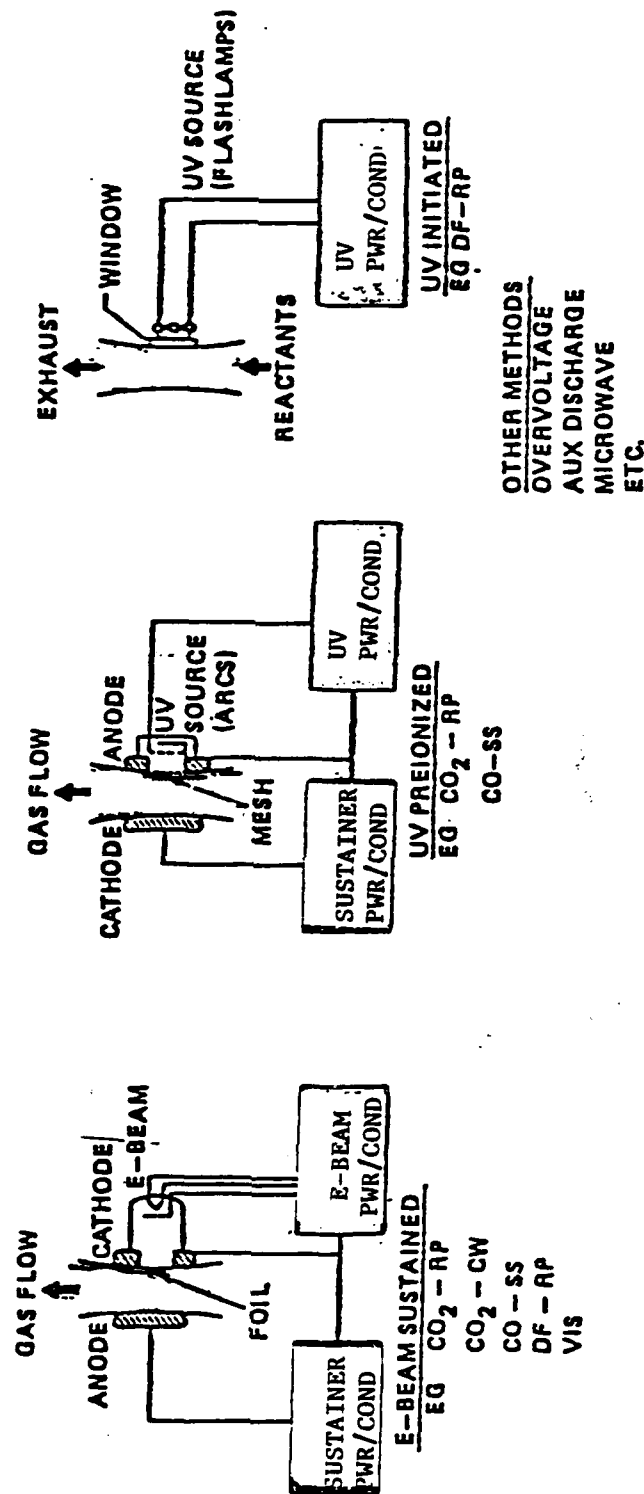


FIGURE 6. Applications in electric discharge lasers.

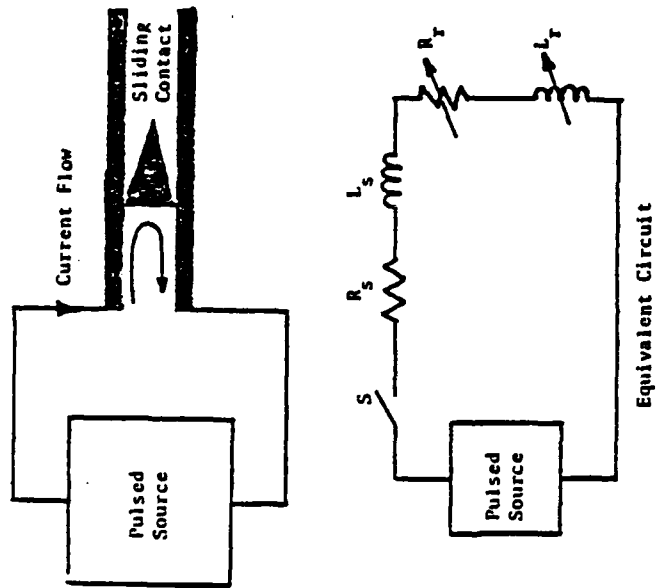
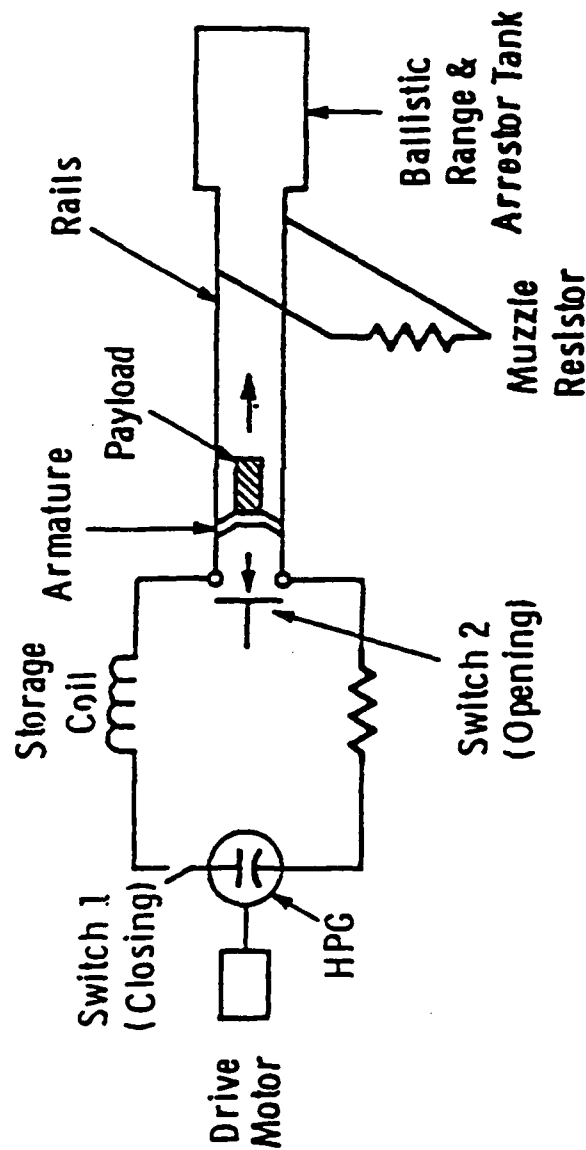


FIGURE 7. Simplified schematic diagram of a rail gun accelerator.

## OPERATION OF DC EM LAUNCHER



### Features

- Inertial Energy Storage In HPG From Prime Mover
- Energy Compression Into Inductor During Charging By Closing Switch 1
- Opening Switch 2 Transfers Inductive Energy Into Armature and Launches Projectile
- Muzzle Resistor Dissipates Unused Stored Energy

FIGURE 8. Operation of a DC EM launcher.

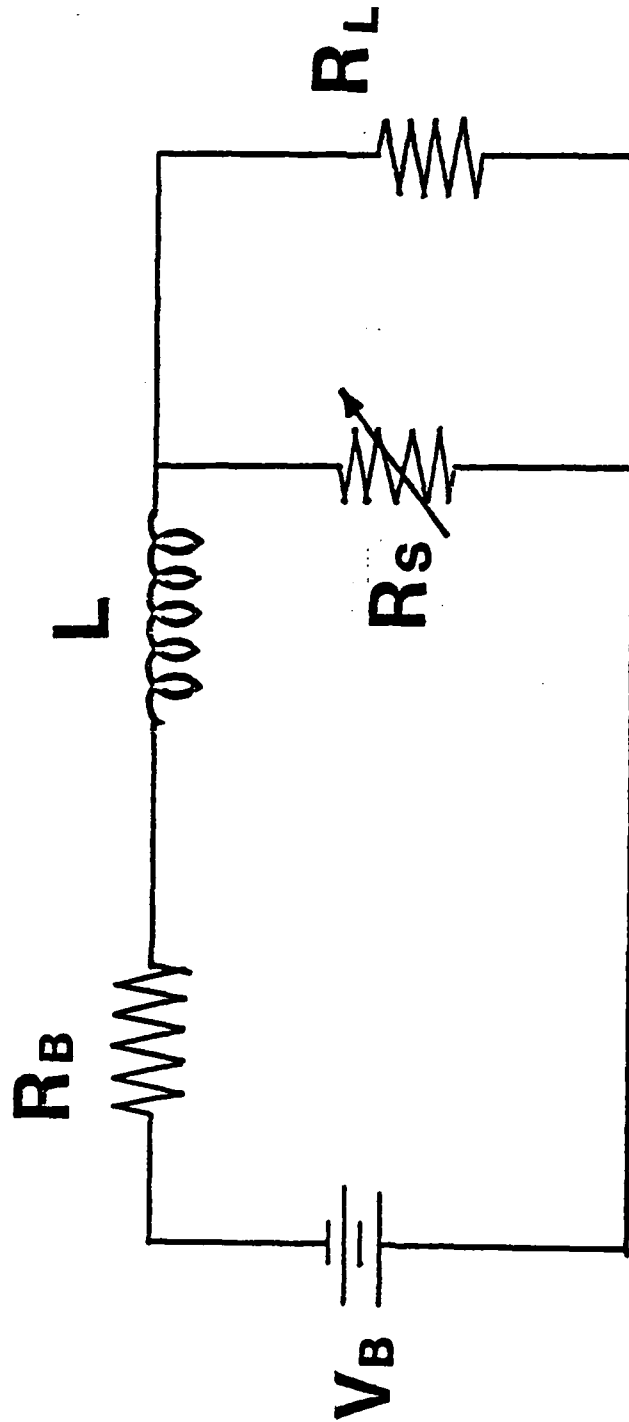


FIGURE 9. Schematic of the circuit used to examine the interaction of the circuit with the switch operation.



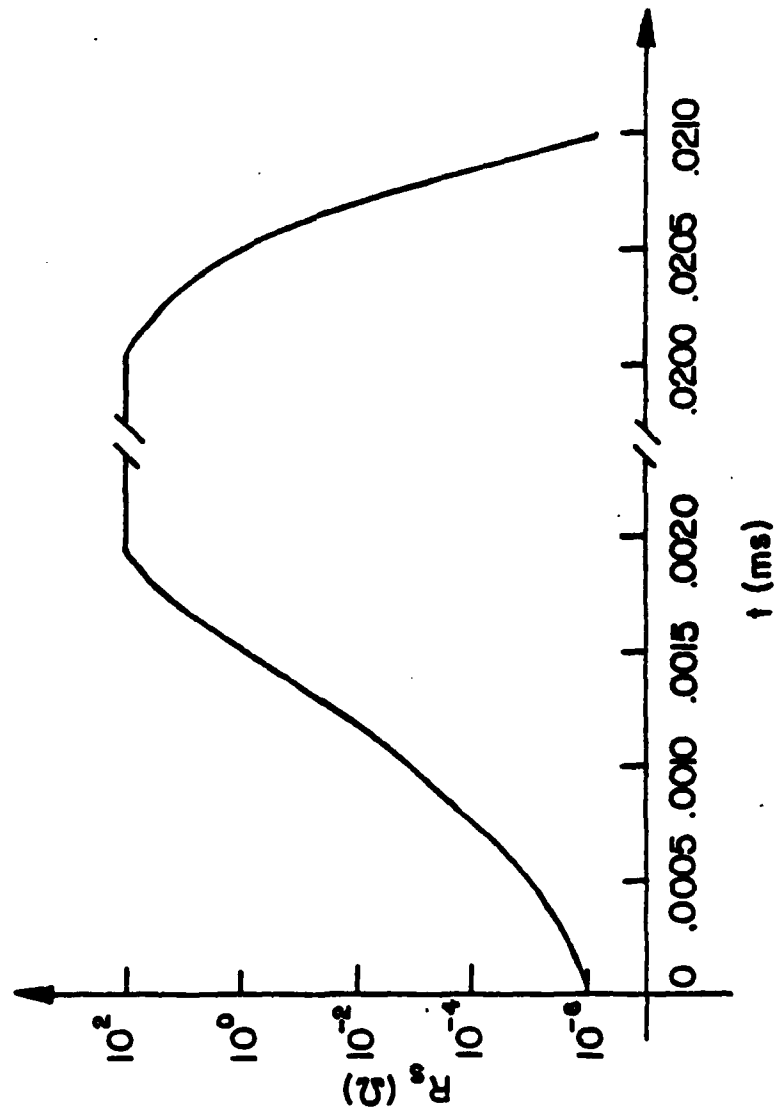


Fig. 10 Time history of the switch impedance

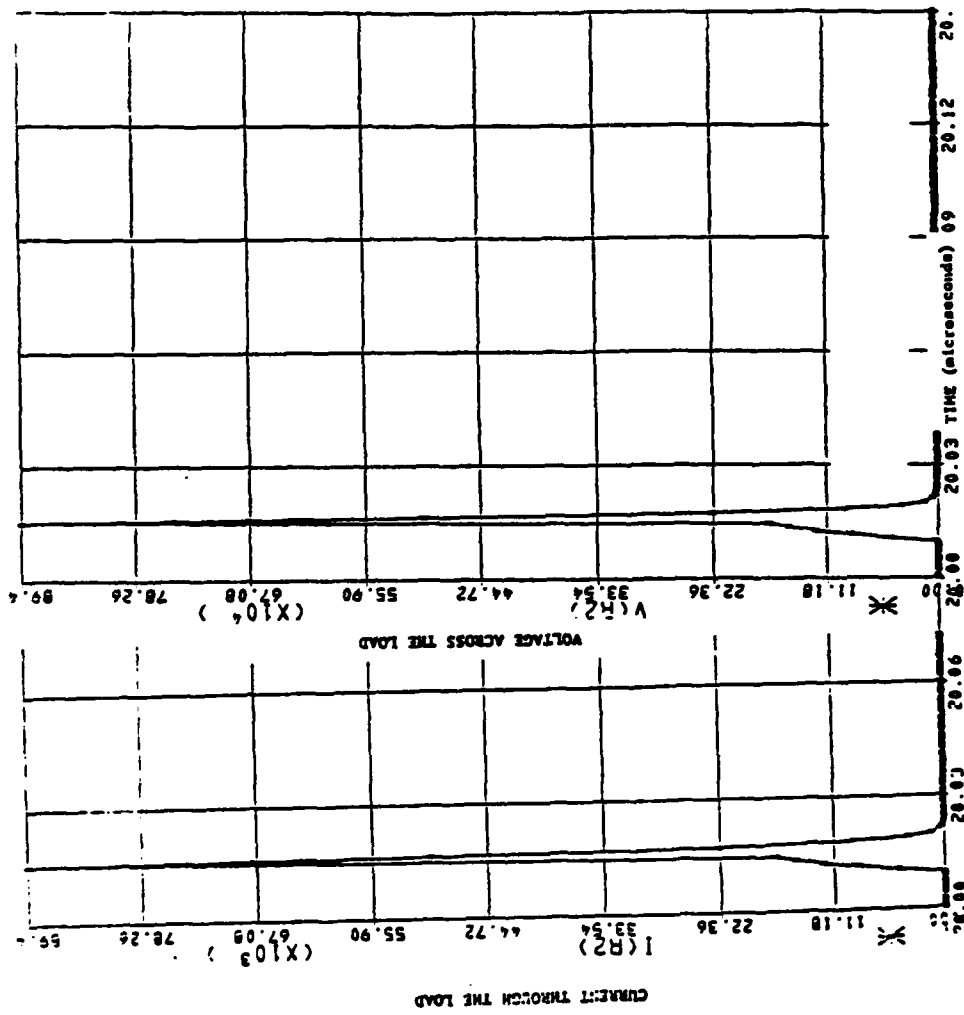


FIGURE 11. Results of NET II calculations.  
The load current and voltage.

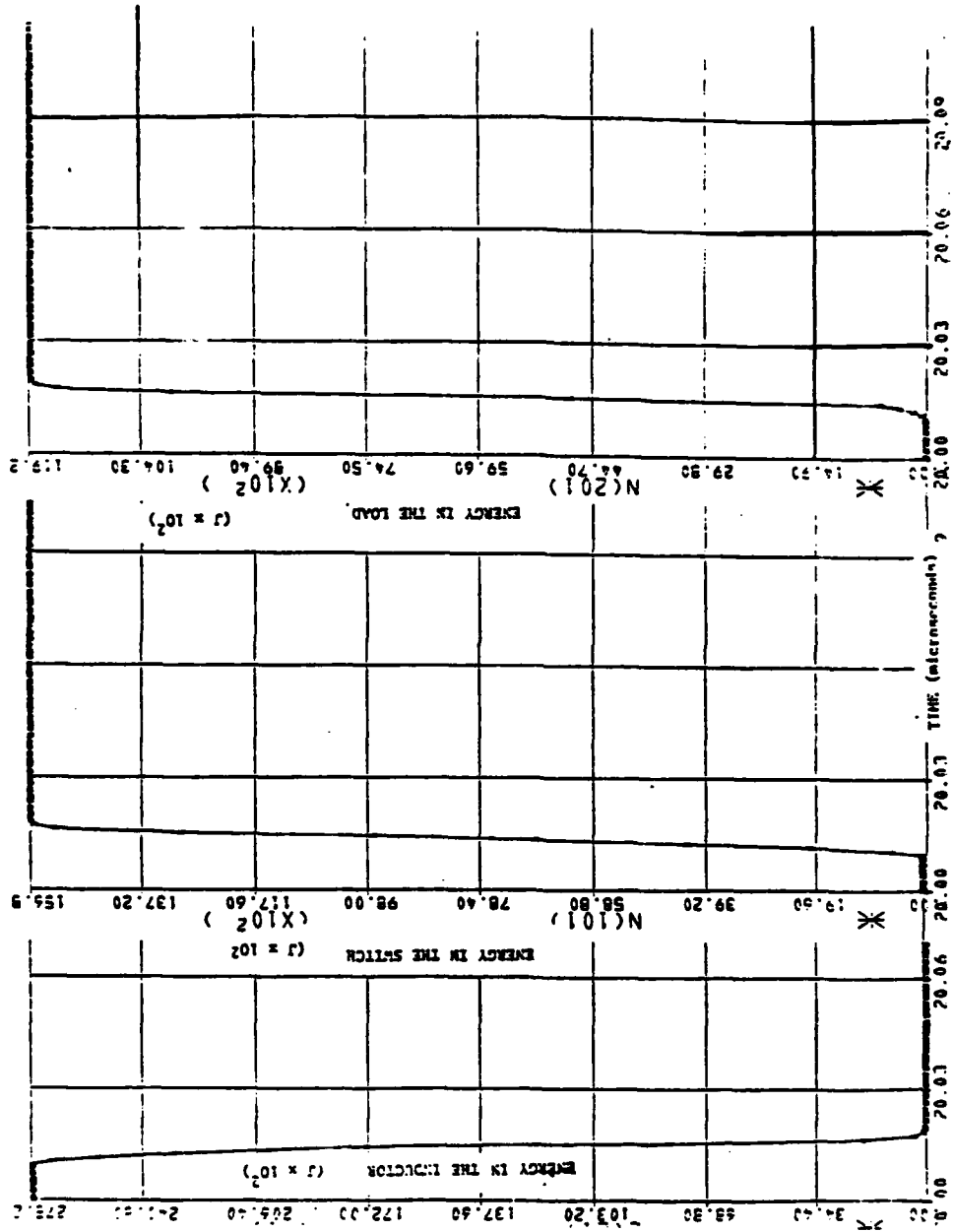


FIGURE 12. Results of NET II calculations.  
The energy in the inductor,  
switch, and load. Note that the  
total energy is conserved.

## INDUCTIVE SWITCHING PRINCIPLES

P. J. TURCHI  
R & D Associates, Inc.  
Washington Research Laboratory

Introduction

In preparation for discussions of diffuse-discharge opening switches, it is useful to review some basic features of inductively-driven pulsed power systems. Such power systems derive their (potential) advantage from the use of high energy density storage techniques (e.g., homopolar generator, high-field inductive store, MHD generator, etc.). For techniques that utilize mechanical energy storage in the form of electrical conductors moving at high speed, constraints are often imposed that the energy storage density is less than mechanical stress limits (e.g., yield strength) and that energy is removed from storage on timescales longer than acoustic transit times in the structure. Either the storage medium (~ moving armature) or the extraction structure (~ stator) may limit the operating energy density and output pulsetime. Typically, high energy sources deliver current pulses in times ranging from 0.1 sec (HPG's) to 100  $\mu$ sec (pulsed MHD). A critical feature of an inductive opening-switch system is the ability to conduct current for these relatively long times, and then to open on command in much shorter times.

The energy required for opening-switch operation is determined by both fundamental and technical factors. These factors depend on the nature of the load (resistive, capacitive, inductive) and the approach utilized to achieve the switching action. For example, if current flow in an inductive circuit is diverted to a purely-resistive load by a purely-resistive opening-switch, the energy dissipated in the switch will mainly depend on the relative resistance-values of the switch and the load and thus on the switching technique. Flow of current in a load, however, is associated with magnetic flux and therefore real loads will always have an inductive component. Similarly, the switch will possess some inductance. It may be shown quite easily (Appendix I) that there are fundamental requirements for energy dissipation in the switch, independent of the switching technique. Such fundamental requirements on energy dissipation and voltage generated in switching (for a desired output pulsetime) must be considered in evaluating the operation and limitations of diffuse-discharge opening switches.

#### Simple Circuit Results

In the Appendix, several elementary inductive pulsed power circuits are considered. It is seen from the derivations that typically the opening-switch must dissipate an amount of energy about equal to that transferred to the inductive component of the load. Energy associated with the inductance

of the switch itself must also be dissipated. The results of the simple circuit analyses are summarized in Table I.

Table I  
Energy Dissipated or Stored in Opening Switch

	$\frac{W/E_o}{}$
Case 1: <u>Inductive-Load, Purely-resistive Switch</u>	$\frac{L_2}{L_1+L_2}$
Case 2: <u>Zero-impedance Load, Inductive Switch</u>	$\frac{L_p}{L_1+L_p}$
Case 3: <u>Inductive-Load, Inductive Switch</u>	$\frac{L_1 L_2 + L_p (L_1 + L_2)}{(L_1 + L_2) (L_1 + L_p)}$
Case 4: <u>Inductive-Load, Purely Capacitive Switch</u>	$\frac{L_2}{L_1+L_2}$
Case 5: <u>Changing Inductance Load/Switch</u>	$\frac{\Delta L}{L}$

The last two cases in Table I do not involve energy dissipation in the switch but are not relevant to diffuse-discharge switching as commonly envisioned (i.e., external excitation).

Note that it is typical for inductive switching operation to transfer magnetic energy to a new volume of space, leave some magnetic energy in the original volume, and to dissipate magnetic energy (and magnetic flux) in the process. A simple illustration of such operation is given in Fig. 1

with the assistance of Poynting's vector  $\vec{S} = \vec{E} \times \vec{B}/\mu$  combined with Ohm's law,  $\vec{E} = \eta \vec{j}$ . Magnetic flux and energy flows out of a storage volume into the switch material of resistivity  $\eta$ . (The direction of the flow is the same as the  $\vec{j} \times \vec{B}$  force acting at the switch surface.) In Fig. 1, two coaxial solenoids are shown in cross-section, with current flow (initially only in the inner solenoid) perpendicular to the plane of the figure. Magnetic field lines from the current flow surround the inner solenoid and some also surround the outer (non current-carrying) solenoid. Let the resistivity of the outer solenoid be much less than that of the inner solenoid. Field line segments of the same magnetic field loop surrounding only the inner solenoid flow into the solenoid from both sides and eventually meet, cancel (or annihilate), and thereby generate heat. For the field loops that surround both solenoids, however, field line segments flow completely through the inner solenoid and never meet oppositely - directed field lines since the resistivity of the outer solenoid is assumed to be low ( $\eta \approx 0$ ). The net result is that field lines surround the outer solenoid, representing current flow in this solenoid and a transfer of magnetic energy to a new region of space. Note that some field lines associated with current flow in the outer solenoid also surround the inner solenoid (which is no longer carrying current), so some magnetic energy remains in the original volume. Visualizing the "flow" of magnetic field lines, including annihilation, may aid in the

conceptual design of opening-switches. For example, the magnetic field surrounding only the switch dissipates its energy in the switch.

#### Some Critical Features for Opening Switches

To guide research in support of repetitive opening-switch technology, it is useful to consider some critical features for switch operations:

1. Ratio of conduction time to opening time - to realize the potential of high energy density inductive power systems, this ratio should be at least 10. Heating (and gas motion) during the conduction phase may limit the ability of diffuse discharges to operate directly with high energy sources for which the conduction time may exceed  $10^{-3}$  sec.
2. Ratio of closed to opening voltage - which, along with the temporal ratio, determines part of the switch efficiency (i.e., flux loss).
3. Rate of rise of dielectric strength and/or resistivity - such rates determine the opening time in the context of the load requirement (voltage and/or current rise).
4. Source of energy (current) to operate switch - clearly affects desirability and practicality of switch concept.
5. Ability to absorb/dissipate required energy - during both the conduction phase and opening/transfer phase of the switch, energy will be dissipated that could critically



affect switch operation (by creating thermal instabilities, for example). The energy density for allowable dissipation will scale the switch size.

6. Size, cost, complexity of the switch (system) - a clear advantage over existing technology must exist.
7. Control and rep-rate - for repetitive operation the switch environment must recover between shots. Also, long term degradation of the switch medium (and other parts of the switch system) must be considered (e.g. introduction of electrode and wall impurities could affect discharge chemistry).

By focusing quantitatively on the parameters that determine the relative advantages of inductive power systems over conventional (capacitive) technology, the operating requirements for repetitive opening - switches can be defined. These operating requirements will then indicate critical basic research areas that must be pursued and, perhaps more importantly, technical approaches that are inadequate for the desired system-operation.

RDA/WRL

FIELD LINE POINT-OF-VIEWPoynting vector

$$\vec{S} = \frac{\vec{E} \times \vec{B}}{\mu}$$

generalized Ohm's Law

$$\vec{E} = \eta \vec{j} - \vec{v}_e \times \vec{B}$$

so

$$\vec{S} = \frac{\eta}{\mu} \vec{j} \times \vec{B} + \vec{v}_e \cdot \frac{B^2}{\mu} - \vec{B} \left( \frac{\vec{v}_e \cdot \vec{B}}{\mu} \right)$$

energy flux  
due to resistive  
diffusion

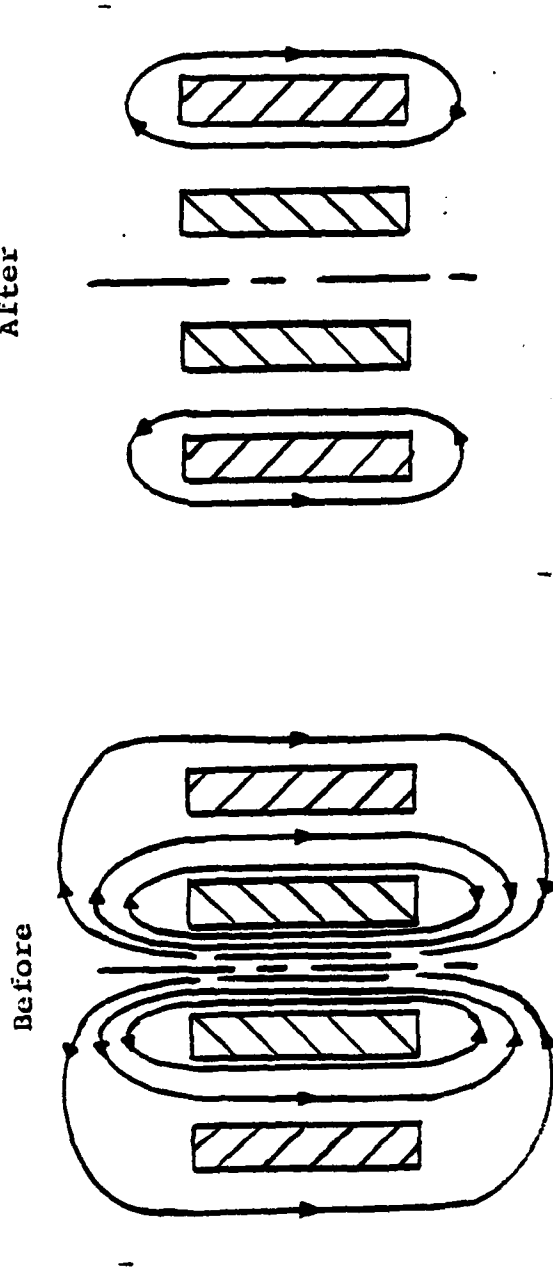
field line  
stretching

$$\frac{B^2}{2\mu} \vec{v}_e \cdot \vec{A} - \text{magnetic pressure work}$$

$$+ \frac{B^2}{2\mu} \vec{v}_e \cdot \vec{A} - \text{new volume of magnetic field}$$

Fig.1 Field Line Point-of-view

# FIELD LINE POINT-OF-VIEW



$$\eta \neq 0, \quad \vec{S} = \frac{\eta}{\mu} \int \vec{j} \times \vec{B} \neq 0$$

$$\eta \approx 0, \quad \vec{S} \approx 0$$

directed into the conductor surface from both sides. Segments of field line (loop) diffuse into conductor, meet, and cancel (annihilate) transforming magnetic energy into heat.

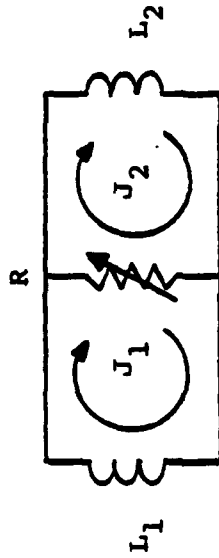
segments of common loop cannot meet, but one segment can pass through resistive conductor without annihilation, thereby transferring magnetic energy to new volume.

Fig. 1 Field Line Point-of-view (con't)

APPENDIX  
RDA/WRL

SIMPLE INDUCTIVE CIRCUITS - CASE 1

Resistive Transfer:



$$L_1 \frac{dJ_1}{dt} = -R(J_1 - J_2) = -L_2 \frac{dJ_2}{dt}$$

$$L \frac{dJ}{dt} = -RJ$$

With  $J = J_1 - J_2$  ; initially  $J = J_0$  and  $L = L_1 L_2 / (L_1 + L_2)$

Energy dissipated in resistor is:

$$W_R = \frac{1}{2} L J_0^2$$

independent of functional form  $R(t)$

Note that dissipated energy scales as system energy:

$$\frac{W_R}{E_0} = \frac{L}{L_1} \quad \text{where} \quad E_0 = \frac{1}{2} L_1 J_0^2$$

SIMPLE INDUCTIVE CIRCUITS - Case 1

Energy left in magnetic field is:

$$\frac{1}{2} (L_1 + L_2) J_f^2 = \frac{1}{2} (L_1 - L) J_o^2$$

so  $J_f = J_o \left( \frac{L_1 - L}{L_1 + L_2} \right)^{\frac{1}{2}} = \frac{L_1 J_o}{L_1 + L_2}$  , as expected by flux conservation

Energy transferred to  $L_2$ :

$$W_{2f} = \frac{L_1 L_2}{(L_1 + L_2)^2} E_o^2 \quad , \quad \text{maximum for } L_2 = L_1$$

Energy dissipation relative to transferred energy:

$$W_R = \left( 1 + \frac{L_2}{L_1} \right) W_{2f}$$

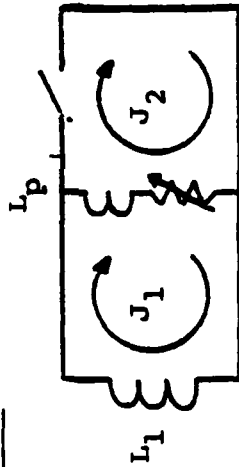
$$= W_{2f} \quad , \quad \text{if load inductance low}$$

$$= 2W_{2f} \quad , \quad \text{if maximum inductive load energy}$$

SIMPLE INDUCTIVE CIRCUITS - Case 2

Parasitic Inductance in Switch:

Zero-impedance Load



$$L_1 \frac{dJ_1}{dt} = 0 = L_p \frac{d}{dt} (J_2 - J_1) + R (J_2 - J_1)$$

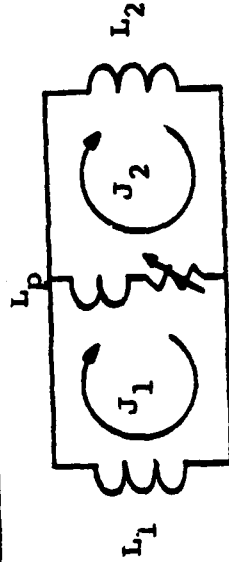
With  $J = J_1 - J_2$  again, the dissipated energy is:

$$W_R = \frac{1}{2} L_p J^2 = \frac{L_p E_0}{(L_1 + L_p)}$$

# SIMPLE INDUCTIVE CIRCUITS - Case 3

## Parasitic Inductance in Switch:

### Inductive Load



$$L_1 \frac{dJ_1}{dt} + L_p \frac{d}{dt} (J_1 - J_2) = -R (J_1 - J_2)$$

$$L_2 \frac{dJ_2}{dt} = -L_1 \frac{dJ_1}{dt}$$

### Energy transferred:

$$W_{2f} \approx \frac{L_1 L_2}{(L_1 + L_2)^2} E_{10}^2, \text{ where } E_{10} = \frac{1}{2} L_1 J_0^2$$

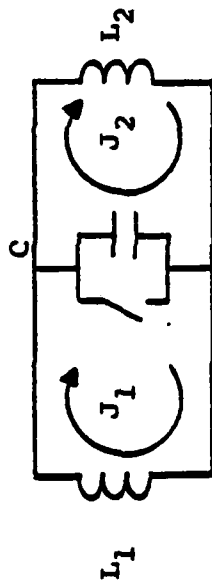
### Energy dissipated:

$$W_R = \left[ \frac{L_1 L_2 + L_p (L_1 + L_2)}{(L_1 + L_2)} \right] \frac{E_{10}}{L_1} = \frac{L_1 L_2 + L_p (L_1 + L_2)}{(L_1 + L_2) (L_1 + L_p)} E_0$$

$$= \left( \frac{L_1 + L_2}{L_1 L_2} \right) \left[ L_2 + L_p \left( 1 + \frac{L_2}{L_1} \right) \right] W_{2f} ; E_0 = \frac{1}{2} (L_1 + L_p) J_0^2$$

# SIMPLE INDUCTIVE CIRCUITS - Case 4

## Capacitive Transfer:



$$L_1 \frac{dJ_1}{dt} = -V = -L_2 \frac{dJ_2}{dt}, \text{ with } V = \frac{1}{C} \int (J_1 - J_2) dt$$

$$L \frac{dJ}{dt} = -V(J)$$

$$\text{with } J = J_1 - J_2$$

$$\text{and } L = L_1 L_2 / (L_1 + L_2) \text{ again.}$$

Peak energy stored in capacitor:

$$W_C = \frac{1}{2} L J_O^2 = \left( \frac{L_1 + L_2}{4 L_1} \right) W_{2f} = \frac{L_2}{L_1 + L_2} E_O, \quad E_O = \frac{1}{2} L_1 J_O^2$$

Maximum transfer to inductive load energy occurs for  $L_1 = L_2$ , so

$$W_C = \frac{1}{2} W_{2f}.$$

Thus, capacitor must be half size of simple capacitive drive.



# SIMPLE INDUCTIVE CIRCUITS - Case 5

## Time-varying Inductances:

$$\frac{d}{dt} LJ = V - RJ$$

Multiply by J:

$$\frac{d}{dt} \left( \frac{1}{2} LJ^2 \right) + \frac{1}{2} \dot{L} J^2 = VJ - RJ^2$$

gain in magnetic energy (M.E.)      gain in kinetic energy (K.E.) or work      power input      resistive loss

By expansion of terms:

$$\frac{d}{dt} \left( \frac{1}{2} LJ^2 \right) = \frac{1}{2} \dot{L} J^2 + LJ \frac{dJ}{dt}$$

So, for rising current -  $\Delta(M.E.) > \Delta(K.E.)$

falling current -  $\Delta(M.E.) < \Delta(K.E.)$

If  $V - RJ = 0$ ,

$$\frac{\Delta(K.E.)}{(M.E.)_0} = \frac{\Delta L}{L}, \text{ accelerator } \Delta L > 0$$

or

$$\frac{\Delta(M.E.)}{(M.E.)_0} = \frac{1}{1 + \frac{\Delta L}{L}}, \text{ flux compressor } \Delta L < 0$$

#### SUMMARY OF SIMPLE PICTURES

1. Opening switch to divert current to a load involves dissipation and/or storage of energy comparable to that required by the inductive portion of the load\* (during transfer). Additional (resistive) impedance in the load increases energy cost. Energy required by the technique may be extra.
2. Kinetic and magnetic energy can be exchanged in circuits with time-varying inductances. Magnetic energy can increase with kinetic energy in switch volumes associated with conductor motion.
3. Magnetic energy of field lines encircling only the opening switch will be absorbed and/or dissipated in the switch itself.
4. Opening switches thus must be capable of absorbing energy associated with both the load and switch inductance on the time scale of current transfer and possibly in competition with the technique employed to lower conductivity.

### CRITICAL ISSUES

1. To use high energy density sources (HPG, MHD, etc.), need to accept current for long times ( $\lambda$  msec) and then on command open circuit in short times ( $\sim \mu$ sec).
2. Energy required for opening circuit operation
  - amount (fundamental; technical)
  - source (size, cost, complexity)

SOME CRITICAL FEATURES FOR OPENING SWITCHES

1. Ratio of conduction time to transfer time
2. Ratio of closed to opening voltage
3. Rate of rise of dielectric strength
4. Source of energy to operate switch
5. Ability to absorb/dissipate required energy
6. Size, cost, complexity
7. Control and rep-rate
8. Performance in system, not simply as a technique by itself

## FUNDAMENTAL PROCESSES IN DIFFUSE DISCHARGES

Manfred A. Biondi

Dept. of Physics &amp; Astronomy, University of Pittsburgh

The purpose of this review is to establish the important processes in diffuse discharge switch plasmas and to present typical rates for the processes under expected switching conditions in order to provide a perspective for engineering designs. In addition, possible problems with suggested plasma density/conductivity modification schemes for the switches will be touched on.

Consider a simplified description of the variation of electron concentration  $n_e$  in a plasma via the continuity equation,

$$\partial n_e / \partial t = P_e - \alpha n_e^2 - \nu_a n_e, \quad (1)$$

where  $P_e$  represents the volume rate of electron (and ion) production via processes such as electron impact ionization, the second term is the volume recombination rate, with  $\alpha$  the effective two-body electron-ion recombination coefficient and the third term is the attachment rate, with  $\nu_a$  the electron attachment frequency to form negative ions (detachment of electrons from negative ions is neglected, and diffusion is slow on the time scale of interest). From Eq. (1), since the recombination rate varies as  $n_e^2$  and the attachment rate as  $n_e$ , in a stationary high density plasma, recombination balances ionization and thus controls the electron density achieved.

### I. Electron-Ion Recombination Processes

Since the plasma conductivity (which controls power transfer and losses in the switch) depends on the electron concentration (and on the electron mobility, which will be discussed in the following paper) it is important to consider the various recombination processes which control the electron removal. The possible forms of electron-ion recombination are

illustrated in reactions (2) through (5)



Reactions (2) and (5) are 2-body in character; however radiative recombination is too slow to be of interest. Reactions (3) and (4) are three-body in character, requiring a third-body to remove energy from the system to cause capture of the free electron. This is shown for reaction (3) in Fig. 1, where two free electrons (open circles) in the vicinity of an ion  $A^+$  interact and exchange energy, leading to initial capture of one to form the neutral excited atom  $A_j^*$ .

The highly efficient two-body dissociative recombination process, reaction (5), in effect carries its own energy-removing third-body in the molecular ion, converting electronic energy into kinetic energy by molecular dissociation following the initial, resonant capture of the electron, as indicated by the potential curves of Fig. 2. The electron capture to form  $(AB^*)_r$  may either be direct (left figure) or indirect, through initial formation of a Rydberg state  $(AB^*)_a$  (right figure). The rates of the direct and indirect processes vary differently with electron energy. The magnitudes and electron temperature dependences of the dissociative recombination coefficients for various ions may be expressed in the form

$$\alpha = \alpha_{300} (T_e/300)^{-x}. \quad (6)$$

Typical values for the various classes of ions are given in Table I.

Table I. Typical values of recombination coefficients.

Ion Type	Examples	$\alpha_{300}(\text{cm}^3/\text{sec})$	x
"Simple" Light Diatomic	$\text{Ne}_2^+, \text{N}_2^+, \text{O}_2^+$	$\sim 2 [-7]$	0.4 - 0.7
Light Rare Gas Trimer	$\text{Ne}_3^+$	$\sim 1 [-6]$	0.3 - 0.4
Molecular Dimer/Trimer	$\text{N}_2^+ \cdot \text{N}_2, \text{CO}^+ \cdot (\text{CO})_{1,2}$	$\sim 2 [-6]$	0.3 - 0.4
Heavy Rare Gas Diatomic	$\text{Kr}_2^+, \text{Xe}_2^+$	$\sim 2 [-6]$	0.5 - 0.6
Polar Cluster Ions	$\text{H}_3\text{O}^+(\text{H}_2\text{O})_n$	2 to 4 [-6]	0.0 - 0.1

To assess the relative importance of the various recombination processes we compare their effective two-body rate coefficients,  $\alpha_{\text{eff}}$ . For reaction (5),  $\alpha_{\text{eff}} = \alpha$ . For reaction (3),  $\alpha_{\text{eff}} = K_{\text{cr}} n_e$ , while for reaction (4),  $\alpha_{\text{eff}} = K_{\text{ns}} n_n$ , where the K's are the appropriate three-body rate coefficients. Fig. 3 compares the rates of the various processes at various neutral concentrations (left side) and electron concentrations (right side) at low and high electron temperatures. It will be seen that for realistic switch pressures and plasma densities, at modestly elevated electron temperatures,  $T_e \geq 1000$  K, dissociative recombination of any molecular ion (the horizontal lines) outweighs any other electron recombination process. Further, the effective rate at elevated temperatures,  $T_e \geq 10,000$  K, is still so large for most molecular ions ( $\alpha_{\text{eff}} \sim 10^{-7} \text{ cm}^3/\text{sec}$ ) that appreciable energy must be expended in creating a large enough ionization rate to yield a high plasma density.

## II. Ion-Ion Recombination Processes

Since electron attachment figures prominently in fast opening switch plans, the fate of the negative ions formed should be considered - are they neutralized by recombination with positive ions or do they release their electrons as a result of collisions with neutrals (detachment)? The two-body, mutual neutralization (ion-ion recombination) coefficients are typically  $\alpha_{\text{mn}} \sim 10^{-7} \text{ cm}^3/\text{sec}$  at  $T_i = T_n = 300$  K, and the coefficient is expected to

decrease as  $T_i^{-1/2}$ . Neutral-stabilized ion-ion recombination, the ion analogue of reaction (4), has an effective recombination coefficient at 1000 Torr pressure and  $T_i = 300$  K,  $\alpha_i = K_i n_n \sim 10^{-6}$  cm<sup>3</sup>/sec, and decreases as  $T_i^{-3}$ . Thus, in a plasma of charged particle concentration  $10^{14}$  cm<sup>-3</sup>, a negative ion has a lifetime of  $\sim 10^{-8}$  sec against neutralization by positive ions, while detachment of the electron may either be very much slower or comparable in rate, depending on the process involved (see discussion in Sec. III A).

### III. Ion-Molecule Reactions

#### A. Electron Detachment at Collisions between Negative Ions and Neutrals

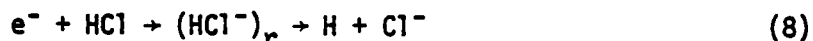
In order to reduce the plasma conductivity for switching, electron attachment to molecules to form stable negative ions is proposed. It is, however, necessary that the negative ion not detach its electron on subsequent collisions with neutrals in the plasma. One means of electron detachment is via impact of a sufficiently energetic negative ion with a neutral,



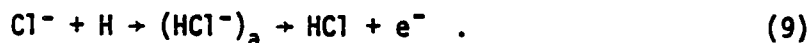
As a rule-of-thumb, there is a threshold for such collisional detachment when the center-of-mass kinetic energy of ion and neutral is of the order of the electron affinity of the negative ion, and the detachment cross section becomes appreciable ( $\sim 10^{-16}$  cm<sup>2</sup>) only at 3 to 10 times this energy. Thus, at low energies,  $\sim 1$  eV, there is no collisional detachment of strongly bound electrons. In a switch plasma, the ion energy distribution provides a few higher energy ions, so that negative ions with weakly bound electrons, e.g.,  $O_2^-$  for which E.A. = 0.4 eV, exhibit some collisional detachment in moderate electric fields, as shown in Fig. 4. Also, for such ions, gas heating to 500-1000 K provides measurable collisional detachment.



Collisional detachment is expected to be negligible in diffuse discharge switches containing a rare gas/halogen-bearing molecule mixture. For example, the  $\text{Cl}^-$  produced by the dissociative attachment reaction



has a strongly bound electron, E.A. = 3.7 eV. However, if the diffuse discharge causes appreciable dissociation of the HCl molecules (e.g., by electron impact), the free hydrogen atoms can cause associative detachment of the electron on collisions with  $\text{Cl}^-$  ions via

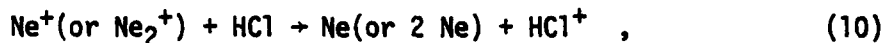


This reaction (essentially the inverse of reaction (8)) has been calculated to proceed at nearly the Langevin rate, i.e.,  $k_{\text{ad}} \sim 10^{-9} \text{ cm}^3/\text{sec}$ , independent of ion energy. If 1% of the HCl molecules (assumed to be present at a pressure of 10 Torr) are dissociated, the lifetime of  $\text{Cl}^-$  against associative detachment is  $\tau_{\text{ad}} = 1/(k_{\text{ad}}[\text{H}]) = 3 \times 10^{-7} \text{ sec}$ . Thus, as the plasma concentration decreases below  $10^{14} \text{ cm}^{-3}$  and/or the ion "temperature" in the applied fields is elevated significantly above 300 K, associative detachment to free the electron will outweigh neutralization of the negative ion by ion-ion recombination. However, the rapid dissociative attachment, reaction (8), assures a negative ion/electron ratio  $\gg 1$ .

#### B. Positive Ion Charge Transfer and Clustering Reactions

Since cluster ions such as  $\text{H}_3\text{O}^+ \cdot \text{H}_2\text{O}$  exhibit large dissociative recombination coefficients over the whole electron temperature range likely to be encountered in diffuse discharge switches, formation of complex ions by transfer or clustering reactions can seriously inhibit maximum plasma densities achieved.

On the basis of known charge transfer and clustering reaction rates for related species, for a hypothetical diffuse discharge containing 1000 Torr Ne and 10 Torr HCl, one postulates the following reaction sequence;



followed by



and perhaps further clustering steps. A likely rate for reaction (10) is  $k_{\text{ct}} \sim 10^{-9} \text{ cm}^3/\text{sec}$ , yielding a time constant for  $\text{HCl}^+$  formation of  $\tau_{\text{ct}} = 1/(k_{\text{ct}}[\text{HCl}]) \sim 3 \text{ ns}$ . For reaction (11),  $K_c \sim 10^{-27} \text{ cm}^6/\text{sec}$ , leading to a clustering time constant for  $\text{HCl}^+ \cdot \text{HCl}$  formation of  $\tau_c = 1/(K_c[\text{HCl}][\text{Ne}]) \sim 0.1 \text{ nsec}$ . Thus, on a nanosecond time scale, our hypothetical plasma might well be dominated by cluster ions, with the attendant problems that that involves.

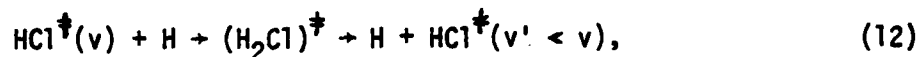
#### IV. Some Potential Problems

In a brief review of this type it is not possible to discuss all relevant atomic collision processes that control the diffuse discharge's behavior. To suggest the wide-ranging nature of the relevant processes, let us consider two that pose possible problems for laser pumping of molecular vibration to enhance electron attachment in molecules such as HCl.

##### A. Vibrational Relaxation

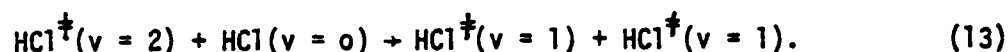
If an adequate population of vibrationally excited molecules (e.g.,  $\text{HCl}^+$ ) is to be attained with reasonable laser pumping powers, vibrational relaxation due to collisions with other atoms/molecules must be slow. Ordinary collisions involving conversion of vibrational energy to translational energy of separation (V-T) are inefficient and do not lead to rapid relaxation. However, using HCl as an example, in the presence of dissociated atoms of H

and Cl, vibrational relaxation via atom transfer can be a fast V-T process; i.e., for the reaction



the rate coefficient may be large,  $k_{\text{VT}} \sim 10^{-10} \text{ cm}^3/\text{sec}$ .

In addition, V-V processes, in which vibration is rapidly exchanged between molecules, tend to defeat selective pumping to a higher vibration state (such as  $v = 2$ ); i.e.,



Again, this reaction probably exhibits a large rate coefficient,  $k_{\text{VV}} \sim 10^{-10} \text{ cm}^3/\text{sec}$ .

#### B. Absorption of Pumping Radiation by Plasma Species

To illustrate rather far-out processes that might frustrate an otherwise promising switch conductivity modulation scheme, consider optical absorption by plasma species created in the diffuse discharge itself. We have seen that cluster ions may form and quickly dominate in the switch plasma. The absorption bands for such ions may lie in awkward spectral regions - such as at the frequency of the vibration-pumping laser, and one must consider the concentration of such ions and their absorption coefficients to decide whether one can neglect the losses they induce. (In rare gas-halide lasers, absorption bands by the principal plasma ions occasionally do inhibit laser gain). While this process is rather unlikely to cause problems in switch plasmas, it is mentioned to suggest the need for great care in searching out potential pitfalls hidden in seemingly innocent atomic collision processes.

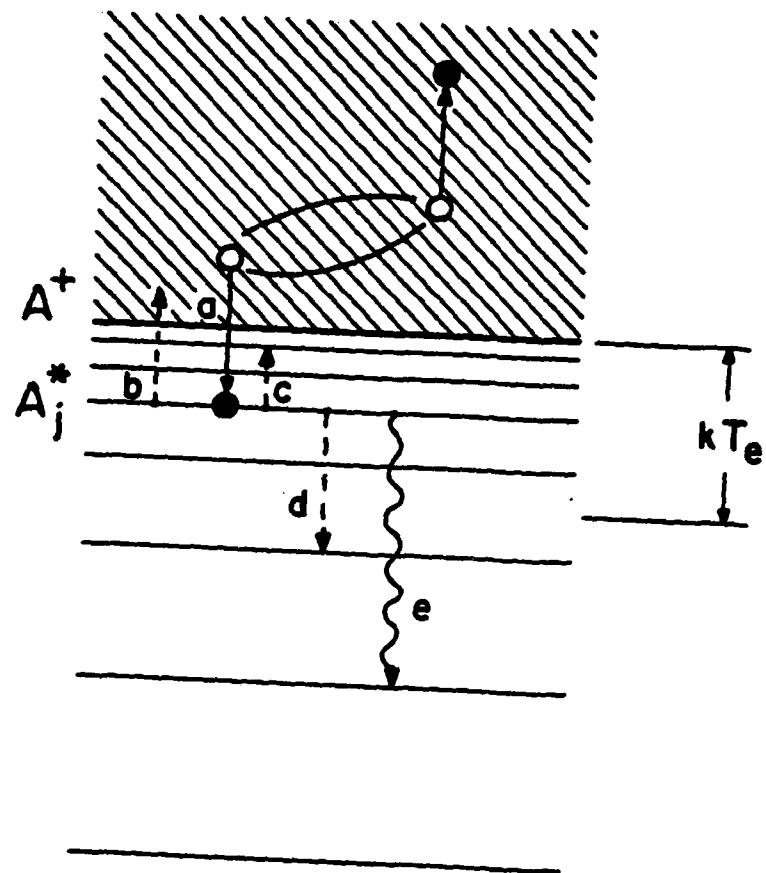


FIGURE 1

FIGURE 2

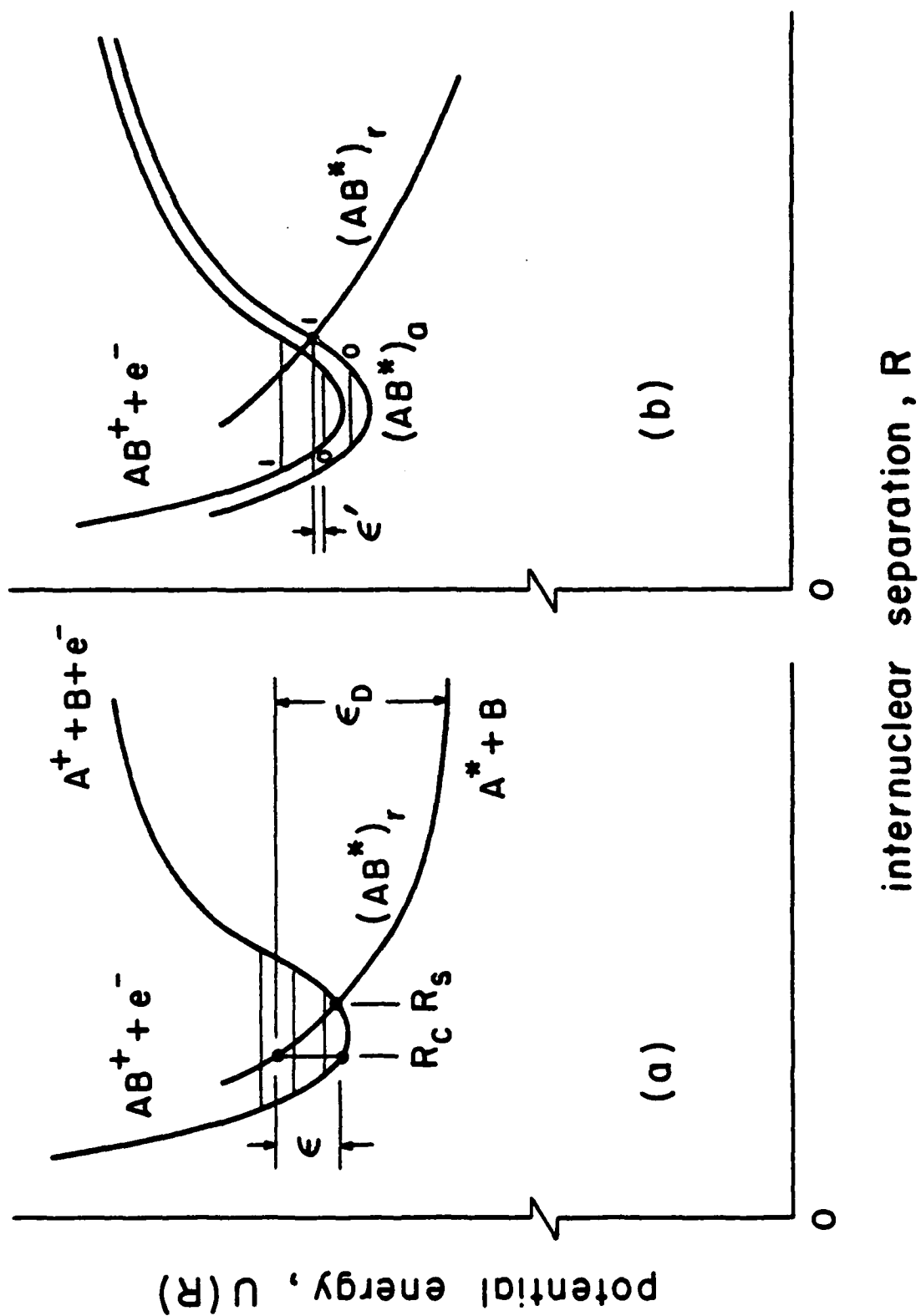


FIGURE 3

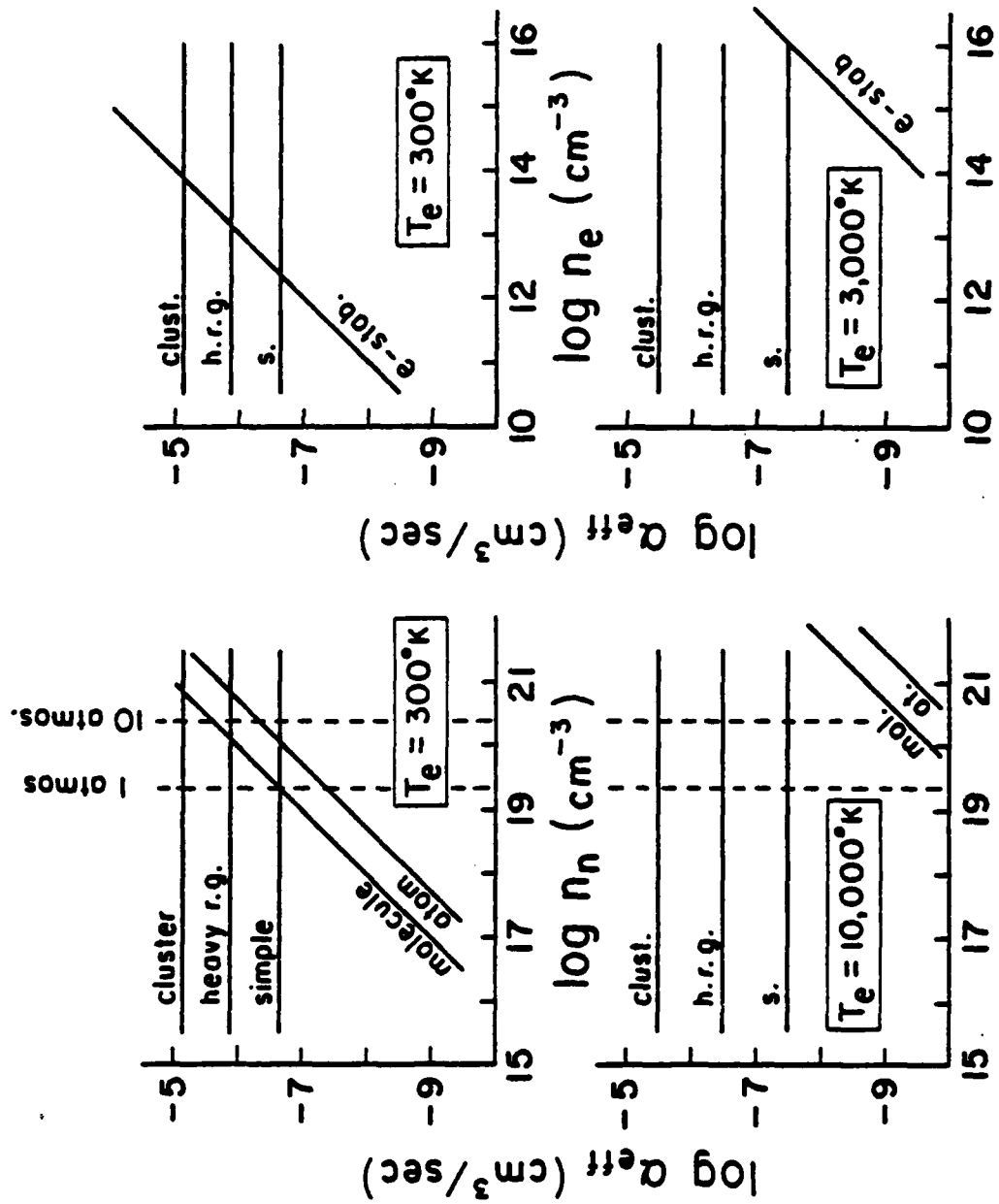
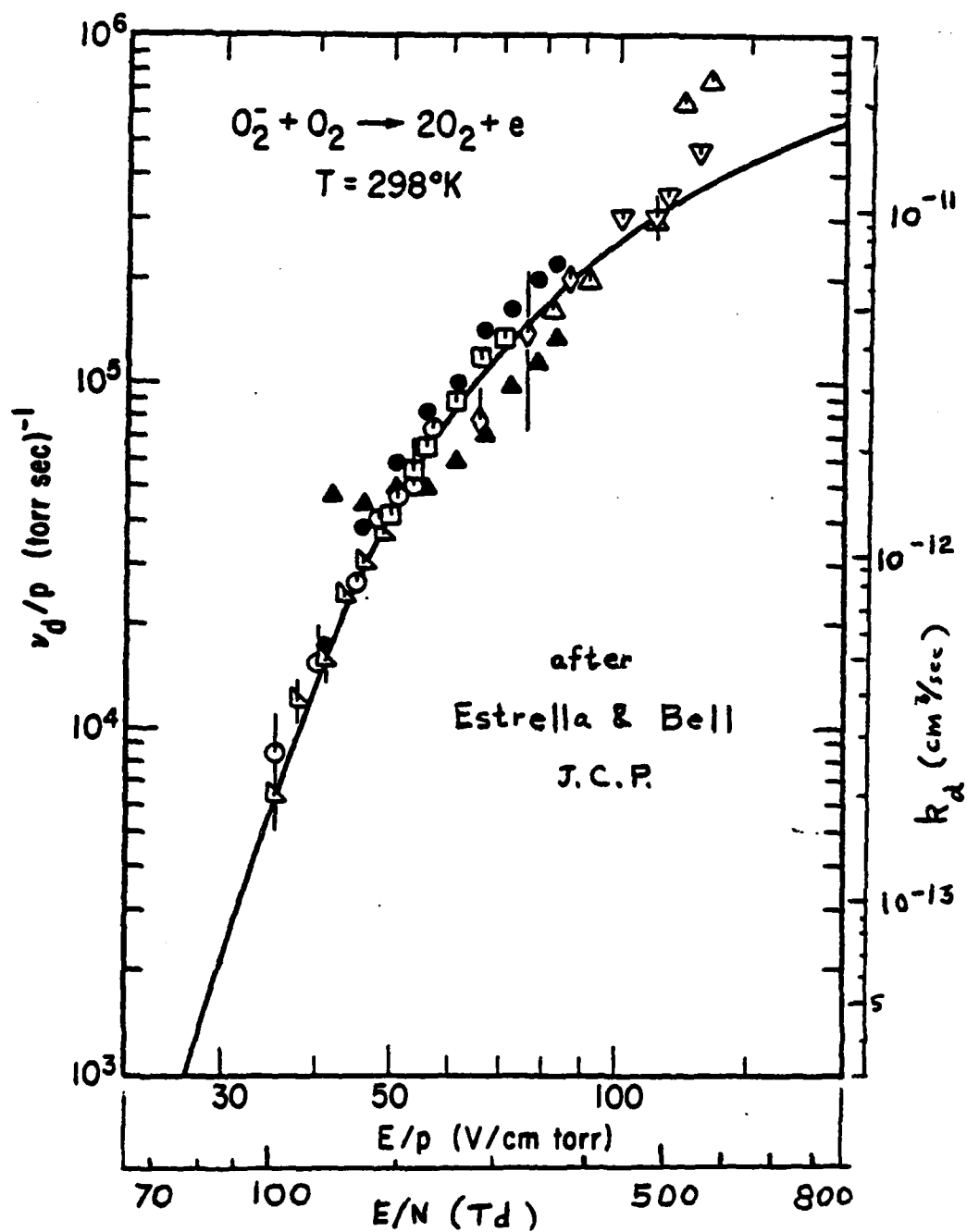


FIGURE 4



FUNDAMENTAL PROCESSES OF IMPORTANCE IN DIFFUSE DISCHARGES  
FOR OPENING SWITCHES\*

A. V. Phelps<sup>†</sup>

Joint Institute for Laboratory Astrophysics  
National Bureau of Standards and University of Colorado  
Boulder, CO 80309

I. INTRODUCTION

We will continue the review of fundamental processes relevant to diffuse discharge opening switches with discussions of various aspects of electron collisions with atoms and molecules. In Sec. II we discuss examples of data concerning the elastic collisions of electrons with molecules. The subject of electron attachment to molecules is reviewed in Sec. III. This will be followed by a consideration of electron collisional ionization in Sec. IV, and finally in Sec. V we consider the topic of gas heating resulting from electron collisions with gas molecules.

II. ELASTIC COLLISIONS

In Fig. 1 we show a recent compilation which we have made of the total cross sections for electron scattering in nitrogen. The uppermost curve is

---

\*This work was supported in part by the U. S. Army Research Office.

<sup>†</sup>Staff Member, Quantum Physics Division, National Bureau of Standards.



the sum of the elastic, excitation and ionization cross sections as measured by attenuation of a beam of electrons.<sup>1,2</sup> The various partial cross sections are shown by the dashed curves. The short dashed curve shows the energy dependence of the total cross section for elastic scattering. This curve is based on experimental data<sup>3</sup> for electron energies up to 400 eV. At higher energies we have made use of theoretical calculations.<sup>4</sup> The total ionization cross section is taken from the work of Rapp and Englander-Golden.<sup>5</sup> The sum of the excitation cross sections shown here is taken from Pitchford and Phelps.<sup>6</sup>

The cross sections shown in Fig. 1 for  $N_2$  are illustrative of the data now available for a few gases such as nitrogen, argon and helium. In addition to these total cross sections, a thorough analysis of electron motion in gases requires a knowledge of the differential cross section for electron scattering, that is, information concerning the angular distribution of the scattered electrons. Figure 2 shows an example of such data again for  $N_2$ . Here we have plotted experimental values<sup>3,7</sup> of the differential cross sections weighted by the sine of the scattering angle, since this is the function which is used to determine the various partial cross sections. The partial cross sections are defined by the equation shown in Fig. 2. This relationship comes from an expansion of the differential scattering cross section in spherical harmonics. If we consider  $n = 0$  we obtain the total cross section for elastic scattering at 10 eV which was shown in Fig. 1. If  $n = 1$  we have an additional cosine weighting of the differential scattering cross section. The difference between  $Q_0$  and  $Q_1$  is the well-known momentum transfer cross section.

I would now like to call your attention to a recent compilation of cross sections for elastic scattering in some of the more common gases by Hayashi.<sup>1</sup>

This report presents graphical and tabular data for the sum of the total cross sections as well as the total transport cross sections for elastic scattering. Although I have checked only parts of this report, I believe these data are the best available in print at the present time. For some gases of interest for diffuse discharge switches, very little experimental data are available, and we must turn our attention to theory. Padial, Norcross and Collins<sup>8</sup> have recently carried out detailed calculations of electron scattering in HCl for electron energies between about 0.3 eV and 10 eV. Of particular interest is the low electron energy range where, contrary to previous theories, the elastic scattering cross section is comparable with or larger than the rotational excitation cross section. This set of theoretical cross sections has been found to be in very good agreement with a set of cross sections derived from very recent measurements of electron transport coefficient for HCl by Davies, as reported by Chantry.<sup>9</sup>

### III. ELECTRON ATTACHMENT

In this section we discuss the process of electron attachment. For the purposes of this discussion we will consider the oxygen molecule, for which the potential energy curves are shown in Fig. 3. These curves show the ground state and the first excited state, the a  $^1\Delta_g$  state, of the neutral molecule. Also shown are the  $X^2\Pi_g$  ground state and one of the excited states, a  $^2\Pi_u$  state, of  $O_2^-$ . At low electron energies, electron attachment occurs to the oxygen molecule via a three-body process involving vibrational states of the  $X^2\Pi_g$  state of  $O_2^-$ . Although this process is of great importance in high pressure gases containing oxygen, the rate coefficients for this process are large only for low energy electrons.<sup>10</sup> It is therefore an undesirable process for diffuse discharge switches. In order to avoid attachment by such low

energy processes one would like to work with molecules which do not have stable negative ion ground states such as is shown in Fig. 3.

The type of potential energy curve associated with attachment processes appropriate to diffuse discharge opening switches is shown by that for the repulsive  ${}^2\Pi_u$  state of  $O_2^-$  shown in Fig. 3. The theory for dissociative detachment via this potential energy curve has been worked out in some detail by O'Malley.<sup>11</sup> The solid vertical lines show the region of internuclear separation for which there is a high probability of electron attachment from the lowest vibrational state of neutral  $O_2$ . According to this theory, electrons with energies above about 6 eV can attach to the  $O_2$  molecule in the dissociating state. The nuclei then begin to move apart. As the nuclei separate the electron can be reemitted, that is, it can be autodetached from the negative ion. If detachment occurs, the oxygen molecule may be left in the vibrationally excited state. If detachment does not occur, then the nuclei will separate forming a neutral oxygen atom and an oxygen atomic negative ion.

If a neutral oxygen molecule is initially in a vibrational excited state, then the range of nuclear separations which can lead to dissociative attachment is indicated by the vertical dashed lines of Fig. 3. One notes that for negative ions formed near the outer turning point, there is less distance to travel before reaching the crossing point for the  $X^3\Sigma$  and  ${}^2\Pi_u$  curves and autodetachment is less likely. This leads to a much larger probability of negative ion formation at low electron energies. Calculated cross sections for electron attachment to the various vibrationally excited states of  $O_2$  as obtained by O'Malley<sup>11</sup> are shown in Fig. 4. One notes that there is approximately a factor of 20 increase in the dissociative attachment cross section in going from the ground vibrational state to the fifth

vibrational state. The potential energy curve and autodetachment lifetime parameters required for this theoretical calculation were obtained by fitting temperature dependent electron attachment coefficient data obtained by Henderson, Fite, and Brackmann.<sup>12</sup>

Similar theoretical calculations have been made for other molecules in response to observations of temperature dependent attachment coefficients. An example is that of HCl where Allan and Wong<sup>13</sup> measured a very significant variation in the attachment coefficient with temperature. Other studies of electron attachment to HCl are those of Davies as reported by Chantry,<sup>9</sup> in which simultaneous measurements were made of electron attachment coefficient and electron drift velocity. The latter measurements were made only at room temperature.

Figure 5 shows a plot of integrated electron attachment coefficients as a function of electron energy of the peak of the attachment cross section for a number of gases,<sup>9,14,15</sup> some of which may be of use in diffuse discharge opening switches. The gases shown here are those with distinct peak cross sections well above zero energy. This plot does not show data for gases with large low energy attachment cross sections. The solid line in the upper right hand corner of this picture shows an approximate theoretical limit for resonance-type electron attachment.<sup>15</sup> Another way of looking at electron attachment data is to plot the attachment coefficient from electron swarm experiments as a function of the mean electron energy. Such a survey has recently been made by Chantry.<sup>9</sup>

#### IV. ELECTRON IMPACT IONIZATION

In this section we discuss data concerned with the process of electron impact ionization of atoms and molecules. A number of surveys and data

compilations have been prepared on this subject and I would particularly like to call attention the articles by Moiseiwitsch and Smith,<sup>16</sup> and by Lotz<sup>17</sup> and by Dutton.<sup>10</sup> The latter article is concerned with data obtained by electron swarm techniques. In addition there is the data compilation by Kieffer.<sup>18</sup>

We now turn to the problem of multi-step or cumulative ionization. This is ionization which occurs in a succession of processes beginning with electron excitation of the atom or molecule and ending with electron impact ionization of an excited atom or molecule.<sup>19</sup> Figure 6 shows a schematic of such processes. In the upper part of the diagram we have shown a simple schematic of the energy levels of an atom. The arrows indicate electron impact excitation and deexcitation. This schematic indicates that ionization of a ground state atom can occur via collisions involving excited atoms. Furthermore, there is the possibility of electron-ion recombination resulting in an excited atom which gradually is deexcited by collisions to the ground state. In the absence of competing processes, such a system would be in a Saha-Boltzmann equilibrium at the temperature of the electrons. In this schematic we have indicated one possible competing recombination process, that is, the process of dissociative recombination discussed at this workshop by Professor Biondi. According to this process, the atomic ions collide with two neutral atoms to form a molecular ion in three-body collision process. Electrons may now collide with this molecular ion causing dissociative recombination. The product of this process will, in general, be an excited atom. Under most discharge situations, this recombination process is not balanced by an ionization process, such as associative ionization. The result is a flow of excitation from the ionization continuum downward to one of the lower excited states of the atom. This is followed by electron impact excitation to the ionization continuum. Models built from this group of

processes can be used to describe the role of multistep ionization in high energy density electrical discharges, such as may be encountered in diffuse discharge opening switches.

The lower diagram in Fig. 6 shows representative excited state populations as a function of the electron energy of the excited state. The dashed curves represent lines with a slope appropriate to the electron temperature. It is only the lower and very highly excited states for which the population ratios follow the electron temperature. An important result of this model is a description of the ionization process in terms of the density of atoms in the lowest excited state in the loop shown in Fig. 6 and in terms of the electron and positive ion densities and the electron temperature. Such results are more conveniently expressed in terms of the collision-recombination coefficient or a three-body electron-ion recombination coefficient rather than in terms of the ionization coefficient because of the slower variation of the recombination coefficient with electron temperature. Figure 7 shows the results of such calculations.<sup>19,20</sup> The dashed curve and the points show calculated collisional-recombination coefficients for a hydrogen-like atom as a function of electron temperature. The calculations are shown for a number of lower excited states considered in the loop of Fig. 6. The solid line at the bottom of the diagram shows a representative collisional recombination coefficient in which neutral atoms are the third body.<sup>19</sup>

We now turn briefly to the subject of electron impact ionization of excited molecules. Very little information is available on this subject. Recently Armentrout, et al.<sup>21</sup> have measured the cross section for the electron impact ionization of nitrogen molecules in the  $A^3\Sigma$  state. These results are found to be in approximate agreement with theoretical calculations of the same quantity.

## V. GAS HEATING BY ELECTRON COLLISION PROCESSES

In this section we review the available data on electron impact heating of gases. The review is very short because data are available only for nitrogen and air. Figure 8 shows the plot of experimental data obtained by a number of authors,<sup>22-25</sup> primarily Russians. The lowest dashed curve in this figure shows the results of theoretical calculations of rotational excitation by Engelhardt, Phelps and Risk,<sup>26</sup> which have been used in most analyses of the subject. The solid curve shows the results of calculations using the cross section set of Pitchford and Phelps.<sup>6</sup> The upper dashed curve shows the results of our, as yet incomplete, calculations in which the cross sections for the rotational excitation of the nitrogen molecule were increased by a factor of two. Napartovich et al.<sup>24</sup> report calculations using theoretical rotational excitation cross sections of Oksyuk<sup>27</sup> which agree well with experiment at  $E/N$  near  $3 \times 10^{-20} \text{ V m}^2$ , but which increase too rapidly as  $E/N$  is decreased. The portion of the solid curve for  $E/N$  electric field to gas density ratios below  $5 \times 10^{-20} \text{ V m}^2$  represents gas heating via rotational excitation of the nitrogen molecule. The portion of this curve at higher  $E/N$  is caused by electronic excitation of the nitrogen molecule and subsequent collisional deexcitation of the excited molecules. One set of similar data has been published for the heating of air by electrons.<sup>28</sup> The values are much larger than we calculate using the available information for electron impact excitation of rotational levels of nitrogen<sup>6</sup> and oxygen.<sup>29</sup> One possible explanation is that the experimental data actually apply to moist air, although the contrary is stated in the publication.<sup>28</sup>

## VI. SUMMARY

We have presented the very brief summary of electron impact data relative to diffuse discharge opening switches. The data set that we have cited for the nitrogen molecule is an example of the rather complete set of information currently available for that gas. Unfortunately, very few data are available for most gases, for example,  $\text{CH}_4$ . Many more experiments using the various techniques of electron scattering and of electron transport measurements are necessary in order to provide the information necessary for the design and optimization of discharge switches.



## References

1. For a very recent analysis of total and elastic collision cross sections see M. Hayashi, Institute of Plasma Physics, Nagoya University, Report IPPJ-AM-19, November 1981.
2. See for example, H. J. Blaauw, R. W. Wagenaar, D. H. Barends and F. J. de Heer, J. Phys. B 13, 359 (1980); G. Dalba, P. Fomasini, R. Grisenti, G. Ranieri and A. Zecca, J. Phys. B 13, 4695 (1980); R. E. Kennerly, Phys. Rev. A 21 1876 (1980).
3. See for example, T. W. Shyn and G. R. Carigan, Phys. Rev. A 22, 923 (1980).
4. M. E. Riley, C. J. MacCallum, and F. Biggs, At. Data Nucl. Data Tables 15, 443 (1975); D. J. Strickland, D. L. Book, T. P. Coffey, and J. A. Fedder, J. Geophys. Res. 81, 2755 (1976).
5. D. Rapp and P. Englander-Golden, J. Chem. Phys. 43, 1464 (1965).
6. L. C. Pitchford and A. V. Phelps, 34th Gaseous Electronics Conf., Boston, Mass., Oct. 1981.
7. S. K. Srivastava, A. Chutjian, and S. Trajmar, J. Chem. Phys. 64, 1340 (1976).
8. N. E. Padial, D. W. Norcross, and L. A. Collins, Phys. Rev. A (submitted)
9. P. J. Chantry, "Negative Ion Formation in Gas Lasers," in Applied Atomic Collision Physics Vol. 3, Gas Lasers, ed. W. L. Nighan (Academic, New York, 1982), Chap. 5.
10. J. Dutton, J. Phys. Chem. Ref. Data, 4, 577 (1975).
11. T. F. O'Malley, Phys. Rev. 155, 59 (1967).
12. W. R. Henderson, W. L. Fite, and R. T. Brackmann, Phys. Rev. 183, 157 (1969).
13. M. Allan and S. F. Wong, J. Chem. Phys. 74, 1687 (1981).

14. H. Ebinghaus, K. Kraus, W. Müller-Duysing, and H. Neuert, Z. Naturforsch. 19a, 732 (1964); M. V. Kurepa, V. M. Pejčev and I. M. Čadež, J. Phys. D 9, 481 (1976); D. K. Davies, J. Appl. Phys. 47, 1920 (1976).
15. L. G. Christophorou and R. P. Blaustein, Chem. Phys. Letters 12, 173 (1971).
16. B. L. Moiseiwitsch and S. J. Smith, Rev. Mod. Phys. 40, 238 (1968).
17. W. Lotz, Z. Physik 216, 241 (1968) and ibid 232, 101 (1970). See also, E. J. McGuire, Phys. Rev. A 16, 73 (1977).
18. L. J. Kieffer, JILA Information Center Report 13, University of Colorado, September 1971.
19. For reviews of collisional-radiative recombination, see for example, L. M. Biberman, V. S. Vorob'ev and I. P. Yakubov, Usp. Fiz. Nauk 128, 233 (1979) [Sov. Phys. Usp. 22, 411 (1979)].
20. T. Fujimoto, I. Sugiyama, and K. Fukuda, Memoirs of Faculty of Engineering, Kyoto University, 34-2, 249 (1972); S. Byron, R. C. Stabler and P. I. Bortz, Phys. Rev. Lett. 8, 376 (1962).
21. P. B. Armentrout, S. M. Tarr, A. Dori and R. S. Freund, J. Chem. Phys. 75, 2786 (1981).
22. A. K. Kosoruchkina, Zh. Tekh. Fiz. 45, 1077 (1975) [Sov. Phys. Tech. Phys. 20, 676 (1976)].
23. F. E. C. Culick, P. I. Shen, and W. S. Griffin, IEEE J. Quantum Electron. QE-12, 566 (1976).
24. A. P. Napartovich, V. G. Naumov, V. M. Shashov, Dokl. Akad. Nauk SSSR 232, 570 (1977) [Sov. Phys. Dokl. 22, 35 (1977)].
25. J. I. Londer, L. P. Menahin, and K. N. Ulyanov, J. Physique C7, 29 (1979).

26. A. G. Engelhardt, A. V. Phelps and C. G. Risk, Phys. Rev. 135, A1566 (1964).
27. Yu. D. Oksyuk, Zh. Eksp. Teor. Fiz. 49, 1261 (1965) [Sov. Phys.-JETP 22, 873 (1966)].
28. A. P. Napartovich, V. G. Naumov, and V. M. Shashov, Fiz. Plazmy 5, 194 (1979) [Sov. J. Plasma Phys. 5, 111 (1979)].
29. S. A. Lawton and A. V. Phelps, J. Chem. Phys. 69, 1055 (1978).

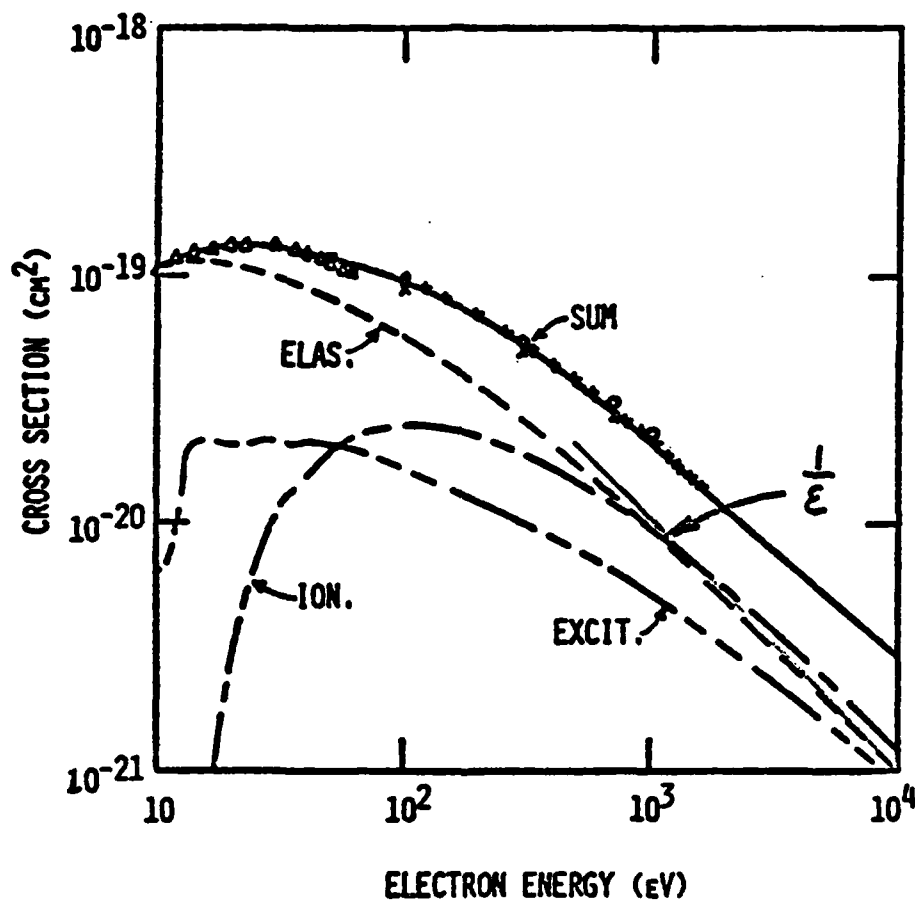


Fig. 1. Total cross sections for electron collisions with  $N_2$ . The solid curve is sum of the total cross sections for elastic, excitation and ionization collisions as shown by the dashed curves.

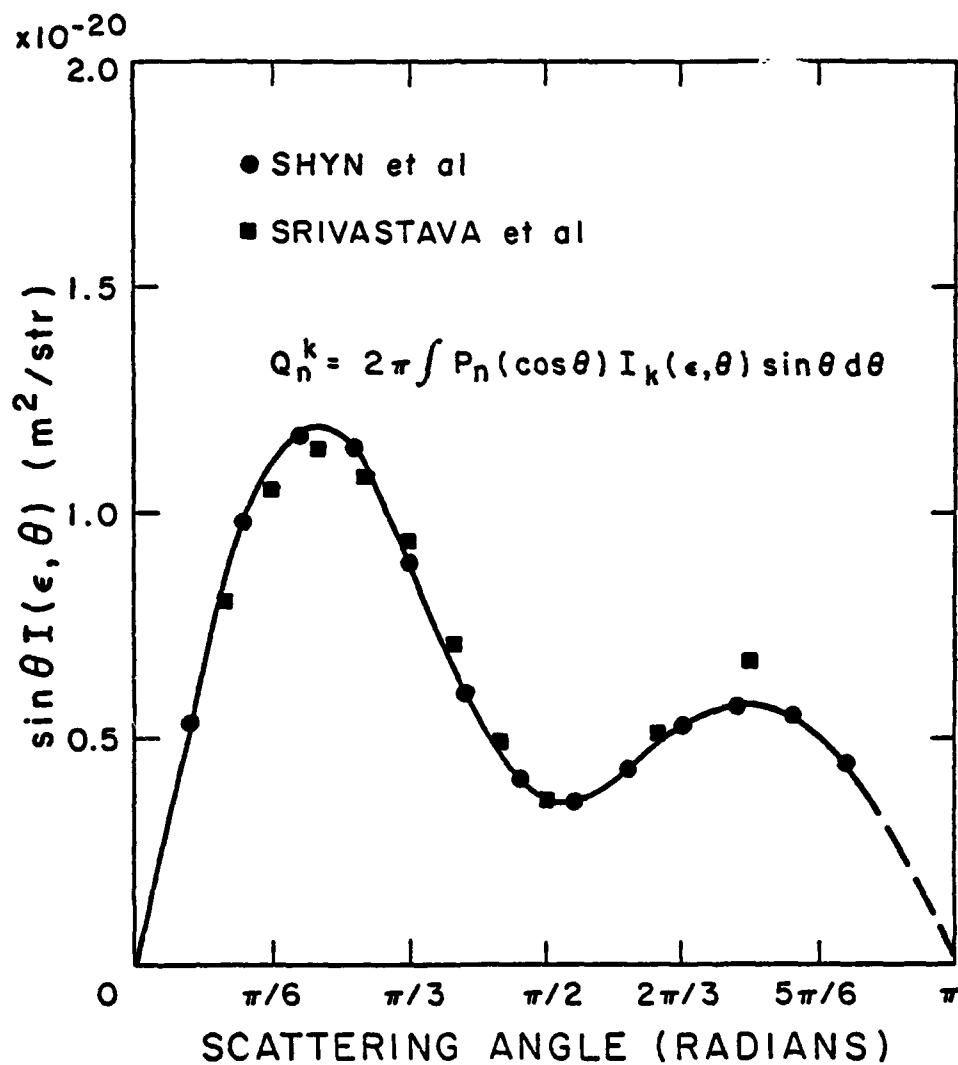


Fig. 2. Weighted differential elastic scattering cross sections for 10 eV electrons in  $N_2$ .

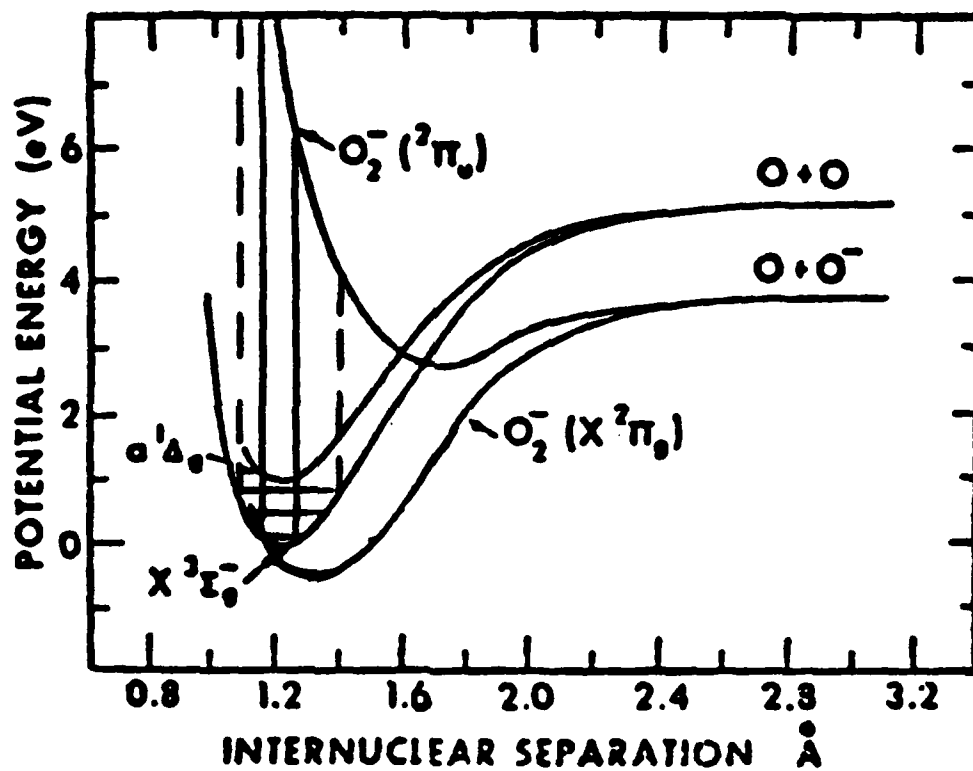


Fig. 3. Potential energy curves for the oxygen molecule showing the  $X^3\Sigma_g^+$  and  $a^1\Delta_g$  states of  $O_2$  and the  $X^2\Pi_g$  and  $^2\Pi_u$  states of  $O_2^-$ .

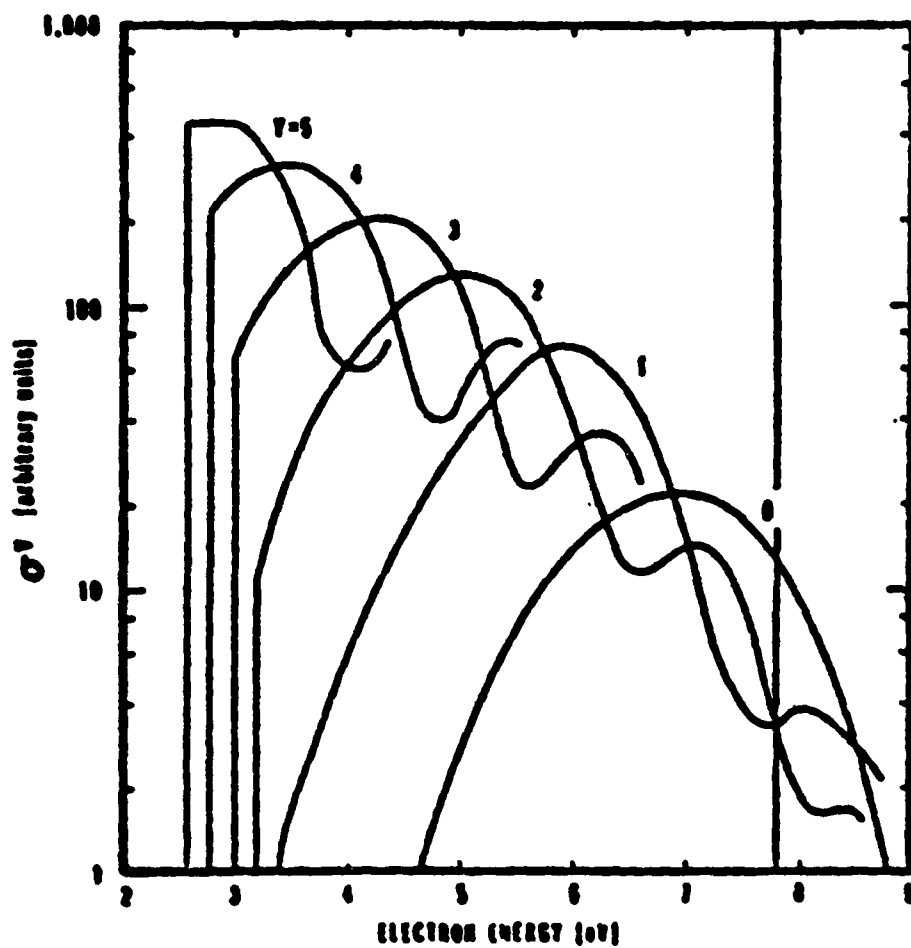


Fig. 4. Calculated dissociative attachment cross sections for various vibrational states of  $O_2$ . From O'Malley.<sup>11</sup>

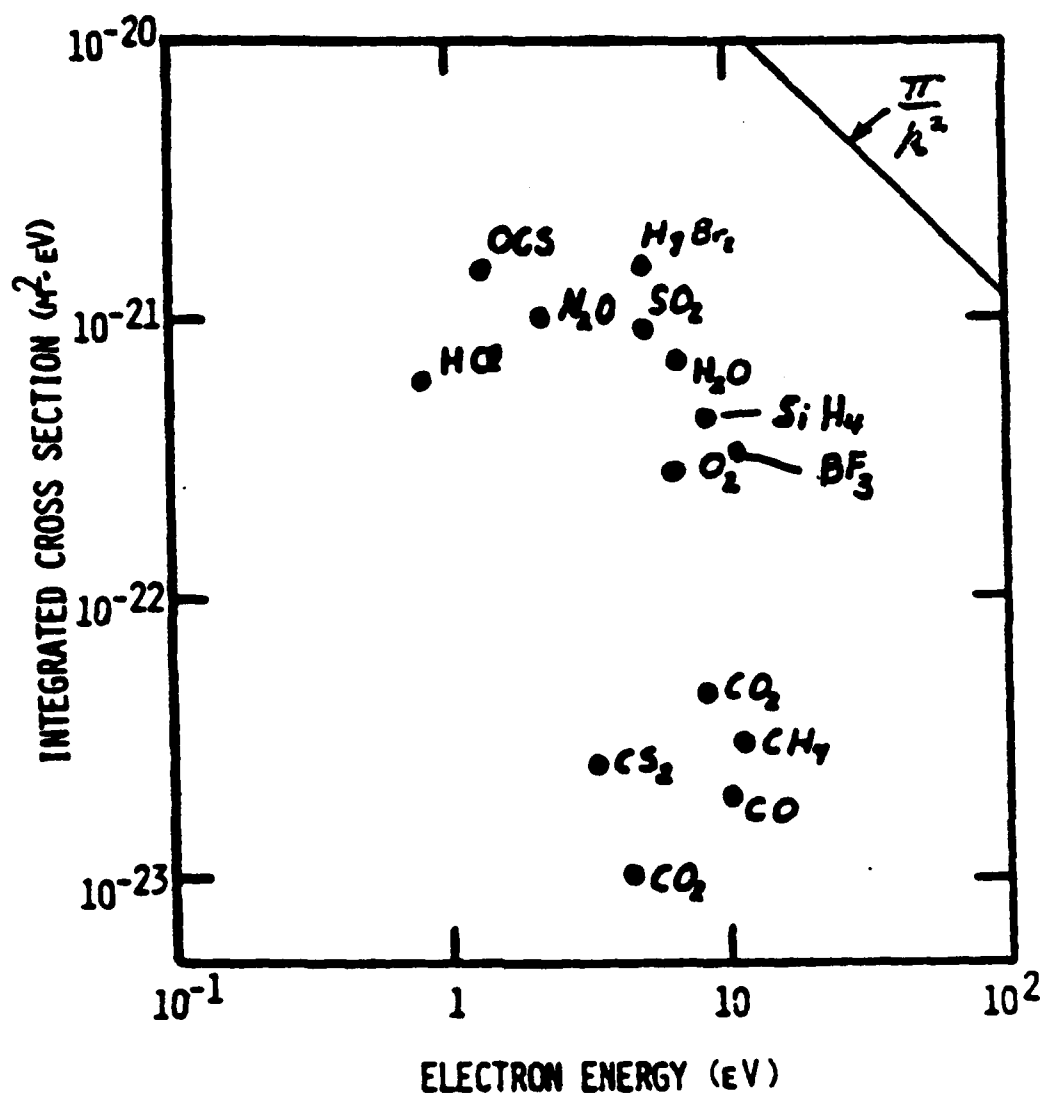


Fig. 5. Integrated dissociative attachment cross sections for various gases of potential usefulness in diffuse discharge opening switches.



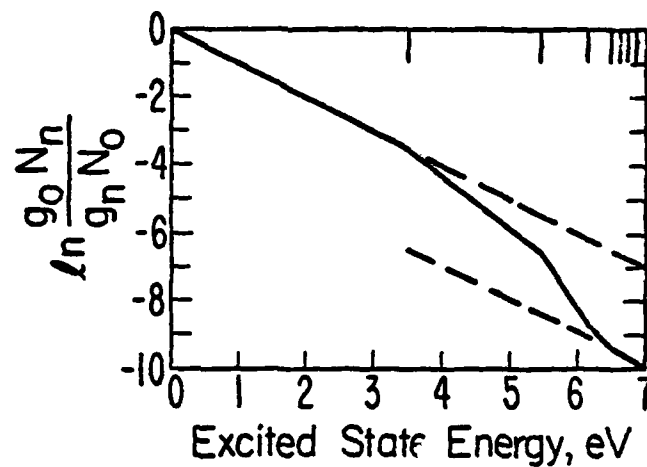
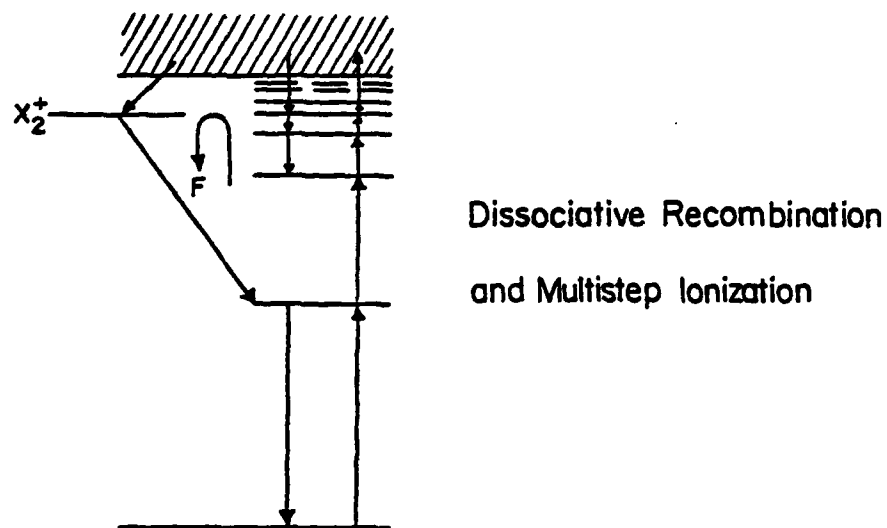


Fig. 6. Representative multistep ionization problem. Top: Schematic of energy levels of atom showing excitation, deexcitation, ionization and collisional recombination via the excited states and dissociative recombination via the molecular ion. Bottom: schematic of relative excited state populations given by model.

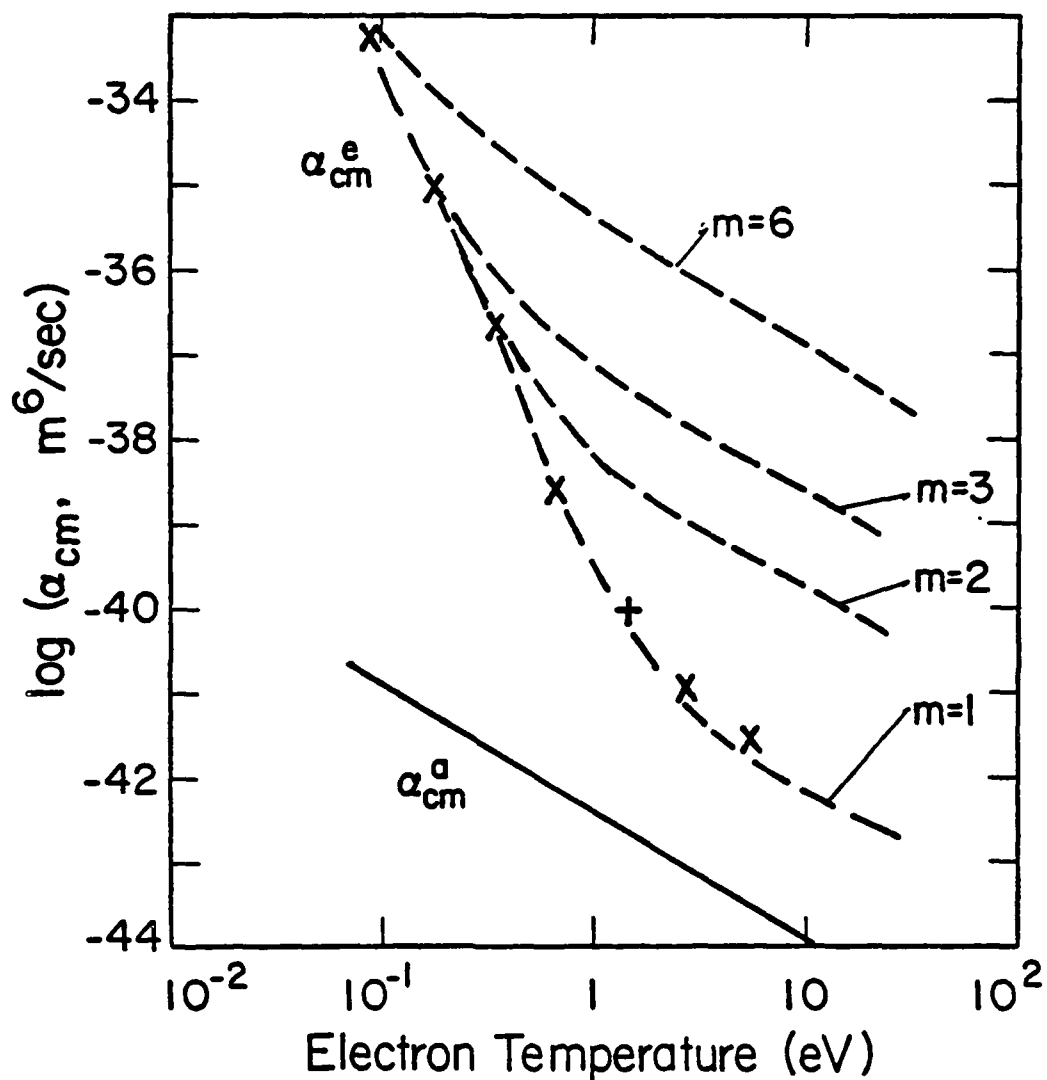


Fig. 7. Collisional electron-ion recombination coefficients for electrons as the third body  $\alpha_{cm}^e$  and for atoms as the third body  $\alpha_{cm}^a$ . Here  $m$  is the principal quantum number of the lowest excited state of the hydrogen-like atom used in the model of multistep ionization.

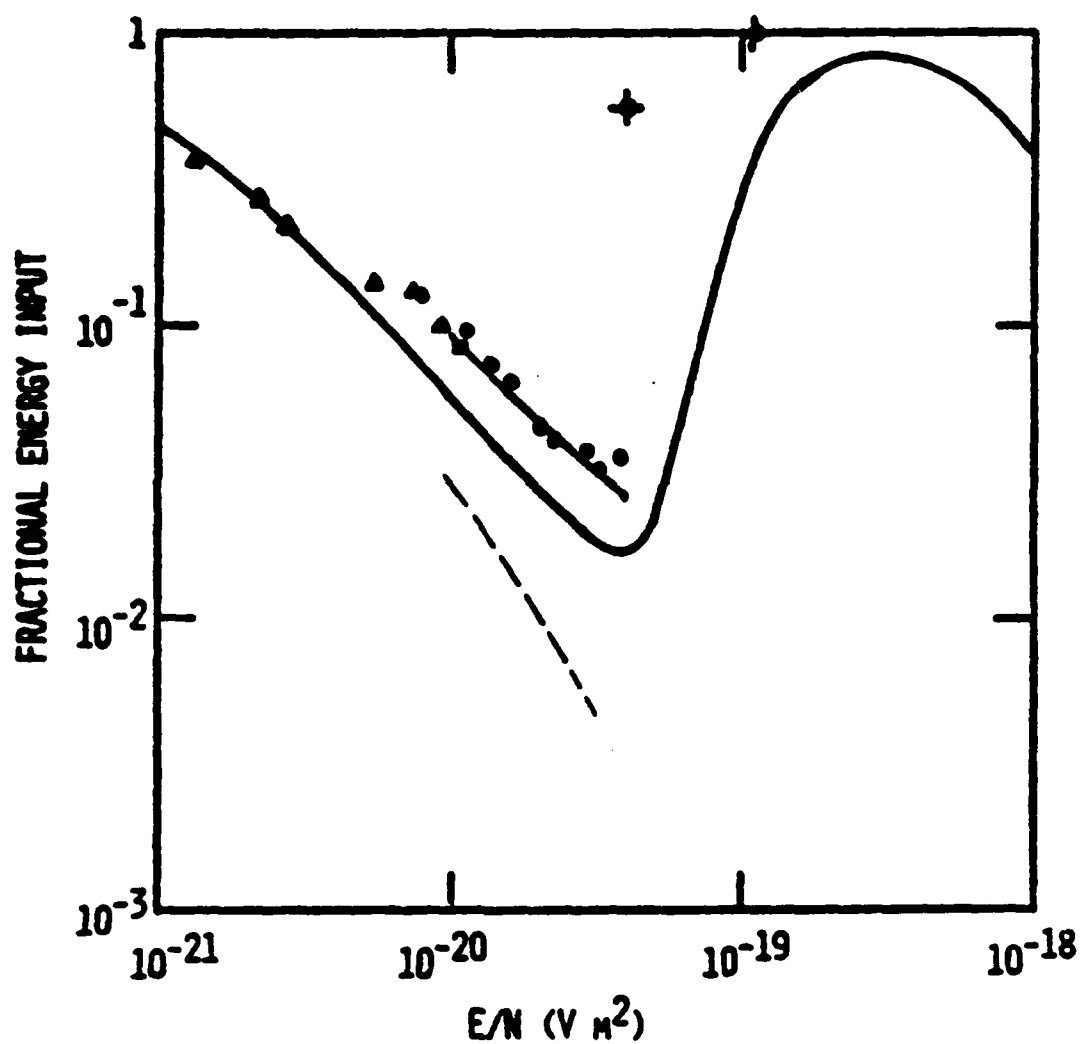


Fig. 8. Fractional energy input to short-time gas heating for electrons in  $N_2$ . The points are experimental data from: +, Ref. 22;  $\blacksquare$ , Ref. 23;  $\bullet$ , Ref. 24;  $\blacktriangle$ , Ref. 25. The smooth curves are calculated values as discussed in the text.

## ARCS vs DIFFUSE DISCHARGES

Alan Garscadden  
 AFWAL/POOC-3  
 Aero Propulsion Laboratory/Energy Conversion Branch  
 Air Force Wright Aeronautical Laboratories  
 Wright-Patterson Air Force Base OH 45433

The purpose of these notes is to answer the question - why diffuse discharge opening switches, that is, why use a diffuse discharge instead of an arc discharge as an opening switch in the context of external optical - or electron beam - control?

First of all, let's define terms. A diffuse discharge is defined as an extended volume non-equilibrium discharge. If externally sustained, e.g. by an electron beam, the ideal diffuse glow discharge has a positive current - voltage characteristic. After sufficient voltage has been applied to establish the electrode sheath conditions the slope of this characteristic depends on the external ionization source. The discharge is in a non-equilibrium state in that the "electron temperature"\* > vibrational temperature > gas temperature.

Arc discharges are of several types (Tables 1 & 2). The name has not been applied consistently so that there are variations in the implied conditions by different authors. However the arc discharge under most situations will have a negative differential current-voltage characteristic. At low pressures the electron gas is not in equilibrium with the gas translational energy and the term arc discharge seems to originate from the condition of small cathode fall of potential<sup>(2)</sup>. More modern usage restricts the use of

---

\* Here "electron temperature" is defined in the generalized sense<sup>(1)</sup>

$$T_e (E/N) \equiv \frac{2}{3} \bar{u} = \frac{2}{3} \int_0^{\infty} u^{3/2} f(u, E/N) du.$$

The vibrational temperature is defined in a similar manner where the distribution function describes the population of the vibrational levels.

arc to the condition that the discharge must have nearly equal electron and heavy particle temperatures (Local Thermodynamic Equilibrium - LTE). We will follow this latter definition.

A classic resource on arc physics is the chapter by Finkelnburg and Maecker in the 1956 Handbuch der Physik 22. From a simplified electron kinetic approach and energy conservation equation, they derive the relationship between the electron temperature and the gas temperature shown in Table 3. When these are applied to a high current argon arc, the results obtained are given in Table 4. It is noted that the assumed condition of LTE in such an arc is satisfied to within a few percent. The electron energy equilibration time is very fast.

Arc discharges have been used as circuit interceptors for many years.<sup>(3)</sup> The principles that have been employed to cool and deionize the gas are

- 1) lengthening the column
- 2) gas blasts
- 3) surface deionization
- 4) high gas pressure or vacuum
- 5) fluid action
- 6) magnetic field blowout

These principles are used singly or in combination in circuit breakers.

Experimenters studying the glow discharge  $\text{CO}_2$  laser noticed that substantial impedance changes occurred during the change from lasing to non-lasing<sup>(4)</sup>. A favorite question was "does lasing heat up or cool the gas"<sup>(5)</sup>. For certain circuit conditions and gas flow it is possible to arrange that the interruption of lasing will switch the discharge off.

AD-A115 883

BATTELLE COLUMBUS LABS OH  
WORKSHOP ON DIFFUSE DISCHARGE OPENING SWITCHES (JANUARY 13-15, --ETC(U)  
APR 82 M KRISTIANSEN, K H SCHOENBACH

F/G 9/5

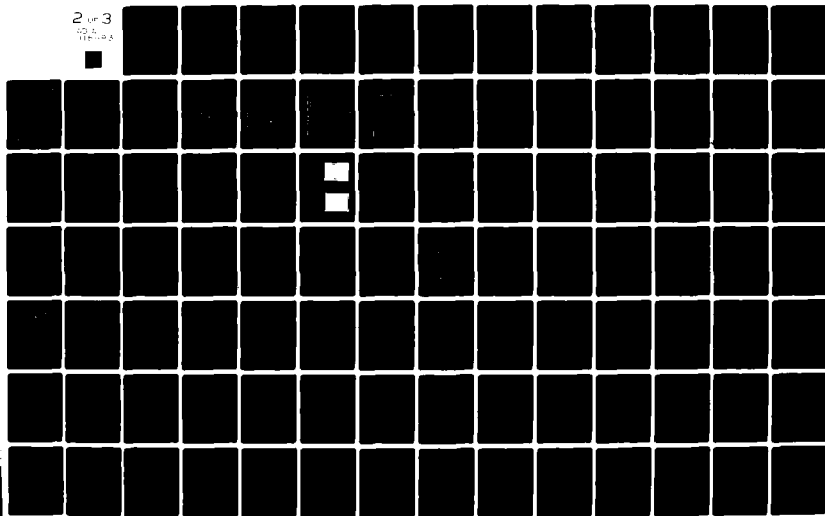
DAA629-81-D-0100

NL

UNCLASSIFIED

2 of 3

AD-A115 883



The requirements for optical or electron beam control of an arc discharge are considerably more demanding than for a glow discharge. It is in concept possible to consider alteration of the discharge characteristic so that the load-line of the ballast resistor no longer intercepts the discharge characteristic. The perturbation required to achieve this would be substantial. In the arc itself, current densities are estimated<sup>(6,7)</sup> to approach  $10^3$  amperes  $\text{cm}^{-2}$  at an electric field of  $10 \text{ kV cm}^{-1}$  in hydrogen. The direct ionization pump rate in this high current atmospheric arc is of the order of  $10^{23} \text{ cm}^{-3} \text{ sec}^{-1}$ <sup>(7)</sup>. To have an external electron beam ionization source compete with this rate would require e-beam ionization power of the order  $10^5 \text{ watts cm}^{-3}$  (for a molecular gas mixture similar to  $\text{He-N}_2\text{-CO}_2$ ). This is a large value to achieve for any extended duration. For switch-off of an arc it is not sufficient to make an instantaneous perturbation as there is an energy reservoir at the same initial temperature comprised of the excited states and translational energy of the gas.

Collisions of the second kind are the coupling mechanism back to the electrons. The gas thermal decay time is then the time constant for decay of the ionization. This is the reason for the use of the macroscopic methods previously listed for arc interruption. The Kauffman criterion for stability of an arc discharge also determines its operational point (Figure 1). This indicates that the external ballast resistor  $R$  must be greater than the differential negative resistance of the arc discharge for this perturbation method to apply. The circuit resistance of the discharge is about the same value. This typically means that the switch cannot be more than 50% efficient even if an optical source or e-beam source can meet the perturbation power requirements. It is noted that these considerations are derived from a pertur-

bation of a steady-state condition. A full time dependent analysis for a pulsed discharge needs to be developed. Thus, while arc discharges can be used as circuit interrupters their disadvantages are the long time to switch-off and also their lifetime which seems to be limited principally by electrode erosion.<sup>(8)</sup> An excellent review of the vacuum arc switch is the paper<sup>(9)</sup> "The Interruption of Vacuum Arcs at High DC Voltages" by A. S. Gilmour and D. L. Lockwood (State University of New York at Buffalo) in 1975.

Opto-galvanic effects with reasonable efficiencies can be found at lower gas pressures.<sup>(11,12)</sup> J. Lawler<sup>(10)</sup> has made a detailed analysis of the laser induced depletion of metastable atoms (helium, and more recently neon). It appears that the switch efficiency comments apply to the low pressure glow discharges also. While the current densities in individual tubes can be quite large, the total current is usually limited to less than an ampere. It is true that optical galvanic effects can be found with reasonable efficiencies. Van den Hoek and Visser<sup>(11)</sup> determined that impedance changes per unit absorbed power in a modest current arc in mercury were  $1.6 \times 10^{-5}$  ohms/milliwatt ( $\lambda = 577$  nm, absorbed power = 20%) and in a sodium arc were  $0.2 \times 10^{-5}$  ohms/milliwatt ( $\lambda = 568.8$  nm, absorbed power > 95%). Here there is also the requirement of achieving control of currents of sufficiently large magnitude to be of interest. If one goes to larger fractional ionization, the electron-electron interaction assumes control and the laser has to compete with rather high electron impact rates that repopulate the perturbed levels. If one tries to get around this by using many discharges in parallel, then each discharge has to be very individually ballasted and the laser illumination has to be very carefully controlled to avoid runaway by one discharge. If, for economic reasons the discharges use a common cold cathode, Emeleus<sup>(13)</sup> (Figs. 2 & 3) has demonstrated that such discharges in parallel require very



exacting identical running and perturbing conditions.

For arcs within the same vacuum chamber, Harry and Knight<sup>(14)</sup> have shown that simultaneous operation from one power supply can be achieved if ballast resistances are included at all electrodes. These resistances must have values approximating the arc differential resistance. While this degrades the switch efficiency in principle, in practice quite low values of ballast resistance are found to be adequate. There does not seem to have been a serious attempt to exploit the astable nature of coupled arcs as a switching device. One might gain the advantage by using the very rapid increase in impedance of one arc rather than having to concentrate on reducing the impedance of the first arc. This comment neglects the eventual problem of circuit interruption after a pulse train of such relaxation oscillations. Even in a low pressure arc the collisional relaxation times are quite short.<sup>(11,12)</sup> The excitation and ionization time is estimated to be  $< 10^{-6}$  secs and the thermal conduction time of the heavy particles is estimated as  $\sim 10^{-4}$  secs. Thus to permit deionization and energy relaxation the perturbation should be on for several times the longest time constant (even for these modest arcs at a few amperes and tens of volts) to prevent the arc re-igniting.

In general, as recognized by Schoenbach et.al.<sup>(15)</sup> for optical control of an opening switch to be effective, some method is needed whereby there is a feedback by the discharge of a process initiated by the incoherent light source or laser. Thus, if the laser triggers dissociation producing an attaching species and the electron impact dissociation rate is an increasing function of  $E/N$  such that the attachment rate at high  $E/N$  is greater than the ionization rate, then the conductivity of the discharge decreases. It has been suggested that an infra-red laser could be used to excite higher

vibrational levels ( $V = 1, 2$ ) of HCl and that the markedly higher dissociative attachment cross-sections for these levels would produce lower conductivity. We point out that the electron impact vibrational excitation of the  $V = 1$  level is reasonably efficient at low electron energies and that the threshold for dissociative attachment decreases with the increase in vibrational level, thus favoring lower energy electrons and low  $E/N$  to increase the attachment rate rather than the increase in  $E/N$  anticipated at current interruption.

The distributed electron beam sustained discharge<sup>(16)</sup> typically uses an ionization rate of  $10^{16} - 10^{19}$  ionizations  $\text{cm}^{-3} \text{sec}^{-1}$ . This requires an ionization power of  $10^{-1} \rightarrow 10^2$  watts  $\text{cm}^{-3}$ . These values are within contemporary e-beam technology. The limitations on the e-beam power are mainly determined by the maximum foil heating permissible (Fig. 4). The e-beam energy is preferably greater than 150 kV. The e-beam energy influences the aperture that can be used in another way. There is a limitation to the total scaling of the e-beam aperture and hence the switch current. This is the influence of the intrinsic magnetic field of the plasma current on the energy and current-voltage characteristics of the externally sustained discharge.<sup>(17,18)</sup> The effect is physically illustrated in Fig. 5. This leads to the relationship between the maximum aperture area and current density product as a function of e-beam energy illustrated in Fig. 6 (after Hsia et.al.<sup>(17)</sup>). Note that the principal effect is on the beam electrons and that the effect on the plasma electrons is small due to their low mobility ( $\mu_e H/c \ll 1$ ). This criterion (Fig. 6) was developed for the optical homogeneity of visible lasers and it is probably too severe. However, it is indicative of the currents at which inhomogeneities in a pulsed discharge are inherent and may, with other combined effects, lead to arcing. Of course a compensating magnetic field can be applied,

however, the switch is becoming more complex and the energy/maintenance costs are significant even with state-of-the-art superconducting fields.

The e-beam sustained discharge can be made reasonably homogeneous below this total current value, provided that the introduction of electrophilic species does not cause the attachment instability<sup>(16)</sup> and the frequently associated glow-to-arc transition.

The electron beam controlled switch scales easier in voltages than in current because at higher current densities the recombination losses become significant. It is advantageous to use a gas or gas mixture with a high drift velocity at low  $E/N$ . One way to achieve this is to use a gas with a Ramsauer minimum in the momentum transfer cross-section (actually, the requirement is a steeply increasing momentum transfer cross-section with increasing electron energy, but one usually implies the other) and an inelastic loss process at low electron energy. Thus gas mixtures such as  $N_2$ -Ar qualify or a single gas such as  $CH_4$  has the desired properties. Such an e-beam switch does work at low switch currents (P. Bletzinger, these proceedings), however in order to satisfy the switch-off time constant requirements, it is usually necessary to add an attaching gas. This adds losses to the on-condition and may complicate the plasma chemistry, especially for high repetition rate operation. Operation of such switches at currents competitive to thyatron capabilities has yet to be demonstrated. The addition of optical control to an e-beam controlled discharge is quite speculative. One can envisage additional vibrational excitation via lasers, however, besides requiring large laser powers, it has to compete with the vibrational-rotational excitation due to electron collisions. Again, if there are excitation thresholds at higher energies that would be accessible to laser control, then it might be possible

to use the laser as a trigger and let the increasing E/N act as a built-in feedback to increase the attachment rate without increasing the discharge ionization rate. Stable appropriate molecules or compounds have not yet been identified and tested. The use of photochemistry or electron impact dissociation to produce macroscopic changes affecting the electron conductivity has not yet been demonstrated. For instance, a very speculative suggestion is to use a compound such as  $\text{SiH}_4$  as a component. It is analogous to  $\text{CH}_4$  and has a very high electron drift velocity. Under intense discharge conditions, it dissociates rapidly and much deposits out as a thin film<sup>19</sup>. The discharge conductivity is predicted to decrease by about a factor of eight for these conditions. There are difficulties with this approach as the amount of gas required is approximately proportional to the current transfer. However discharges under conditions where there is essentially a change of phase seem to offer the potential for the desired macroscopic changes in electronic conductivity within reasonable volumes, and are an attractive basic research area that is relatively unexplored. (see Fig. 7)

# REFERENCES

1. W. L. Nighan, "Stability of High Power Molecular Laser Discharges" in Principles of Laser Plasmas, ed. G. Bekefi, J. Wiley and Sons, New York, (1976).
2. J. H. Ingold, "Anatomy of the Discharge" in Gaseous Electronics, eds. Hirsh and Oskam, Academic Press, New York (1978).
3. J. D. Cobine, "Gaseous Conductors", Dover Publications, Inc., New York, (1958).
4. P. Bletzinger and A. Garscadden, 'Laser Perturbation Measurements in CO<sub>2</sub>-N<sub>2</sub>-He Discharges', Proceedings of Ninth International Conference on Phenomena in Ionized Gases, (1969).
5. The answer is both; which one is measured depends on the observation time. Initially lasing causes a faster vibrational relaxation and so a faster gas heating; however as energy is extracted from the discharge system, the eventual heating is less compared to the non-lasing case.
6. M. C. Cavenor and J. Meyer, Australian J. of Physics, 22, 155 (1969).
7. G. L. Rogoff, Physics of Fluids, 15, 1931 (1972).
8. P. E. Stover, private communication.
9. A. S. Gilmour and D. L. Lockwood, IEEE Transactions on Electron Devices, ED-22, 173 (1975).
10. J. Lawler, paper C-1, 33rd Annual Gaseous Electronics Conference, Oklahoma, 1980.
11. W. J. van den Hoek and J. A. Visser, J. Appl. Phys. 51, 5292 (1980).
12. E. F. Zalewski, R. A. Keller, and R. Englemann, J. Chem. Phys., 70, 1015 (1979).
13. K. G. Emeleus, Phys. Letters, 61A, 391 (1977).
14. J. E. Harry and R. Knight, IEEE Transactions on Plasma Science, PS-9, 248 (1981).
15. K. H. Schoenbach, G. Schafer, E. E. Kunhardt, M. Kristiansen, L. L. Hatfield and A. H. Guenther, Proceedings of the Third International Pulsed Power Conference, Albuquerque, NM (1981).
16. J. D. Daugherty "Electron Beam Ionized Lasers" in "Principles of Laser Plasmas", editor G. Bekefi, Wiley-Interscience, New York, (1976).

17. J. C. Hsia, J. H. Jacob, J. A. Mangano and M. Rokni, DARPA Semi Annual Report, Feb. 1977-Aug. 1977. (AVCO Everett Research Laboratory).
18. V. V. Vladimirov, V. N. Gorshkov and A. I. Shchedrin, Sov. J. Quantum Electronics 11, 18 (1981).
19. B. Drevillon, J. Huc, A. Lloret, J. Perrin, G. deRosny and J. P. M. Schmitt, Appl. Phys. Letters 37, 646 (1980).

Table 1

## ARC DISCHARGES

- (a) THERMIONIC ARC IN WHICH THE CATHODE IS HEATED BY AN EXTERNAL SOURCE AND THE ARC IS NOT SELF-MAINTAINING
- (b) THERMIONIC ARC IN WHICH THE CATHODE IS HEATED BY THE DISCHARGE AND THE ARC IS SELF-MAINTAINING
- (c) FIELD EMISSION ARC IN WHICH THE ELECTRON CURRENT AT THE CATHODE IS DUE TO A VERY HIGH ELECTRIC FIELD AT THE CATHODE SURFACE
- (d) METAL ARCS MOST COMMONLY MERCURY
- (e) HOLLOW CATHODE ARCS IN WHICH THE GAS IS FED THROUGH THE CATHODE AND CONTINUOUSLY PUMPED

Table 2

## ARC DISCHARGES

CHARACTERIZED AS DISCHARGES THAT CARRY TENS TO THOUSANDS OF AMPERES AND WHERE THE VOLTAGE DROP ACROSS THE DISCHARGE IS TENS OF VOLTS

ARCS ARE USUALLY CLASSIFIED BY THE EMISSION PROCESS THAT OCCURS AT THE CATHODE, AND BY THE GAS PRESSURE



Table 3

## FINKELNBURG &amp; MAECHKER

$$\text{ENERGY EQUATION} \quad \frac{3}{2} k (T_e - T_g) \frac{2 m_e n_e}{m_s \tau_{es}} = e n_e b_e E^2$$

$$\text{COLLISION TIME} \quad \tau_{es} = \frac{1}{v_e (\eta_0 Q_{eo} + n_i Q_{ei})}$$

$$\left( \frac{T_e T_g}{T_e} \right) = \frac{m_s}{4m_e} \left( \frac{\lambda_e e E}{\frac{3}{2} k T_e} \right)^2$$

Table 4

## EXAMPLE: HIGH CURRENT ARGON ARC

$$E = 13 \text{ VOLTS cm}^{-1} \quad \lambda_e = (\sum_k n_k Q_{ek})^{-1} = 3 \times 10^{-4} \text{ cm}$$

$$\frac{m_A}{m_e} = 7 \times 10^4$$

$$T = 30,000 \text{ } ^\circ\text{K}$$

$$\frac{\Delta T}{T} = 2\%$$

$$\tau_R (\text{ELECTRONS}) \leq 10^{-12} \text{ SECS (ROMPE \& WEIZEL)}$$

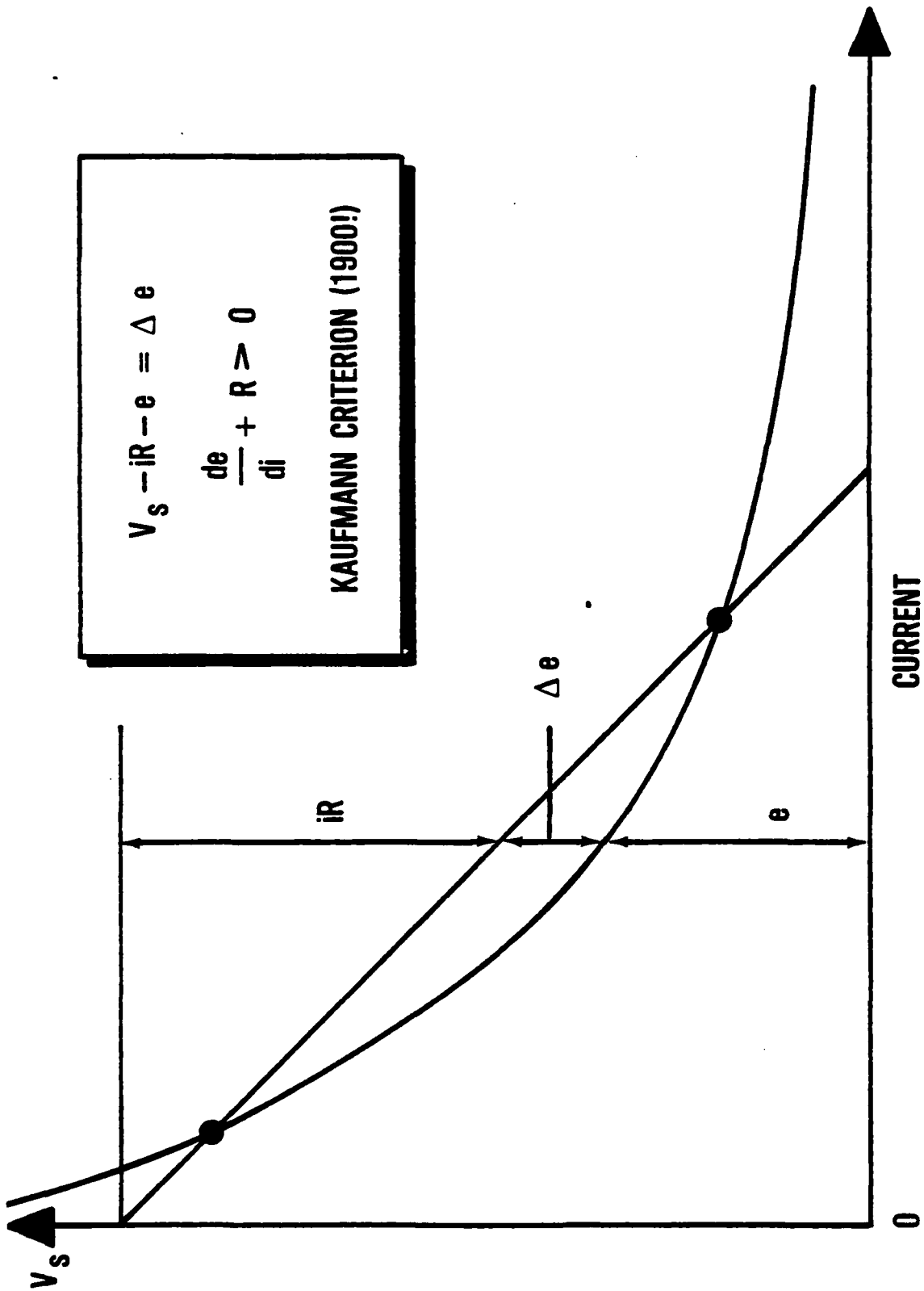
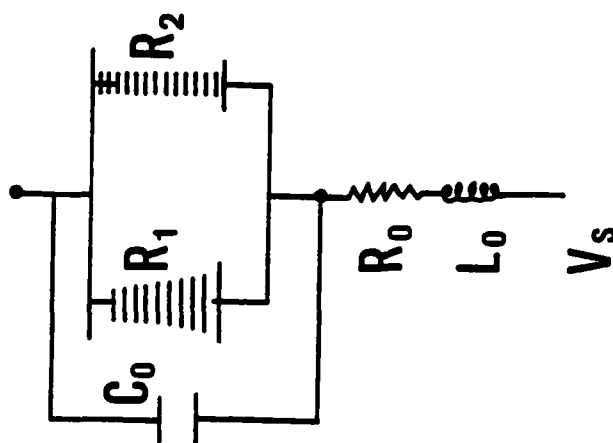


Fig. 1

# TRANSVERSE INHOMOGENEITY (EMELEUS 1978)



FOR STABILITY

$$\frac{1}{R_0} + \frac{f_1 S}{r_1} - \frac{(1 - f_1) S}{r_2} < 0$$

SUBNORMAL DISCHARGE  $R_2 = - \frac{r_2}{(1 - f_1) S}$

ABNORMAL DISCHARGE  $R_1 = \frac{r_1}{f_1 S}$

$f_1$  = FRACTION OF CATHODE SURFACE COVERED BY CATHODE GLOW  
 $R_1, R_2$  ARE DIFFERENTIAL RESISTANCES

Fig. 2

G→

REQUIRES BOTH

$$R_0 > \frac{r_2}{(1 - f_1) S}$$

$$\frac{r_1}{f_1 S} > \frac{r_2}{(1 - f_1) S}$$

Fig. 3

64

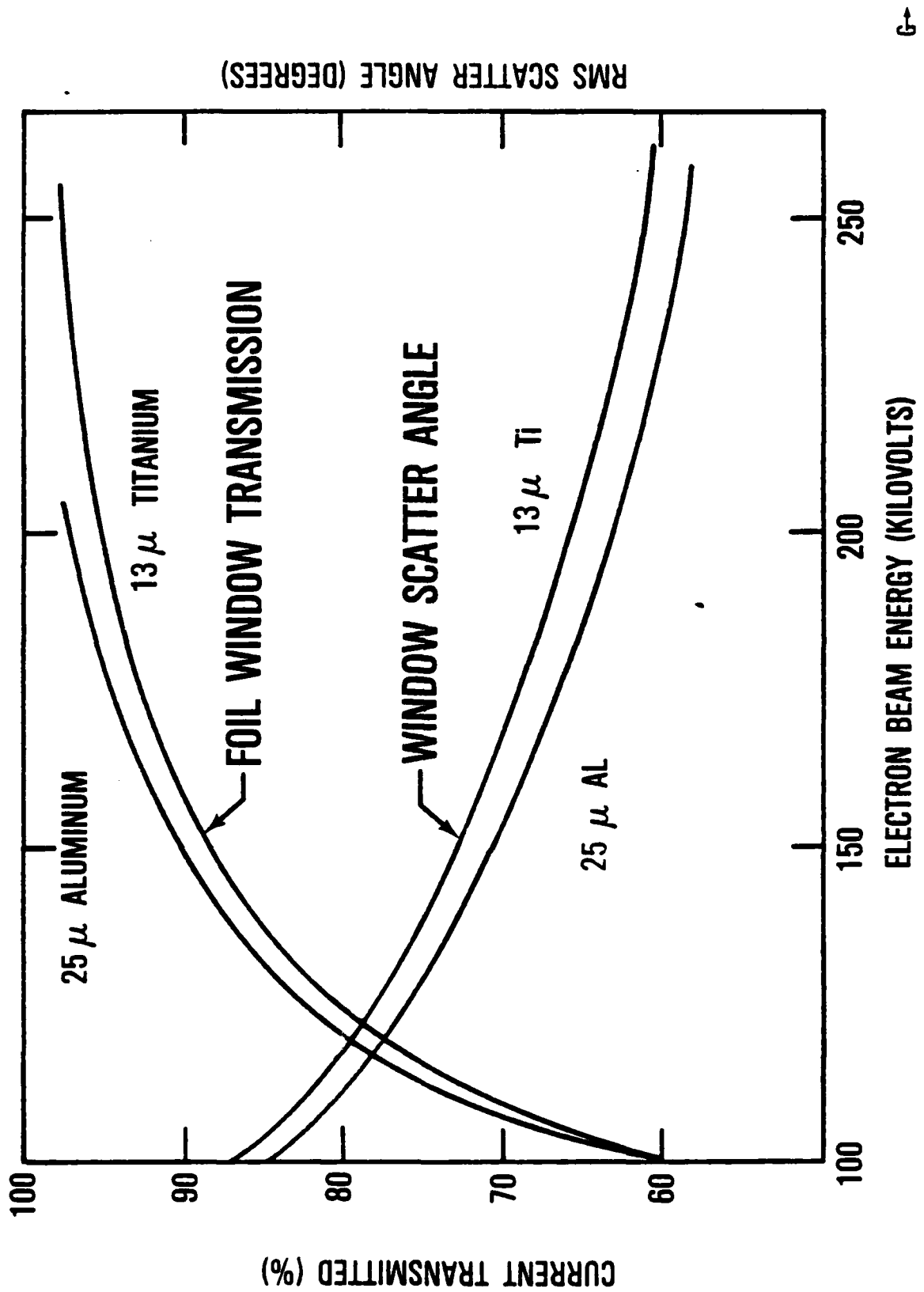


Fig. 4

# E-BEAM PINCHING BY THE MAGNETIC FIELD GENERATED BY THE DISCHARGE CURRENT

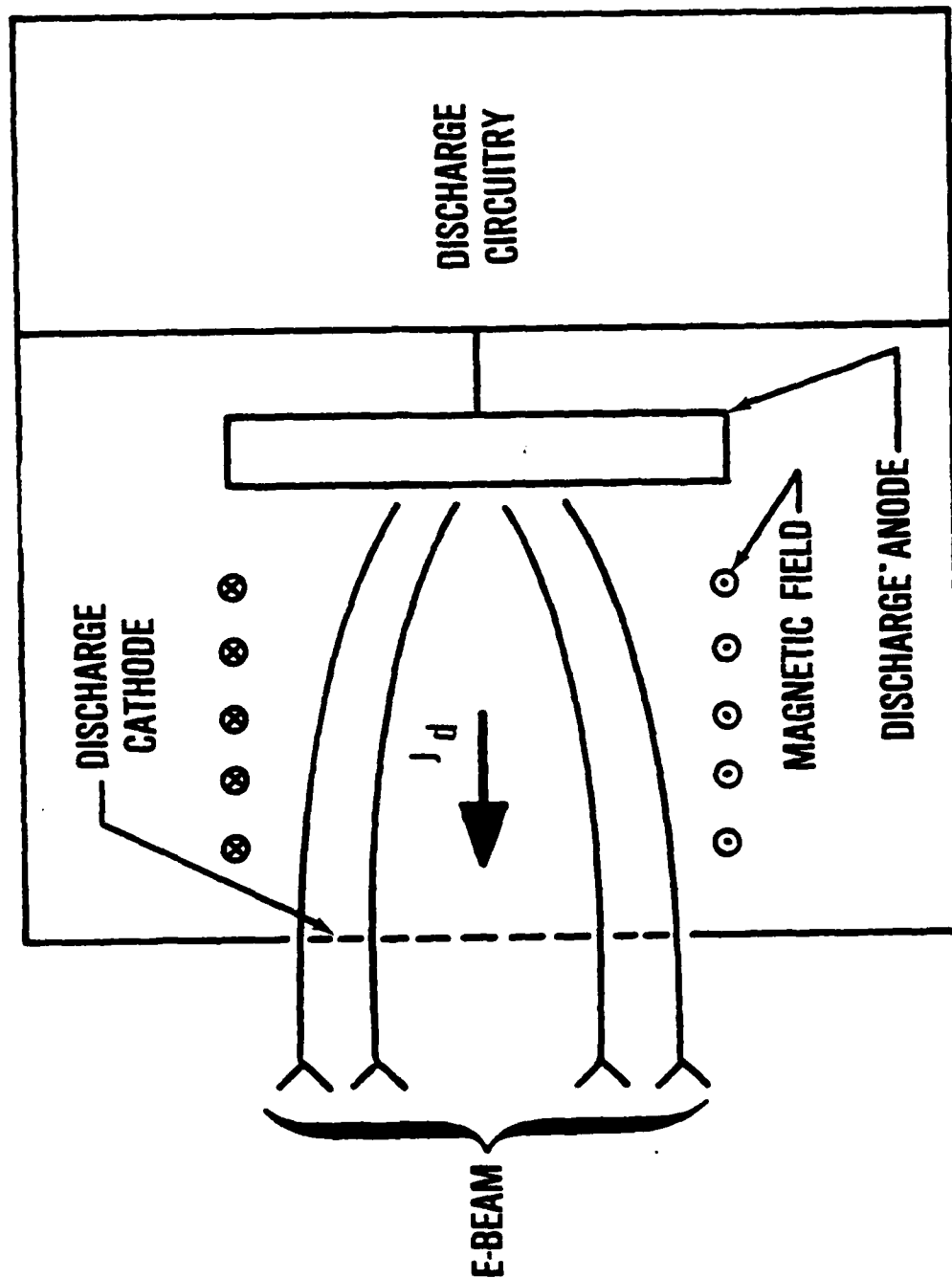


Fig. 5

# MAXIMUM APERTURE AREA AND DISCHARGE CURRENT DENSITY PRODUCT AS A FUNCTION OF E-BEAM ENERGY

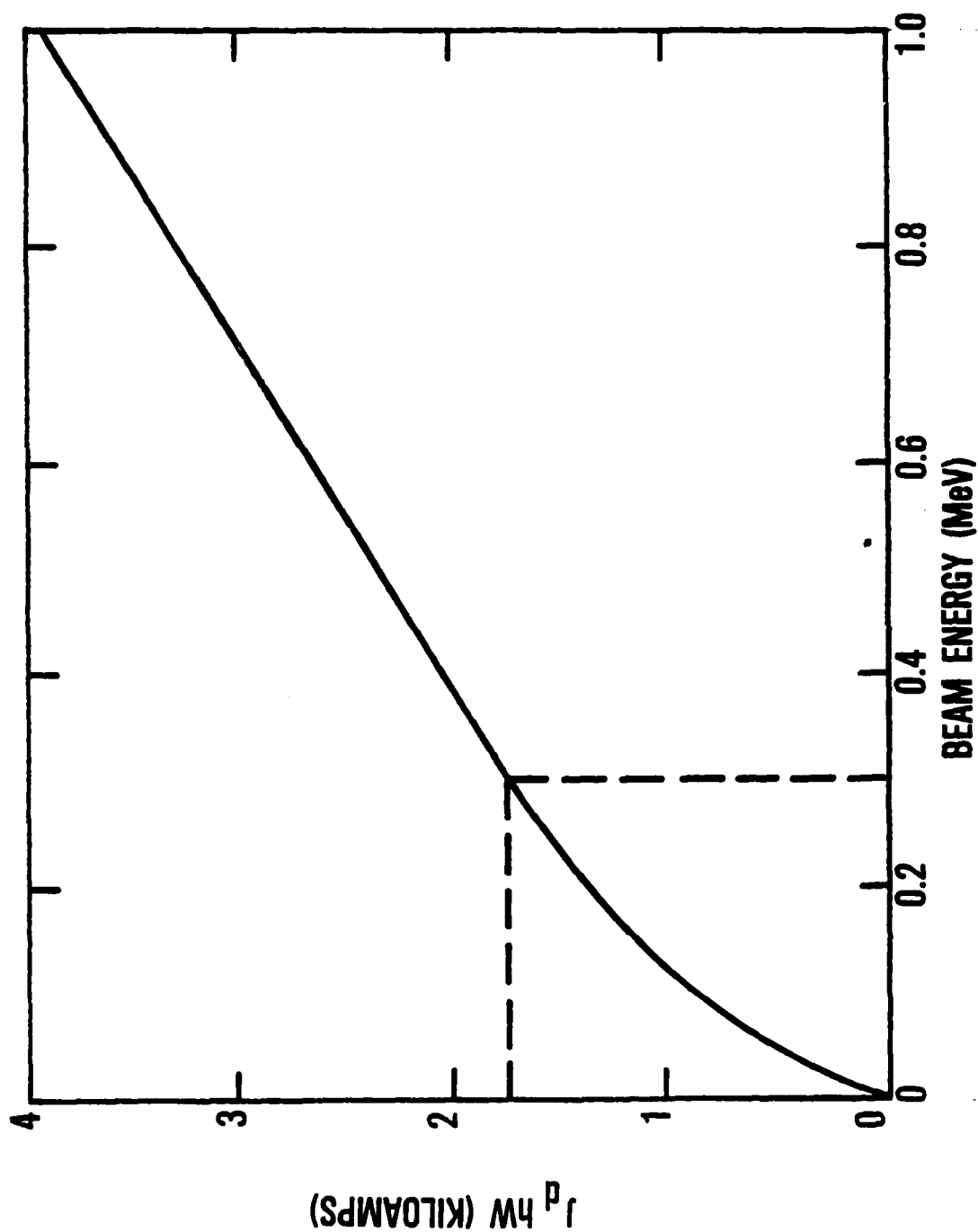


Fig. 6



# DRIFT VELOCITY IN SILANE MIXTURES

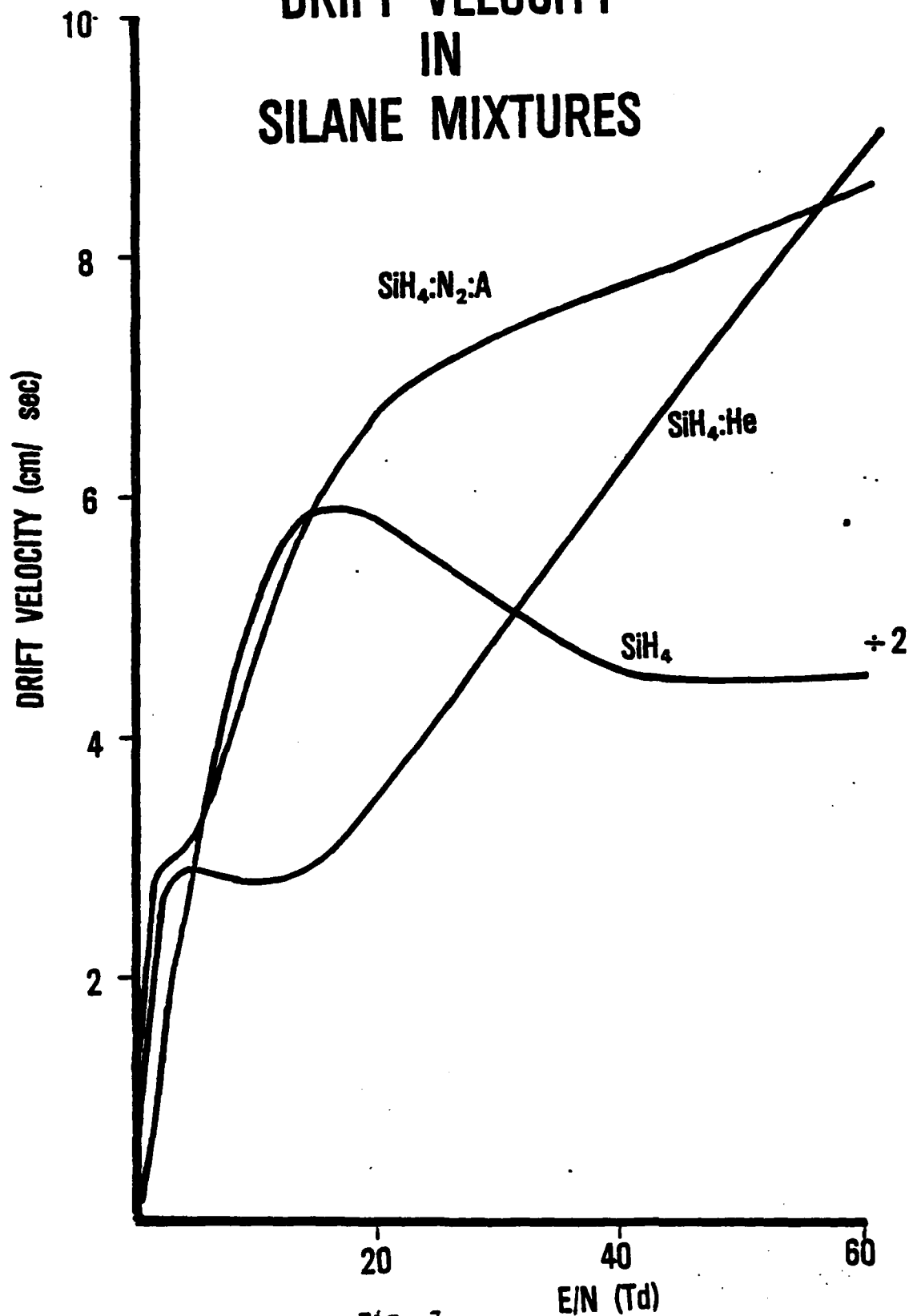


Fig. 7

E-BEAM EXPERIMENTS  
INTERPRETATIONS AND EXTRAPOLATIONS

P. Bletzinger  
AFWAL Propulsion Laboratory

Abstract

A short summary of the theory of externally ionized plasmas using the continuity equation is given and the limitations of some simplifications are noted. A comparison of previous experiments is made. Experimental results using methane as the discharge gas are presented in the form of I-V curves, cathode fall voltages and some temporal waveforms for pulsed discharges. The discharge decay is used to derive effective recombination and attachment rates and this information is used to compute theoretical I-V curves for comparison with the experimental results. Also, the experimental results are extrapolated to higher current densities. In an appendix, calculations of the I-V curves with consideration of the cathode sheath effects are compared with the experiments and the influence of secondary emission and ionization using metastables is demonstrated.

NOTE: Portions of this material have been submitted for publication elsewhere.

## INTRODUCTION

Initial experiments with a small (5 x 15 cm aperture, 1.5 mA/cm<sup>2</sup> max. pulsed beam current after the foil) E-beam ionized discharge system have been reported at the previous ARO workshop. In these measurements, the discharge characteristics in argon were shown to be strongly influenced by additional ionization in the cathode sheath, resulting in a much lower discharge voltage drop and higher conductivity than expected from consideration of the argon drift velocity alone. Unfortunately, argon has a very low breakdown strength for post-discharge arcs (600 V/cm in pure argon in our experiment). The experiments to be reported here were performed in methane, which is known to have a very high drift velocity in the range of reduced electric fields (E/N) of interest for an E-beam controlled switch. As will be shown, methane discharges also have increased conductivity due to cathode sheath effects, although to a lesser degree than argon. Methane's breakdown strength, avoiding post-arcs, was much higher (5KV/cm). Also, due to an unexpected high recombination rate and small attachment rate, the discharge decay (switch-off time) was less than  $3 \cdot 10^{-5}$  sec. Since the E-beam ionized discharge is to be used as a switch element, it is best described by its I-V characteristic and several examples will be shown.

It is felt necessary to first define the discharge by one-dimensional continuity equations and show the approximations which can be made as well as the implications of these approximations. A comparison of published E-beam experiments will be made. The experimental results with our low-current E-gun will be discussed next and a comparison with theory follows. In conclusion, extrapolations of the low current results to higher E-beam and discharge currents will be made.

The E-beam ionized discharge is best described by one-dimensional continuity equations and, if space charge is to be considered, by Poisson's equation. Following (1) we can write for the electron density  $n_e$ :

$$\frac{\partial n_e}{\partial t} = S + n_e a |w| - \alpha n_e n_+ - \frac{\partial j_e}{\partial x} \quad (1)$$

where  $S$  is the source function (ion-electron pairs  $\text{sec}^{-1} \text{ cm}^{-3}$ ) which can be obtained for the E-beam parameters from the well-known tables of Berger and Seltzer (2),  $a$  is Townsend's first ionization coefficient,  $w$  the electron drift velocity,  $\alpha$  the recombination coefficient,  $n_+$  is the ion density,  $j_e$  the electron current density (in number of electrons per  $\text{cm}^2$  per sec) and is defined as

$$j_e = n_e w - D \frac{\partial n_e}{\partial x} \quad (2)$$

where  $D$  is the electron diffusion coefficient. If attachment is to be included, then the ionization coefficient can be replaced by a net ionization coefficient which includes the losses by attachment. If we now restrict ourselves to a homogeneous discharge ( $\frac{\partial j_e}{\partial x} = 0$ ) and assume  $n_e = n_+$ , then

$$\frac{dn_e}{dt} = S + n_e a w - \alpha n^2 \quad (3)$$

Equivalent continuity equations can be written for the ions; for the discharge current, the contribution of the ion current is usually neglected because of the much lower ion mobility; therefore the discharge current density is simply

$$j_D = n_e \cdot w \quad (4)$$

For I-V characteristics the steady-state value of  $n_e$  ( $\frac{dn_e}{dt} = 0$ ) can be obtained from eqn. 3, and since for the switch-discharge case the applied electric field is much below the self-breakdown threshold, the ionization term in eqn. 3 can also be set to zero. With no attachment, we then obtain for the electron density

$$n_e = \sqrt{\frac{S}{\alpha}} \quad (5)$$

which, with (4) and the equation for S gives us the ratio of discharge current density to E-beam current density, or the switch gain

$$jD/jB \sim \frac{1}{\sqrt{jB}} \quad (6)$$

If attachment is included, we obtain from the modified eqn. (3) (and  $\frac{dn_e}{dt} = 0$ )

$$n_e = \left(\frac{S}{\alpha} + \frac{\beta^2}{4\alpha^2}\right)^{1/2} - \frac{\beta}{\alpha} \quad (7)$$

where  $\beta$  is the attachment frequency ( $\text{sec}^{-1}$ ). If attachment dominates, then

$$n_e = S/\beta \quad (8)$$

Note that in this case the switch gain is constant.

While these approximations have very much simplified the equation for the discharge current density, they are still very useful since they now allow a first order estimate of the influence of the functional variation of the materials parameters  $\alpha$ ,  $W$  and also  $\beta$  with the reduced electric field  $E/N$  on the I-V characteristics, as has been done by L. Kline (3). As will be shown later, for low E-beam currents and especially for certain gases like argon, the simplified equation (2) is no longer valid and boundary effects will cause noticeable deviations from characteristics derived from the simple theory.

In general, however, the above equations can be used to derive scaling parameters and to interpret reported experimental results. Table I gives a summary of some of the relevant experiments

TABLE I

	NOTES	GAS	$J_B/E_B$	$J_{SWITCH}$	SWITCH GAIN	$\tau_R$ [SEC]	$\tau_F$	$E_{SW}$
Kovalchuk & Mesyats 1971	E-Beam Initiated Patent (71)	$N_2$ 1-16 Atm	1-5 A/cm <sup>2</sup> 100-350KV	2KA/cm <sup>2</sup> MAX	(2000)	delay $10^{-8}$ - $10^{-9}$ $<10^{-6}$ - $10^{-8}$ ?	N/A	700KV MAX
Kovalchuk & Mesyats 1976		$N_2$ 1-3.6 Atm	0.4 A/cm <sup>2</sup>	40A/cm <sup>2</sup>	8-100	delay $>3 \cdot 10^{-7}$ $10^{-6}$ - $10^{-9}$	$10^{-6}$ - $10^{-9}$	175KV
Hunter 1976	Patent (1977)	$CH_4$ 1 Atm	5 A/cm <sup>2</sup> 250KV	27 A/cm <sup>2</sup>	$\sim 5$	$4 \cdot 10^{-7}$	$4 \cdot 10^{-7}$	50KV
McDonald et.al. Texas Tech. 1980	E-Beam Initiated	$N_2$ , $N_2 + Ar$ , $N_2 + SF_6$ 1-3 Atm	110 A/cm <sup>2</sup> 145-280KV	1.6-3.2 KA/cm <sup>2</sup>	(29)	delay 52ns $2.8$ - $3 \cdot 10^{-9}$	N/A	500KV
L. Kline Westinghouse 1980	Theory	$CH_4$ (8 other) 1-3 Atm	5 mA/cm <sup>2</sup>	2.5 A/cm <sup>2</sup>	500-1000	$<1 \cdot 10^{-6}$	$>1 \cdot 10^{-6}$	100KV
Bletzinger AFMIL 1980-81	Pulsed & CW	$N_2$ , Ar, $CH_4$ & Attachers 1 Atm	1.5mA/cm <sup>2</sup> MAX 175KV	1.5 A/cm <sup>2</sup> MAX	1000+	$\geq 1 \cdot 10^{-6}$	$\sim 1 \cdot 10^{-5}$	12KV MAX

EB: E-beam voltage

$\tau_R$ : Risetime of discharge pulse

$\tau_F$ : Falltime of discharge pulse

$E_{SW}$ : Switched discharge voltage

Koval'chuk & Mesyats (1971)<sup>(4)</sup> and McDonald et.al.<sup>(5)</sup>(1980) refer to experiments with electron beam triggered sparkgaps and are listed for comparison only.

As can be seen from the table, the early experiments of Koval'chuk & Mesyats<sup>(6)</sup> and of Hunter<sup>(7)</sup> used large E-beam current densities, resulting in low gain (eqn. 6). Also their guns, derived from laser experiments, were cold cathode types requiring the full E-beam voltage to be switched and therefore resulting in even lower power gain. On the other hand, they achieved very fast risetimes and could afford to work with added attaching gases (impurities) which resulted in fast fall times. Hunter<sup>(7)</sup> recognized the importance of having a gas with a high electron drift velocity and therefore chose methane. As can be seen from Fig. 1, methane has an electron drift velocity peaking at more than  $10^7$  cm/sec. at about 3

Townsend. In actual switch devices the reduced electric field may be somewhat lower and there the addition of argon will slightly increase  $W$  over the value in methane alone (8).

As reported at last year's ARO workshop, we have used a small 5x15 cm aperture E-beam with energy of 175 KeV and maximum peak current

density of  $1.5 \text{ mA/cm}^2$  to test E-beam ionized discharges at low  $j_B$ . At very low

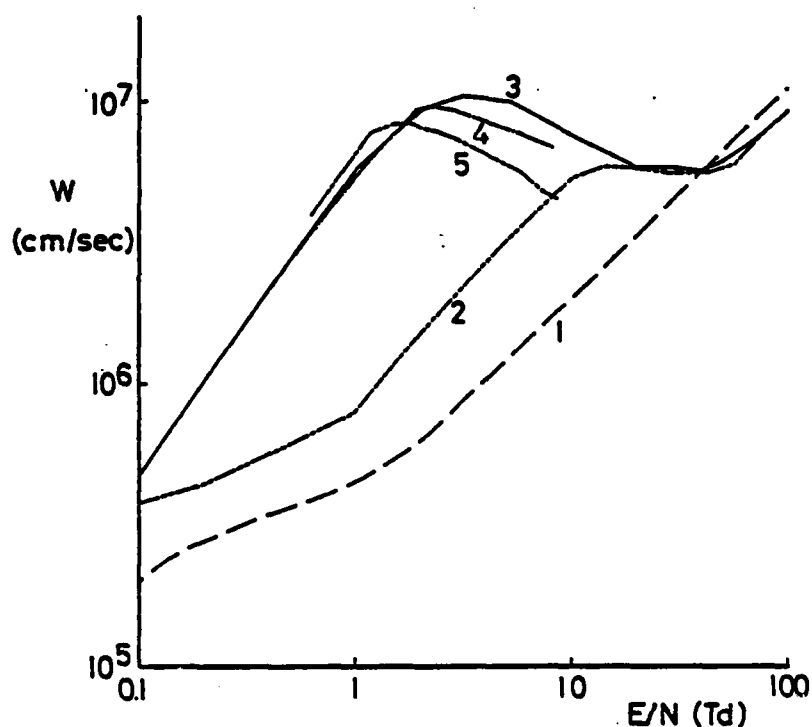


FIG. 1 Electron Drift velocity vs reduced electric field for 1:nitrogen, 2:nitrogen/argon, 3:methane, 4:methane/argon 80:10%, 5:methane/argon 50:50% (1-3 from ref (3), 4 and 5 from ref (7))

(CW) E-beam currents and constant current load ( $R_L \rightarrow \infty$ ), the very nonlinear characteristic of these discharges becomes apparent (Fig. 2).

As shown for the right hand argon curve, the characteristic starts out with a very low conductivity and at a certain electric field switches over to a very high conductivity (impedance 10-20 Ohm for argon). Comparing conductivities of the various gases (including methane, Fig. 3) one finds that there is no correlation between

the conductivity and the drift velocities of these gases in the high conductivity range of the characteristics. In this operating range, ionization in the cathode sheath has a larger influence than ionization by the E-beam. The non-monotonic I-V characteristic has been predicted theoretically by Velikhov et.al. (9), Zakharov et.al. (10) and, in a more consistent manner covering a wider range of discharge parameters by Lowke and Davies (1). Also it has been observed experimentally by Averin et.al. in nitrogen (11). As the

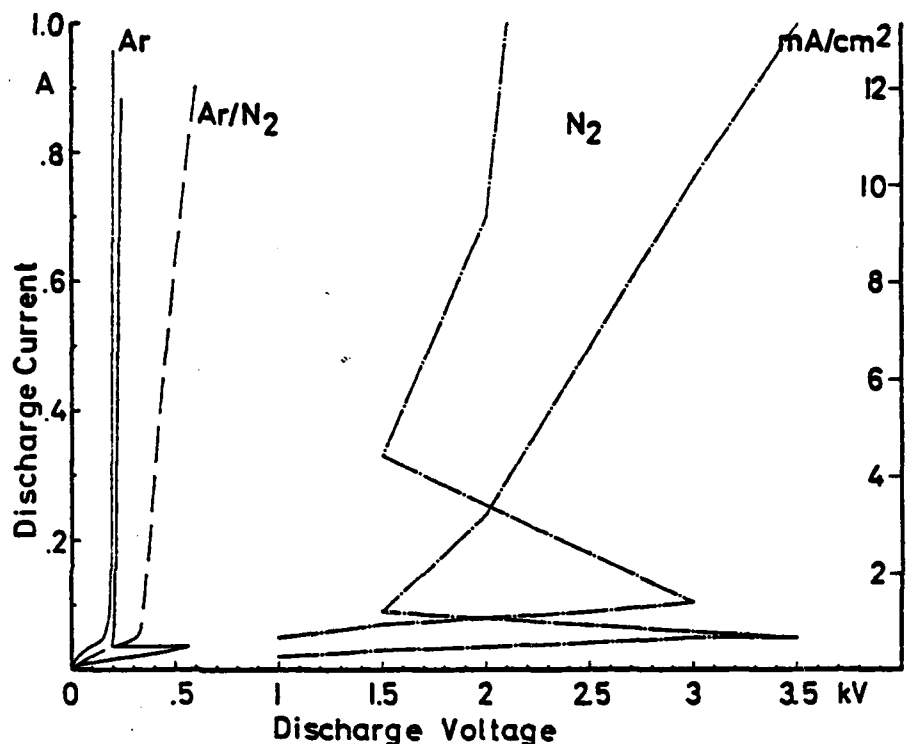


FIG. 2 I-V characteristics at very low (CW current densities,  $j_B$  for these curves (left to right,  $5 \cdot 10^{-5}$ ,  $8 \cdot 10^{-6}$ ,  $2.8 \cdot 10^{-5}$ ,  $2.8 \cdot 10^{-5}$ ,  $9.3 \cdot 10^{-6}$  A/cm<sup>2</sup>). All gases at 760 Torr.



FIG. 3

I-V characteristics for methane (pulsed) R load = 400 Ohm, 760 Torr.

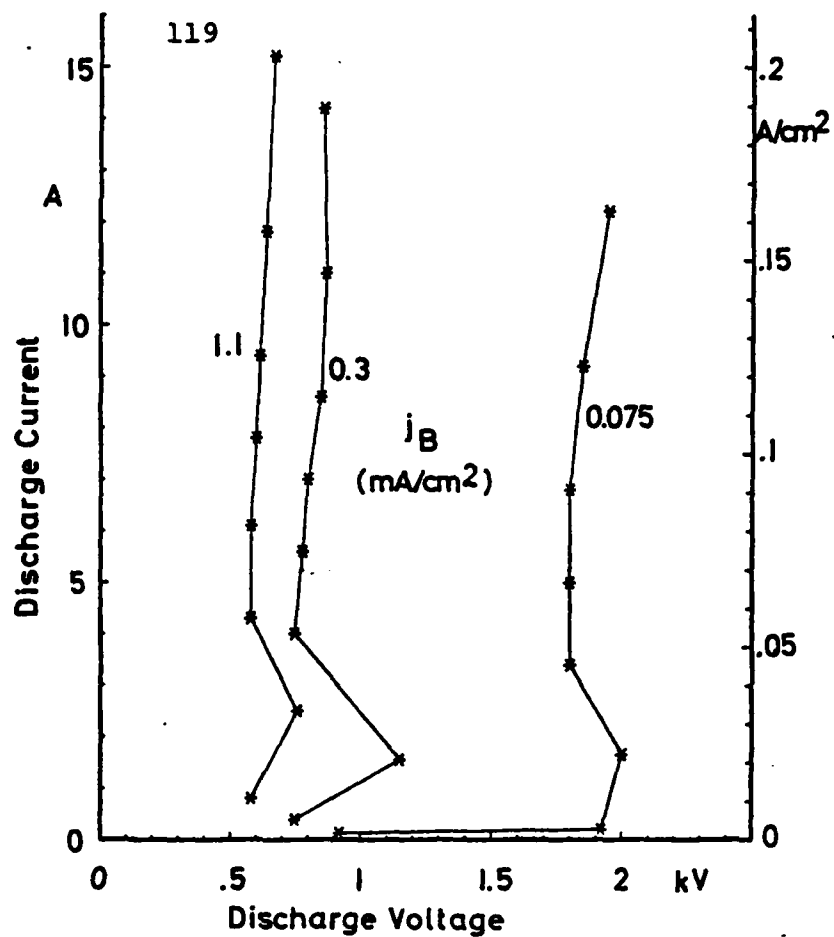
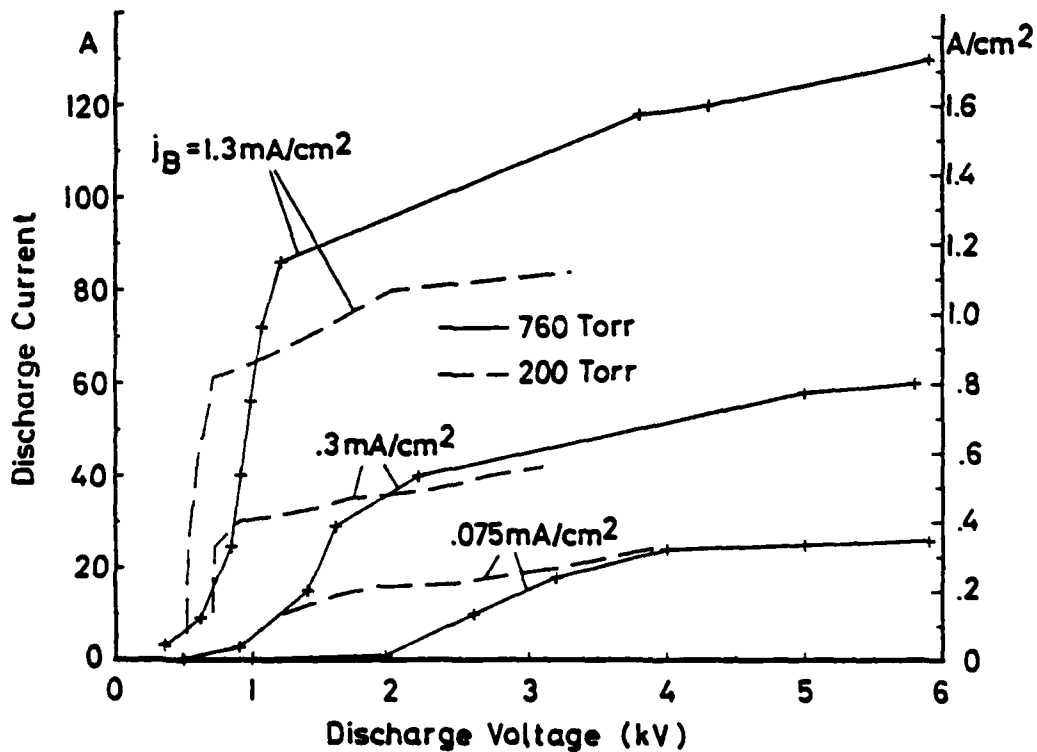


FIG. 4

I-V characteristics for methane (pulsed) R load = 40 Ohm at different pressures



E-beam and discharge current densities are increased using pulsed operation and lower load resistances (Fig. 4), a third regime of the I-V characteristic is observed, where eqn. 5 becomes valid. In Fig. 4 we see that at reduced pressure at lower currents (in the high conductivity regime) the higher E/N causes higher conductivity while at the higher currents, where the cathode sheath effects no longer dominate, the lower source function reduces the conductivity. For efficient operation of a switch, one would however try to operate at the highest current density which is still in the high conductivity-low voltage drop regime and therefore still make use of cathode sheath effects. The dual role of argon when added to methane is illustrated in Fig. 5. In

the high conductivity range it increases conductivity due to its high ionization efficiency and in the third regime by increasing the effective electron drift velocity of the mixture in the E/N range used (See Fig 1.).

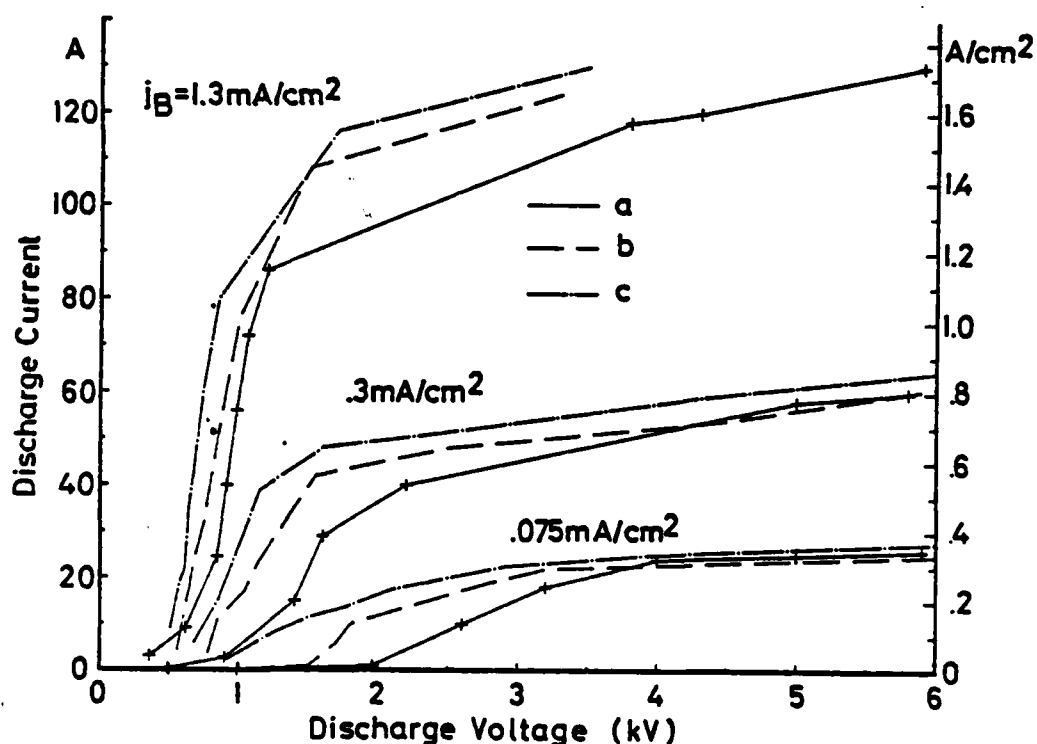


FIG. 5

- a: Methane 760 Torr
- b: Methane + 60 Torr of Argon, 760 Torr total
- c: Methane + 250 Torr of Argon, 760 Torr total

At the high percentages of argon, however, the threshold voltage for post-discharge arcs is lowered. When adding an attaching gas, the conductivity is lowered, as expected (Fig. 6). According to M. A. Biondi (comment at the ARO workshop), the strong effect of water vapor observed could also be caused by a large increase in the recombination coefficient due to the formation of large cluster

ions. The fall time of the discharge current pulse after E-beam switch-off was decreased only with relatively large amounts (10 Torr) of water vapor added.

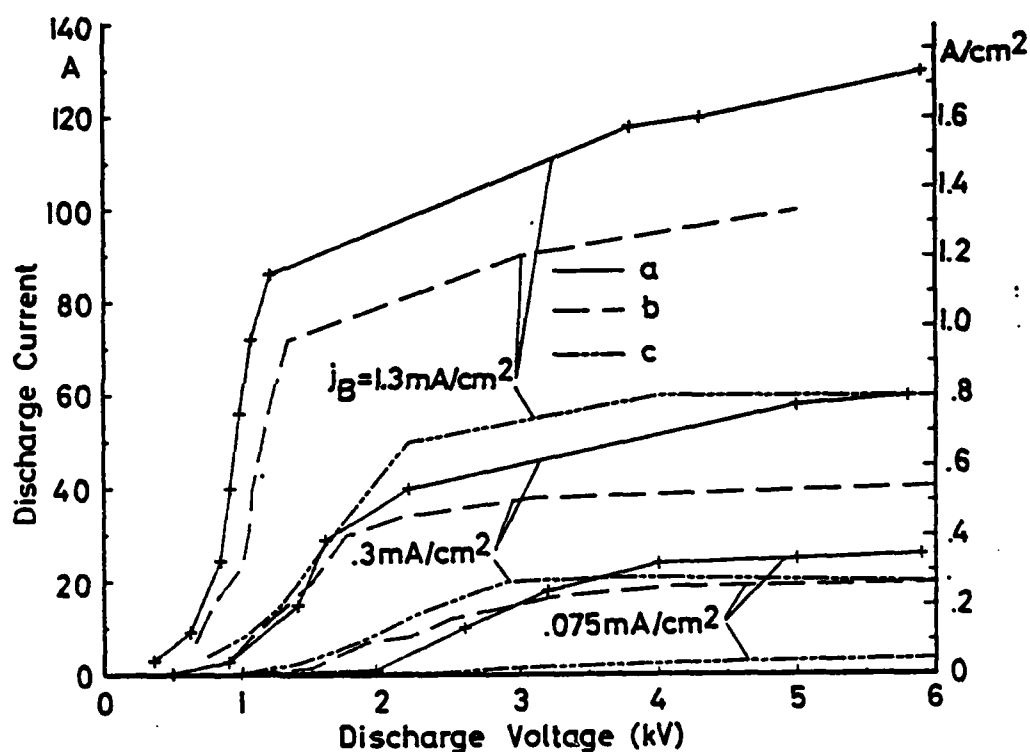


Fig. 6 a: Methane 760 Torr  
b: Methane + 1 Torr H<sub>2</sub>O, 760 Torr total  
c: Methane + 10 Torr H<sub>2</sub>O, 760 Torr total

Another characteristic important for the understanding of discharges is the distribution of the electric field between the electrodes. In particular the voltage drop across the positive column and across the cathode fall are of interest. When changing the position of the movable cathode the linear voltage drop across the positive column can be measured, the extrapolation to

zero electrode distance results in a voltage offset which corresponds to the cathode fall. For these measurements it was assumed that if the current at each distance was held to the same value, then the E/N value also would be the same for each measurement. Fig. 7 shows the cathode fall voltages measured for argon and methane. Note that the cathode fall voltages for each gas are a strong function of E-beam current and have a weaker dependence on discharge currents. In all gases the cathode fall voltages were much larger than the voltage drops per cm in the discharge volume, therefore except for very long discharge paths the cathode fall voltages will represent a major portion of the total discharge voltage. Cathode fall

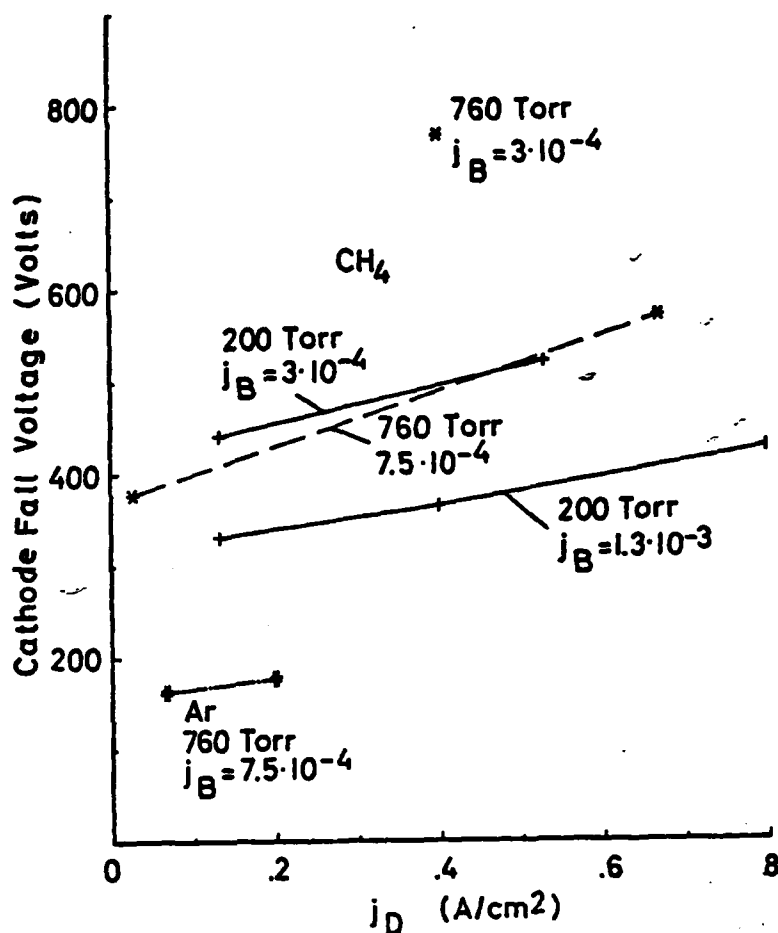


Fig. 7 Cathode fall voltages in methane and argon as a function of  $j_D \cdot j_B$  (A/cm<sup>2</sup>) parameter.

voltages in nitrogen were considerably higher and ranged from 1.1kV for a  $j_b = 7.5 \cdot 10^{-4}$  A/cm<sup>2</sup> to 2kV at  $j_b = 3 \cdot 10^{-4}$  A/cm<sup>2</sup>, both at  $j_d = .2$  A/cm<sup>2</sup>. The reduced electric field in the positive column for argon and methane are shown in Fig. 8 where the E/N values for argon were only in the range of .005 to .023 Td. For nitrogen E/N was measured to be 1.3 and 1.7 Td for the values of  $j_b$  and  $j_d$  listed above.

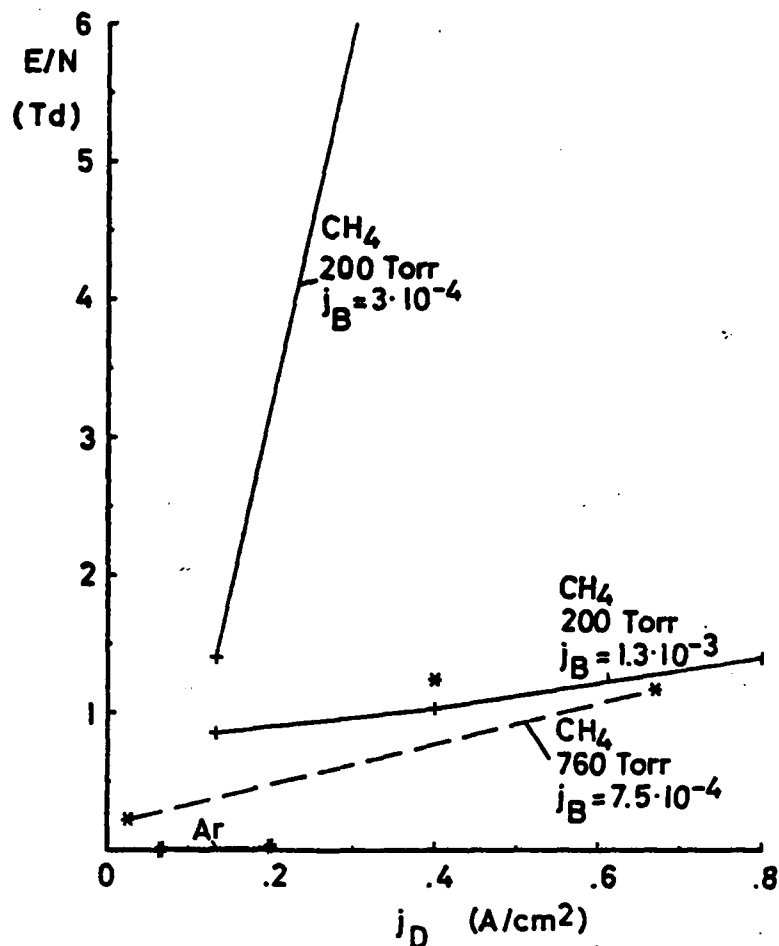


FIG. 8 Reduced electric field in methane and argon discharge as function of  $j_D$ ;  $j_B$  ( $A/cm^2$ ) parameter

Temporal characteristics for methane are shown in Figs. 9a and b. As predicted by theory (12) the risetime is a function of the E-beam current until at the largest currents it is limited by the risetime of the E-beam pulse ( $\sim 1$   $\mu$ sec). The fall time shows a typical recombination dominated behavior and is independent to first order from E-beam current. High frequency oscillations may be caused either by the negative slope in the methane drift velocity, although this would be expected to occur at higher  $E/N$ , or by cathode sheath effects. A careful analysis of the decay of the discharge

Fig. 9a

Discharge Current in  
Methane (760 Torr)  
(5  $\mu\text{sec/div.}$  hori-  
zontal, 10 A/div.  
vertical) E-beam  
current densities  
 $7.5 \cdot 10^{-5}$ ,  $1.5 \cdot 10^{-4}$ ,  
 $3 \cdot 10^{-4}$ ,  $7.5 \cdot 10^{-4}$  A/cm<sup>2</sup>

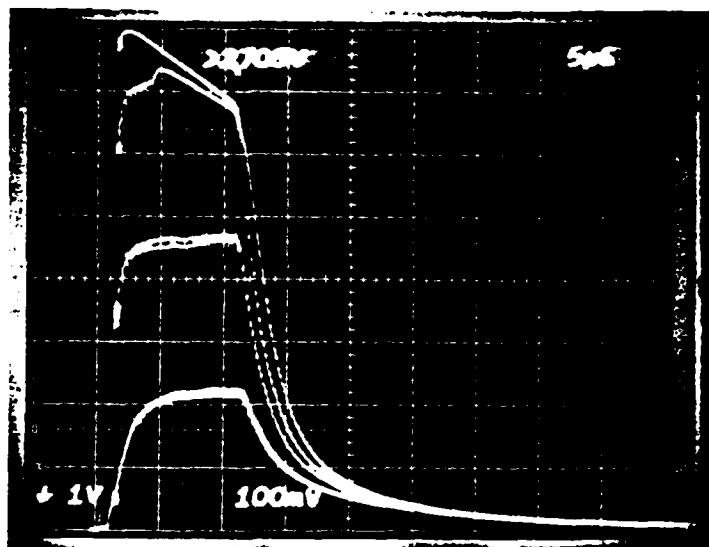
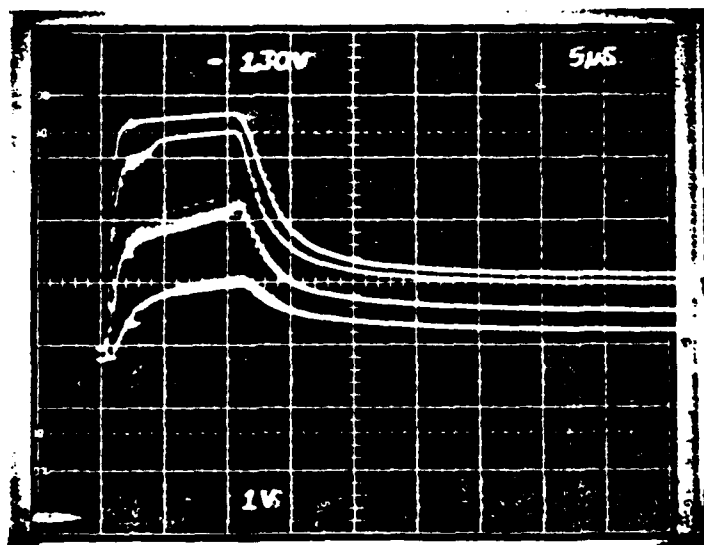


Fig. 9b

Discharge Voltage in  
Methane (760 Torr)  
(5  $\mu\text{sec/division}$   
horizontal, 1 KV/  
division vertical,  
zero voltage at top  
of picture). E-beam  
current densities  
same as Fig. 9a.



current (Fig. 10) allows us to obtain values for the recombination and attachment coefficients. When the recombination data of (3) were increased by a factor of 10 and a small, E/N independent attachment coefficient was added, a very good fit of the experimental data was achieved (Curve a). The effect of using the original recombination data (Curve c) or no attachment (Curve b) is also shown. A less satisfactory fit was obtained by using an E/N independent recombination rate of  $8.3 \cdot 10^{-6} \text{ cm}^3/\text{sec}$  and an attachment frequency of  $1.8 \cdot 10^5 \text{ sec}^{-1}$ .<sup>(1)</sup>

Using the modified recombination coefficients and the original electron drift velocity data from (3), a comparison between theoretical and measured I-V curves was made (Fig. 11). The source terms of the theoretical curves

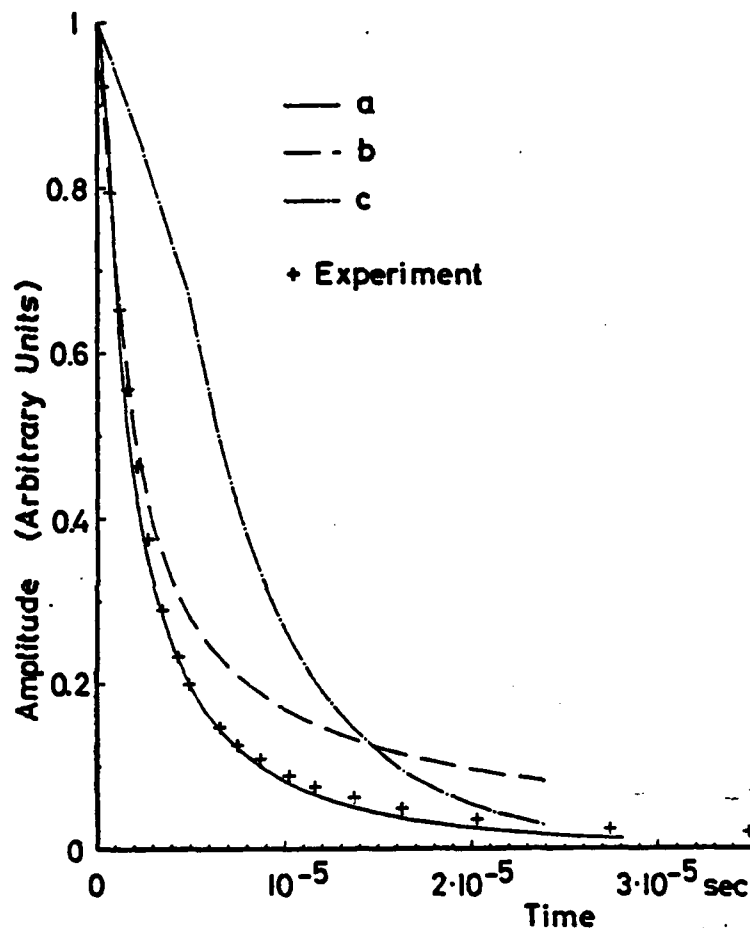


Fig. 10 Comparison of measured decay and computed decay in methane.

- a: Recombination data  $\times 10$ , E/N independent attachment frequency  $3.7 \cdot 10^4 \text{ sec}^{-1}$ .
- b: Recombination data  $\times 10$ , attachment frequency = 0.
- c: Original recombination data, attachment frequency =  $1.4 \cdot 10^5 \text{ sec}^{-1}$ .

1) The much larger recombination rate observed could be caused by the appearance of larger molecules at the higher pressures used here in contrast to the low pressures generally used for the measurement of recombination coefficients. (Comment by M. A. Biondi at the ARO workshop).

were adjusted for best match between theoretical and experimental characteristics. The theoretical values for  $S$  are equal to the experimental ones within experimental limits. The values for the cathode fall were taken from the measurements in

Fig. 7. The difference between theoretical and experimental curves at low

discharge voltages is due to the neglect of the cathode sheath effects in the theoretical model. Also at the higher discharge voltages, the negative differential conductivity, caused in the theoretical model by the decrease in drift velocity between 3 and 30 Townsends, is not observed. Expected instabilities are also not observed in this region.

Assuming a recombination dominated discharge, the experimental I-V curves can be extrapolated to higher E-beam and discharge current densities (Fig. 12a), indicating that discharge current densities of  $10 \text{ A/cm}^2$  are feasible using  $50 \text{ mA/cm}^2$  E-beam current densities. Fig. 12b indicates a gain of 200 for these conditions.

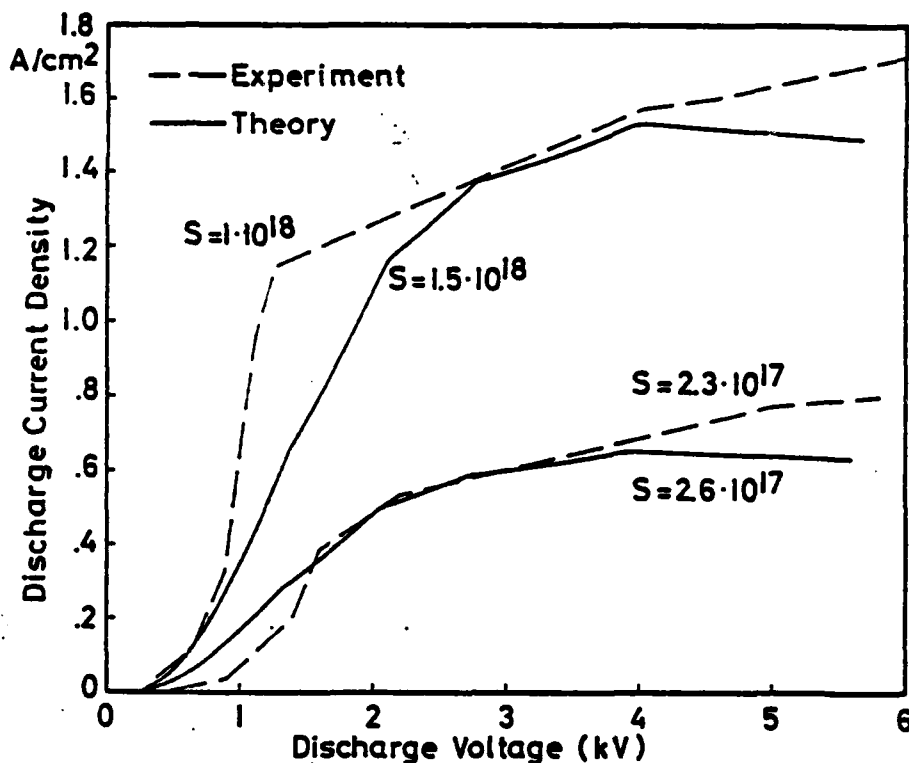


Fig. 11 Comparison of I-V curves, 760 Torr methane.

$S$ : Source term (electron-ion pairs  $\text{sec}^{-1} \text{ cm}^{-3}$ ).



Fig. 12a

Extrapolation of discharge current densities in 760 Torr Methane and Methane + 60 Torr of argon assuming recombination dominated discharge. Discharge voltage 2 KV. Crosses indicate experimental points for pure methane.

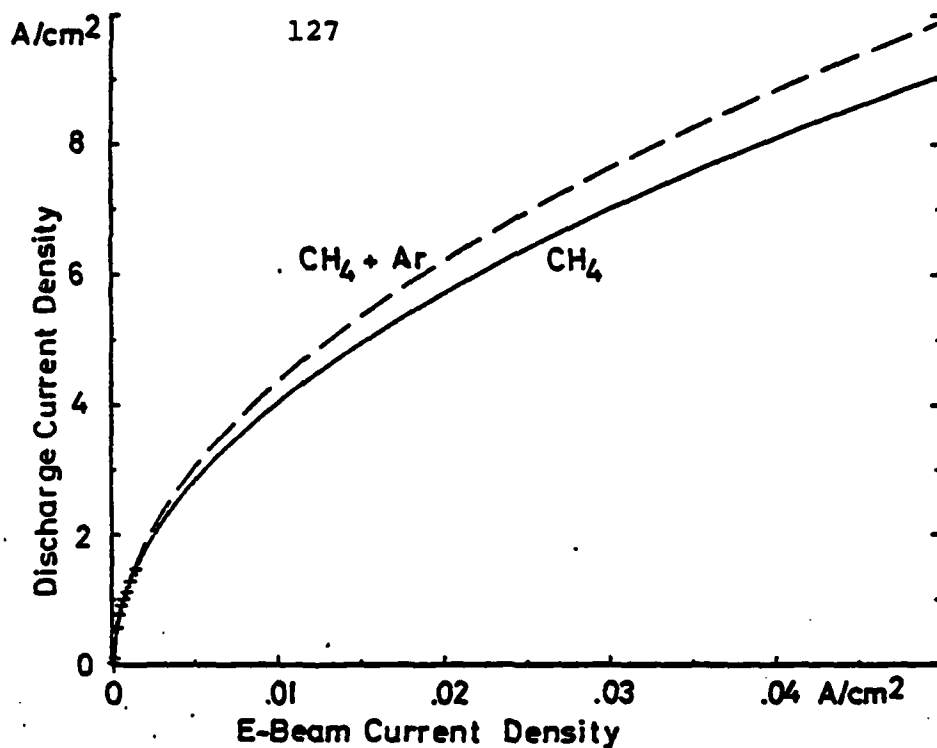
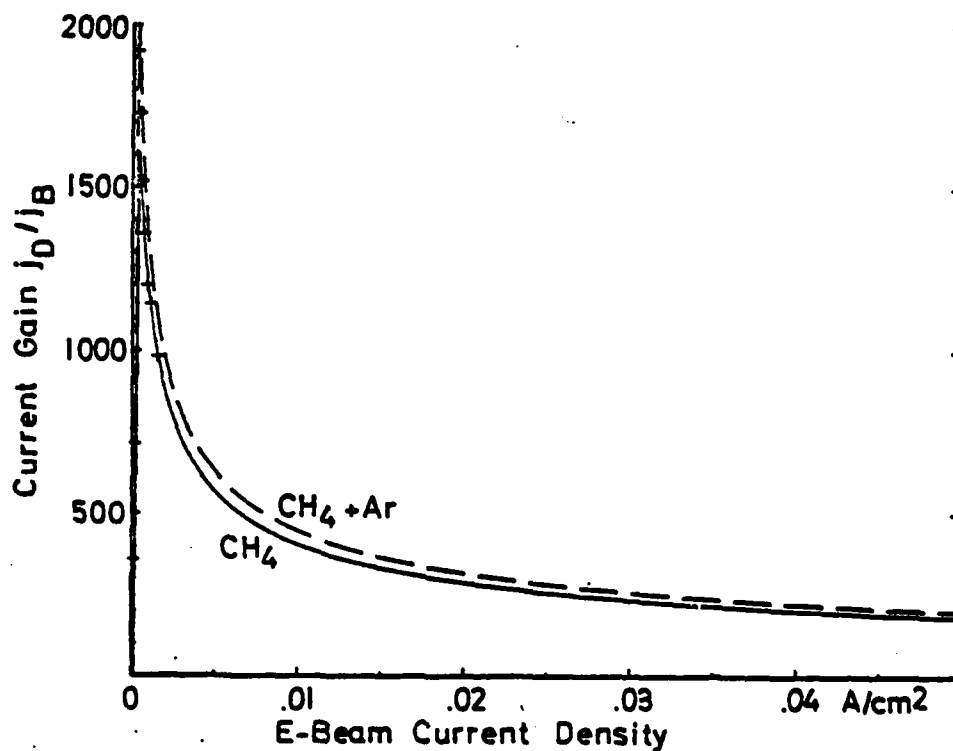


Fig. 12b

Extrapolation of current gain for Methane and Methane plus argon. Crosses indicate experimental points for pure Methane.



Finally, the effect of attachment (which can, of course, be varied by addition of an attaching gas such as  $\text{SF}_6$ ) on the electron density will be considered. Fig. 13 is a plot of eqn. 7 for various recombination rates and attachment frequencies.

Since the discharge decay of a recombination dominated plasma is probably too slow for a practical off-switch (Fig. 9), an attaching gas will have to be added, which of course will reduce the plasma conductivity during the "on" phase. However, it can be argued that a large enough E-beam current density will reduce the effect of attachment (see Fig. 13; at higher source strengths the curves with attachment merge with the curves where  $\beta = 0$ ). As a practical example for methane,

assuming  $\alpha = 1.10^{-7}$  and  $\beta = 1.10^6$  - only about one

order of magnitude larger than the measured value - at  $S = 10^{20}$  electron ion pairs per sec, the attachment still reduces the electron density by 14%.

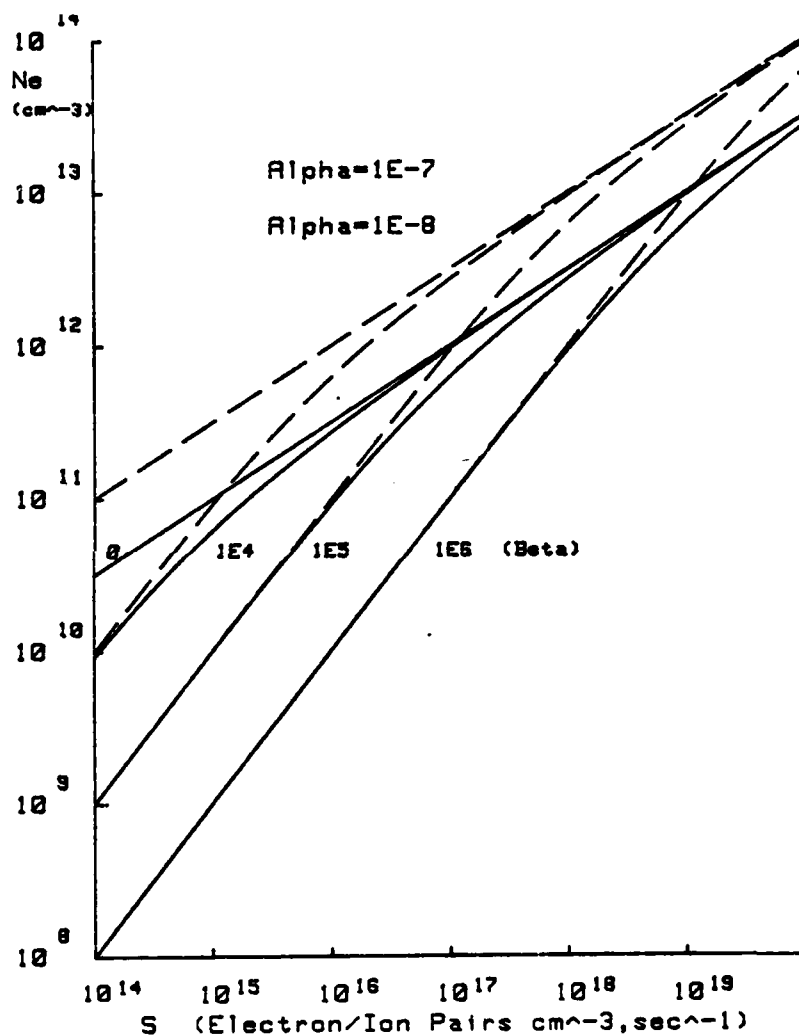


Fig. 13 Electron density as function of the source term  $S$  with recombination/coefficient ( $\alpha$ ) and attachment frequency ( $\beta$ ) as parameter.

Since this source strength corresponds to an E-beam current density of  $.13\text{A}/\text{cm}^2$  (after the foil), it is clear that rather large E-beam currents will be necessary to overcome the effects of attachment. Alternate schemes, such as variable or externally controlled attachment rates <sup>(13)</sup> would bring considerable advantages.

REFERENCES:

1. J. J. Lowke and D. K. Davies, J. Appl. Phys. 48, 4991 (1977).
2. M. J. Berger, and S. M. Seltzer, Tables of Electron Ranges in Various Materials, National Bureau of Standards.
3. J. W. Dzimianski and L. R. Kline, AFWAL-TR-80-2041, April 1980, (Available from NTIS).
4. B. M. Koval'chuk, V. V. Kremnev, G. A. Mesyats and Yu. F. Potalitsyn J. Appl. Mech. & Tech. Phys. 12, 803, Dec. 71.
5. K. McDonald, M. Newton, E. E. Kunhardt, M. Kristiansen and A. H. Guenther, I.E.E.E., Trans. Plasma Science, PS-8, 181, Sept. 80.
6. B. M. Koval'chuk, Yu. D. Korolev, V. V. Kremnev and G. A. Mesyats, Sov. Radio Eng. & Electron Phys. 21, 1513 (1976).
7. R. O. Hunter, Proc. IEEE Int. Pulse Power Conf., paper IC8-1 (1976); U. S. Patent 4, 063, 130.
8. L. Foreman, P. Kleban, L. D. Schmidt and H. T. Davis, Phys. Rev. A, 23, 1553 (1981).
9. E. P. Velikhov et.al., Sov. Phys. JEIP, 38, 267 (1974); Sov. Phys. Usp. 20, 586 (1977).
10. V. V. Zakharov, A. A. Karpilov, and E. V. Chekhonov, Sov. Phys. Techn. Phys. 21, 1074 (1976).
11. A. P. Averin, Ye. P. Glotov, V. A. Danilychev, V. N. Koterov, A. M. Soroka and V. I. Yugov, Pis'ma V. Zhurn, Tekhn. Fiziki 6, 405 (12 April 1980).
12. D. H. Douglas-Hamilton, J. Chem. Phys. 58, 4820 (1973).
13. K. H. Schoenbach, C. Schaefer, E. E. Kunhardt, M. Kristiansen, L. L. Hatfield and A. H. Guenther, 3rd Int. Pulse Power Conf., Albuquerque (1981) (to be published).
14. M. Hallada, M.S.Thesis, Air Force Inst. Techn., NOV 81 (unpublished).

## APPENDIX

Calculation of I-V characteristics using the approach by Lowke and Davies, including secondary emission from the cathode and ionization via metastable states. (M.S. Thesis, Marc R. Hallada, Air Force Institute of Technology, Dec. 1981)

The following data is extracted from the thesis quoted and is added to show how features of the measured I-V characteristics can be explained with these theoretical calculations of the effect of the additional ionization in the cathode sheath.

These calculations are extensions of the ones performed by Lowke and Davies (1). In particular, they have been extended to higher discharge currents, higher E-beam currents and now also include effects of secondary emission from the cathode by ion bombardment and increased ionization due to the presence of metastable states. The calculations consist of numerical solutions of eqn. (1) and the Poisson equation, the electron current density being expressed by eqn. (2).

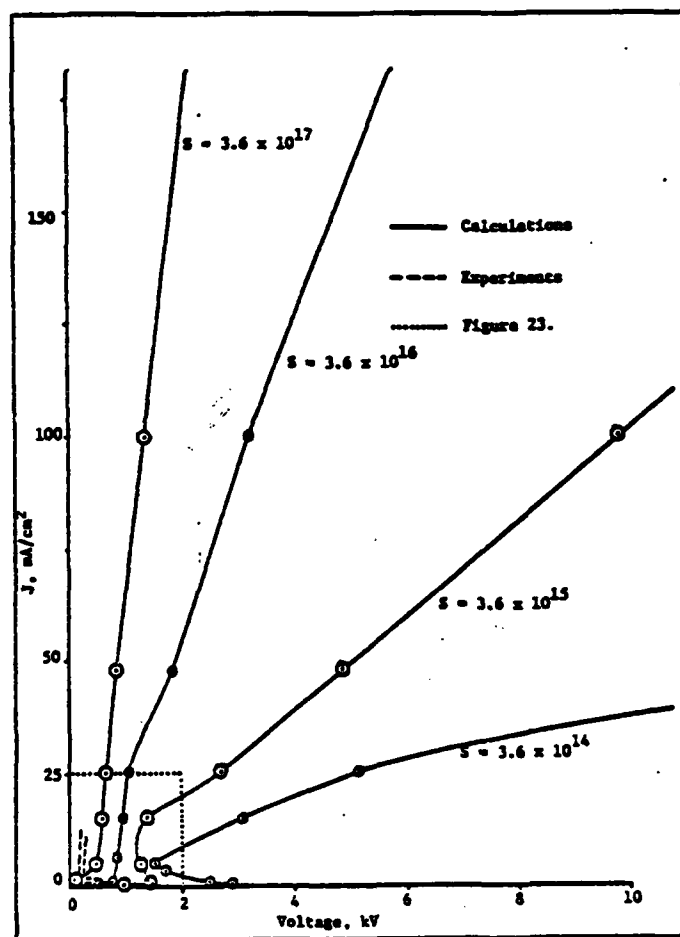


Fig. A1 I-V Characteristics-Calculated for an Argon Discharge (760 Torr,  $\gamma = .02$ ,  $d = .3$  cm, no metastable ionization)

( $\gamma$ : secondary emission coefficient)

The calculations result in a description of the electric field, electron and ion densities and potential across the discharge length giving one data-point of the I-V curve for a particular electron beam

current, pressure and gas species. The calculated curves of Fig. A1 show the non-linear behavior of the experimental curves of Fig. 2. As already pointed out in (9) and (10), the negative portion of the characteristic is unstable. As the E-beam current density is being increased, the influence of the cathode sheath decreases. The enlarged portion (Fig. A2) shows that the experimental characteristics have a much steeper slope and lower voltage drop for comparable source functions, at least for argon. The agreement is much

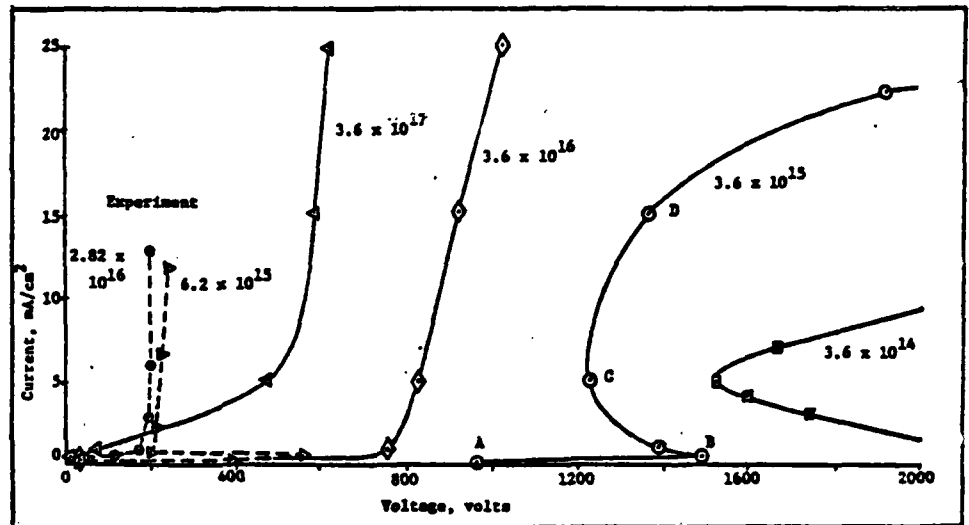


Fig. A2 I-V Characteristics-Calculated for an Argon Discharge (expansion of low current and voltage region of Fig. A1.)

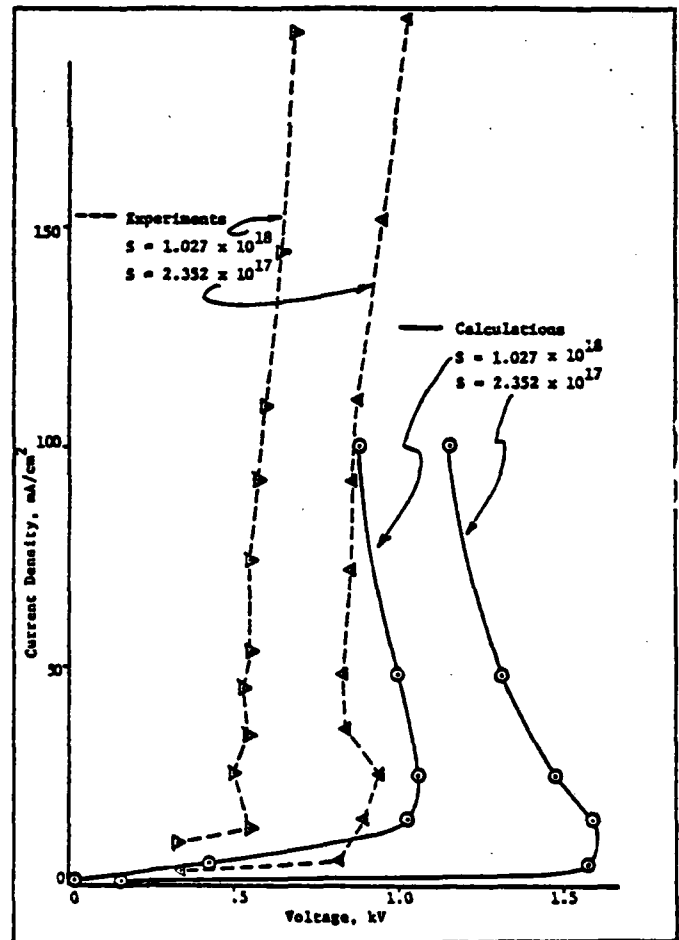


Fig. A3 I-V Characteristics-Experimental and Calculated for a Methane Discharge (760 Torr,  $\gamma = .02$ ,  $d = 2.2$  cm)

better for methane (Fig. A3). The agreement can be improved by including secondary emission (Fig. A4) which increases the slope of the I-V curve in the high conductivity regime. The effective ionization cross sections for argon will be increased and the ionization threshold will be lowered if two step ionization via metastables is being considered. Using calculated effective ionization cross sections for argon, the new characteristic has a much lower voltage drop (Fig. A5). Including both corrections, the theoretical characteristics then can be matched both in slope and in voltage drop to the experimental characteristics.

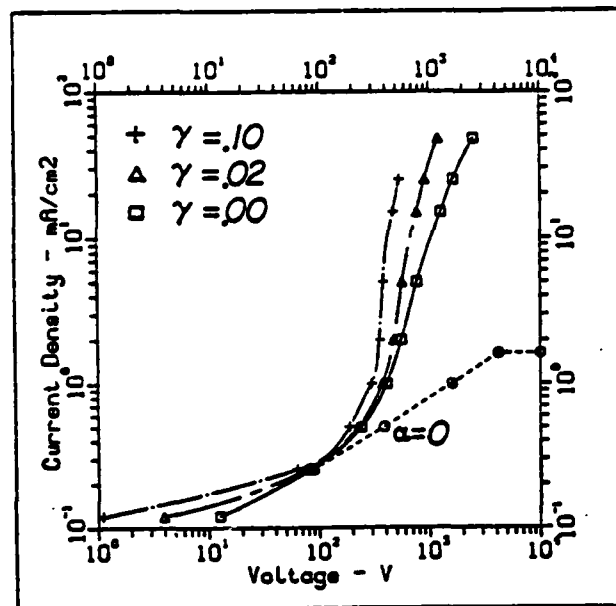
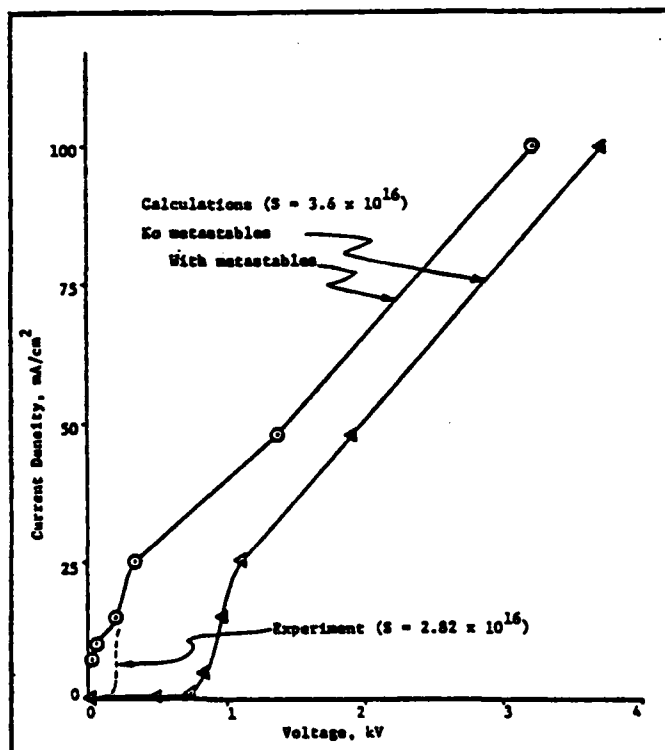


Fig. A4 Calculated I-V Characteristics for Three Secondary Emission Coefficients (Argon, 240 Torr,  $S = 3.6 \times 10^{16}$ )

Fig. A5

I-V Characteristics-Experimental and Calculated for an Argon Discharge (same parameters as Fig. A1, but with metastable ionization)



OPTICAL CONTROL OF DIFFUSE  
DISCHARGE OPENING SWITCHES\*

K. H. Schoenbach, G. Schaefer, M. Kristiansen, L. L. Hatfield  
Texas Tech University, Lubbock, Texas 79409 USA

A. H. Guenther  
Air Force Weapons Laboratory  
Kirtland Air Force Base, New Mexico 87117 USA

Diffuse discharge opening switches seem to be prime candidates for repetitively operated ( $> 10^3$  pps), fast, opening devices ( $\tau < 1 \mu s$ ) in inductive storage systems. The switch performance is mainly determined by the type of gas fill. In order to achieve fast opening of the switch, attachers are to be used at a partial pressure which makes the switch attachment dominated during the opening phase. On the other hand, additives of attachers increase the power losses during conduction. Both low forward voltage drop and fast opening can only be obtained by choosing gases or gas mixtures which satisfy the following conditions:

- a) for low E/N values (conduction phase) the gas mixture should have a high drift velocity and low attachment rate coefficients
- b) for high E/N values (opening phase) the gas mixture should have lower drift velocities and high attachment rate coefficients.

---

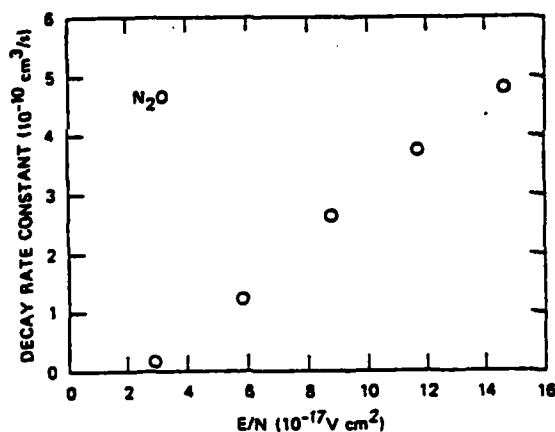
\*Supported By Air Force Office of Scientific Research



Gas mixtures with the desired behavior can be found among mixtures of Ar and  $\text{CF}_4$ <sup>1</sup>. Gas mixtures which at least satisfy the attachment conditions contain attachers with a maximum of the attachment cross-section at electron energies of 1 to 2 eV. An example for such an attacher is  $\text{N}_2\text{O}$ . Figure 1 shows the electron decay rate constant for  $\text{N}_2\text{O}$  in 350 Torr  $\text{N}_2$  as buffergas<sup>2</sup>. The decay rate has a low value at  $E/N$  below 5 Td and is increasing by at least one order of magnitude between 5 and 30 Td.

Figure 1.

Decay Rate Constant of the Electron Conduction Current in  $\text{NO}$  in an Atmosphere of 350 Torr of  $\text{N}_2$  at various  $E/N$ .



The requirements for the gas mixture used in a fast, low loss diffuse discharge opening switch do not depend on the type of sustainment of the discharge. They hold for e-beam as well as for optically controlled discharges. What laser control makes attractive for diffuse discharge opening switches is:

- a) the variety of possible resonant electron production and depletion mechanisms

- b) the fact that the control system can be separated physically from the switch
- c) the ease by which laser beams can be manipulated (shape, rise and fall time, power density).

Concepts for using lasers for electron production (i.e. for sustainment of diffuse discharges) are shown in Fig. 2. The opening process after turn-off of the laser in each case is determined by attaching processes of an added attacher that satisfies the conditions mentioned earlier.

#### A. Optically Enhanced Electron Density

The simplest conceptual way to generate electrons optically in a gas is single step photo-ionization from the ground state. However, considering that available lasers produce photons only up to energies of 7 eV efficiently, only certain gases like alkali vapors are suitable for direct ionization<sup>3</sup>. Alkali vapors on the other hand react very aggressively with most attachers. A better way to generate electron-ion pairs seems to be resonant two-step photo-ionization by means of UV-laser radiation. In organic gases, like Dimethylaniline, Fluorobenzene, or Tripropylamine, resonant two-step processes can produce<sup>4,5</sup> electrons with densities of up to some  $10^{15} \text{ cm}^{-3}$ . With  $\text{Cs}_2$  a maximum yield was achieved for visible light<sup>6</sup>. Two-step ionization in atoms is resonant for the first step while for the second step also a flashlamp might be used<sup>3</sup>.

Tunable, visible lasers offer a wider variety of ionization mechanisms, which, however, have to be collisionally assisted. A self sustained discharge has to be ignited to provide either collisional ionization from an optically excited state<sup>7</sup> or collisional excitation and successive one or two-step photo ionization<sup>8-11</sup>. The laser serves to change the conductivity of the diffuse discharge from a low level to a higher level and thereby closes the switch for a certain time, the conduction time. After laser turn-off the initial state of low conductivity is approached on time scales determined by the loss processes in the gas.

Two-step photoionization from a collisionally excited state was considered in more detail for a gas system consisting of  $N_2$  as buffer gas, NO as gas which is photoionized and an attacher with the desired attachment properties<sup>12</sup>. Pertinent transitions in such a system are shown in Fig. 3. Resonant two-step photo ionization from the NO A-state through the NO E-state provides for conduction electrons. The NO A-state is collisionally excited via the metastable  $N_2$  state which is highly populated and serves as a reservoir for the two-step photoionization in NO. Once the laser is turned off, the ionization process is interrupted and the electrons are removed by the attaching gas. Although a molecular system has the disadvantage that according the additional vibrational and rotational states the absorption cross-section is low, the  $E^2\Gamma^+ \rightarrow A^2Z^+$  system in NO has the advantage of having nearly the same molecular constants for both electronic states<sup>13</sup>.

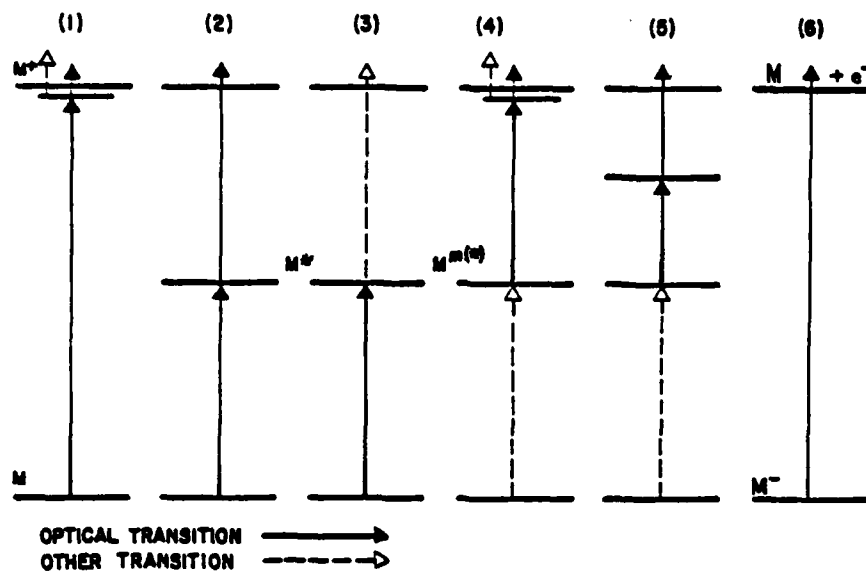
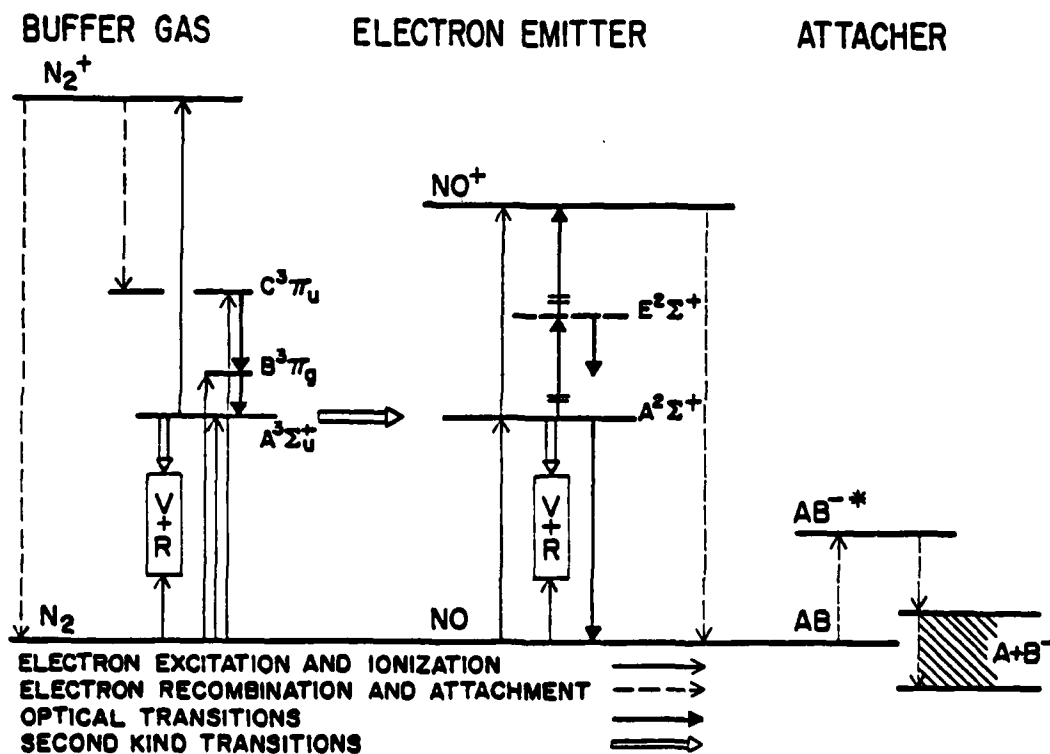


Fig. 2 Optically Controlled Electron Generation

Fig. 3 Energy Level Diagram for the  $N_2$ -NO System

Instead of molecular gases like NO, atomic gases can be used for two-step photoionization from a collisionally excited state. Advantages of atomic system like Hg<sup>14,15</sup> (Fig. 4) are the higher absorption cross-section and a reduction in complexity, which makes it easier to predict the behavior in diffuse discharge systems. Two possible ways for two-step ionization are sketched in the energy diagram of Hg; one from the resonant  $6^3P_1$  state and a second one from the metastable  $6^3P_0$  state. The density of these states very much depends on the discharge conditions. For the metastable state  $6^3P_0$  the density can be higher than 50% of the gas density.

A similar concept is based on optical detachment by means of laser radiation. In this case an attacher with a noticable attachment rate also for the conduction phase (low E/N) is used. In the conduction phase the attachment is then compensated by photodetachment.

#### B. Optically Decreased Electron Density

A second way to use lasers to control diffuse discharges is optical stimulation of electron loss processes. In contrast to the considerations discussed so far, the laser is used now to induce and control processes which lead to a reduction of conductivity, an effect which is used in the opening phase of the diffuse discharge.

In systems where the electron production is determined by collisional ionization via a metastable state the ionization rate can be reduced by optically depopulating the meta-

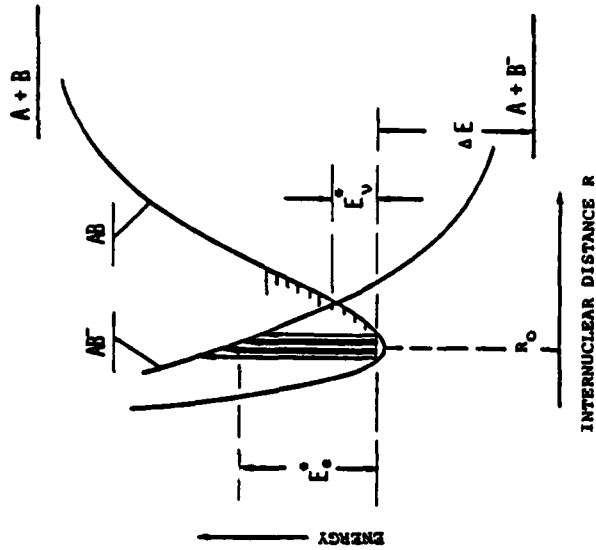


Fig. 5 Resonance Dissociative Electron Attachment

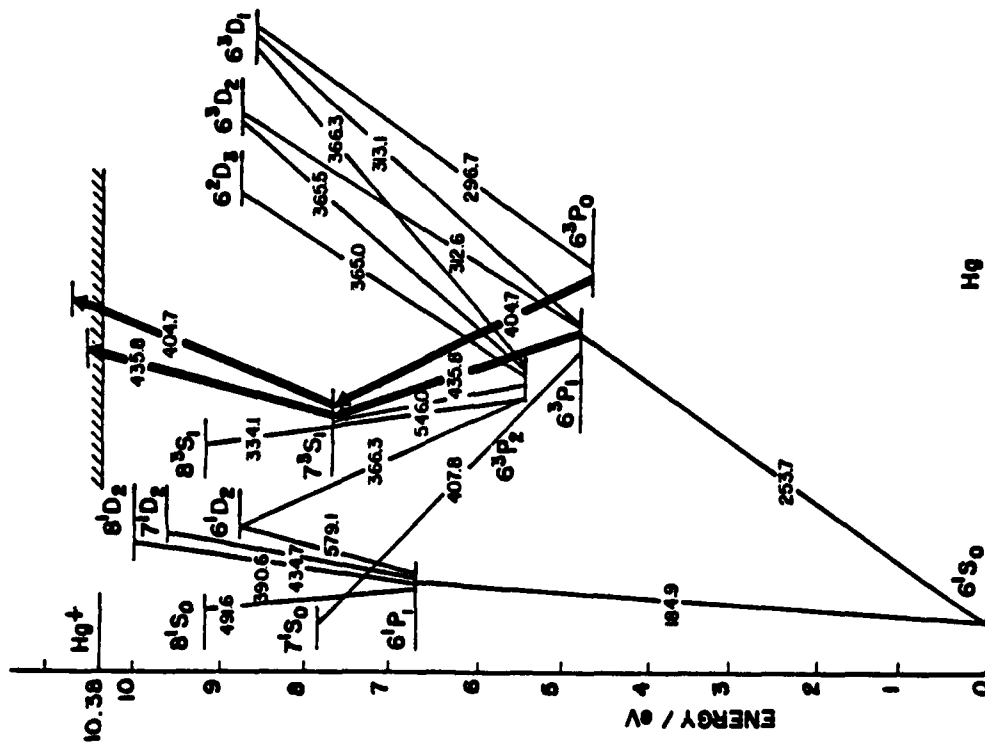


Fig. 4 Energy Level Diagram of Hg with Proposed Two-Step Photoionization from Excited States

stable level. A laser is used to populate a higher state which is optically connected to the ground state <sup>15-18</sup>. The density of atoms in the metastable state, which serves as reservoir for collisional ionization, is then reduced and so is the total ionization rate.

Another method to reduce the electron density and hence the conductivity by means of a laser is given by optical decomposition of molecules. The objective is to produce fragments, radicals or ions, where at least one of them has a higher attachment cross-section than the original molecule.

A third method to stimulate loss processes optically is based on photoenhanced attachment by excitation of molecules. Certain attachers as, for instance,  $\text{HCl}$  have a higher attachment cross-section in their rotational and/or vibrational excited states. The mechanism can be understood by considering the potential energy curves of an attacher and its ion. In Fig. 5 a general type of dissociative electron attachment process is illustrated. The potential energy curve of a neutral diatomic molecule  $\text{AB}$  is crossed at an energy  $E_v^*$  above the ground state by a repulsive branch of the negative ion  $\text{AB}^-$ . The probability of electron attachment and succeeding dissociation is depending on the energetic state of the vibrationally excited molecule relative to the curve crossing. For the example shown the attachment cross-section increases with vibrational excitation up to  $v = 4$ . On the

other hand the electron energy necessary to form the negative ion  $AB^-$  shifts to smaller values if the molecule  $AB$  is excited into a state closer to the curve crossing.

Figure 6 shows attachment cross-sections for the ground state and the first two vibrationally excited states of  $HCl$  <sup>19</sup>, demonstrating both the strong increase in attachment cross-

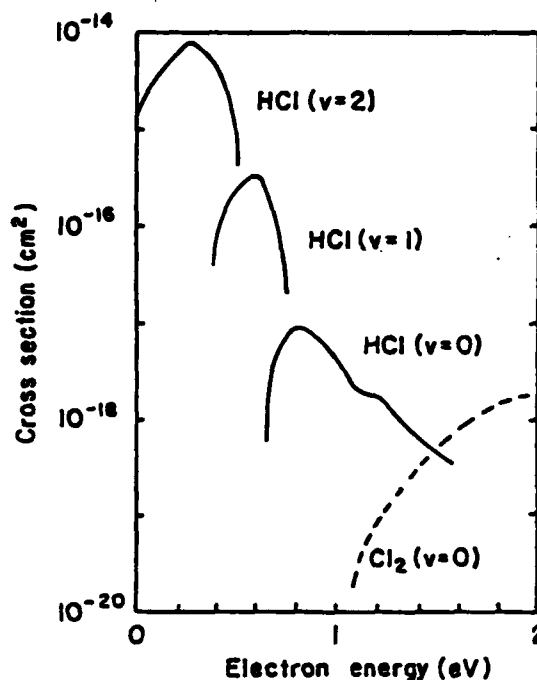


Fig. 6

Dissociative Attachment  
Cross Sections for  
Vibrationally Excited  
 $HCl$  Molecules

section and the related shift of the attachment peak towards lower electron energies. The results shown in this figure are based on attachment cross-section measurements for different temperatures in  $HCl$ .<sup>20</sup> More detailed calculations yielding cross-sections for different vibrationally and rotationally excited states of  $HCl$  have recently been performed <sup>21</sup>. By



means of an IR-laser it should be possible to excite vibrational states selectively, thus increasing the attachment cross-section in a controlled way. Photoexcitation in competition with collisional excitation may be effective if the curve crossing is several  $kT_e$  above the ground state at a internuclear distance  $R > R_0$ . For a curve crossing at  $R \gtrsim R_0$  vibrational excitation will only cause a small increase of the attachment cross-section as has been shown<sup>22</sup> for  $I_2$ .

$HC\dot{L}$  seems to be the molecule where most data are available, but due to its attachment cross-section peaking at low energies ( $E_e < 1$  eV), it is not the best choice for a gas suitable for opening switch operation. A way to select gases for the special purpose of using them as triggerable attachers in diffuse opening switches is to look at first for gases with molecular structures which promise strong absorption in spectral regions where efficient IR-lasers (for example  $CO_2$  lasers) are available. Figure 7 shows groups of gases with bondings which show strong absorption in the spectral region between 9 and 11  $\mu m$  (of course there are several others).

A second step is to consider the attachment properties of these gases. A criterion for suitable gases where the curve crossing is a few  $kT$  above the potential minimum is the temperature behavior; in particular, the rate of increase of attachment rate with increasing temperature. A strong increase was, for example, found for some halo-generated hydro carbons<sup>23, 24</sup>. More detailed information is obtained by measure-

Compounds	Strong Absorption Bands ( $\mu\text{m}$ )	Absorbing Bond or Group
NON-AROMATIC ALCOHOLS	8 - 10	C-O Stretch
NON-AROMATIC ESTERS, ACETATS AND EPOXIDES	8 - 11	C-O Stretch
NON-AROMATIC AMINES	8.1 - 9.4	C-N Stretch
NON-AROMATIC ALDEHYDES	8.5 - 9.5	C-O Stretch
NON-AROMATIC ESTERS AND LACTONES	9 - 10	$\overset{\text{O}}{\parallel}$ C-O-C Stretch
NON-AROMATIC ANHYDRIDES	8 - 11	$\overset{\text{O}}{\parallel} \quad \overset{\text{O}}{\parallel}$ C-O-C Stretch
NON-AROMATIC ACID HALIDES	10 - 11	$\overset{\text{O}}{\parallel}$ C-Cl
NON-AROMATIC AMIDES	8.4 - 9.5	C-N Stretch
NON-AROMATIC PHOSPHORORUS COMPOUND	9 - 11.5	P-O-C Stretch
AROMATIC HALOGENATED HYDROCARBONS	9 - 10	$\phi$ -Cl, $\phi$ -Br, $\phi$ -I
AROMATIC ETHERS	9.5 - 10	<u>C-O</u> - $\phi$ Stretch
AROMATIC NITRO AND NITROSO COMPOUNDS	9.5 - 10.5	N-O Stretch
AROMATIC ESTERS AND LACTONES	7.8 - 10	C-O Stretch
AROMATIC ACID HALIDES	10 - 11.7	$\overset{\text{O}}{\parallel}$ C-Cl

Fig. 7 Chemical Compounds which Absorb Radiation within the Emission Range of the CO<sub>2</sub> Laser. The Spectral Range of Strong Absorption Bands and the Absorbing Bands or Groups are Indicated

ments of the temperature dependence of the attachment cross-section which is available <sup>25-27</sup> for gases like  $N_2O$ ,  $O_2$  and  $SF_6$ . It can be assumed that gases with increasing attachment rate with increasing  $E/N$  show the same temperature dependence <sup>1, 28, 29</sup>. The temperature dependent change of the cross-section in  $SF_6$  occurred at too low electron energies for switching applications in these experiments <sup>27</sup>. However, in this case an increase of the attachment rate after laser excitation was observed for the first time.

The number of gases suitable for opening switches is reduced by the further consideration the the attachers should have the attachment cross-section at moderate electron energies (a few eV) to get a low attachment rate at  $E/N \approx 3$  Td and a strong increase of the attachment rate at  $E/N \geq 5$  Td. Finally, chemical properties like materials compatibility and toxicity have to be considered.

The disadvantage of this type of attachers, the shift of attachment peak cross-sections to lower energies with increasing vibrational energy, can be compensated by adding another attacher with  $E/N$  characteristics which satisfy the previously mentioned desirable properties for opening switch gases.

According to the limited number of small molecules that satisfy all the mentioned requirements, larger molecules should also be considered. In recent experiments with  $C_2F_5Cl$

it has been shown, that there can be a strong spectral structure in the quasicontinuum <sup>30</sup>, which indicates that there are states with appropriate lifetimes to allow attachment before internal thermalization.

### C. Experimental Arrangement

To test the concepts of optical control of diffuse discharges, two experimental arrangements have been designed and tested. One is shown in Fig. 8. It consists of a 50  $\Omega$  line which can be DC charged up to  $V = 120$  kV. Pulse charging is possible up to  $V = 250$  kV. The line is discharged by means of a laser triggered switch into a self-sustained, high pressure, volume discharge between two 10 cm diameter electrodes, 1 cm apart. The anode is a mesh with  $\sim 75\%$  transparency, which allows axial irradiation of the diffuse plasma and homogeneous preionization. The pulse length for the matched line is 100 ns which can be increased by a factor of 5 by changing the dielectric of the line. Current and voltage measurements, together with optical measurements (streak camera) are planned to get information about the time development of the diffuse plasma with and without optical control.

A second apparatus, an electron beam sustained discharge, is under construction. The experimental set up is shown in Fig. 9. An electron beam with an aperture of  $\sim 100$  cm<sup>2</sup>, a current of up to  $I = 100$  A at electron energies of up to  $E_e = 250$  keV is generated in a grid controlled system with a heated cathode. The electrons penetrate a 1 mil Ti-foil and provide

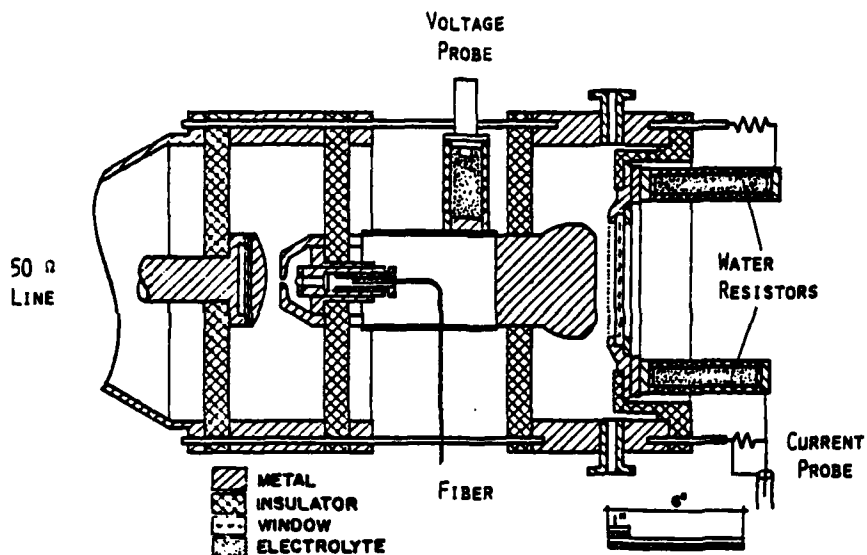


Fig. 8 Experimental Arrangement for Optical Control of Diffuse Discharges

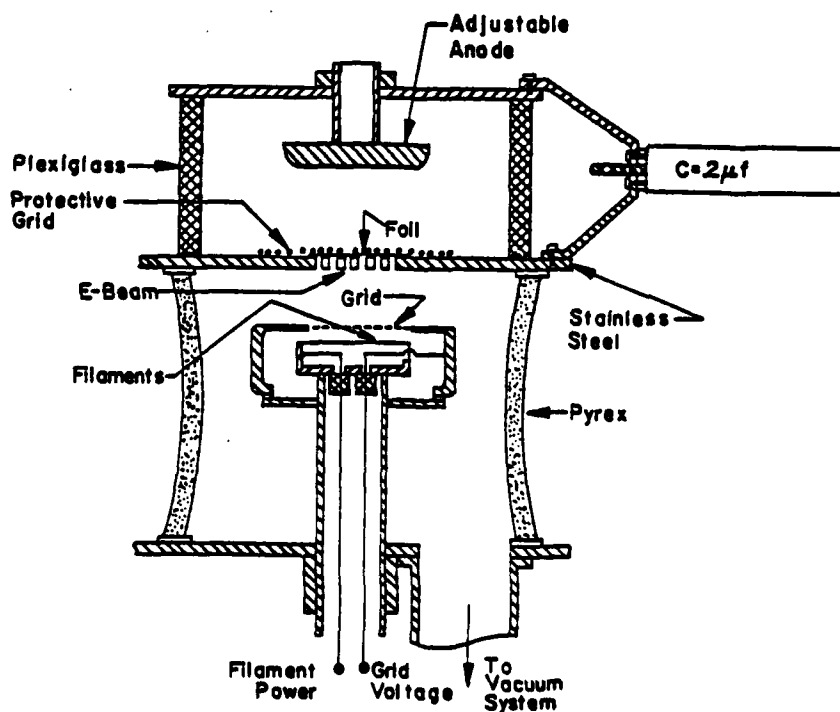


Fig. 9 Experimental Arrangement for E-Beam Control of Diffuse Discharges

ionization in a high pressure, gas-filled switch. Side-on windows allow for optical access and hence for testing the feasibility of optically assisted attachment processes. It is planned to use both experimental arrangements to test the applications of optical control concepts for diffuse discharge opening switches. The concept of "Optically Control of Diffuse Discharge Opening Switches" has been discussed in several recent papers 31-35.

### References

1. L. G. Christophorou, S. R. Hunter, J. G. Carter and S. M. Spyrou, "Gases for Possible Use in Diffuse-Discharge Switches, (to be published\*).
2. L. C. Lee, C. C. Chiang, K. Y. Tang, D. L. Huestis and D. C. Lorents, "Gaseous Ele-Tronic Kinetics for e-beam Excitation of Cl, NO and N<sub>2</sub>O in N<sub>2</sub>, (to be published).
3. Ali Javan and Jeffrey S. Levine, "The Feasibility of Producing Laser Plasma via Photo ionization," IEEE Journal of Quantum Electronics, QE-8, 827, (1972).
4. J. R. Woodworth, C. A. Frost and T. A. Green, "UV Laser Triggering of High-Voltage Gas Switches," (to be published in J. Appl. Phys.).
5. L. C. Lee and W. K. Bischel, "Two-Photon-Ionization Coefficients of Propane, 1-Butane, and Methylamines," (to be published).
6. E. H. A. Granneman, M. Klewer, K. J. Nygaard and M. J. Van der Wiel, "Two-photon ionization of Cs<sub>2</sub>, Rb<sub>2</sub> and RBCs using an Ar-ion laser," J. Phys. B: Atom. Molec. Phys., 9, 865 (1976).
7. R. B. Green, G. J. Havrilla and T. O. Trask, "Laser-enhanced Ionization Spectrometry: Characterization of Electrical Interferences," Applied Spectroscopy, 34, 561 (1980).
8. William B. Bridges, "Characteristics of an opto-galvanic effect in cesium and other gas discharge plasmas," J. Opt. Soc. Am., 68, 352 (1978).
9. P. Camus, M. Dieulin and C. Morillon, "Optogalvanic detection of barium high-lying levels with a two-step pulsed laser excitation," Le Journal de Physique, 40, L-513 (1979).
10. D. Feldmann, "Opto-Galvanic Spectroscopy of some Molecules in Discharges: NH<sub>2</sub>, NO<sub>2</sub>, H<sub>2</sub> and N<sub>2</sub>," Optics Communications, 29 67 (1979).
11. E. P. Glotov, V. A. Danilychev, A. I. Milanich and A. M. Soroka, "Self-sustained electric photoionization discharge in three component mixtures containing rare gases and hologen bearing molecules," Sov. J. Quantum Electron, 9, 1176 (1979).
12. In collaboration with D. Lorents and L. C. Lee, SRI.

---

\* See Appendix A of this Workshop Proceedings

13. M. W. Feast, "Two New  $^2\Sigma-^2\Sigma$  Systems Due to the Molecule NO," Canadian Journal of Research, 28, 492 (1950).
14. W. J. van den Hoek and J. A. Visser, "Optogalvanic spectroscopy and thermal relaxation in high-pressure mercury and sodium arc discharges," J. Appl. Phys., 51, 5292, (1980).
15. Carl Kenty, "Role of Metastable ( $^3P_2$ ) Hg Atoms in Low Current Discharges in Hg Rare Gas Mixtures," Phys. Rev. 80, 95 (1950).
16. Kermit C. Smyth, "Photon-Induced Ionization Changes in a Neon Discharge," Chemical Physics Letters, 55, 473 (1978).
17. A. C. Tam, "Quenching Effect of Helium 2- $\mu$  Light On a Weak Helium Discharge," (to be published).
18. J. E. Lawler, "Experimental and Theoretical Investigation of the Optogalvanic Effect in the Helium Positive Column," Physical Review A, 22, 1025 (1980).
19. W. L. Morgan and M. J. Pound, "Kinetics of E-Beam Excited XeCl," Proceedings of the 33rd Gaseous Electronics Conf. Oklahoma, Abstract FB-3, Oct., 1980.
20. M. Allan and S. F. Wong, "Dissociative attachment from vibrationally and rotationally excited HCl and HF" J. Chem Phys. 74, 1687 (1981).
21. J. Morman Bardsley, private communication.
22. R. J. Hall, "Dissociative attachment and vibrational excitation of  $F_2$  by slow electrons," J. Chem. Phys. 68, 1803 (1978).
23. W. E. Wentworth, R. George and H. Keith, "Dissociative Thermal Electron Attachment to Some Aliphatic Chloro, Bromo, Iodo Compounds," Journal Chemical Physics, 51, 1791 (1969).
24. D. Spence and G. J. Schulz, "Temperature dependence of electron attachment at low energies for polyatomic molecules," Journal Chemical Physics, 58, 1800 (1973).
25. P. J. Chantry, "Temperature Dependence of Dissociative Attachment in  $N_2O$ ," Journal of Chemical Physics, 51, 3369 (1969).
26. W. R. Henderson, W. L. Fite and R. T. Brackmann, "Dissociative Attachment of Electrons to Hot Oxygen," Physical Review, 183, 157 (1969).



27. C. L. Chen and P. J. Chantry, "Photon-enhanced dissociative electron attachment in SF<sub>6</sub> and its isotopic selectivity," J. Chem. Phys., 71, 3897 (1979).
28. T. G. Lee, "Electron Attachment Coefficients of some Hydrocarbon Flame Inhibitors, J. Phys. Chem., 67, 360 (1963).
29. L. M. Chanin, A. V. Phelps and M. A. Biondi, "Measurements of the Attachment of Low-Energy Electrons to Oxygen Molecules," Physical Review, 128, 219 (1962).
30. E. Borsella, R. Fantoni, A. Giardini-Guidoni and C. D. Cantrell, "Observation of Structure in the Quasicontinuum of Multiple-Photon-Excited C<sub>2</sub>F<sub>5</sub>Cl, (to be published in Chemical Physics Letters).
31. K. H. Schoenbach, L. Hatfield and E. E. Kunhardt, "An Opening Switch Using a Diverter." First Annual Report on Coordinated Research Program in Pulsed Power Physics, Texas Tech University, Lubbock, TX, 158 (1980).
32. K. H. Schoenbach, M. Kristiansen, E. E. Kunhardt, L. L. Hatfield, and A. H. Guenther, "Exploratory Concepts of Opening Switches," Proceedings of the Workshop on Repetitive Opening Switches, Tamarron, Co., 66 (1981).
33. K. H. Schoenbach, G. Schaefer, E. E. Kunhardt, M. Kristiansen, L. L. Hatfield and A. H. Guenther, "An Optically Controlled Diffuse Discharge Switch," Proceedings of the 3rd IEEE International Pulsed Power Conference, Albuquerque, N.M., 142 (1981).
34. K. H. Schoenbach, G. Schaefer, M. Kristiansen, L. L. Hatfield and A. H. Guenther, "Diffuse Discharge Opening Switches," Proceedings of the NATO Advanced Study Institute: Electrical Breakdown and Discharges in Gases, Les Arcs, France, (in press).
35. K. H. Schoenbach, G. Schaefer, L. L. Hatfield, M. Kristiansen, H. C. Harjes, G. Hutcheson, and G. Leiker, "Opening Switches," Second Annual Report on Coordinated Research Program in Pulsed Power Physics, Texas Tech University, Lubbock, Tx., 209 (1981).

## MODELING OF DIFFUSE DISCHARGES

Laurence E. Kline  
Westinghouse R&D Center  
Pittsburgh, PA 15235

A. Introduction

A wide variety of models have been developed for the analysis of diffuse discharges. In this paper some of these models will be discussed in the context of diffuse discharge opening switches. The discussion will be limited to models of externally sustained diffuse discharges, i.e., discharges where an external beam of high energy electrons, U.V. photons, x-rays, etc. provides the electron production needed to offset the electron losses due to recombination and attachment. Externally sustained discharges appear to be well suited to the opening switch application.

The various models which have been developed are discussed in order of increasing complexity. The motivation for, and application of the various models are also described. After describing some of the models which have been developed, several important physical limitations on switch operation are discussed which have not been quantitatively modeled and are not fully understood.

A useful, and rather complete review of diffuse discharges sustained by high energy electron beams is given by Bychkov, et al.<sup>(1)</sup> Additional information is given in a review by Daugherty.<sup>(2)</sup> Both of these papers contain many references to earlier work.

B. Rate Equation Models.

The discharge steady state voltage-current (V-I) characteristics and transient (i.e., turn-on and turn-off) characteristics can

be predicted by using simple rate equation models. Models of this kind have been used to predict the characteristics of e-beam discharge switches by Koval'chuk<sup>(3)</sup> et al., Hunter,<sup>(4)</sup> Bletzinger<sup>(5)</sup> and others.<sup>(1)</sup> A scaling and gas selection study which used this type of model is described by Dzimianski and Kline.<sup>(6)</sup>

#### C. Electron Beam Deposition.

The one- and two-dimensional characteristics of the ionization and power deposition by the high energy electrons has been studied using a variety of models. Monte Carlo on simulation models which follow a large number of electron trajectories are particularly useful for this purpose because they accurately model a wide range of experimental conditions. The Monte Carlo approach to studying the interaction of the high energy electron beam with the gas is described by Srivastava, et al.,<sup>(7)</sup> Smith,<sup>(8)</sup> and the references therein. See also the review papers, Refs. 1 and 2.

#### D. Two-Dimensional Discharge Characteristics.

The non uniform ionization produced by the e-beam leads to nonuniformities in discharge properties such as current density, electric field and power density. If the gas in the switch is flowing this gas flow adds an additional source of nonuniformity in the discharge properties. These spatial variations of the discharge properties have been modeled by Srivastava, et. al.,<sup>(7)</sup> Filcoff, Roache and Money,<sup>(9)</sup> Parazzoli<sup>(10)</sup> and the references listed therein.

#### E. Cathode Sheath Models.

The regions near each electrode in these diffuse e-beam discharges are regions of higher electric field and higher power density, compared with the positive column which occupies most of the interelectrode volume. Many of the existing models of these sheath regions are reviewed by Bychkov, et.al.<sup>(1)</sup> The non-equilibrium nature

of the electron energy distribution in the cathode sheath region is discussed by Tran Ngoc et al.<sup>(11)</sup>

#### F. Discharge Stability.

The macroscopic discharge nonuniformities discussed in Section D and the sheath regions discussed in the last section are both possible causes of instabilities in these diffuse discharges. Instabilities predicted by analyzing the properties of the positive column as discussed for example by Douglas-Hamilton and Mani,<sup>(12)</sup> Long,<sup>(13)</sup> Brown and Nighan<sup>(14)</sup> and the references therein.

However, the discharge instability which is normally of interest is the glow-to-arc transition (GAT), i.e., the development of a highly conducting filamentary channel which "shorts out" the diffuse discharge and which is unaffected by the external ionization source. Although the development of the GAT has been correlated with the predictions of simple analyses in some cases,<sup>(11-14)</sup> the detailed physics of the GAT are not well understood. There has been a recent study of similar physical processes in point-plane gaps in air.<sup>(15)</sup>

Experimental observations described in Ref. 1 and by Douglas-Hamilton and Rostler<sup>(16)</sup> show that the first visible evidence of the GAT is observed in the cathode sheath region. Similar observations have been made in self-sustained diffuse discharges.<sup>(17)</sup> A simple model for these developing arc precursors is described in Ref. 16.

#### G. Electron Energy Distributions.

The electrons are usually the primary conducting medium in diffuse discharge switches because they are much more mobile than positive or negative ions. The electrons gain energy from the applied electric field and lose energy in collisions with the neutral gas-molecules and atoms. The resulting electron energy distribution (EED) determines the transport properties of the electrons such as their

drift velocity and their recombination and attachment rate coefficients. A forthcoming paper by Pitchford and Phelps<sup>(18)</sup> discusses the various models which have been developed to predict the EED's and describes the conditions for which these methods are applicable, as well as giving many additional references.

#### H. Status and Research Needs.

The models which are briefly described in this paper are capable of predicting many of the properties of externally ionized diffuse discharges which are of practical interest for diffuse discharge switch design. For example, the rate equation models described in Section B can be used to determine the required switch gas properties, gas pressure, physical dimensions and e-beam properties for various applications. Calculations of this type for a simple non-inductive circuit are described by Dzimanski and Kline.<sup>(6)</sup> The author is not aware of any similar studies of diffuse discharge opening switches in inductive energy storage systems.

The e-beam deposition and two-dimensional discharge models described, respectively, in Sections C and D can be used to study and design the two-dimensional properties of switch discharges. Similar studies performed in the context of laser discharge design are described in Refs. 7, 9 and 10.

Existing models of the electrode sheath regions, discussed by Bychkov, et al.,<sup>(1)</sup> can be used to make approximate predictions of sheath region properties. However, our understanding of these regions is incomplete, as discussed in Ref. 1 and by Tran Ngoc, et al.<sup>(11)</sup> Furthermore, the author is not aware of any studies of sheath region properties during the turn off phase of a diffuse discharge. The evolution of the sheath region during this period may be important in determining the development of the glow-to-arc transition and the ability of the switch to open.

REFERENCES

1. Yu I. Bychkov, Yu D. Korolev, and G. A. Mesyats, "Pulse Discharges in Gases Under Conditions of Strong Ionization by Electrons", Sov. Phys. Usp. 21, 944-958 (1978).
2. J. D. Daugherty, "Electron Beam Ionized Lasers", in Principles of Laser Physics, G. Bekefi, Ed (Wiley, New York, 1976).
3. B. M. Koval'chuk, Yu D. Korolev, W. V. Kremnev, and G. A. Mesyats, "The Injection Thratron - A Completely Controlled Ion Device", Soviet Radio Engr. and Electr. Phys., 21, 112-115 (1976).
4. R. O. Hunter, "Electron Beam Controlled Switching", Proc. IEEE Int'l Conf. Pulse Power Conf., Paper IC8 (1976); U.S. Patent 4-063-130 (1977).
5. P. Bletzinger, "Electron Beam Switching Experiments in the High Current Gain Regime", Proc. 3rd IEEE Int'l Pulsed Power Conf. (1981).
6. J. Dzimianski and L. E. Kline, "High Voltage Switch Using Externally Ionized Plasmas", Final Report No. AFWAL-TR-80-2041 (1980). (Air Force Weight Aeronautical Lab, Dayton, OH).
7. B. N. Srivastava, G. Theophanis, R. Limpaecher and J. C. Comly, "Flow and Discharge Characteristics of Electron-Beam-Controlled Pulsed Lasers", AIAA J., 19, 885-892 (1981).
8. R. C. Smith, "Use of Electron Backscattering for Smoothing the Discharge in Electron-Beam-Controlled Lasers: Computations", Appl. Phys. Lett. 25, 292-295 (1974).

9. J. A. Filcoff, P. J. Roache and W. M. Money, "Polarization and Space Charge Effects in Electrode Design", Proc. 3rd IEEE Int'l. Conf. on Pulsed Power (1981).
10. C. G. Parazzoli, "Electron-Beam-Stabilized Discharge in a Flowing Medium: Numerical Calculations, AIAA J., 16, 592-599 (1978).
11. Tran Ngoc An, E. Marode and P. C. Johnson, J. Phys. D 10, 2317-2328 (1977).
12. D. H. Douglas-Hamilton and S. A. Mani, "Attachment Instability in an Externally Ionized Discharge", J. Appl. Phys. 45, 4406-4415 (1974).
13. W. H. Long, Jr., "Discharge Stability in e-Beam Sustained Rare-Gas Halide Lasers", J. Appl. Phys. 50, 168-172 (1979).
14. R. T. Brown and W. L. Nighan, "Stability Enhancement in Electron-Beam-Sustained Excimer Laser Discharges", Appl. Phys. Lett. 35, 142-144 (1979).
15. E. Marode, F. Bastien and M. Bakker, "A Model of the Streamer-Induced Spark Formation Based on Neutral Dynamics", J. Appl. Phys. 50, 140-146 (1979).
16. D. H. Douglas-Hamilton and P. S. Rostler, "Investigation of the Production of High Density Uniform Plasmas", Final Report No. AFWAL-TR-80-2087 (1980).
17. R. R. Mitchell, L. J. Denes and L. E. Kline, "Electrode Surface Field and Preionization Effects on the Spatial Distribution of Arcs in CO<sub>2</sub> Laser Discharges", J. Appl. Phys. 49, 2376-2379 (1978).
18. L. C. Pitchford and A. V. Phelps, "Comparative Calculations of Electron-Swarm Properties in N<sub>2</sub> at Moderate E/N Values", to appear in Phys. Rev., Jan. 1982.

GROUP REPORTS



## REPETITIVE OPENING SWITCHES

I.M. VITKOVITSKY

(Chairman)

Introduction

The group's meetings have focused its attention on the range of applications of interest to DoD which require repetitive opening switches. Selecting one application, a straw-man switch design has been carried out. By using this approach, the major research needs for this type of switching became clear. The selection of the specific design was based on the perception of the group obtained from discussions at the general workshop meetings and from the conversations with members of other Working Groups. Two main points regarding the scenarios, where repetitive opening switches might be used, are:

- a) Charging of capacitive loads by inductive storage is becoming an important task (due to the need to reduce the pulse power supply weight, cost and reliability)
- b) Both CW and burst operations are important.

Applications

Review of the applications developed last year at the US ARO Workshop on Repetitive Opening Switches has indicated that additional applications should be considered. Thus, one of the categories, the directed energy application, has been explained and in Table I. Four subcategories are listed:

TABLE I: TYPICAL REQUIREMENTS

PULSED PARAMETERS		DIRECTED ENERGY				OTHER	
		ATA	Mod Betatron*	Laser A	Laser B	SREMP	EM PROPULSION
$V_{oc}$		0.1-1.0 MV	0.5 MV	10-100 KV	10-20 KV	MV's	5-20 KV
Rep Rate		~ 10 KHz (Burst)	1 shot (10 KHz)	10-100 Hz (CW)	100 Hz	100 Hz (Burst)	100-500 Hz
$I_{Peak}$		10-100 KA	200 KA	1-30 KA	20 KA	10 KA	1-5 MA
Life		$10^6-10^8$ Shots	Long	$10^6-10^8$ Shots	$10^8$ Shots	Short	$10^6-10^8$ Shots
Type of Load		Capac.	Induct.	Capac.	Resistor (Flash)	Capac.	Resistor (dL/dt)
C S H T W A I I R M T A E C C S H T E R	Cond.	20 $\mu$ s	1 sec	100 $\mu$ s	100's $\mu$ s	msec's	1sec
	Open	<1 $\mu$ s	1 ms	<1 $\mu$ s	few $\mu$ s	1 $\mu$ s	~100 $\mu$ s
	Hold Off	2-5 $\mu$ s	ms	2-10 $\mu$ s	100 $\mu$ s	10 $\mu$ s	1-5 ms

\* Accelerating Field Coil

ATA, Modified Betatron Accelerator, Laser A and Laser B. ATA parameters are unchanged from last year. The modified betatron requires large (~ 150 MJ) inductive store to drive accelerator and guide coils. Laser designs include pulse-line (Laser A) and flashlamp source (Laser B). A new Army requirement for Source Region EMP (SREMP) is also included. Electromagnetic Gun requirement is unchanged from last year.

In considering systems that use repetitive opening switches it became clear that more detailed specification of the time characteristics of the opening switch is needed. Consideration of circuits employing inductive stores and opening switches show that periods required to characterize the switch are:

- $T_{ch}$  - Conduction time needed to charge the inductor
- $T_{open}$  - Opening time
- $T_{hold-off}$  - Hold-off time, which allows the switch to maintain voltage necessary to drive the discharge into the load.

By including all three of these times in Table I, rather than opening time only, as was done last year, and recognizing that in repetitive operation  $T_{pp}$  (pulse-to-pulse interval) can be longer than inductor charging time, the importance of conduction time became evident. Its importance is due to the need to maintain ionization level of the diffuse discharge of the switch and due to absorption of the energy from the inductor (which arises from the non-vanishing forward resistance)

during relatively long conduction time (in contrast to short opening time).

### Strawman

As a basis for developing a switch design that points to limitations of, and opportunities presented by, the use of repetitive opening switches, parameters of ATA were used. It was assumed that ATA's 50 pulse lines are to be charged by an inductor.

Parameters chosen for the straw-man design are the following:

Pulse line voltage	=	250 kV
Output current	=	40 kA
Pulse length	=	40 ns
Burst	=	40 pulses with 100 $\mu$ s pulse-to-pulse separation
Total ATA pulse energy	=	800 kJ

The inductor is to store 8 MJ, so that pulse energy represents only 10% of the stored energy. This allows the inductor to charge the pulse lines at approximately constant current. It also provides a reserve of energy for the switch dissipation. Assuming further that the pulse lines are to be charged from an inductor in a period 40 times longer than the pulse time, the charging current is about 50 kA. The size of the inductor needed to store 8 MJ at this current is 6.4 mH. Since the required capacity for all 50 pulse lines is 0.5  $\mu$ F,

the charging time  $\sqrt{LC} = 60 \mu\text{s}$ , i.e., too long for water dielectric PFL. Thus, one solution would be to divide L into 10 parallel sections driving 1/10 of the pulse lines at 50 kA per inductor resulting in 6  $\mu\text{s}$  charging time.

The switch requirements follow from the above considerations:

During opening phase:

$$\begin{aligned} T_{\text{open}} &= T_{\text{hold-off}} &&= 6 \mu\text{s} \\ \text{Switch } R_{\text{open}} &&&= 5 \Omega \\ I^2 R_{\text{open}} &&&= 10^{10} \text{ W} \\ E_{\text{dissip}} &&&= 10 \text{ kJ/pulse for ramp} \\ &&&\text{charging waveform.} \end{aligned}$$

During conduction phase:

	Assumption 1	Assumption 2
$T_{\text{cond}}$	$= 100 \mu\text{s}$	$100 \mu\text{s}$
$V_{\text{switch}}$	$= 200 \text{ V}$	$1 \text{ kV}$
$R_{\text{cond}}$	$= 4 \text{ m}\Omega$	$20 \text{ m}\Omega$
$I^2 R_{\text{cond}}$	$= 10^7 \text{ W}$	$5 \times 10^7 \text{ W}$
$E_{\text{Dissip}}$	$= 1 \text{ kJ/pulse}$	$5 \text{ kJ/pulse}$

For Assumption 2, the total 40-pulse dissipation (including opening phase contribution) is 600 kJ. The amount of gas (at 1 Atm) needed to absorb  $0.1 \text{ J/cm}^3$  (result presented by the Modelling Work Group) and operate properly is  $6 \times 10^6 \text{ cm}^3$ .

Adding the volumes of switches for 10 inductors the total volume is  $6 \times 10^7 \text{ cm}^{-3}$ .

Switch performance is derived from assuming gas  $\rho$  of  $10 \text{ } \Omega\text{-cm}$  and  $E_{\text{breakdown}}$  of  $10 \text{ kV/cm}$  (1 Atm). From  $R = \rho d/A = 0.02$  and  $dA = 6 \times 10^7 \text{ cm}^{-3}$ , switch area is about  $10^5 \text{ cm}^2$ . This suggests  $d$  of more than a meter, so that hold-off is at least 1 MV. Using injected beam energy of 200 keV, the electron range in gases suggests that the switch may be redesigned for somewhat larger area and several sections in series. At this point it makes more sense to consider improvements in higher gas energy density, lower resistivity and in circuit techniques, rather than further refining the straw-man design parameters. This becomes even more evident, when the requirement on the electron beam injection is folded in.

The injected electron beam energy at  $1 \text{ A/cm}^2$  of discharge current (requiring about  $10^{-2} \text{ A/cm}^2$  of beam current for volume discharge and resistivity control) is 2 MJ. Gas conductivity decay data and the long opening time suggests that it may be possible to inject the electron beam pulse for about 1/10 of the total conduction time, reducing the e-beam energy to 200 kJ (at the expense of having to turn the control beam on and off at appropriate times). This is discussed in the Appendix A.

As the ATA system requirements are changed to 10 pulse bursts, the switch becomes a much more manageable device.

### Recommendations

The long conduction time required by many switch applications and the resulting energy absorption is one of the problems affecting the switch design. The gas resistivity during conduction is another related problem. Both of these considerations lead to increased gas volumes and, in turn, lead to more demanding requirements on the electron beam generation. These consideration and possibility of reducing electron beam injection requirements lead to the following recommendations for research topics:

1. Determine gas mixtures with lowest resistivity (below 30  $\Omega$ -cm available at present).
2. Determine gas mixtures which retain desirable electrical characteristics after energy deposition into the mixture substantially exceeds 0.01 J/cm<sup>3</sup>.
3. Study conductivity decay time and volume-to-channel discharge transition as a function of e-beam density and duration, with the idea of reducing e-beam requirements for switches with long conduction time.

In addition to research topics above, the Working Group also recognized that variety of engineering difficulties exists. These include injection window heating, storage and control of the e-beam circuit, possible gas flow requirements. Any one of these problems may suggest worthwhile research.

The most important issue arising from the limits on switch performance that will require evaluation is the nonlinearities that can be expected from modularizing of given switch design for use in parallel and series combinations.

The overall recommendation of this Working Group is that the potential pay-off from the type of research proposed is very significant, that the switches can be expected to work in several scenarios and that the problems while difficult are not insurmountable.



## Appendix A

Fig. 1A provides an example of the experimentally measured current flow in the  $N_2-O_2$  gas mixtures ionized by an electron beam current,  $i_e$ . The conduction period depends on the relative amounts of electronegative and non-attaching molecules. For 100%  $N_2$  the conduction decays over  $\sim 0.5 \mu s$  period. Using Ar gas, conduction can be extended to very long times without turning-off at an appropriately high applied electric field. This property can be used to minimize the electron beam energy required for practical switches in the following manner. Selecting a gas mixture with long turn-off time, the ratio of the switch conduction time to e-beam injection time,  $T_{ch}/T_e$ , can be much greater than unity. The value of the ratio will depend on the opening time requirement. That is, the conductivity decay time can not be longer than the switch opening time, because e-beam cut-off is used for switching action. In the example discussed by the Working Group, this value was  $\sim 6 \mu s$ . Assuming the e-beam injection time of 200 ns is sufficient to ionize the gas to provide a required level of resistivity,  $T_{ch}/T_e$  of 15 can be easily utilized.

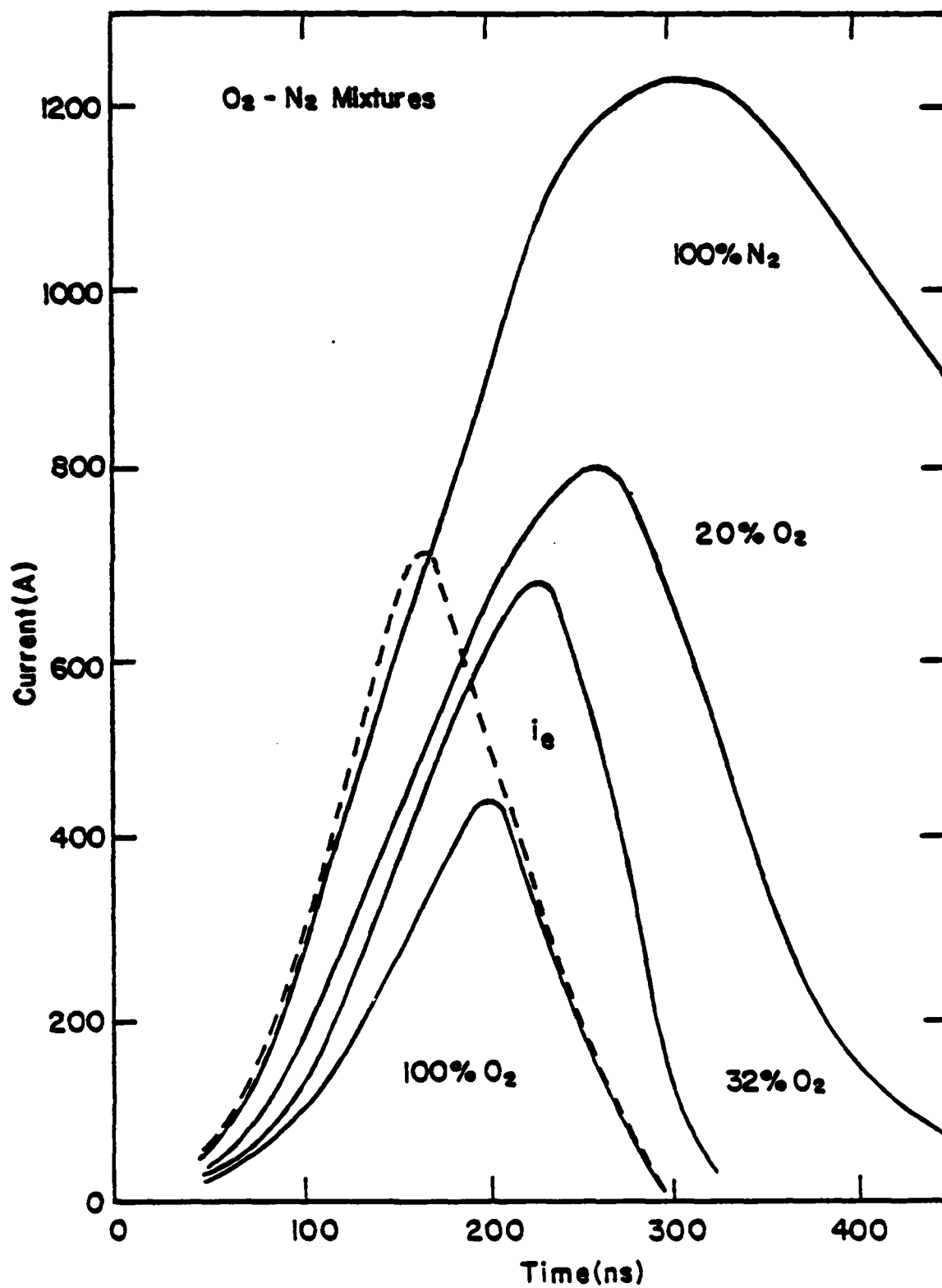


Fig. 1A

DIFFUSE DISCHARGE PRODUCTION  
(ELECTRON BEAM DISCHARGE SWITCH)

D. H. Douglas-Hamilton  
(Chairman)

A. INTRODUCTION

The salient results of the workshop discussion on diffuse discharge switching are summarized here. The discussions were limited to electron beam generated diffuse discharges. We list the equations describing conductivity and gas heating in the discharge, point out the important practical limits on gas heating in the controlled discharge regime, and give the expressions for calculating discharge onset and cutoff behavior (important since a large fraction of switch heating can occur at onset and cutoff). The results assumed for gas heating limits are comparable with experimental results obtained at Northrop and AVCO Everett.

Complete definition requires knowledge of external circuitry. For the present purpose, external circuitry is of two types; constant voltage (e.g. capacitor) or ballasted (e.g. resistive or inductive). In the latter case the effect of changing current on the electric field must be taken into account. In principle this requires computer solution of the discharge and circuit equations. We have analyzed a possible switch for the constant-voltage case, using discharge properties measured in  $\text{CH}_4$ .

Thermal, acoustic and attachment instabilities are all going to be important in this type of switch, which for reasons of efficiency and volume reduction is likely to be operated as near the discharge arcing limits as possible.

We therefore recommend that further research should be done on attachment and thermal/acoustic instabilities.

### 1. Summary of Discharge Equations

The elementary equations describing the electron beam sustainer (EBS) discharge are derived here, and then put into a form in which the power into the EBS switch can be obtained.

The electron beam ionizes the gas producing a steady-state secondary electron density  $n_e$ . This density is described by the differential equation:

$$\frac{dn_e}{dt} = \frac{\overline{j_{eb}} D^{-1} (\partial E / \partial m) \rho}{e E_1} - \alpha n_e^2 - \beta n_e ;$$

where  $\overline{j_{eb}}$  is the mean EB current density within foil-melting limitations,  $D$  is the EB duty cycle (so that  $D^{-1} \overline{j_{eb}}$  represents the EB current density during the pulse),  $\partial E / \partial m$  is the mass stopping power for the gas being irradiated, typically  $\sim 2 \times 10^6$  eV cm<sup>2</sup>/g at beam energies of interest, and  $\rho$  is the gas density.  $E_1$  is the effective ionization potential: typically  $E_1 \sim 35$  eV. The recombination coefficient  $\alpha$  and attachment coefficient  $\beta$  determine the volume electron loss rate in the discharge. For an efficient switch, in the EB-on state the major electron loss will be recombination; the attachment phenomena are important only in onset and cutoff, steepening the current pulse. In

steady state the electron density is then described well by the expression:

$$n_e = \left[ \frac{\overline{j_{eb}} D^{-1} (\partial E / \partial m) \rho}{e E_i \alpha} \right]^{\frac{1}{2}},$$

and the discharge gas conductivity  $\sigma = n_e e V_o / E$ , where  $V_o$  is the electron drift velocity and  $E$  is the electric field in the discharge. We then obtain the expression for the conductivity:

$$\sigma = \left[ \frac{\overline{j_{eb}} D^{-1} (\partial E / \partial m) e \rho}{\alpha E_i} \right]^{\frac{1}{2}} \cdot \frac{V_o}{E} \cdot \frac{\rho_o}{\rho}$$

For the gas mixture 90%  $CH_4$ , 10%Ar at 10 atm, we take the values

$$\overline{j_{eb}} \approx 1 \text{ mA/cm}^2 \text{ (foil heating limitations).}$$

$$D = 1$$

$$\frac{\partial E}{\partial m} = 2 \times 10^6 \text{ eV cm}^2/\text{g}$$

$$\rho(10 \text{ atm}) = 8.4 \times 10^{-3} \text{ g cm}^{-3}$$

$$V_o = 10^7 \text{ cm/sec}$$

$$E = 500 \text{ V/cm atm}$$

$$\alpha = 10^{-7} \text{ cm}^3/\text{sec}$$

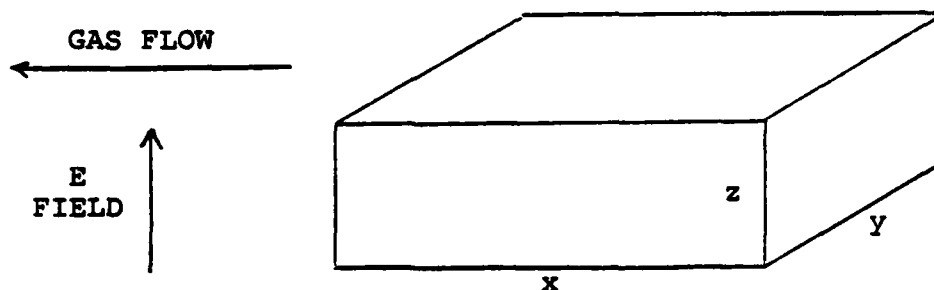
$$E_i = 35 \text{ eV}$$

Each of these numbers can be separately justified. Note however that the mean electron beam current density, averaged over time, of  $1 \text{ mA/cm}^2$  is optimistic; conventional multi-pulsed lasers operate at  $\sim 0.1 \text{ mA/cm}^2$ , and we are assuming that foil

material and foil cooling technology can be improved up to the above level. In the later estimate of the switch calculated in section 6, we adopt the more conservative current density of  $200 \mu\text{A}/\text{cm}^2$ . It will be shown that in any event the switch area only depends on the EB current density as  $j_{\text{eb}}^{1/4}$ , so the switch area changes slowly with assumed EB current density. We have chosen  $E = 500 \text{ V/cm}$  because this is the experimental Ramsauer minimum for the above gas mixture, and at this point the electron drift velocity is  $10^7 \text{ cm/sec}$ ;  $\partial E/\partial m$  is taken from Berger and Seltzer [Table of Electron Energy Losses, NAS-NRC #1133 (1964)]. We then find  $\sigma_{10 \text{ atm}} = 1.8 \times 10^{-3} \text{ mho/cm}$  and  $\sigma_1 \text{ atm} = 5.5 \times 10^{-3} \text{ mho/cm}$ .

Heating per unit volume (molecular gas, not vibrationally excited):

$$\Delta T = 845 \frac{\rho_0}{\rho} \cdot \frac{z}{\sigma_{xy}} I^2 \cdot \frac{\tau}{xyz}$$



$\rho_0$  = Gas density, NTP,  $\text{g}/\text{cm}^3$

$\tau$  = Pulse duration

$$\text{Area: } xy = I \left[ \frac{845 \rho_o \tau}{\rho \sigma \Delta T} \right]^{\frac{1}{2}} = I \left[ \frac{845 E \tau}{V_o \Delta T} \right]^{\frac{1}{2}} \left[ \frac{\alpha E_i}{j_{eb} D \frac{\partial E}{\partial m} e} \right]^{\frac{1}{4}} \cdot \frac{1}{\rho^{1/4}} .$$

Gas Flow Rate:  $F = xyzN$

N: Repetition Rate, Hz.

Gas Mass Flow:  $\dot{M} = \rho F = \rho xyzN$ .

Power into Switch:  $P_{\text{switch}} = \dot{M}(1+\gamma) \frac{R\Delta T}{M} = \frac{zI^2}{\sigma xy}$  .

$\gamma = 1.4$

$R = 8.3 \text{ j/mole}$

$M = \text{molecular weight of gas}$

Discharge Width:  $z = (V_e/E_{\text{crit}}) \frac{\rho_o}{\rho}$  .

$V_e$ : Switch-off voltage standoff required

$E_{\text{crit}}$ : Maximum hold-off field possible for NTP discharge after discharge cutoff ( $E_{\text{crit}} = 6\text{-}12 \text{ kV/cm}$ ).

In Section 6 we will use these relations to derive parameters for a "Strawman" switch suitable for ATA inductive storage.

Limit on  $\Delta T$ : Wide experience at Avco, Northrop and elsewhere drives us to the conclusion that typical attainable EB-sustainer discharge loadings up to the arcing limit result in  $\Delta T \sim 500^\circ\text{K}$  for NTP discharges in a molecular gas. This limit on  $\Delta T$  might perhaps be improved for peculiar gases such as CO, in which discharge energy is retained for long times in upper vibrational states; but the addition of attaching electron scavengers to the gas is also likely to deactivate the stored vibrational energy

by VT transitions. Another approach is use of optically polished electrodes, for which Denes & Kline (Westinghouse) found 2 to 3 times better stand-off in self-sustaining discharges. It is an open question whether this technique can be applied to EB sustainer discharges.

## 2. Turn-on and Turn-off Behavior

A large fraction of the total power deposited in the switch will be deposited during the impedance-change phase of the switch at turn-on and turn-off.

For an attachment-dominated process, the electron density will be given by:

$$\frac{dn_e}{dt} = -\beta n_e,$$

$n_e$  = electron density

$\beta$  = attachment rate.

Typically we select an attaching gas mixture where  $\beta$  is an increasing function of  $E$

$$\beta = \beta(E)$$

and the discharge field  $E$  is determined by the external circuit of which the switch is a component.

The total energy deposited in the switch during this phase is then

$$\epsilon = \int_0^t j E \cdot xyz \, dt$$



where  $j = n_e e \mu E$ , and  $\mu$  is electron mobility, we use  $\mu \sim \frac{10^7}{500} = 2 \times 10^4 \text{ cm}^2/\text{Vsec}$  at 1 amagat in the methane-argon mixture discussed above.

The external circuitry must therefore be known before the energy deposited in the switch during onset and cutoff can be estimated.

In the case where  $E$  is constant, during onset the electron density becomes

$$n_e = n_{e0} (1 - e^{-\beta t}),$$

where we are neglecting recombination and  $n_{e0}$  is the steady-state electron density. The energy deposited in the switch is then

$$\begin{aligned} \epsilon &= \int_0^t j \cdot E \cdot xyz \, dt \\ &= P t \left( 1 - \frac{1 - e^{-\beta t}}{\beta t} \right) \end{aligned}$$

where the steady-state power deposited is  $P = n_{e0} e V_0 E_{xyz}$ .

The ratio of the actual energy deposited in the switch to the energy deposited if it reached steady-state instantaneously is then

$$R = \frac{\epsilon}{Pt} = 1 - \frac{1 - e^{-\beta t}}{\beta t}.$$

Note that for  $t \sim 2/\beta$ , by which time the discharge has essentially reached steady-state, we find  $R = 57\%$ . Under these circumstances the power deposited during onset is

less than that deposited in steady-state. If the electric field increases when the current is low, as in a ballasted discharge, the situation is different and the discharge behavior will depend on the specific circuitry. In this case a large fraction of total energy can be deposited during the discharge onset and cutoff.

### 3. Instabilities.

#### a. Attachment Instabilities.

Any system in which  $\beta$  is a rapidly increasing function of  $E$  will be subject to attachment instability\* (increasing local field reduces local electron density, thereby further increasing local field and further reducing local electron density, etc).

We are considering gases with this type of attachment rate to provide rapid cutoff and onset. Optical or other less than uniform changes in attachment rate will lead to this instability. Analysis of the parameter field within which this problem exists for the attaching gas mixture recommended for switches will be required.

Therefore we recommend investigation of attachment instability interaction with the EB switch, and its dependence on the variable  $E$  which will result from certain switch circuits.

---

\*Douglas-Hamilton and Mani, J. Appl. Phys. 45, 4406 (1974).

#### b. Flow and Acoustic Phenomena and Instabilities

The effective run times for the selected opening switch are quite long, ~ 500  $\mu$ sec. The switch gas is repetitively heated to an approximate  $\Delta T$  of ~ 500°K. This will lead to a gas overpressure. Moreover the repetitive nature of the 10 pulse burst can create a series of sound waves that can rattle around in the switch during the discharge. The dimensions of the switch are such that the sound waves travelling at 10-50 cm per ms (dependent on the nature of the gas and the temperature) can make several transverse transits in the strawman switch. Such waves, depending on their strength, can cause significant local density fluctuation which can lead to discharge instabilities or arc formation. Thus the ideal switch needs to be designed with an emphasis on gas dynamics and acoustic damping that is at least as detailed as the discharge phenomena and the coupling of the switch to the circuit. It is recommended that an acoustic scaling analysis be performed to develop designs for switch geometry and acoustic damping that will allow the gas medium to perform as close to its "homogeneous density" limit as possible. Effects of the repetitive pulsed loading need to be considered in this analysis.

#### 4. Beam Pinch in the Switch

The e-beam being used to ionize and sustain the discharge will be subject to a magnetic field created by the current flow in the discharge. This field will tend to pinch the

ionizing beam in the discharge. This effect requires the use of an external magnetic field to compensate the discharge magnetic field if the currents exceeds a critical value depending on aspect ratio. For the selected switch the effect is minor, but switches carrying several tens or hundreds of kiloamps is expected to require external fields of order 2 kGauss.

### 5. Methane Datapoints

For the Strawman switch we will use discharge parameters based on methane: and for convenience summarize here results obtained from discharges in methane.

#### a. Drift velocity:

Data computed by L. Kline indicate a drift velocity  $V_0$  peaking at 3 Td (Ramsauer minimum) at  $> 10^7$  cm/sec. By adding Argon, the peak can be shifted to lower E/N (L. Foreman et al., Phys. Rev. A, 23, 1553 (1981)) at some decrease in  $V_0$  (but relative increase vs. pure methane). Using L. Kline's methane data, a comparison between the AF-propulsion lab data and the theoretical data resulted in the same discharge current density values at higher discharge voltages, if the E-beam source function was increased 10-50% for the theoretical curves. This discrepancy is within error limits of determining the experimental source functions. (At lower discharge voltages the experimental values were considerably higher, due to the cathode sheath/ionization effects.)

#### b. Switch-on

As predicted by theory the current risetime decreases as a function of E-beam current, such that at  $\overline{j_{eb}} = 1.3 \text{ mA/cm}^2$

(post-foil) the risetime was limited by the E-beam current risetime ( $\leq 1\mu\text{s}$ ).

c. Switch-off, recombination attachment

Observed 90%-10% current decay times for  $1\text{ A/cm}^2$  discharge current density were  $\sim 10^{-5}\text{ s}$  (for lower  $j_0$ , the long recombination tail will increase this value). Modelling the decay using E/N dependent recombination rates, a good match was achieved, if L. Kline's recombination data was increased by 10X and an E/N independent attachment frequency  $\nu_a = 2.8 \cdot 10^4\text{ 1/s}$  was added. According to M. Biondi, the increased recombination rate can be explained by the much larger molecular ions which will be encountered at atmospheric pressure vs. the  $\text{CH}_4^+$  ion measured in the low pressure cross section experiments. Using E/N independent recombination rates, a least-square fit to the decay data resulted in  $\alpha = 8.3 \cdot 10^{-7}\text{ cm}^3/\text{s}$  and  $\nu_a = 1.8 \cdot 10^5\text{ 1/s}$ ; the fit was not as good as with the E/N dependent data.

d. Discharge voltage

Using a variable electrode spacing the cathode fall voltage at  $\overline{j_{\text{eb}}} = .75\text{ mA/cm}^2$ ,  $j_b = .7\text{ A/cm}^2$  was 600 V; at  $\overline{j_{\text{eb}}} = .3\text{ mA/cm}^2$ ,  $j_b = .4\text{ A/cm}^2$  it was 750 V. Since  $V_{\text{cath}} \approx f(j_b)$ ,  $V_{\text{cath}} \approx f(\sqrt{j_{\text{eb}}})^{-1}$  as expected.

The discharge voltage was as low as 1 kV at  $1\text{ A/cm}^2$  at 2.2 cm electrode spacing ( $j_0 = 1.3\text{ mA/cm}^2$ ), so with consideration of  $V_{\text{cath}}$ ,  $E < 500\text{ V/cm}$ .

e. Summary

A. drift velocity  $V_0 \sim 10^7$  cm/sec has been predicted and observed in  $\text{CH}_4$  and Ar mixtures at  $E \sim 500$  V/cm. No attaching electron scavengers were added to this gas mixture. M. Biondi points out that addition of such species may increase the recombination rate to the neighborhood of  $10^{-6}$   $\text{cm}^3/\text{s}$ . However, in practical EB sustainer gas laser discharges, which are by no means ideal pure gases, typically  $\alpha \sim 2 \times 10^{-7}$   $\text{cm}^3/\text{s}$ ; therefore we believe  $\alpha \sim 10^{-7}$   $\text{cm}^3/\text{s}$ ,  $V_0 \sim 10^7$  cm/s at  $E \sim 500$  V/cm atm are attainable practical discharge parameters.

6. Straw Man Calculation

Taking the ATA requirement:

$$V_e = 250 \text{ kV} \quad [\text{Capacitor } 400 \times 10^{-9} \text{ f}].$$

$$I = 10 \text{ kA through switch}$$

$$\tau_{\text{on}} = 50 \text{ } \mu\text{s} \text{ [charging time]}$$

$$\tau_{\text{off}} = 10 \text{ } \mu\text{s}$$

for a burst of 7 pulses, repeated 4 times per second. Effective on-time is then  $\tau = 50 \times 7 \text{ } \mu\text{s}$ , between clearings. We assume a gas pressure of 10 atm, in 90%  $\text{CH}_4$ , 10% Ar, with a stand off capability of  $E_{\text{int}} = 5 \text{ kV/cm}$  at NTP.

Then  $z = (V_e/E_{\text{int}}) \rho_o/\rho = 5 \text{ cm}$ . We make the conservative assumption  $\overline{j_{\text{eb}}} = 200 \text{ } \mu\text{A/cm}^2$ , with  $D = (50 \times 10^{-6} \times 7 \times 4) = 1.4 \times 10^{-3}$ . Then  $\sigma = 2.1 \times 10^{-2} \text{ mho/cm}$ .

$$\text{Area:} \quad xy = 10^4 \sqrt{\frac{845 \times 50 \times 7 \times 10^{-6}}{10 \times 2.1 \times 10^{-2} \times 500}} = 531 \text{ cm}^2.$$

$$\text{Volume:} \quad xyz = 2.7 \text{ liter}$$

Gas Flow:  $F = xyz N = 11 \text{ liter/sec. } \Delta 89 \text{ g/sec.}$

Power into Switch: a) Discharge:  $\frac{ZI^2}{\sigma xy} = \frac{5x(10^4)^2}{531x2.1x10^{-2}} = 45 \text{ MW}$

For a 200 kV EB, we have:

$$b) \text{ EB: } xyD \frac{1}{j_{eb}} V_{eb} = 531x200x10^{-6}x200x10^3 = 15 \text{ MW}$$

This is EB energy into the gas. Allowing, conservatively, structure and foil EB losses as ~ 30%, we obtain the required EB power as:

$$P_{eb} \sim 22 \text{ MW.}$$

Mean power into capacitor:

$$P = \frac{1}{2} CV^2/\tau = \frac{1}{2} x \frac{400x10^{-9}x250000^2}{50x10^{-6}} .$$

$$= 250 \text{ MW.}$$

Switch Efficiency

$$\eta = \frac{P_{cap}}{P_{cap} + P_{eb} + P_{dis}} = \frac{250}{250 + 45 + 22} = 80\%.$$

Summary

The strawman ATA charging switch does not appear to require physically impossible dimensions or discharge parameters.

Note that a more precise analysis would include the time-variation of current and field across the switch during the charging cycle. As pointed out above, the discharge behavior is highly interactive with the external circuitry. This will be especially significant in a reactive circuit, and the danger of inductive triggering of attachment instability phenomena must be considered.

## 7. Conclusion and Recommendations

We conclude that EB controlled discharges can be used for switching high-current, high-voltage loads under certain circumstances, within discharge gas-heating limitations. We have given a sketch of plausible dimensions for a switch capable of handling the ATA power supply, using a methane-argon mixture. The switch efficiency was ~ 80%.

The use of electron scavenging gases such as fluoro-carbons will result in sharpening the switch onset and cutoff. Precise predictions of onset and cutoff behavior and efficiency can be made by considering the discharge and the circuit as a whole. In general this will need computer analysis.

Electron attachers will expose the switch to problems due to attachment instability. This instability has been observed in high power discharges in gas lasers at AERL, and in general the higher the energy density used in the discharge, the further one progresses into the instability region. Triggering of attachment instability is expected to be a significant problem in switch discharges.

Thermal and acoustic instabilities will also result from multipulse switch operation. We have taken the experimental effective single pulse thermal limit as  $\Delta T \sim 500^\circ\text{K}$ ; multipulse operation on the same gas is very likely to reduce that limit. Acoustic damping will be needed to avoid arc triggering from acoustically generated instabilities.

We recommend work in the field of finding gases with a suitable combination of recombination coefficient ( $\alpha \sim 10^{-7} \text{ cm}^3/\text{s}$ ),



transport coefficients ( $V_0 \sim 10^7$  cm/s), and attachment rate (low at  $\sim 2$  Td, high at  $\sim 30$  Td).

We recommend further study of the attachment instability and investigation of the parameter space of interest for switching. Further understanding of streamers and streamer propagation and initiation in this parameter space is also needed.

We also recommend examination of the problem of acoustically generated instabilities. Experience gained in multipulse high pressure gas laser discharges should be applied to the switch problem.

## GASES

## BASIC DATA AND EXPERIMENTAL METHODS

L. Christophorou (Chairman), L.L. Hatfield

There are several approaches to realize a diffuse discharge opening switch: externally sustained or enhanced discharges or selfsustained discharges with externally controlled loss mechanisms. As none of these approaches has been developed to a stage that makes it necessary to discuss the properties of specific gas mixtures the aim of this group was to identify general requirements that should be fulfilled by a gas or gas-mixture that is used in any type of diffuse discharge opening switch. The most important consideration is based on the general requirement that the properties of the gas mixture have to be chosen in that way that the response of the gas discharge on the external control mechanism, especially during the opening phase, works in the same direction as the control mechanism itself (Table 1), while other consideration aim towards practical or even simple devices.

In the second step (Table 2) the group focussed on needed basic data that are necessary for suggested gases and gas mixtures to predict the behavior of a gas in a diffuse discharge opening switch or, even better, to compose mixtures that fulfill the requirements given in Table 1.

The following tables present the recommendations of the group in an abbreviated form.

Table 1. Desirable Properties of Candidate Gases

- High dielectric strength (effected by strong attachment)

- Attachment properties depend on option

- (i)  $k_a$  low at low E/N and high at high E/N.
- (ii)  $k_a$  high at fixed E/N.

Options (i) and (ii) offer enough flexibility for discharges controlled by either electron beams or lasers, and in the latter case, whether the laser sustains or shuts off the switch.

- High conductivity at low E/N.
  - high electron mobility
  - low rate of electron loss

A low rate of electron loss is a relative measure. The electron loss rate during the conducting phase should be low compared to that during the turn off phase. Some trade off is necessary since the opening time of the switch depends on the electron loss rate during turn off.

- Chemically unreactive; "simple chemistry" (this is of course a relative term). One of the important considerations is that a practical switch has a reasonable lifetime.
- Compatible with e-beam transmission foil, which has to be at high T.

Table 2. Needed Basic Data

- Electron Scattering Cross Sections
  - Total inelastic cross sections down to threshold for diatomics and polyatomics (candidate gases) for processes such as ionization, excitation, etc.
  - Overall (gross) inelastic cross sections to aid modeling and guide choice and tailoring of gases, i.e., a simple measurement which gives some idea as to how effective a gas is in modifying the electron energy distribution.
- Electron transport coefficients for candidate mixtures, especially at high P and high E/N.
  - High p ( $> 1$  atm) and high E/N (at least 120 Td) are both necessary for reasonable opening switch performance.
- Electron attachment coefficients for candidate mixtures over wide ranges of p, E/N, and T.
  - The ranges for p, E/N, and T depend on the gas mixture tested. There is no point in using such high temperatures that one of the constituent gases dissociates, for example. Pressures below one atm. are probably not practical, E/N down to zero is desirable, and temperatures from 300K to 1000K are reasonable.
- Recombination, including ion mobility and clustering over wide P ranges, especially high p ( $> 1$  atm).
- V-T and V-V data to determine how the energy dissipated in the discharge will be distributed among the many degrees of freedom available in the candidate mixture.
- Collisions of atoms, molecules, electrons and ions with excited species. These excited species may be produced in the discharge by photons from an external source or electrons in the discharge. Cross section for processes of interest are needed.

Table 3. Experimental Studies &amp; Tests

The following studies of candidate gases should provide sufficient information for adoption or rejection of the gas for use in a diffuse discharge switch.

- Degradation and recovery
  - To obtain a fast history of the products produced from the gas in a discharge.
  - Use externally sustained source with high pressure mass spectrometry.
  - Time-resolved (laser) spectroscopy.
  - Determine rate of recovery of the gas, i.e. lifetimes of undesirable products
  - Determine chemistry for both charged and neutral species produced from the gas.
  - Does initial gas reform or transform to a product having good insulating properties?
- Thermal Properties
  - Investigate thermal instabilities
  - Energy-density dependent reaction
  - Excitation-relaxation processes.
- Total System studies pertaining to the switch
  - Insulating gas
  - Solid conductors
  - Solid insulators
- Quick switching test for screening of candidate gases
  - Establish empirical indicators of merit
  - Give feedback to those measuring basic data

For use in models the best estimates at present for suitable gases are:

- Electron drift velocity  $\sim 10^7$  cm/s
- Ion recombination coefficient  $\sim 10^7$  cm<sup>3</sup>/s

#### Summary

The following remarks apply to gas mixtures suitable for diffuse discharge opening switches controlled either by a laser or an electron beam.

The mixture must have high dielectric strength which can be obtained through the use of an attaching gas. The conductivity of the discharge must be high for low E/N and low for high E/N. This dictates the functional dependence on E/N of the electron attachment coefficient and electron mobility. The chemistry of the mixture must be simple so that predictions of reactions with the rest of the system (electrodes and insulators) are not too difficult.

Certain gases are already known to satisfy some of the above criteria. Mixtures of gases which have the potential to satisfy virtually all of the requirements should be tested in a pulsed discharge apparatus to determine dielectric strength, conductivity, and chemical reactivity. This kind of quick test could eliminate unsuitable mixtures and identify desirable component gases. In this way, gases could be identified for the more detailed basic data measurements recommended in Table 2.

AD-A115 883

BATTELLE COLUMBUS LABS OH

WORKSHOP ON DIFFUSE DISCHARGE OPENING SWITCHES (JANUARY 13-15, --ETC(U)

APR 82 M KRISTIANSEN, K H SCHOENBACH

DAA629-81-D-0100

F/6 9/5

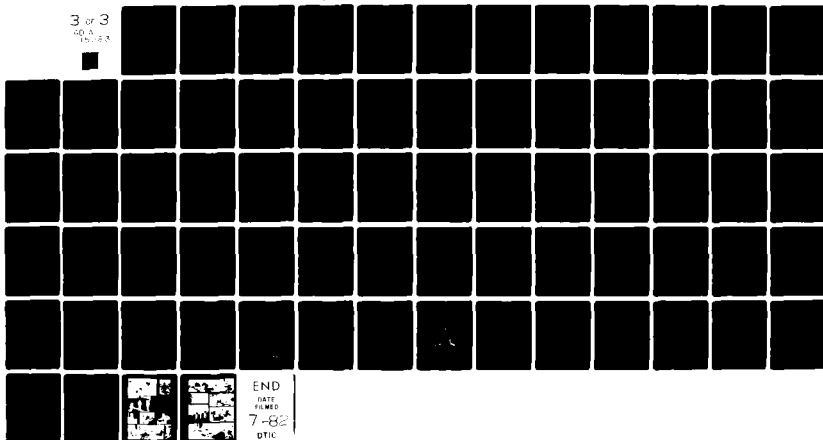
NL

UNCLASSIFIED

3 of 3

NO. 3

15/12/82



END

DATE

FILED

7-82

DTIC

One general statement can be made; only a fraction of the basic data needed is presently available in the literature. However, it is clear that limited resources dictate that care must be exercised in the selection of gases or gas mixtures for which the necessary measurements are to be made.



## OPTICALLY INDUCED PROCESSES

ARTHUR H. GUENTHER

(Chairman)

The members of this working group are to be congratulated not only for their written contributions but for their vigorous involvement in our group discussions and willingness to participate in an open and frank interchange.

The summaries of the group discussions given in this report have mainly been written

by:	Section:
J. N. Bardsley	B.3
P. J. Chantry	B.4
C. Frost	B.8
M. Gundersen	B.2,6
T. Lawler	B.7
T. Leventhal	B.9
G. Schaefer	B.2,4
S. Srivastava	B.5

## A. INTRODUCTION

At last year's Army Research Office workshop<sup>1</sup> on "Repetitive Opening Switches" for inductive energy storage, two principal areas were identified for additional attention. One was the development of a model of discharges which could be employed in circuit analyses programs. The degree of comprehensiveness needed in such a switch model is a question, however, which remains to be addressed before effective progress can be made in this area. The other principal conclusion was that one of the most promising approaches for achieving a repetitive opening switch for use with inductive energy storage was by employing diffuse discharges, potentially controlled by external means (e-beams or photons), either in the open or closed phase. Because the payoff compared to the risk involved was very high for this latter concept it was decided that it should be the theme of this year's workshop, i.e., diffuse discharges in opening switches.

The question asked was not if it would work, (we have some solid evidence that external control of diffuse discharges by both electron and photons does work<sup>2-4</sup>) but rather, the principal problem was to bound the operational range of such switches, e.g. current density, fields, conductivity, geometry, etc. Thus, once we have bound the range of operation, determine if that range is interesting, i.e., can they be made to operate under conditions of interest to the pulsed power community. Our initial considerations are outlined in Table I.

Before proceeding to the individual contributions from our group regarding the topics listed in Table I it is important to point out some differences between the activities of the optically induced processes group and the other groups at the workshop. These other groups generally considered only electron beam controlled discharges and did not dwell to any extent on photon controlled discharges. Our group, unlike the others did not have the "benefit" (?) of the, relatively speaking, wealth of experience and history that e-beam controlled discharges enjoy. Therefore, we were not as inhibited or constrained in our thinking. One must realize that optical control offers distinctly unique advantages such as the efficiency of resonant interaction and the selection of which molecule and transition the energy is deposited (although lasers, in general have lower generation efficiency than e-beams). It also allows for a greater variety in the chemical reactions associated with the discharge species and kinetics as well as a wide selection of controlling optical sources. Photon control, unlike electron control, offers opportunities not only for sustaining and initiating the discharges but also for enhancing the recovery of the dielectric strength i.e., turn-on, sustain, turn-off. Thus, we have concentrated on the desirable characteristics, those chemical kinetic variables which control the behavior of the dielectric medium. We were not system or engineering oriented but more fundamental in our approach. The \$64,000 question is: What are the important or optimum characteristics of an optically controlled

processes? Our initial thoughts and discussions proceeded along the items outlined in Table II.

We have thus addressed issues such as photon-enhanced attachment or the competition between photon and electron processes (See Table III.). We have also looked at screening procedures for candidates, relative to photon enhanced attachment with an emphasis on vibrational processes (See Table IV.). These will be discussed in detail, addressing such issues as a comparison between collisional and optical processes, including electron impact excitation, attachment, and molecule-molecule interactions.

Briefly, we need to identify a mode of excitation of a molecule which leads to enhanced attachment, which can be excited by a laser during the opening phase, and which is not excited significantly by the electrons when the switch is closed. We debated the relative merits of electronic excitation versus vibrational excitation and simple molecules versus polyatomics.

We feel that next year, if one wishes to continue the thrust of this and previous meetings, we should address other points, such as the pressure level under which such switches might operate; include engineering issues, e.g., the potential for placing capillaries in parallel across the switch electrodes for enhancing wall effects, and consider future possibilities, e.g., the state of the art in optogalvanic effects. Secondly we need to select and agree upon key parameters such as the appropriate electron density or conductivity. It is difficult

for each group to work this problem using different assumption or baseline data. Further, there is a need for a stronger interaction between the various groups such that we, individually, don't go our own way. Each group needs to have the benefit of the thinking of members of other groups. There must be a collation of the reports of these committees, i.e., an effective integration upon which there is some consensus. But most importantly we all need to work continuously between these meetings and have experimental results circulated in a timely manner. I would add one note, that we not overlook the opportunity for optically controlled solid state elements in performing the opening switch function with reliability.

#### REFERENCES

1. Workshop on Repetitive Opening Switches, Tamarron, Co., January 28-30, 1981, M. Kristiansen and K. Schoenbach editors, Texas Tech University, Lubbock, Tx. 79409.
2. A. C. Tam, "Quenching Effect of Helium 2- $\mu$  Light on a Weak Helium Discharge," (To be published in IEEE Transactions on Plasma Science)
3. R. O. Hunter, "Electron Beam Controlled Switching," Proc. 1st. Int'l. Pulsed Power Conf., Lubbock, Tx., 1975, IEEE Cat. CH. 1147-8, Paper IC8.
4. A. H. Guenther, "Optically Controlled Discharges," Workshop on Repetitive Opening Switches, pp. 47-64, Tamarron, Co., 1981.

TABLE I

## SUBJECTS DISCUSSED IN THE SESSION "OPTICALLY INDUCED PROCESSES"

## 1. Complete Listing of Possible Processes

- Classification according to pressure - regime
- electron production mechanism
- electron loss mechanism

## 2. Negative V/I Characteristic Suitability

- Desirable during turn-off?
- Tolerable during conducting phase?
- Candidate species identification

## 3. Low Pressure Discharges - Why Not?

## 4. Vibrationally Enhanced Attachment

- Large vibrational excitation by photons
- Collision cross sections with electrons
- Molecule size
- Optical diagnostics

TABLE II

## OPTICALLY INDUCED PROCESSES THAT AFFECT CONDUCTIVITY

During Pulse (Conduction phase)

- Photoionization by one or more photons
- Collisionally assisted ionization
- Excited state phenomena
- Inverse Bremsstrahlung

After Pulse (opening phase)

- Optical quenching of metastable species by optically induced radiative relaxation
- Photoenhanced attachment.

TABLE III  
PHOTOENHANCED ATTACHMENT  
(COMPETITION: PHOTON-ELECTRON EXCITATION)

1. Vibrational Excitation (small molecules)

In gas discharge: e-collision + energy sharing → mainly  
 $v = 1$

needed: molecules with  $k_{\text{attach}}$  strongly increasing  
only for  $v \geq 2$  and (selective) excitation of  $v \geq 2$

- overtone excitation
- $E \rightarrow V, R$  collisions
- $E \rightarrow V, R$  radiative

2. Laser excitation of larger molecules

3. Electronic excitation

4. Photochemical reactions, (multi) photon decomposition

- fragments with higher attachment rate
- vibrationally excited fragments
- radicals



TABLE IV  
SCREENING PROCEDURE FOR CANDIDATES FOR PHOTOENHANCED  
ATTACHMENT BY VIBRATIONAL EXCITATION

1. Absorption at available laser wavelengths (practical consideration)
2.  $k_{\text{attach}}$  (E/N) increasing as E/N increases, and  
 $k_{\text{attach}}$  (E/N) small at conductive E/N of gas mixture
3.  $k_{\text{attach}}$  (T) increasing as T increases
4.  $\sigma(E_e, v = 0)$  maximum, threshold
5.  $\sigma(E_e, v > 0)$
6. a)  $v^*$  - quenching by buffer gas?  
b)  $v^*$  - quenching by attacher?
7. Chemistry, including buffer gas and gas flow.

## B. GROUP DISCUSSIONS

### 1. Introduction

In general two different groups of optically controlled processes for switch applications were considered: The optically controlled electron generation and the optically controlled electron depletion.

Optical processes that either increase or decrease the conductivity are possible. The general decision whether a laser may be used for the conduction phase or for the opening phase mainly depends on the specific application. For applications where the length of the conduction phase is on the order of the length of the opening phase either process may be used. For conduction times much larger than the opening time, processes that increase the conductivity have the disadvantage that the laser has to operate for a long time.

Processes that decrease the conductivity can also be used in combination with e-beam sustained opening switches to achieve shorter opening times and higher hold-off voltages.

### 2. Optically Controlled Electron Generation

The processes considered for control of the electron generation were shown in Table II and are summarized in Fig. 1 and discussed below.

#### (1)-(6) Optically Enhanced Electron Generation

- (1) The "one" photon ionization from the ground state has only been demonstrated in alkali atoms. UV lasers are required.

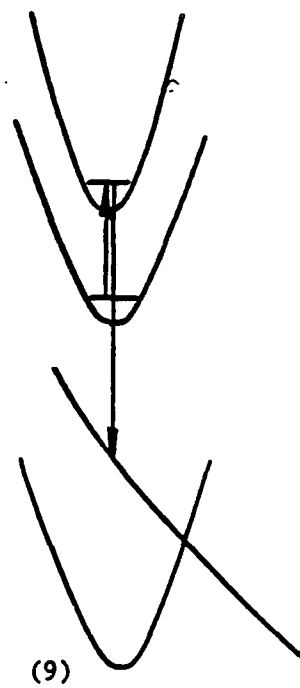
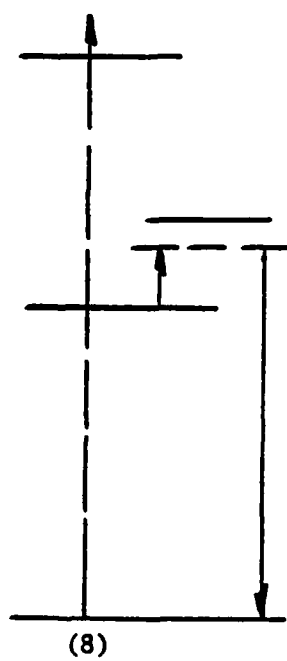
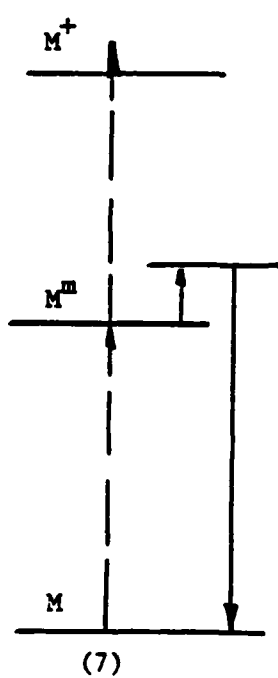
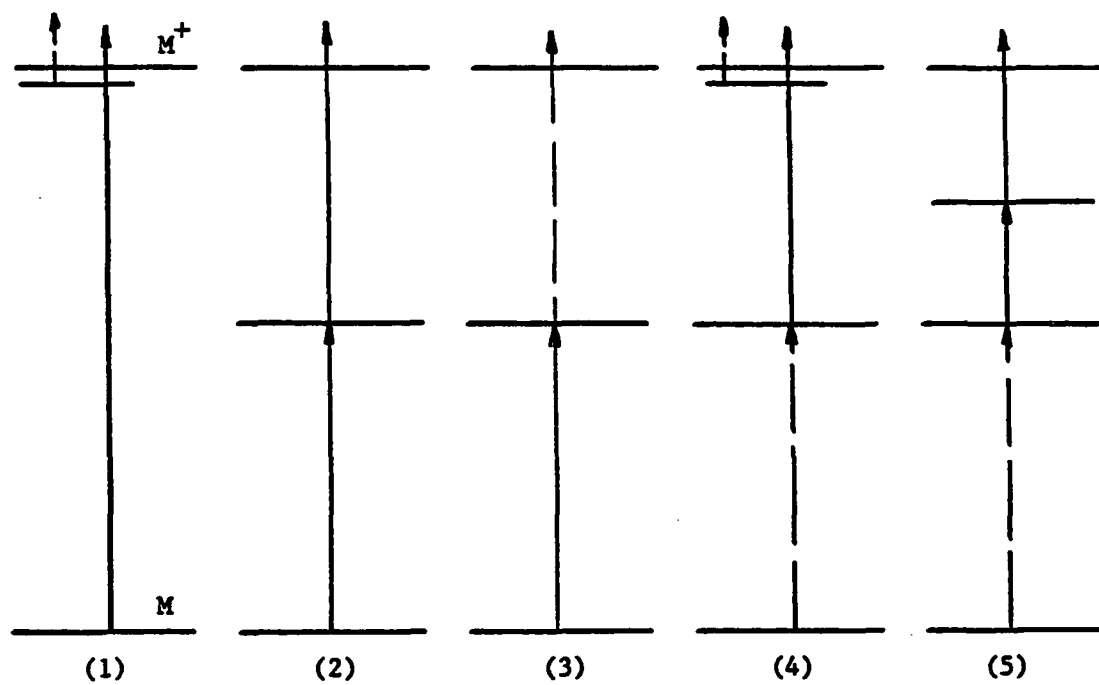


Figure 1.

Processes for optically controlled electron generation

- (2) The two photon ionization from the ground state via a resonant intermediate state has been shown for some molecules with low ionization energy, such as  $(\text{CH}_3)_3\text{N}$ . In this case also UV lasers are required.

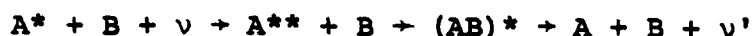
These processes, (1) and (2), can be used for optically sustained discharges while the processes, (3) to (6), below involve collisional excitation.

- (3) The excitation of an intermediate state can enhance the electron generation either through an additional e-collision ionization from this intermediate state, as has been shown for alkali and Hg, or through Penning ionization according to collisions of two excited atoms as known for Na.
- (4) The photoionization starting from an excited state is suggested mainly for systems with metastable states. An example is Hg where high metastable densities can be achieved (>50%).
- (5) The photon ionization from an excited state via an additional intermediate state has the advantage that relatively low photon energies are necessary. Consider the cases, for  $\text{NO}(\text{A} \rightarrow \text{E} \rightarrow (\text{NO})^+)$ ,  $h\nu = 2 \text{ eV}$  or for  $\text{Hg}(6^3\text{P}_0 \rightarrow 7^3\text{S}_1 \rightarrow \text{Hg}^+)$ ,  $h\nu \approx 3 \text{ eV}$  are necessary.
- (6) Inverse Bremsstrahlung: Electrons can absorb energy from the electric field of a laser and transfer the energy through collisions into ionization. This process requires high intensity, high collision frequency, seed electrons, and favors longer laser wavelengths.

## (7)-(10) Optical Quenching

- (7) De-excitation of metastables into resonant states with subsequent stimulated emission or spontaneous emission.
- (8) Raman Processes as in (7), but off-resonance.

## (9) Excimer formation



## (10) Electric field induced emission

3. Optically Enhanced Electron Attachment

The processes considered for optically enhanced electron attachment were shown in Table III.

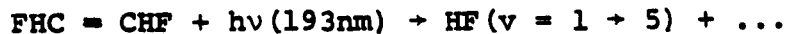
In order to achieve rapid opening without a significant increase in the energy lost in the switch, it is necessary that the attachment rate during the opening phase be much larger than that appropriate to the conduction phase. This can be achieved by including in the gas a molecule which is weakly attaching in the ground state, but which possesses one or more excited states with very large attachment cross sections. The number of molecules in these excited states should be very low during the conduction phase and should be rapidly increased by laser irradiation during the opening phase.

There are several molecules, such as  $H_2$ ,  $HCl$ ,  $HF$ ,  $O_2$ , and  $N_2O$ , for which dissociative attachment is enhanced by several orders of magnitude when the molecule is vibrationally excited. However, large cross sections for dissociative attachment usually imply large cross sections for vibrational exci-

tation by electron impact. Thus, many vibrationally excited molecules (at least with  $v = 1$ ) will be formed when the switch is opened, unless the mean electron energy can be kept below the vibrational excitation threshold in the attaching gas molecules.

Several ideas have been suggested to increase the ratio of photon-induced attachment to electron-induced attachment.

1. Use diatomic molecules containing hydrogen atoms, which have relatively large vibrational spacings.
2. Choose molecules for which the enhancement of the attachment rate is important only for  $v \geq 2$ . If this procedure is followed, then one needs to find optical mechanisms for producing these levels. Some possibilities are:
  - a. overtone excitation
  - b. multi-photon absorption
  - c. electronic to vibrational energy transfer from a different atom or molecule, e.g.
 
$$\text{Na}(3_p) + \text{CO}(v = 0) \rightarrow \text{Na}(3_s) + \text{CO}(v = 7)$$
  - d. radiative decay from an excited electronic state of the attaching molecule
  - e. production of the excited state of the attaching gas as a dissociation fragment in a photochemical reaction involving a larger molecule, e.g.



When one has identified a suitable attaching molecule one must check that the vibrational excitation is not quenched too rapidly by the buffer gas. This may be a serious problem if molecular gases, such as  $\text{CH}_4$  are present. A rapid quenching rate would necessitate increased power of the laser which drives the optical control. In a subsequent section we will outline a series of steps which could be used to screen possible candidates for vibrationally enhanced attachment, and will summarize the data that are available for one promising candidate. An alternative way to minimize the attachment during the conduction phase are to base the enhancement on an electronic excitation for which the threshold is much higher than the mean electron energy. However, there is very little experimental data on attachment to electronically excited molecules. Theoretically one expects that such cross sections may often be smaller than those for the corresponding ground states. Nevertheless this suggestion is worthy of further study.

One attractive possibility is to search for attaching excimers, i.e., molecules which are only very weakly bound in the ground state but which possess excited states with large cross sections for dissociative attachment. One way of implementing this idea is outlined below. Another promising approach would be to search for molecules in which the ground electronic state is singlet and is weakly attaching, but which has a strongly attaching excited triplet state.

Such a state would be excited by optical pumping on an allowed transition followed by internal conversion. Acetone ( $\text{CH}_3\text{COCH}_3$ ) seems to possess such properties.<sup>1</sup> Clearly many new data are needed before either enhancement mechanism, via vibrational or electronic excitation, can be fully evaluated.

An example of vibrationally enhanced attachment:

In order to clarify the issues involved in optical control of attachment, it is useful to consider a specific molecule, namely  $\text{HCl}$ , in which vibrationally enhanced attachment has been demonstrated, and for which much of the relevant data are known.

(a) Attachment cross sections:

Allan and Wong<sup>2</sup> have measured the cross section for attachment of electrons for  $\text{HCl}$  and  $\text{DCl}$  at gas temperatures between 300 K and 1200 K with electron energies up to 1.2 eV. From their results, Bardsley and Wadenra<sup>3</sup> have deduced the cross sections for attachment of electrons to specific vibrational states ( $v = 0 - 3$ ) and rotational states ( $J = 0 - 25$ ). Figure 2 shows the cross section for each of these vibrational states, averaged over a thermal distribution of rotational states at 300 K. This shows that for electrons with energy of the order of 0.1 eV, the rate of attachment to molecules in state  $v=0$  and  $v=1$  is small, whereas for  $v=2$  and  $v=3$  it is large. However, this advantage disappears if the electron energy is  $\geq 0.5$  eV.



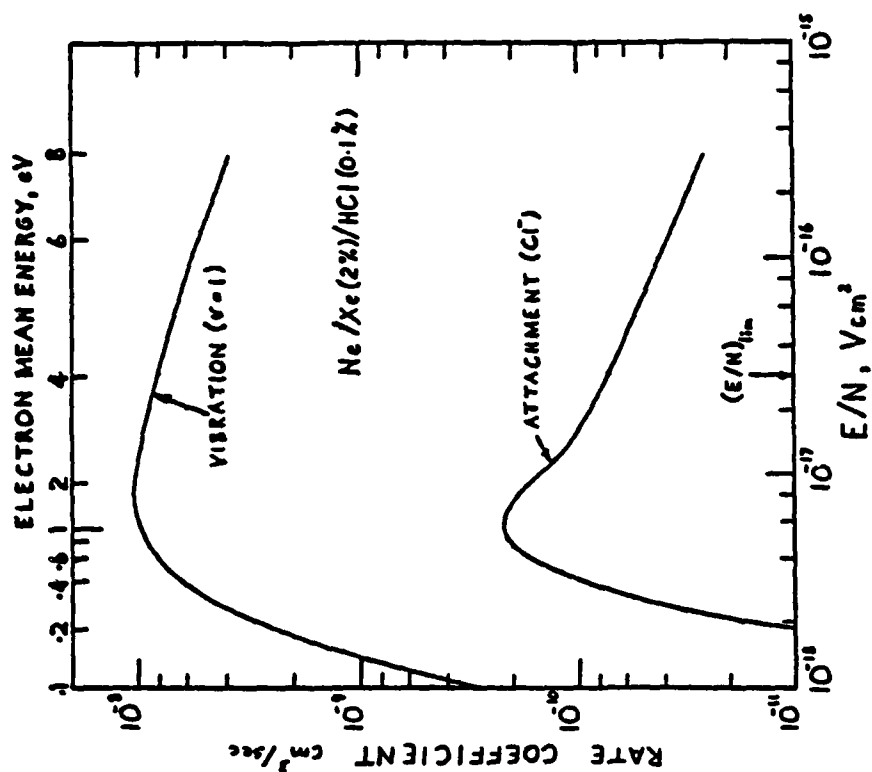


Figure 3.  
Rate of vibrational excitation and  
attachment of HCl from the vibrational  
groundstate

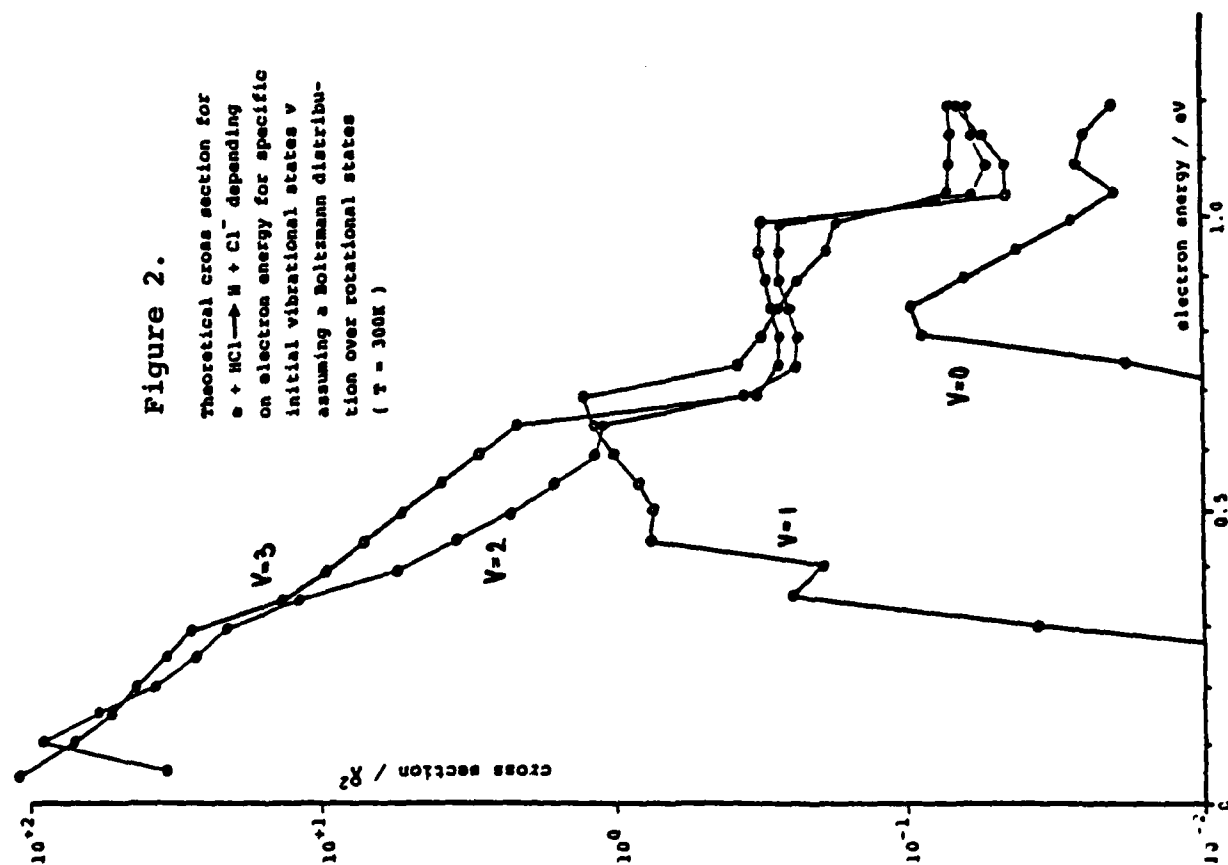


Figure 2.

Theoretical cross section for  
 $e + \text{HCl} \rightarrow \text{H} + \text{Cl}^-$  depending  
on electron energy for specific  
initial vibrational states  $v$   
assuming a Boltzmann distribu-  
tion over rotational states  
( $T = 300\text{K}$ )

(b) Optical versus electronic excitation of vibrational modes.

Since  $\text{HCl}$  is a polar molecule it can be easily pumped directly using a suitable infrared laser. Vibrationally excited molecules may also be produced as dissociation fragments in optically controlled processes involving larger molecules. It has the further advantage that the large vibrational spacing (0.35 eV) means that in the conducting phase vibrational excitation will result only from collisions of hot electrons. However, the cross section for vibrational excitation by electron impact is very large, close to threshold. Figure 3 shows the rate of vibrational excitation as deduced by Davies<sup>4</sup> from an analysis of transport properties. This again shows the gain that can accrue from minimizing the mean electron energy in the switch during the conducting phase.

(c) Quenching of excited vibrational states

As discussed above, the enhancement of electron attachment will be reduced if the vibrational excitation is quenched in collisions of  $\text{HCl}^*$  with ground state  $\text{HCl}$  or buffer gas molecules. The rates of these relaxation processes have been measured, by Chen and Moore,<sup>5</sup> for several molecules, including  $\text{CH}_4$ .

(d) Research Needs

More detailed experimental data are needed on electron attachment to specific excited states and on the cross sections for electron-impact excitation of levels with  $v \geq 2$  (e.g.,  $0 \rightarrow 2$ ,  $1 \rightarrow 2$  transitions). The efficiency of optical

procedures for producing this vibrational excitation should also be surveyed.

#### References:

1. D. C. Lorents, private communication.
2. M. Allen and S. F. Wong, J. Chem Phys. 74, 1687 (1981).
3. J. N. Bardsley and J. M. Wadehra, University of Pittsburgh, preprint (1982).
4. D. K. Davies, private communication.
5. H. L. Chen and C. B. Moore, J. Chem Phys. 54, 4072 (1971) and 54, 4080 (1971).

#### 4. Screening Procedure for Candidate Gases for Photoenhanced Attachment (Vibrational Excitation)

Table IV was generated as a viewgraph for purposes of discussion. The points addressed are in order of priority from the point of view of the experimentalist wishing to choose a gas for testing a switch with an optically controlled attachment rate. From a longer range point of view, consideration of possible candidates need not be constrained by the present availability of laser wavelengths (Point 1).

Point 2 is not directly related to considerations of photoenhanced attachment. It arises from the desire to take advantage of the increasing E/N in the decaying switch medium during the turn-off phase. Since this behavior of  $k_{\text{attach}}$  is entirely compatible with the other considerations of vibrationally enhanced attachment we can take full advantage of it. The

important consideration here is that  $k_{\text{attach}}$  be sufficiently small at the operating  $E/N$  during the conduction phase. The electron mean energy in mixtures chosen for high drift velocity is likely to be a few tenths of an electron volts. Again, the choice of an attaching mechanism compatible with the total gas mixture properties is emphasized.

Point 3 reflects the fact that most of the relevant experimental data available in the literature relate to attachment measurements (cross sections or rate coefficients) as a function of gas temperature. From such data, the vibrationally enhanced process is inferred, in some cases quantitatively by unfolding techniques<sup>1,2</sup> or with the aid of theory.<sup>3</sup> Candidate gases for which there are no data can be screened experimentally by studying their temperature dependence rather than via optical excitation experiments.

Points 4 and 5 concern the energy dependences of the individual cross sections for  $v=0$  and  $v>0$ . This information is equivalent to, but more fundamental than, the information from point 3. The required  $E/N$  dependence of  $k_{\text{attach}}$  implies constraints on the threshold and peak position of  $\sigma(E_e, v=0)$ . Availability of the separate  $v$ -state cross sections facilitates theoretical prediction of photo-induced effects.

Point 6 addresses the general concern that the proposed enhanced attachment mechanism must not be "undone" by an inappropriate combination of attaching and buffer gases. This is being addressed in more detail in Sec. 3, treating  $\text{HCl}$  as a particular example of the overall process.

Point 7 is perhaps the most difficult to address a priori, and its low priority position on this list reflects this fact. There is no implication that plasma chemistry effects need not be considered troublesome. This issue is of concern regarding whether or not an attaching species introduced in relatively low concentrations will survive the conducting phase to perform properly during the opening phase, and may impose the need to flow the gas, with the attendant engineering costs.

#### References:

1. Allan, M. and Wong, S. F., Phys. Rev. Lett. 41, 1791 (1978).
2. Allan, M. and Wong, S. F., J. Chem. Phys. 74, 1687 (1981).
3. Bardsley, J. N. and Wadehra, J. M., Phys. Rev. A 20, 1398 (1979).

#### 5. Photochemical Enhancement of Electron Attachers in the Plasma of the Switch (Electronic Excitation):

##### A. Statement of Concept:

It is proposed that by optical absorption a temporary high attaching molecule be produced in the plasma.

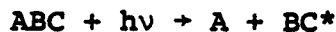
##### B. Discussion

Energies for exciting rotational and vibrational levels in molecules are small. Therefore, the molecules may be excited by the plasma electrons. The method proposed for exciting these levels by a laser, then, will not be very effective unless the intensity of the laser beam is very high

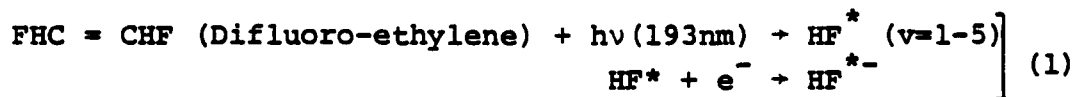
or the cross sections for electron impact excitation are quite low compared with the photoabsorption cross sections. In order to overcome the above difficulties it was also suggested that photochemical reactions, resulting from excitation to the electronic states of the molecules or atoms, be utilized for the production of temporary attachers in the plasma. This will be further clarified by the following examples:

a) Photo-dissociation:

The plasma of the switch can be seeded with molecules which can be photodissociated by an external laser to produce fragments. One of the fragments can be highly electronegative and can attach plasma electrons to open the switch, viz:

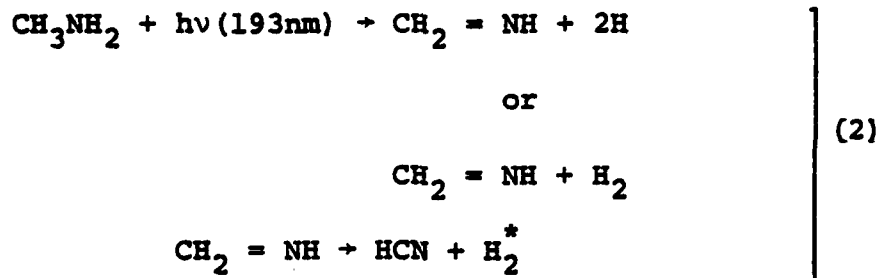


where ABC is a molecule which upon photodissociation gives rise to a vibrationally excited radical  $BC^*$ . The  $BC^*$  may have large attachment cross sections and may combine with plasma electrons to generate a temporary negative ion  $BC^{*-}$ . As an example, consider the following reaction:<sup>1</sup>



It is expected that, just like vibrationally excited  $HCl$ ,  $HF^*(v = 1-5)$  will also have high attachment cross section.

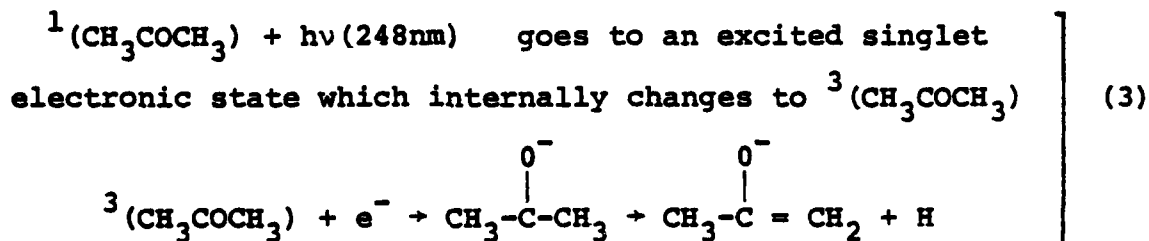
Or, consider the following reactions:<sup>2</sup>



Both HCN and  $\text{H}_2^*$  (\* indicates vibrationally excited state) are electron attaching molecules. The above reaction is found to be very efficient ( $\approx 70\%$  converts to HCN).

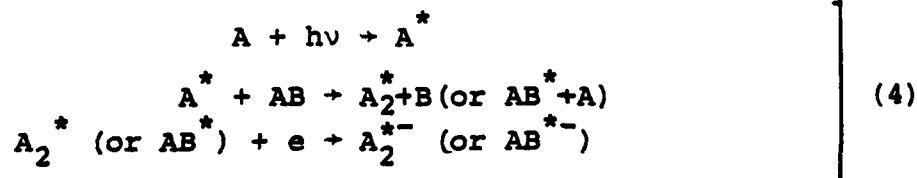
b) Internal Conversion of an Excited Electronic State:

By photoabsorption certain molecules can be excited to electronic states which internally convert to highly attaching ones. For example:<sup>1</sup>



c) Generation of An Attaching Molecule by an Excited State of an Atom:

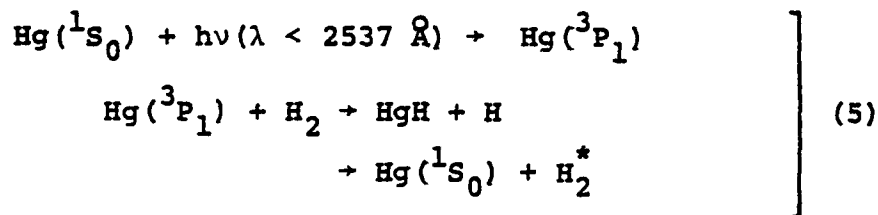
Consider a reaction of the following type:



where \* denotes the excited state of the atom or the molecule. Reaction of the type represented by (4) are of special interest because they offer the possibility of closed cycle oper-

ation i.e. a continuous flow of gases is not needed.

As an example, consider the mercury sensitized reaction:<sup>3</sup>



Reaction (5) is just an example. Much more research is needed to identify suitable atom sensitized reactions for our purpose.

#### C. Suggested Research Approach

- i) Look into the literature for radical molecules which have the possibility of strong electron attachment cross sections and small thresholds for attachment energy.
- ii) Look into the various possible ways to produce these radicals by using a laser or an e-beam.
- iii) Perform the experiment and measure the attachment cross sections. At the same time theoretical calculations will help in understanding their detailed properties.

#### References:

1. D. Lorents, private communication.
2. Ed. Gardner, private communication.
3. K. Yang, J. D. Paden and C. L. Hassell, J. Chem. Phys. 47, 3824 (1967).



## 6. Low Pressure Considerations

Higher pressure tends to produce equilibrium, or LTE, and a process employing a laser is a nonequilibrium non-LTE process. Thus there is an intrinsic tradeoff in pressure and optical power. At lower pressures it is possible to consider several significantly different approaches, summarized here:

Low pressure makes it possible to employ a wall-dominated process. The walls may be either

- 1) The confining walls of the discharge, as in an ion laser, or:
- 2) The electrodes, which may be large, and closely spaced. An interesting advantage of closely spaced electrodes is the capability of increasing the hold-off voltage by operating on the left-hand side of the gas Paschen curve. It may be possible to obtain high currents, for at least short times. Densities of more than  $100 \text{ A/cm}^2$  are possible, particularly with a hot cathode. At pressures of  $1/2$  torr, ( $N \approx 2 \times 10^{16} / \text{cm}^3$ ) the electron density may be approximately  $10^{14} / \text{cm}^3$  in this environment. The electrons will equilibrate rapidly, but the molecules won't, and thus an optical excitation process will not have to compete with molecule-molecule collisions.

### Suggested Research Approach

- 1) Consider candidates at low pressures, subject to the constraints discussed above, and delineate the limits on pressure imposed by this idea for an opening switch. A fairly simple

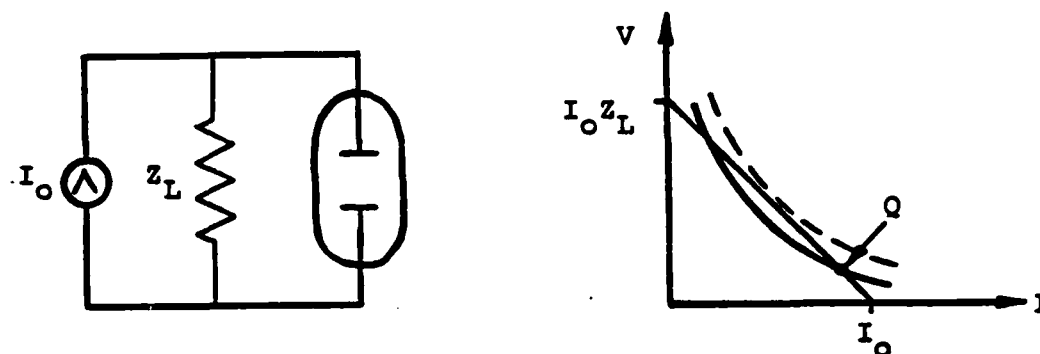
experimental apparatus could be employed. Certainly existing switch gases should be studied, initially at least.

2) Understand some existing low-pressure devices, such as lasers (e.g., ion) and closing switches, by studying the physics of these where necessary. Consider the effect on these through addition of attaching gases, light (photons), or electrons.

#### 7. Negative Dynamic Resistance Consideration

The cost of laser photons requires that they be used very efficiently in any switching scheme. Schemes that involve using the laser only during the opening phase of a self-sustained discharge have a significant advantage over schemes that involve using the laser to sustain the discharge. If the discharge switch must remain closed for long periods, then the requirements on a laser to sustain the discharge are severe.

Diffuse discharges with large negative dynamic resistances make possible efficient use of laser energy during the opening phase of a discharge switch. A large negative dynamic resistance has two advantages that are apparent in steady state models. The first advantage is that a small change in  $V/I$  characteristics can switch large currents into a resistive load. This advantage is illustrated in the circuit diagram and load line analysis, which follows.



Point "Q" represents a macroscopically stable operating point for which most of the source current is carried by the low impedance discharge. A relatively small change in  $V/I$  characteristics, represented by the shift from the solid curve to the dotted curve, drives all of the source current into the load.

The second advantage of large negative dynamic resistance is that the magnitude of the linear optogalvanic effect for a fixed energy input is proportional to the dynamic resistance. This statement follows from applying perturbation theory to the balance equations which describe a discharge.<sup>1</sup> A first order perturbation theory approach describing optogalvanic effects is useful if the laser power is a small ( $\leq 10\%$ ) fraction of the total power being dissipated in the discharge.

There are several processes which can cause negative dynamic resistance. Molecules with attaching rates which increase strongly with  $E/N$  can produce negative dynamic resistance. Multistep ionization processes can also produce a negative dynamic resistance.

#### Reference:

1. J. E. Lawler, Phys. Rev. A, 22, 1025 (1980).

## 8. Diagnostics for Diffuse Discharges

Lasers can be useful not only for controlling discharges but also as probes to determine basic parameters and conditions in the switch. Diagnostics beyond simply measuring voltages and currents are essential to understanding the diffuse discharges used for opening switches. Almost all the diagnostic techniques developed for the study of e-beam sustained laser discharges are applicable to switches and should be considered. Laser-based measurement techniques can give time and space resolved measurement of  $N_e$ , gas density, and species and also yield the temporal evolution of the excited state distribution. Emission spectroscopy of the discharge should not be ignored since it is a simple technique which provides valuable information, particularly about impurities.

A few diagnostics worth considering are:

- 1) Optical interferograms
- 2) Framing camera
- 3) Pressure rise transducer
- 4) Emission spectroscopy
- 5) Laser induced fluorescence spectroscopy
- 6) Coherent antistokes Raman spectroscopy (CARS)
- 7) Microwave interferometry

CARS can give information about the distribution of vibrationally excited states, crucial to the investigation of certain concepts. Microwave interferometry can give time resolved measurements of  $N_e$  in the discharge and has already been employed to study electron production by 2-step

photoionization and decay by recombination and attachment. The microwave technique can be employed to study attachment rate as a function of  $E/N$  and vibrational excitation.

#### Microwave Measurements

A microwave interferometer, shown schematically in Figure 4, has been used at Sandia National Laboratories to study electron production by laser photoionization of organic molecules. This apparatus provides time-resolved measurements of electron densities from a few times  $10^9$  through  $10^{12} \text{ cm}^{-3}$  by observing transmission amplitude and phase retardation of 10 GHz traveling waves passing through the excited gas which is contained in the waveguide section. Resonant 2-step photoionization (see Figure 5) is achieved by passing the beam from a pulsed UV laser through the gas. In this manner, photoionization coefficients have been determined for a large number of active molecules. For most of the compounds studied, the electron density scales with  $I^2$  as shown in Figure 6.

Recombination and attachment have also been studied by observing the decay of electron density for various buffer gases. Figures 7 and 8 show the microwave transmission as a function of time. Cutoff ( $T = 0$ ) corresponds to  $N_e$  of  $10^{12} \text{ cm}^{-3}$ . Figure 7 shows the behavior of  $N_e$  using argon, a non-attaching buffer.  $N_e$  rises rapidly during the 20 ns laser pulse (lower trace) and decays very slowly thereafter. In the case of mildly attaching gases such as air,  $N_e$  decays more rapidly, as shown in Figure 8. For strong attachers, such

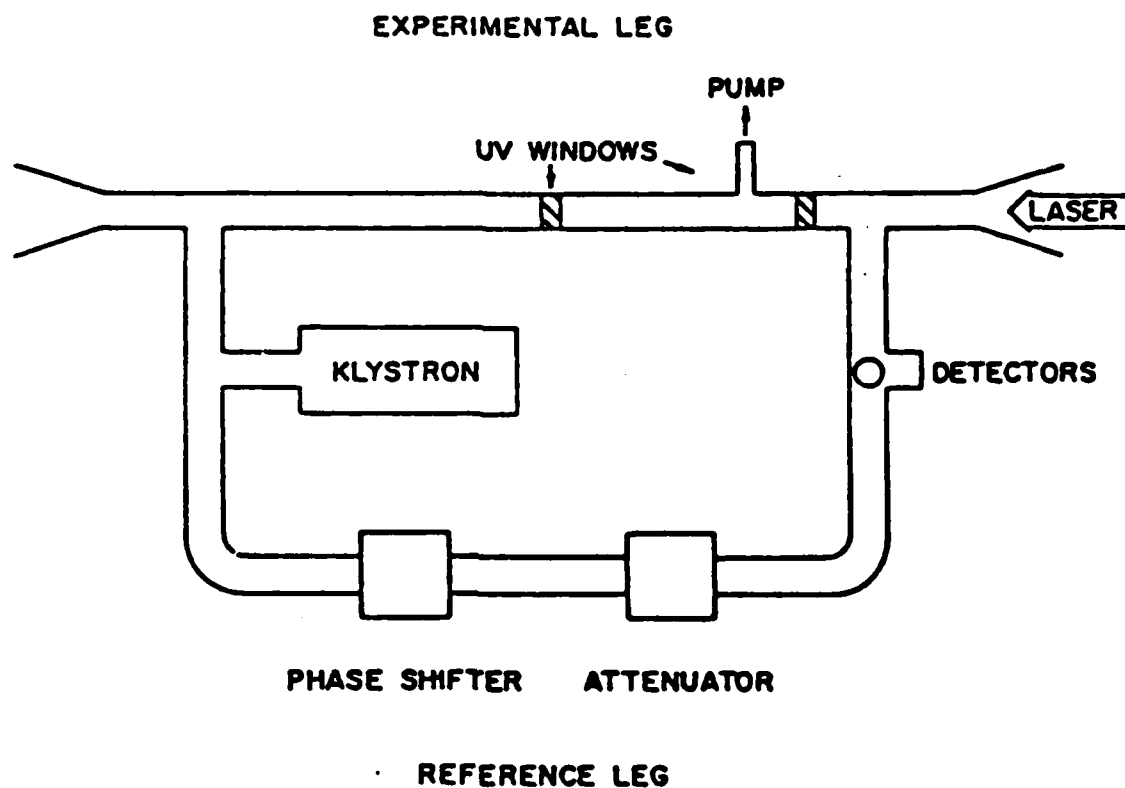
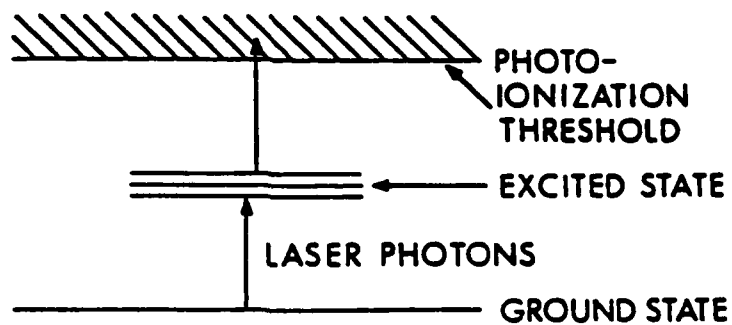


Figure 4. Microwave apparatus.



**EXAMPLES:**

TRIPROPYLAMINE + KrCl LASER (221nm)  
 FLUOROBENZENE + KrF LASER (248nm)  
 DIMETHYANILINE + XeCl LASER (307nm)

Figure 5. Resonant 2-step photoionization.

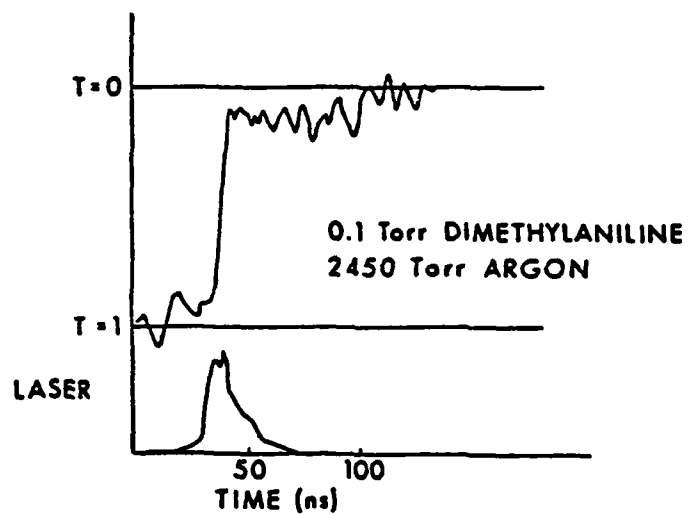


Figure 7. Slow decay of  $N_2$  with non-attaching buffer.

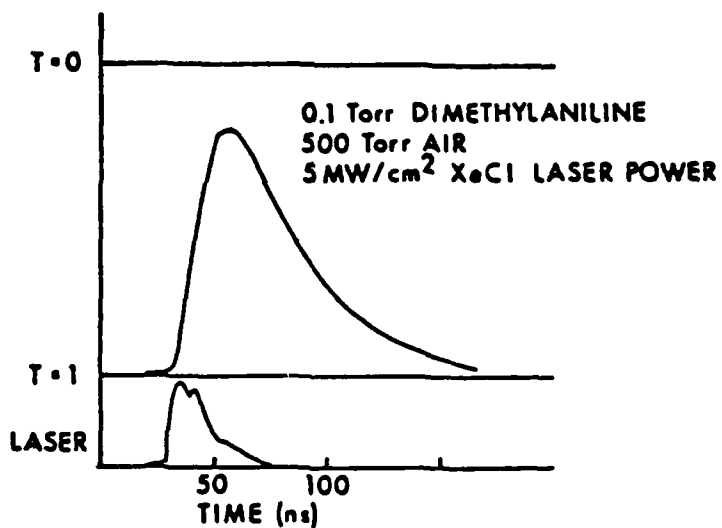
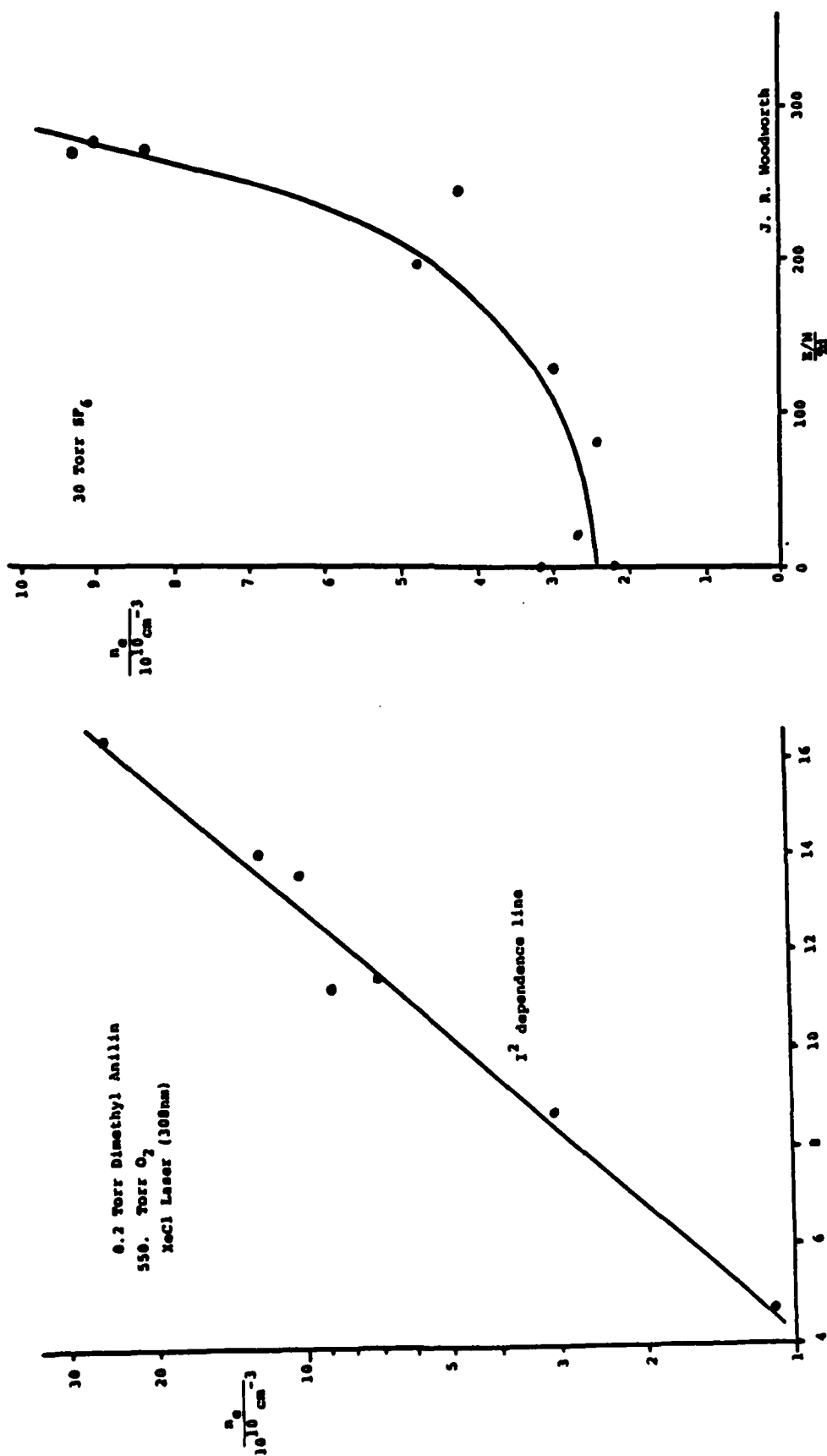


Figure 8. Rapid decay of  $N_2$  with attaching buffer.

Figure 6.  $N_e$  as a function of intensity.Figure 9.  $N_e$  as a function of  $E/N$  for  $\text{SF}_6$ 

(preliminary data).



as  $\text{SF}_6$ ,  $N_e$  falls very rapidly after the end of the laser pulse and the peak electron density is reduced even at low pressure due to attachment during the buildup phase. Plate electrodes inside the waveguide section allow application of an E field. For  $\text{SF}_6$  buffer,  $N_e$  (for a fixed laser excitation) is observed to increase with E/N (see Figure 9). This is the expected behavior based on the shape of the  $\text{SF}_6$  attachment curve. With  $\text{O}_2$  as buffer, however,  $N_e$  appears to decrease as the voltage is increased. This is exactly the type of behavior which is of interest for opening switches. The microwave technique should be considered not only to obtain basic parameters but also to provide time-resolved measurements of  $N_e$  in opening switches.

#### 9. Field Strength Dependant Laser Induced Processes

Statement of Concept: The strong electromagnetic (EM) field associated with a high power laser may be used to enhance or inhibit certain inelastic processes occurring in a discharge so that switching may be facilitated.

Discussion: The advent of high intensity lasers has made it possible to study atomic and molecular reactions in the presence of a strong EM field. The reaction may be either enhanced or inhibited relative to the reaction rate under field-free conditions. In these "laser-induced" processes the laser provides an intense EM field (not necessarily on a real atomic or molecular resonance) which perturbs the quasimolecular potential energy curves, relative to the field-

free case, and the reaction can be either enhanced or inhibited.

The study of such processes is still in its infancy; to date the most studied of these laser-induced processes are associative ionization and laser-induced Penning ionization in collisions between two Na(3p) atoms.<sup>1-7</sup> These processes may be represented as  $h\nu + \text{Na}(3p) + \text{Na}(3p) \rightarrow \text{Na}_2 + e^-$  and  $h\nu + \text{Na}(3p) + \text{Na}(3p) \rightarrow \text{Na}^+ + \text{Na}(3s) + e^-$ . The symbol  $h\nu$  refers to the EM field and not to the laser photons required to effect the 3s  $\rightarrow$  3p transition. Of course, the experiment may be conducted with a single high intensity laser tuned to a D-line, but the EM field enhancement effect does not require the precise D-line wavelength. Although there are still uncertainties about the exact mechanisms that lead to the enhancement, it is clear that the ion yield, especially from associative ionization increases dramatically (orders of magnitude) when an intense field is applied ( $\sim 10^3 - 10^6$  W/cm<sup>2</sup>).

Although the sodium reactions briefly described above show enhancement in the presence of the strong EM field, there is no reason why, in some other properly chosen system, the reaction could not be inhibited.<sup>8</sup> If such a process could be found it could have application for fast opening switches. For example, if a given atomic collision process which provides conduction electrons in a "conventional" discharge switch could be turned off (i.e., reduced by orders of magnitude) by nonresonant laser light, the switch would then be in

the open position during the laser pulse. The switch would be closed between laser pulses. Only during the short laser pulse would the switch be open. Such a scheme takes advantage of the low duty cycle of most pulsed lasers to provide the desired open/closed characteristics. Not inconsequentially, the expensive laser photons would then only be used during the short open period.

Suggested Approach. Because there exists so little data of a fundamental nature on these laser-induced processes, additional work should be undertaken. It is considered important that the sodium system, which of course was studied because of experimental convenience, be thoroughly understood and characterized. Subsequent experiments on different types of systems, such as rare gas/rare gas collisions, should also be performed. Naturally, theoretical guidance should be added in appropriate doses. Primarily though, it should be noted here that there currently exists very little data. More basic research is needed.

Questions. Can a reaction be found, which under field-free conditions causes conduction, but under intense irradiation ceases to conduct?

#### References:

1. S. Geltman, J. Phys. B 10, 3057 (1977).
2. G. H. Bearman and J. J. Leventhal, Phys. Rev. Lett 41, 1227 (1978).
3. A. deJong and F. van der Volk, J. Phys. B 12, L561 (1979).

4. F. Roussel, P. Breger, G. Spiess, C. Manus and S. Geltman, J. Phys. B 13, L631 (1980).
5. V. S. Kushawaha and J. J. Leventhal, Phys. Rev. A 22, 2268 (1980).
6. J. Weiner and P. Polok-Dingels, J. Chem. Phys. 74, 508 (1981).
7. V. S. Kushawaha and J. J. Leventhal, Phys. Rev A 25, 346 (1982).
8. K. C. Kulander and A. E. Orel, J. Chem. Phys. 74, 6529 (1981).

## MODELING OF DIFFUSE DISCHARGE OPENING SWITCHES

W.H. Long, Jr.  
(Chairman)

The committee sought to identify a) types of models that are needed to address the current problem, b) codes which already exist to analyze similar phenomena in other devices, and c) areas where additional research is required. Model capabilities were expressed in terms of basic processes and dimensionality. Table 1 presents a matrix of model capabilities, where existing codes are indicated with a cross.

It was generally agreed that no single code could, or should, contain all the processes of importance or all the possible dimensions, but that more could be learned by analyzing important aspects of the problem with small, specialized and interactive models. For example, divisions can be made on the basis of a scale of time or distance. Long term chemistry in a closed gas loop can be considered separately from the short term chemistry and plasma kinetics during conduction, which itself can be treated independently of the transients associated with opening and closing. The various codes are then coupled through initial or periodic boundary conditions. In a similar way, spatial divisions exist between bulk flow, boundary layer, plasma sheath, and surface phenomena.

Further separation can be made by grouping related processes in individual codes which are then coupled together through specific parameters or common variables. This is generally done in joining electron kinetics codes to models treating plasma kinetics, and then to general gas dynamics codes. The coupling between these subsystems is indicated in Figure 1.

The basic processes which must be considered in repetitive, diffuse discharge, opening switches are listed in Table 1. Others may have to be added for specific switch concepts not considered here. Electron kinetics in the positive column of a glow discharge is usually treated by solving the Boltzmann equation for the electron energy distribution in a constant, uniform field. The angular dependence of the distribution is expanded in Legendre polynomials, retaining only the first two terms. (In the presence of magnetic fields an expansion in spherical harmonics is made.) The transport coefficients and rate constants are then determined for a given gas mixture as a function of  $E/N$ , the ratio of electric field strength to neutral particle density. The plasma kinetics is modeled by using electron collision rate constants together with neutral and heavy ion rate constants in a set of coupled continuity equations covering all the species of interest in the plasma. Significant excited state populations must be coupled back into the electron kinetics model, self-consistently. Neutral chemistry is treated in the same way.

Repetitive switches using gas as the dielectric medium will require flow to remove heat and unwanted chemical by-products from the electrode region. The determination of density, velocity, and temperature in the switch is derived from a solution of the gas dynamic equations with an ohmic heating term. The contribution of charged species to continuity or momentum balance will be negligible in a diffuse glow. The boundary layers can be treated separately using appropriate boundary layer theories. They could seriously impact the efficiency and stability of the switch if significant density variations exist. The plasma sheaths at the anode and cathode are also areas of concern due to enhanced fields and subsequent gas heating in these regions. Electron kinetics in the sheath must be treated differently from that in the positive column because of steep field and

density gradients. Surface properties are important in determining gross sheath characteristics and stability.

The types of instabilities which must be considered in determining the maximum rate of rise of recovery voltage are space charge, ionization-attachment and thermal. Space charge instabilities include corona emission from sharp surface protrusions and localized streamer formation. They are characterized by space charge-enhanced fields and very fast propagation times. Ionization-attachment instabilities consist of coupled fluctuations in the plasma density and electric field which grow exponentially with time. Both of these types of instability can develop into a thermal instability, which results in an arc. However, a thermal instability can also occur directly, due to nonuniform conditions on the electrodes or in the gas flow. The study of instabilities is essential in determining the useful operating regime for a diffuse-glow switch.

Computer codes and theories exist to cover all the situations mentioned above. However, most of them are not in a form which is suitable for the general user. Many have been developed to model specific phenomena or devices and may employ approximations which are not universally applicable. Nevertheless, these codes can be modified and used to design a workable switch within a limited parameter range, if the incentive exists. The most serious impediment to this end lies in obtaining basic data on gases of interest for use in the models. This data can be obtained experimentally if the gases are first identified. One of the conclusions of this meeting was to use a general interactive model of a switch in a given application to obtain information about the desirable properties of the working gas. This would facilitate the work of experimentalists trying to identify useful candidates.

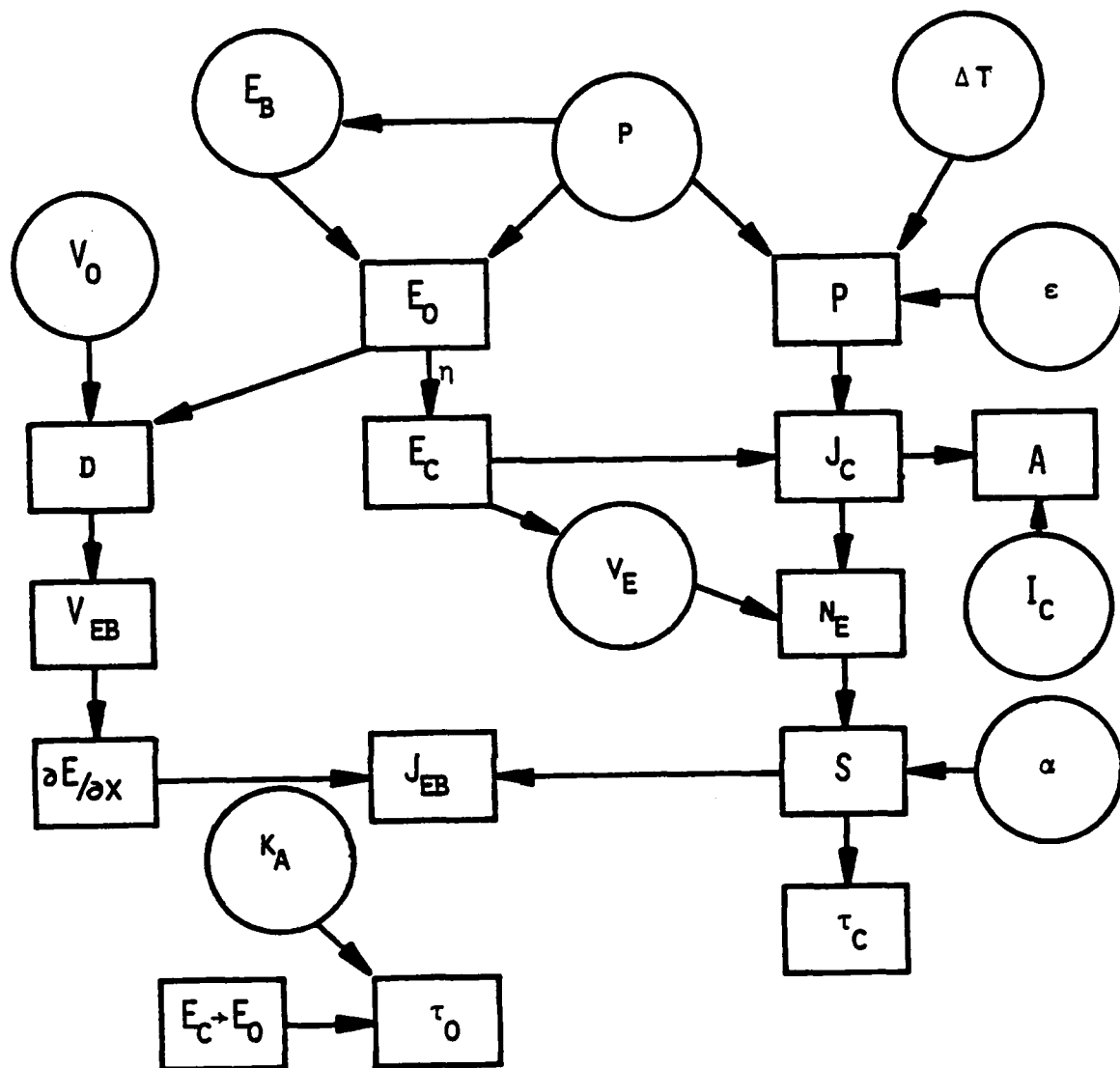
The types of problems which require further work are listed in Table 2. Most importantly, any model of the electrical characteristics of a diffuse-glow opening switch must incorporate the driving circuit as well as the load. The response of the plasma during switch opening is strongly dependent on the configuration of the external circuit. A study needs to be made of the transient sheath development and its extinction. It may be necessary to look at the time-dependence of the electron energy distribution in a changing electric field, particularly in the high energy tail which responds more slowly than the rest. As stated previously, all forms of instability should be examined further in order to identify a practical operating regime. Finally, a general, interactive model should be formulated to identify scaling relationships and to link specific engineering requirements to basic data in a transparent manner.



## Bibliography

- C. M. Bowden, J. F. Perkins, and R. A. Shatas, "Range and Energy Deposition Enhancement of a Fast Electron Beam by External Electric Fields," J. Vac. Sci. Technol. 10, 1000 (1973)
- R. T. Brown and W. L. Nighan, "Stability Enhancement in Electro-Beam-Sustained Excimer Laser Discharges," Appl. Phys. Lett. 35, 142 (1979)
- A. J. Davies, C. J. Evans and F. Llewellyn Jones, "Electrical Breakdown of Gases: The Spatio-temporal Growth of Ionization in Fields Distorted by Space Charge," Proc. Roy. Soc. A 281, 164 (1964)
- D. H. Douglas-Hamilton and P. S. Rostler, "Investigation of the Production of High Density Uniform Plasmas," Tech. Rep. AFWAL-TR-80-2087 (October 1980)
- J. W. Dzimianski and L. E. Kline, "High Voltage Switch Using Externally Ionized Plasmas," Tech. Rep. AFWAL-TR-80-2041 (April 1980)
- L. Friedland, "Novel Computer Simulation of Electron Swarm Motion," Phys. Fluids 20, 1461 (1977)
- D. B. Henderson, "Electron Transport in Gas Discharge Lasers," J. Appl. Phys. 44, 5513 (1973)
- J. H. Jacob, "Diffusion of Fast Electrons in the Presence of a Magnetic Field," Appl. Phys. Lett. 31, 252 (1977)
- L. E. Kline and J. G. Siambis, "Computer Simulation of Electrical Breakdown in Gases; Avalanche and Streamer Formation," Phys. Rev. A 5, 794 (1972)
- W. H. Long, Jr., "Discharge Stability in E-Beam-Sustained Rare-Gas Halide Lasers," J. Appl. Phys. 50, 168 (1979)
- W. H. Long, Jr., "Plasma Sheath Processes," Tech. Rep. AFAPL-TR-79-2038 (April 1979)
- C. B. Mills, "Current Continuity in Dense Plasma," J. Appl. Phys. 45, 2112 (1974)
- W. L. Morgan, R. D. Franklin and R. A. Haas, "Electron Energy Distribution in Photolytically Pumped Lasers," Appl. Phys. Lett. 38, 1 (1981)
- W. L. Nighan, "Investigation of the Stability of Ionized Molecular Gas Flows," ONR Report R76-921325-6 (September 1976)
- C. G. Parazzoli, "Turbulent Boundary Layer over the Cathode of a High Current Density Discharge: Numerical Calculation and Experimental Results," AIAA 15th Aerospace Science Meeting, Los Angeles, Calif. (24 January 1977)
- L. C. Pitchford and A. V. Phelps, "Comparative Calculations of Electron-Swarm Properties in  $N_2$  at Moderate E/N Values," Phys. Rev. A (1981)

- M. Shimosuma, Y. Sakai, H. Tagashira, and S. Sakamoto, "Prebreakdown Current Growth and the Ionization Coefficients in Hydrogen," J. Phys. D: Appl. Phys. 10, 1671 (1977)
- R. C. Smith, "Computed Secondary-Electron and Electric Field Distributions in an Electron-Beam-Controlled Gas-Discharge Laser," Appl. Phys. Lett. 21, 352 (1972)
- G. A. Theophanis, J. H. Jacob, and S. J. Sackett, "Discharge Spatial Nonuniformity in E-Beam-Sustainer CO<sub>2</sub> Lasers," J. Appl. Phys. 46, 2329 (1975)
- C. M. Wiggins and D. N. Mansell, "Chemical Laser Computer Code Survey," NRL Report 8450 (December 1980)



$E_b$  : e-beam energy  
 $V_{eb}$  : e-beam voltage  
 $J_{eb}$  : e-beam current density  
 $\Delta t$  : conduction time  
 $\tau_c$  : closing time  
 $\tau_o$  : opening time  
 $p$  : pressure  
 $E_o$  : open field  
 $E_c$  : closed field  
 $V_o$  : open voltage  
 $d$  : electrode separation

$A$  : discharge cross-section  
 $\epsilon$  : energy density  
 $P$  : power density  
 $I_c$  : current  
 $J_c$  : current density  
 $S$  : source function  
 $n_e$  : electron density  
 $v_e$  : drift velocity  
 $k_a$  : attachment rate coefficient  
 $\alpha$  : recombination coefficient  
 $\eta$  : efficiency

Fig. 1

	STEADY-STATE				TIME-DEP.			
SPACE DIMENSIONS	0	1	2	3	0	1	2	3
ELECTRON KINETICS	X	X			X			
PLASMA KINETICS	X	X	X		X	X	X	
SHEATHS		X				X		
EXCITED STATES	X	X	X		X	X	X	
NEUTRAL CHEMISTRY	X				X	X	X	
PHOTON PROCESSES	X	X	X					
GAS DYNAMICS		X	X	X		X	X	X
BOUNDARY LAYERS		X	X					
MAGNETIC FIELDS	X	X	X					
STABILITY	X	X	X		X	X	X	
EXTERNAL CIRCUIT	X				X			

Table 1

### RECOMMENDATIONS

- FORMULATE SCALING RELATIONSHIPS
- COUPLE CIRCUIT TO SIMPLE MODELS
- DETERMINE SYSTEMATICS FOR TIEING ENGINEERING REQUIREMENTS TO BASIC DATA
- ONE-DIMENSIONAL ANALYSIS OF SHEATH DURING OPENING PHASE
- TIME-DEPENDENT ELECTRON KINETICS (RELAXATION OF HIGH ENERGY TAIL)
- INCORPORATE GASDYNAMICS
- STABILITY ANALYSIS (PUSH BACK ARCING LIMIT)
- MODELS SHOULD BE DYNAMIC (I.E. INTERACTIVE)

Table 2

**APPENDICES**

## APPENDIX A

## GASES FOR POSSIBLE USE IN DIFFUSE-DISCHARGE SWITCHES\*

L. G. Christophorou,<sup>†</sup> S. R. Hunter, J. G. Carter, and S. M. Spyrou

Atomic, Molecular and High Voltage Physics Group  
Health and Safety Research Division  
Oak Ridge National Laboratory  
Oak Ridge, Tennessee 37830

It has been pointed out recently (e.g., see Refs. 1 and 2) that in pulsed-power applications, energy storage using inductive elements could be advantageous because of the high intrinsic energy density; about  $10^2$  to  $10^3$  times that for capacitive systems. It appears<sup>1-3</sup> that the main technological problem in inductive storage systems for pulsed-power applications is the need for an opening switch--capable of repetitive operation--to transfer the energy from the storage loop to the load (see Fig. 1). In this paper we wish to suggest gas mixtures for possible use in externally sustained (e-beam) diffuse-discharge switches.

The basic requirements of a gaseous medium for use in a diffuse-discharge switch can be understood by referring to the inductive-energy discharge circuit in Fig. 1 (Ref. 3). In the first (*conducting*) stage, the switch  $S_2$  is open, and the switch  $S_1$  is conducting by means of a diffuse discharge which is sustained by either an external pulsed electron or laser beam.<sup>2</sup> In this stage, the gas number density  $N$  (or total pressure  $P$ ) and the electric field  $E$  applied across the electrodes of  $S_1$

---

\*Research sponsored by the Division of Electric Energy Systems, U.S. Department of Energy, under contract W-7405-eng-26 with the Union Carbide Corporation.

<sup>†</sup>Also Department of Physics, The University of Tennessee, Knoxville, Tennessee 37916.

By acceptance of this article, the publisher or recipient acknowledges the U.S. Government's right to retain a nonexclusive, royalty-free license in and to any copyright covering the article.

must be such that for the resulting low value of  $E/N$  ( $\sim 3 \times 10^{-17}$  V cm $^{-2}$ ), the electron drift velocity,  $w$ , (and thus, conduction) is maximum and the electron attachment rate constant,  $k_a$ , is minimum (electron production must be maximized and electron loss minimized). In the second (*opening*) stage at time  $t = 0$  the external (electron or laser beam) ionization source is terminated, the switch  $S_1$  is opened, and the switch  $S_2$  is closed—to allow the stored energy in the inductor  $L_s$  to be transferred to the load  $Z_L$ . It is known,<sup>2,3</sup> however, that in an inductive system where one attempts to rapidly open a conducting switch, a very large voltage is induced across the switch due to the term  $V_i = L \frac{di}{dt}$  ( $L$  is the inductance of  $L_s$  in Fig. 1, and  $i$  is the current). The induced voltage increases the  $E/N$  value (to  $\sim 120 \times 10^{-17}$  V cm $^{-2}$ ) and tends to maintain a conducting arc between the electrodes of switch  $S_1$  and to quote Kristiansen *et al.*,<sup>2,3</sup> "How to interrupt the conduction process against a high driving voltage is the essence of the opening switch." The gas, which in the conducting stage was such as to optimize conduction, must now serve as a high voltage insulant in order to sustain the high driving voltage and prevent breakdown.

A basic difference between the conducting and the opening stages of the switch (at least in the e-beam-sustained discharge) is the effective value of  $E/N$  (or  $E/P$ ). In the conducting stage  $E/N$  is low, while in the opening stage  $E/N$  is very high. This is most significant and remains a key variable in efforts to tailor gases for the optimum performance of  $S_1$  in both stages.

In Fig. 2 we show schematically the desirable characteristics of the gas in terms of  $w(E/N)$  and the attachment rate constant  $k_a(E/N)$ . The drift velocity  $w$  must be maximum at the  $E/N$  values (indicated by



the shaded region in Fig. 2) characteristic of the conduction stage, and  $k_a$  must be as small as possible in this E/N range. In the opening stage (Fig. 2)  $w$  must be as small as possible and  $k_a$  as high as possible at the E/N values (indicated by the shaded region in Fig. 2) characteristic of this stage.

Fast gases having the general characteristics of  $w(E/N)$  shown in Fig. 2 have been reported by us<sup>4</sup> (e.g., Ar + CF<sub>4</sub> mixtures) which are free of electron attachment at low E/N. Promising mixtures that are comprised of Ar and CF<sub>4</sub> are shown in Fig. 3. The mixture composition and E/N can be chosen such as to maximize  $w$  in the conducting stage. It is also seen that at high E/N, the  $w$  of such mixtures falls off considerably,\* a property desirable in the opening stage of the switch (see Fig. 2).

To become effective for the opening stage of the switch, such gases must have a high dielectric strength. To achieve this, the *mixture must effectively remove electrons by electron attachment forming negative ions*.<sup>5,6</sup> Since in the opening stage of the switch E/N is very high, the gas must be capable of removing electrons with energies well in excess of thermal energy. It thus seems that a fast gas mixture (i.e., one with high  $w$ ) such as Ar + CF<sub>4</sub> must be mixed with a third gas which does not attach thermal and near-thermal energy electrons but which attaches electrons at higher energies (say, from ~0.5 to 2 eV).<sup>†</sup> Candidates for

---

\*In this regard such measurements must be extended to higher E/N values.

<sup>†</sup> It is well known<sup>5,7</sup> that electron attachment processes at energies  $\leq 15$  eV are resonant processes and that their cross sections decrease rapidly as the resonance energy increases. When the positions of such resonances are located at energies  $\geq 4$  eV or so, it is doubtful that the magnitude of the attachment cross sections are sufficiently large to effectively reduce the number density of electrons and thus affect the value of the breakdown voltage. We argued earlier<sup>5,6,8</sup> that enhanced scattering cross sections shifting the electron energies to lower energies where electron attachment is strong can be more beneficial in increasing the breakdown strength.

such electron attaching gases to mix with the fast mixtures of Ar + CF<sub>4</sub> are shown in Fig. 4.

Special attention is drawn to the gas (CF<sub>3</sub>)<sub>2</sub>S which is seen (Fig. 4) to capture electrons rather strongly above thermal energies and which itself is an excellent gas dielectric having a DC uniform field breakdown strength 1.5 times that of SF<sub>6</sub> (Ref. 10). A mass spectrometric study of (CF<sub>3</sub>)<sub>2</sub>S has shown (Fig. 5) that the dominant anion is CF<sub>3</sub>S<sup>-</sup> whose yield peaks at ~0.65 eV, a finding consistent with the  $k_a$  vs  $\langle \epsilon \rangle$  data in Fig. 4. A weak F<sup>-</sup> ion is also produced at higher energies (Fig. 5). The electron affinity of CF<sub>3</sub>S<sup>•</sup> is 1.8 eV<sup>11</sup> which would render electron detachment difficult.

It should be noted that the use of (CF<sub>3</sub>)<sub>2</sub>S may be advantageous in the conducting stage of the switch as well. The ionization potential of Ar is 15.76 eV<sup>12</sup> and that of CF<sub>4</sub> ~14.7 eV,<sup>13</sup> while the ionization potential of (CF<sub>3</sub>)<sub>2</sub>S is only ~11.15 eV.<sup>14</sup> Thus, an increase in electron production in the conducting stage (when the external source is an e-beam) may result due to the Penning ionization process



Process (1) is not likely to affect the insulating property of the mixture in the opening stage in view of the work of Christophorou *et al.*<sup>8</sup> which has shown that—at least for uniform fields—the breakdown voltage is mostly affected by the electron attaching rather than by the ionization properties of the gas. It should be noted also that CF<sub>4</sub> itself attaches electrons at higher energies (see Fig. 5 in Ref. 15) than does (CF<sub>3</sub>)<sub>2</sub>S and may thus act synergistically with (CF<sub>3</sub>)<sub>2</sub>S as an electron attacher in the opening stage of the switch. The vapor pressure of (CF<sub>3</sub>)<sub>2</sub>S at ~20°C is ~4.4 atm.

It follows from the above discussion that ternary mixtures comprised of Ar + CF<sub>4</sub> and (CF<sub>3</sub>)<sub>2</sub>S (or other electron attaching additive with the appropriate properties, Figs. 2 and 4) are good candidates for diffuse-discharge switches. It is, however, preferable to have a binary rather than a ternary mixture and to identify, for example, a gas which would serve the role of both CF<sub>4</sub> and (CF<sub>3</sub>)<sub>2</sub>S when mixed with Ar. In search for such a gas we focused on C<sub>3</sub>F<sub>8</sub>. The attachment rate constant  $k_a$  as a function of  $\langle \epsilon \rangle$  for C<sub>3</sub>F<sub>8</sub> is shown in Fig. 4. Although the  $k_a$  for C<sub>3</sub>F<sub>8</sub> is lower in magnitude than that for (CF<sub>3</sub>)<sub>2</sub>S, it has a very desirable  $\langle \epsilon \rangle$ -dependence (i.e., it is very small at low  $\langle \epsilon \rangle$  and large at high  $\langle \epsilon \rangle$ ). Mass spectrometric studies have shown (Fig. 6) that the dominant anion is F<sup>-</sup> with a peak at 2.9 eV. (The electron affinity of the F atom is 3.45 eV.<sup>17</sup>) Other fragment anions (CF<sub>3</sub><sup>-</sup>, C<sub>2</sub>F<sub>3</sub><sup>-</sup>, C<sub>3</sub>F<sub>5</sub><sup>-</sup>, C<sub>3</sub>F<sub>7</sub><sup>-</sup>) with maximum yields in the range 3.2 to 3.8 eV (see Fig. 6) are produced but with very much lower probabilities. From our earlier work on fast gases<sup>4</sup> it seemed that mixtures of C<sub>3</sub>F<sub>8</sub> and Ar would exhibit a similar behavior in terms of the  $w$  vs  $E/P$  function as the Ar + CF<sub>4</sub> mixtures (Fig. 3) (i.e., provide a large  $w$  for specific, low values of  $E/N$  and compositions). Although we have not conducted these latter measurements as yet, we have made preliminary  $w(E/N)$  measurements on Ar + C<sub>2</sub>F<sub>6</sub> mixtures. Our preliminary measurements on this system are shown in Fig. 7. The observed large  $w$  values and sharply peaked  $w(E/N)$  functions in the  $E/N$  range characteristic of the conducting stage of the switch, the high sensitivity of the  $w(E/N)$  functions to the percentage of C<sub>2</sub>F<sub>6</sub> in Ar, and the decline in  $w$  with increasing  $E/N$  are all most interesting and desirable characteristics. Similar measurements on Ar + C<sub>3</sub>F<sub>8</sub> are planned over wide  $E/N$  ranges and mixture compositions. While final

judgment has to await these measurements, on the basis of the data in Figs. 4, 6, and 7, it can be suggested that appropriate binary mixtures of Ar + C<sub>3</sub>F<sub>8</sub> may possess both of the required characteristics (see Fig. 2) of a switching gas and are thus suggested as good candidates for diffuse-discharge switches.\*

---

\*The vapor pressure of C<sub>3</sub>F<sub>8</sub> at ~20°C is ~7.8 atm; C<sub>3</sub>F<sub>8</sub> is listed<sup>18</sup> as nontoxic, nonflammable, unreactive, and thermally stable; its DC uniform field breakdown voltage is 0.9 that of SF<sub>6</sub>.

## REFERENCES

1. J. K. Burton, D. Conte, R. D. Ford, W. H. Lupton, V. E. Scherrer, and I. M. Vitkovitsky, Proc. 2nd IEEE Intern. Pulsed Power Conf., Lubbock, Texas, p. 284 (1979).
2. K. H. Schoenbach, G. Schaefer, E. E. Kunhardt, M. Kristiansen, L. L. Hatfield, and A. H. Guenther, Proc. 3rd IEEE Intern. Pulsed Power Conf., Albuquerque, New Mexico, June 1-3, 1981 (in press); see also relevant papers in *IEEE Transactions on Plasma Science*, Vol. PS-8 (No. 3), September 1980.
3. M. Kristiansen and K. H. Schoenbach, Final Report on Workshop on Repetitive Opening Switches, April 20, 1981, Department of Electrical Engineering, Texas Technological University.
4. L. G. Christophorou, D. V. Maxey, D. L. McCorkle, and J. G. Carter, *Nucl. Instr. Methods* 163, 141 (1979); 171, 491 (1980).
5. L. G. Christophorou, Proc. XIIIth Intern. Conf. on Phenomena in Ionized Gases, Berlin (Leipzig; VEB Export-Import) pp. 51-72 (1978).
6. L. G. Christophorou, in *Electron and Ion Swarms* (L. G. Christophorou, Ed.), Pergamon Press, New York, 1981, pp. 261-277.
7. L. G. Christophorou, *Atomic and Molecular Radiation Physics*, Wiley-Interscience, New York, 1971, Chapt. 6.
8. L. G. Christophorou, D. R. James, and R. A. Mathis, *J. Phys. D: Appl. Phys.* 12, 1223 (1979).
9. D. L. McCorkle, L. G. Christophorou, and S. R. Hunter, in *Electron and Ion Swarms* (L. G. Christophorou, Ed.), Pergamon Press, New York, 1981, pp. 21-34.

10. L. G. Christophorou, D. R. James, R. Y. Pai, R. A. Mathis, I. Sauers, D. H. Smith, L. C. Frees, M. O. Pace, D. W. Bouldin, C. C. Chan, A. Fatheddin, and S. R. Hunter, *Oak Ridge National Laboratory Report ORNL/TM-7624* (1981).
11. F. M. Page and G. C. Goode, *Negative Ions and the Magnetron*, Wiley-Interscience, New York, 1969, p. 140.
12. Ref. 7, p. 614.
13. H. M. Rosenstock, K. Draxl, B. W. Steiner, and J. T. Herron, J. *Phys. Chem. Ref. Data* 6 (Suppl. 1) (1977), p. 352.
14. Ref. 13, p. 445.
15. L. G. Christophorou, *Environ. Health Perspec.* 36, 3 (1980).
16. L. G. Christophorou, D. R. James, R. Y. Pai, R. A. Mathis, I. Sauers, D. H. Smith, L. C. Frees, S. R. Hunter, M. O. Pace, D. W. Bouldin, S. M. Spyrou, and A. Fatheddin, *Oak Ridge National Laboratory Report ORNL/TM-7862* (1981), p. 14.
17. Ref. 7, p. 547.
18. *Matheson Gas Data Book* (5th Edition), W. Braker and A. L. Mossman (Eds.), New Jersey, 1971, p. 467.

## FIGURE CAPTIONS

Fig. 1. Inductive energy discharge circuit (from Ref. 3).

Fig. 2. Schematic illustration of the desirable characteristics of the  $w(E/N)$  and  $k_a(E/N)$  functions of the gaseous medium in an externally (e-beam-sustained) diffuse-discharge switch. Indicated in the figure are rough estimates of the  $E/N$  values for the conducting and the opening stage of the switch.

Fig. 3.  $w$  vs  $E/P_{298}$  for Ar and Ar/CF<sub>4</sub> mixtures (from Ref. 4).

Fig. 4. Electron attachment rate constant,  $k_a$ , as a function of mean electron energy,  $\langle \epsilon \rangle$ , for (CF<sub>3</sub>)<sub>2</sub>S and C<sub>3</sub>F<sub>8</sub> (present work) and 1,2-C<sub>2</sub>Cl<sub>2</sub>F<sub>4</sub>, 1,1,2-C<sub>2</sub>Cl<sub>3</sub>H<sub>3</sub>, and 1,1-C<sub>2</sub>Cl<sub>2</sub>H<sub>4</sub> (from Ref. 9). The relative breakdown strengths  $V_g^R$  shown in the figure are from Ref. 6 except those for (CF<sub>3</sub>)<sub>2</sub>S, which are from Ref. 10.

Fig. 5. Energy dependence of the yield of the negative ions produced by electron impact on (CF<sub>3</sub>)<sub>2</sub>S.

Fig. 6. Negative ion intensity as a function of electron impact energy for C<sub>3</sub>F<sub>8</sub>. Note the multiplication factors (Ref. 16).

Fig. 7.  $w$  vs  $E/N$  for Ar/C<sub>2</sub>F<sub>6</sub> mixtures.

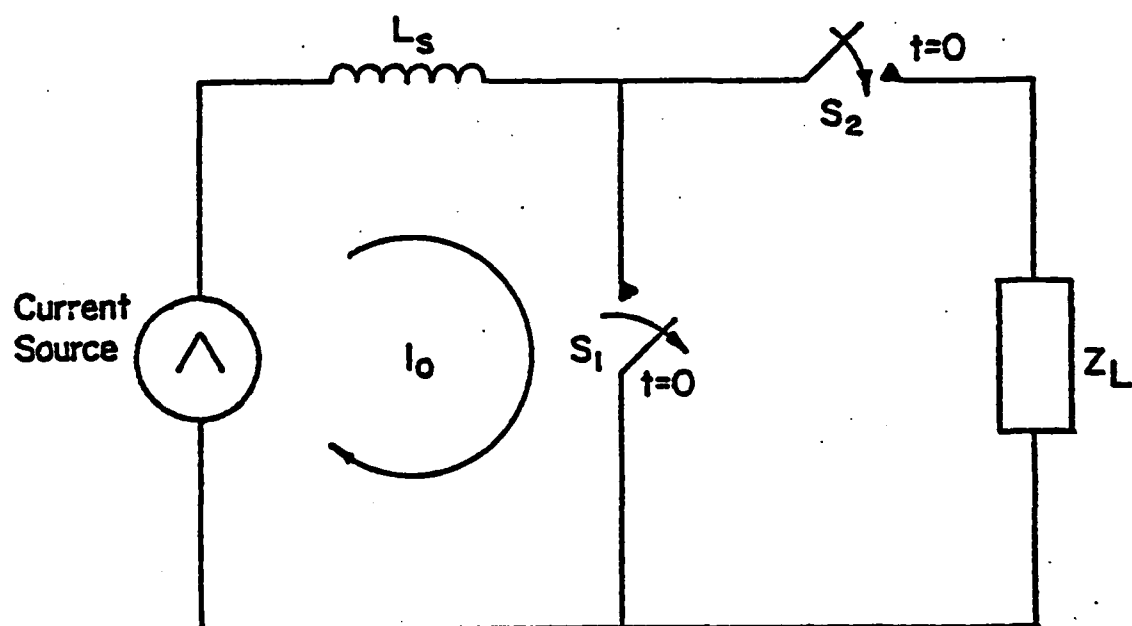


Fig. 1. Inductive energy discharge circuit (from Ref. 3).



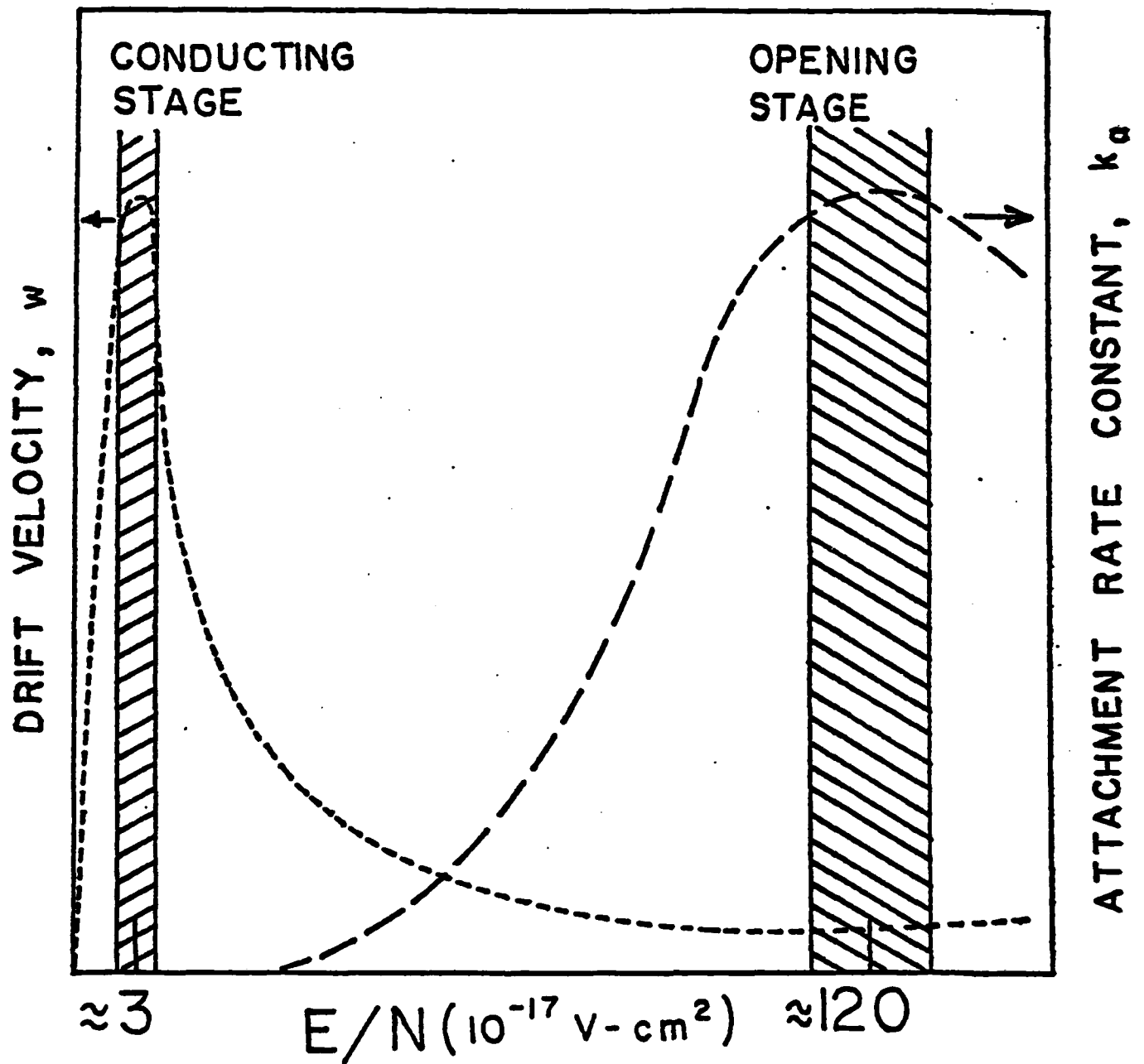


Fig. 2. Schematic illustration of the desirable characteristics of the  $w(E/N)$  and  $k_a(E/N)$  functions of the gaseous medium in an externally (e-beam-sustained) diffuse-discharge switch. Indicated in the figure are rough estimates of the  $E/N$  values for the conducting and the opening stage of the switch.

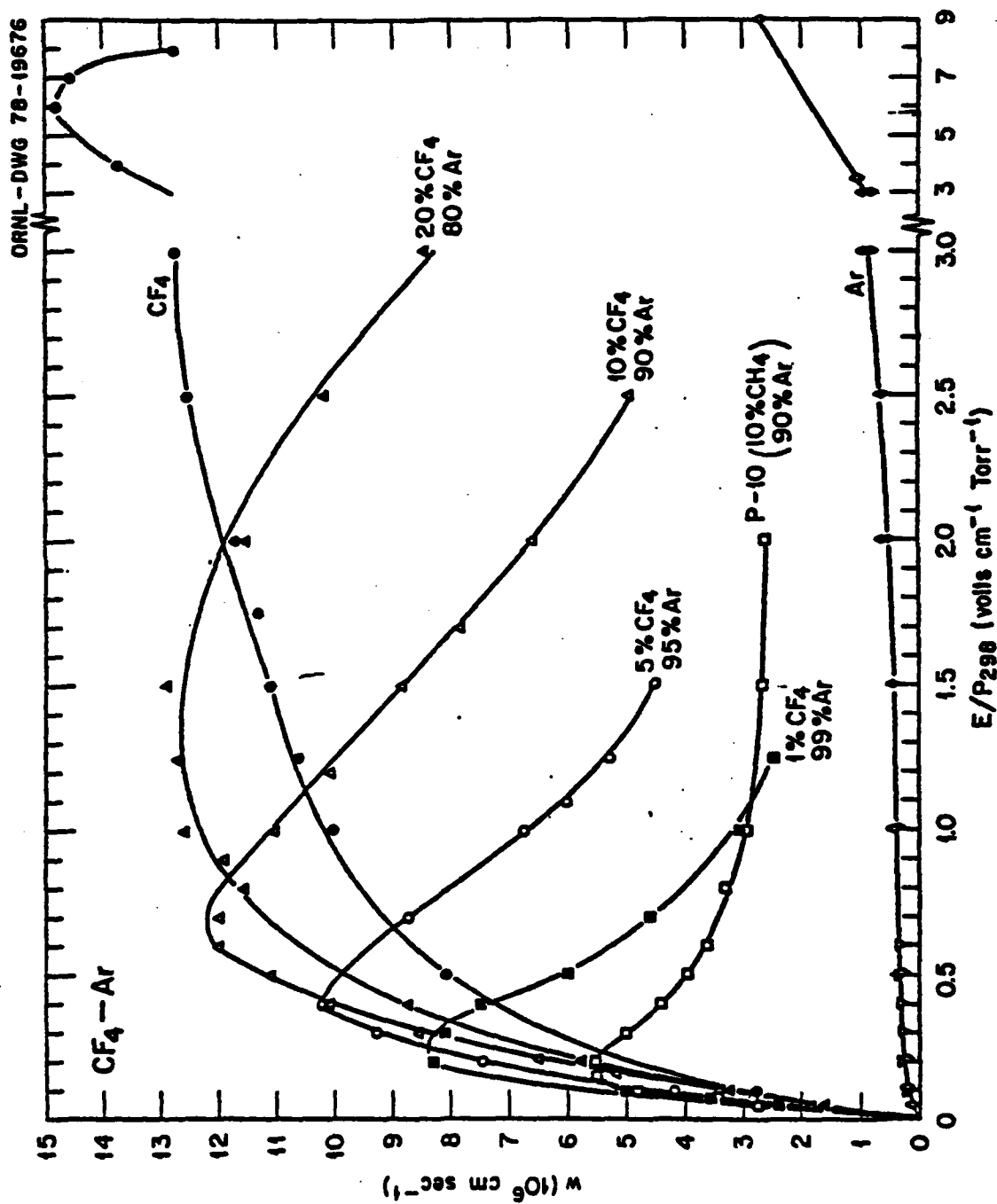


Fig. 3.  $w$  vs.  $E/P_{298}$  for Ar and Ar/ $\text{CF}_4$  mixtures (from Ref. 4).

ORNL-DWG 81-20671R

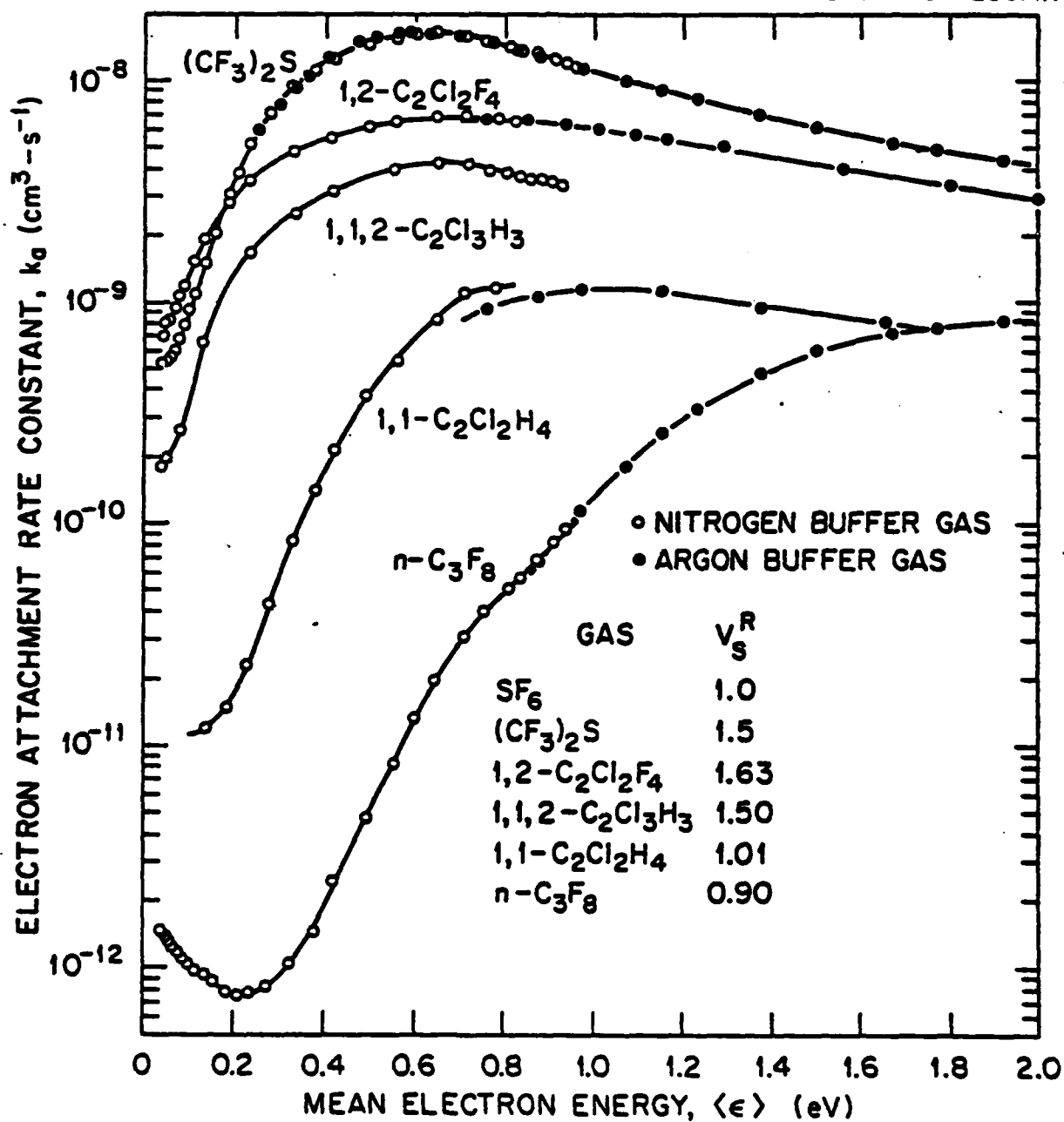


Fig. 4. Electron attachment rate constant,  $k_a$ , as a function of mean electron energy,  $\langle \epsilon \rangle$ , for  $(\text{CF}_3)_2\text{S}$  and  $\text{C}_3\text{F}_8$  (present work) and  $1,2\text{-C}_2\text{Cl}_2\text{F}_4$ ,  $1,1,2\text{-C}_2\text{Cl}_3\text{H}_3$ , and  $1,1\text{-C}_2\text{Cl}_2\text{H}_4$  (from Ref. 9). The relative breakdown strengths  $V_s^R$  shown in the figure are from Ref. 6 except those for  $(\text{CF}_3)_2\text{S}$  which are from Ref. 10.

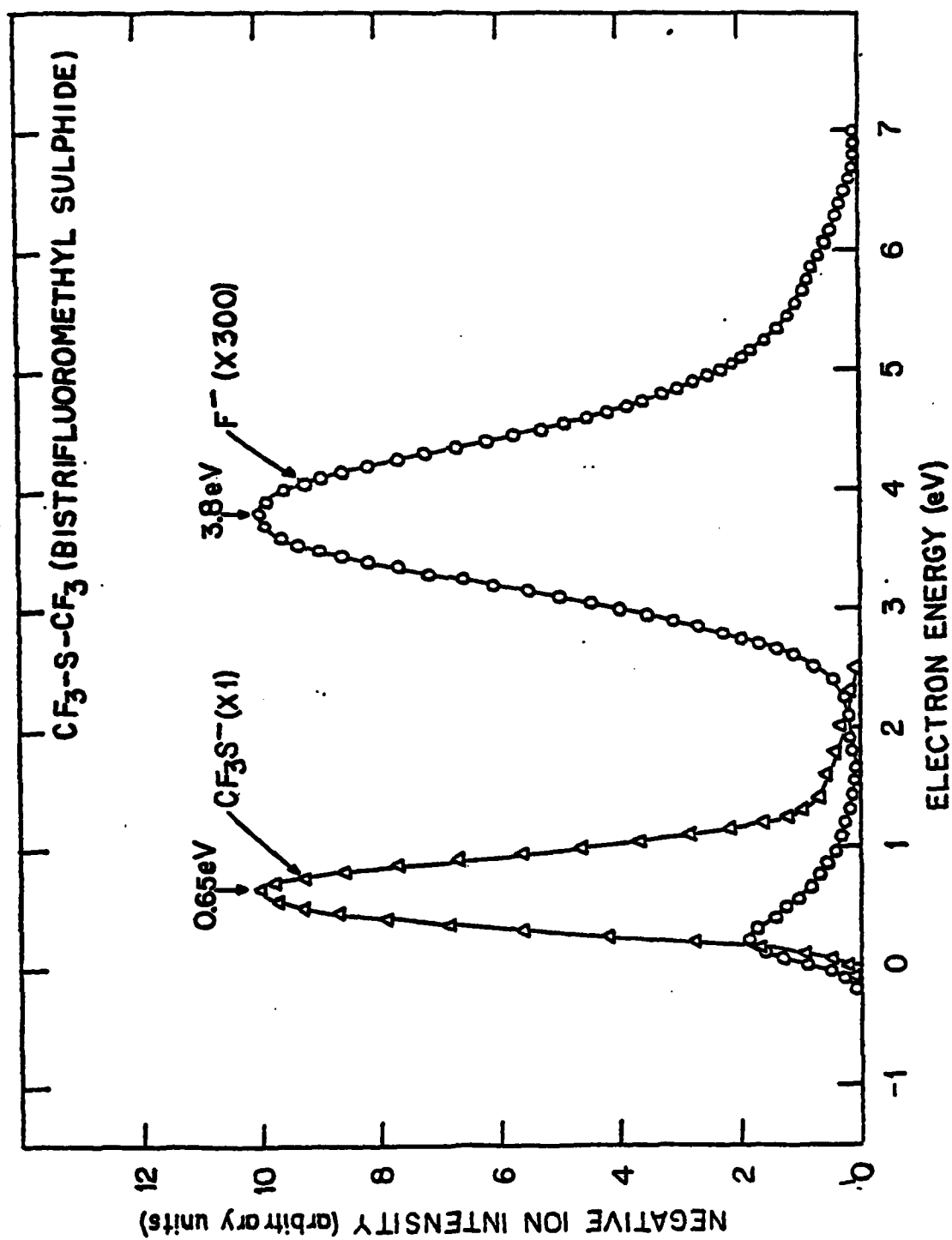


FIG. 5. Energy dependence of the yield of the negative ions produced by electron impact on  $(\text{CF}_3)_2\text{S}$ .

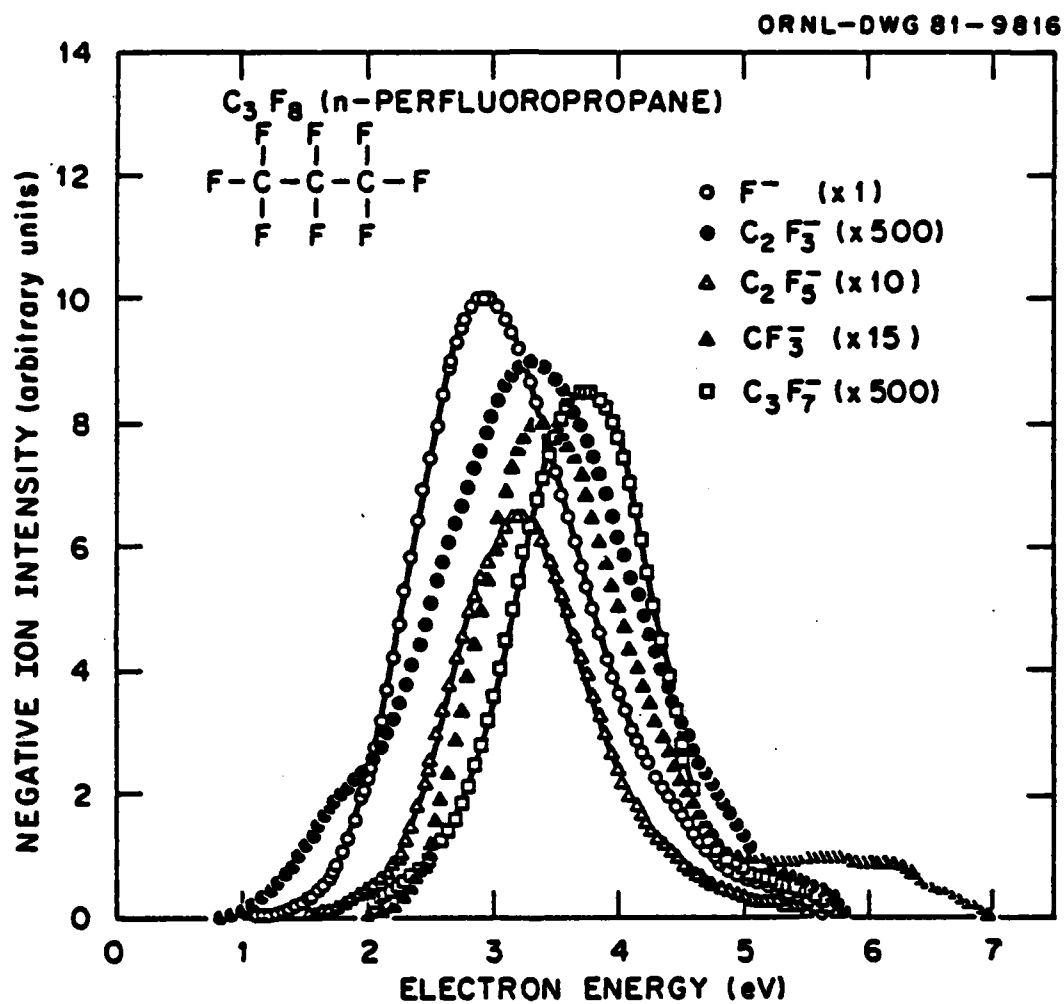


Fig. 6. Negative ion intensity as a function of electron impact energy for  $C_3F_8$ . Note the multiplication factors (Ref. 16).

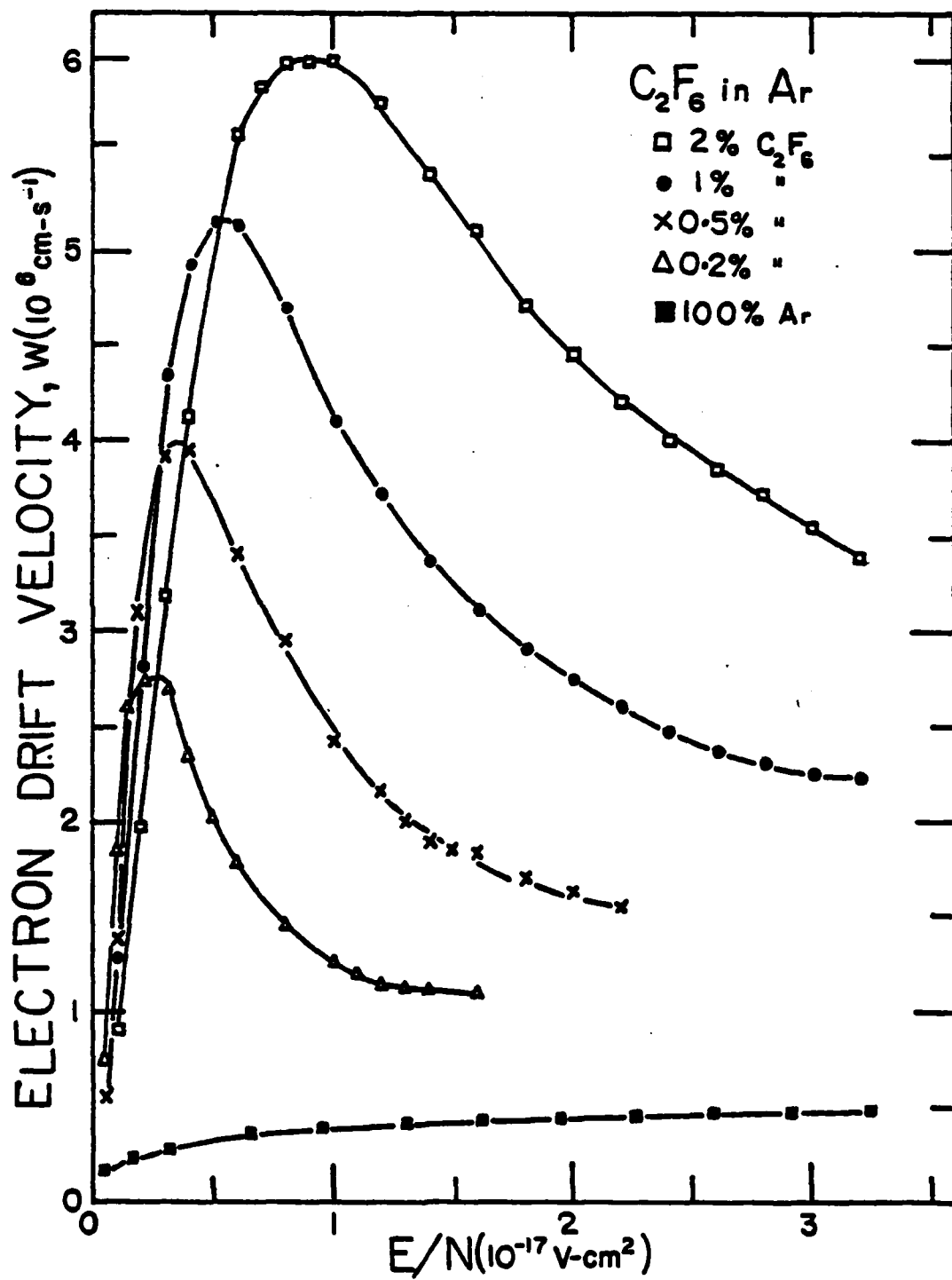


Fig. 7.  $w$  vs  $E/N$  for Ar/C<sub>2</sub>F<sub>6</sub> mixtures.

## APPENDIX B

## Summary of Meeting On

"Diffuse Discharge Opening Switches"  
at Texas Tech University on Sept. 23-24, 1981

K. Schoenbach and M. Kristiansen

A meeting on "Basic Processes in Diffuse Discharge Opening Switches" was held in Lubbock on September 23-24, 1981. It brought together 20 atomic and plasma physicists and electrical engineers. The goal of the meeting, set up especially to discuss the opening switch concepts developed at Texas Tech, was:

- a) to identify the limitations of diffuse discharge switch concepts
- b) to identify the unresolved problems
- c) to identify research areas that must be supported to resolve the problems
- d) to identify where the needed research expertise resides
- e) to establish cooperative, coordinated research efforts.

The meeting was opened with a brief review on the state-of-the-art of repetitive opening switches with special emphasis on concepts developed at Texas Tech. Discussion sessions on "Production of High Pressure Diffuse Discharges", "Optical Control of Diffuse Discharges", "Basic Data" and "Diffuse Discharge Modeling" followed. The results of the discussions were summarized in a final session:

1. Limitations on current density and time of conduction in atmospheric pressure diffuse discharges are due to instabilities which are mainly developing on the electrode surface. To prevent instabilities or, at least, to delay their onset, the establishment of a high uniformity of pre-ionization and electric field in the gap and of the controlling e-beam or laser power has to be attempted. With respect to the application as rep-rated switches, where excessive

heating of the gas must be avoided, gas exchange systems have to be considered.

2. The conditions for gas mixtures, usable in attachment dominated diffuse discharge switches are:

- a) High mobility at low  $E/N$
- b) Low attachment rate at low  $E/N$
- c) High attachment rate at high  $E/N$
- d) High dielectric strength

Whereas agreement on these general features existed, the opinion about the "best" gases differed. As appropriate attachers for opening switches  $\text{NO}$ ,  $\text{N}_2\text{O}$ ,  $\text{I}_2$ , some halogenated hydro-carbons, and  $\text{HCl}$  in buffer gases like  $\text{N}_2$ ,  $\text{CH}_4$ , and noble gases were considered. Basic data for commonly used gases ( $\text{N}_2$ , noble gases) are fairly complete, whereas they are limited for the other gases. Predictions about the behavior of gas mixtures containing ions, radicals, and excited molecules, however, (a research object of plasma chemistry) are rather vague for most opening switch gas mixtures. It is therefore important to increase the appropriate plasma chemical investigations.

3. An effort which should also be increased is modeling of diffuse discharges in diverter circuits. Rate equation codes and Boltzmann equation codes are available or under development. A major obstacle for using the codes in opening switch calculations is the lack of data for appropriate gases. Experiment-theory comparisons could fill gaps in the data base.
4. Generally, the importance of experiments for both e-beam and optically controlled diffuse discharges was emphasized together with development of fast diagnostic techniques. Special atten-



tion should be payed to experimental investigations of laser induced effects (opto-galvanic effects).

To proceed in the field of diffuse discharge opening switches further interaction of the three communities present at this meeting (scientists, engineers, "appliers") was highly recommended.

#### Attendees at Meeting in Lubbock

M.A. Biondi	University of Pittsburgh
P. Chantry	Westinghouse Research Lab
L.G. Christophorou	Oak Ridge National Laboratory
D.H. Douglas-Hamilton	Avco Everett Research Lab
A. Garscadden	Air Force Wright Aeronautical Laboratories
A.H. Guenther	Air Force Weapons Laboratory
B.D. Guenther	U.S. Army Research Office
A.K. Hyder	Air Force Office of Scientific Research
B. Junker	Office of Naval Research
L.E. Kline	Westinghouse Research Lab
J.E. Lawler.	University of Wisconsin
W.H. Long, Jr.	Northrop Research and Technology Center
J.T. Mosely	University of Oregon
A.V. Phelps	Joint Institute for Laboratory Astrophysics
L. Pitchford	Sandia National Laboratories
M.F. Rose	Naval Surface Weapons Center
G. Schneider	Air Force Wright Aeronautical Laboratories
M. Kristiansen	Texas Tech University
E.E. Kunhardt	" " "
G. Schaefer	" " "
K. Schoenbach	" " "

## APPENDIX C

## List of Participants

Tammaron - 1982

J. Norman Bardsley  
Physics Department  
University of Pittsburgh  
Pittsburgh, PA 15260  
412/624-4359

Ara Chutjian  
Jet Propulsion Laboratory  
California Institute of Technology  
Mail Code 183-601  
4800 Oak Grove Drive  
Pasadena, CA 91109  
213/354-7012 (2141 - message)

M.A. Biondi  
Department of Physics & Astronomy  
University of Pittsburgh  
Pittsburgh, PA 15260  
412/624-4354

Frank DeLucia  
Department of Physics  
Duke University  
Durham, NC 27796  
919/684-8232

Peter Bletzing  
Air Force Wright  
Aeronautical Laboratory  
Wright-Patterson AFB, OH 45433  
513/255-2923  
ext. 36

D.H. Douglas-Hamilton  
AVCO Everett Research Lab  
2385 Revere Beach Parkway  
Everett, MA 02149  
617/389-3000  
ext. 568

Rudy Buser  
Night Vision and Electro Optics  
Laboratory  
DELVN-L  
For Belvoir, VA 22060  
703/664-4956

Albert G. Engelhardt  
Los Alamos National Laboratory  
MS 554  
Los Alamos, NM 87545  
505/667-7440 (lab - 7557)

Peter J. Chantry  
Westinghouse R&D Center  
1310 Beulah Road  
Pittsburgh, PA 15235  
412/256-3675

J.J. Ewing  
Mathematical Science N.W. Inc.  
2755 Northup Way  
Bellevue, WA 98004  
206/827-0460

Lucas Christophorou  
Oak Ridge National Laboratory  
Building 4500-S, H-158  
P.O. Box X  
Oak Ridge, TN 37830  
615/574-6199

Richard Fernsler  
Naval Research Laboratory  
Code 4770  
Washington, D.C. 20375  
202/767-2724

Charles Frost  
Org. 4212  
Sandia National Laboratories  
Albuquerque, NM 87185  
505/844-9102

A.K. Hyder  
Directorate of Physics  
Room C 225  
Bldg. 410  
Bolling Air Force Base  
Washington, D.C. 20332  
202/767-4908

Alan Garscadden  
Air Force Wright Aeronautical  
Laboratories  
POOC/3  
Wright-Patterson AFB, OH 45433  
513/255-2923

Bob Junker  
Office Naval Research  
Code 421  
800 N. Quincy  
Arlington, VA 22217  
202/696-4220

A.H. Guenther  
Chief Scientist  
AFWL/CA  
Kirtland AFB, NM 87117  
505/844-9856

Larry E. Kline  
Westinghouse R&D Center  
1310 Beulah Road  
Pittsburgh, PA 15235  
412/256-7552

B.D. Guenther  
U.S. Army Research Office  
P.O. Box 12211  
Research Triangle Park, NC 27709  
919/549-0641

M. Kristiansen  
Electrical Engineering Department  
Texas Tech University  
P.O. Box 4439  
Lubbock, Texas 79409  
806/742-2224

Martin Gundersen  
Electrical Engineering Department  
University of Southern California  
University Park  
Los Angeles, CA 90007  
213/743-6195 (lab - 5320)

Erich E. Kunhardt  
Electrical Engineering Department  
Texas Tech University  
P.O. Box 4439  
Lubbock, Texas 79409  
806/742-3545

Lynn L. Hatfield  
Department of Physics  
Texas Tech University  
P.O. Box 4180  
Lubbock, Texas 79409  
806/742-3783

James E. Lawler  
Physics Department  
University of Wisconsin  
Madison, WI 53706  
608/262-2918

Jacob Leventhal  
Department of Physics  
University of Missouri/St. Louis  
St. Louis, MO 63121  
314/553-5933

W.H. Long, Jr.  
Northrop Research and  
Technology Center  
1 Research Center  
Palosverdes Peninsula, CA 90274  
213/377-4811  
ext. 861

Donald C. Lorents  
SRI International  
333 Ravenswood Ave.  
Menlo Park, CA 94025  
415/326-6200  
ext. 3167

Lawrence H. Luessen  
Naval Surface Weapons Center  
Code F-12  
Dahlgren, VA 22448  
703/663-8057

Michael Mando  
U.S. MERADCOM  
DRDME-EA  
Fort Belvoir, VA 22060

William M. Moeny  
Tetra Corporation  
1325 San Mateo S.E.  
Albuquerque, NM 87108  
505/256-3595

Marshall Molen  
Old Dominion University  
Department Electrical Engineering  
Norfolk, VA 23508  
804/440-3750

R.M. Patrick  
AVCO Everett Research Lab  
2385 Revere Beach Parkway  
Everett, MA 02149  
617/389-3000

A.V. Phelps  
Joint Institute for Laboratory  
Astrophysics  
University of Colorado  
Boulder, CO 80309  
303/492-7850

Leanne Pitchford  
Division 4211  
Sandia National Laboratories  
Albuquerque, NM 87185  
505/846-1262

Joseph M. Proud, Jr.  
GTE Laboratories, Inc.  
40 Sylvan Road  
Waltham, MA 02154  
617/466-2539

Larry Rapagnani  
AFWL/ARAC  
Kirtland AFB, NM 87117  
505/844-9836

M. Frank Rose  
 Naval Surface Weapons Center  
 Code F-04  
 Dahlgren, VA 22448  
 703/663-8026

Jim Thompson  
 University of South Carolina  
 College of Engineering  
 Columbia, SC 29208  
 803/777-7304 (4195 - message)

Wolfgang Seelig  
 Institut für Angewandte Physik  
 Technische Hochschule  
 Schlossgartenstr. 2  
 61 Darmstadt  
 FRG  
 001 49 6151 162580

Ihor Vitkovitsky  
 Naval Research Laboratory  
 Code 6770  
 Washington, D.C. 20375  
 202/767-2724

Gerhard Schaefer  
 Electrical Engineering Department  
 Texas Tech University  
 P.O. Box 4439  
 Lubbock, Texas 79409  
 806/742-3501

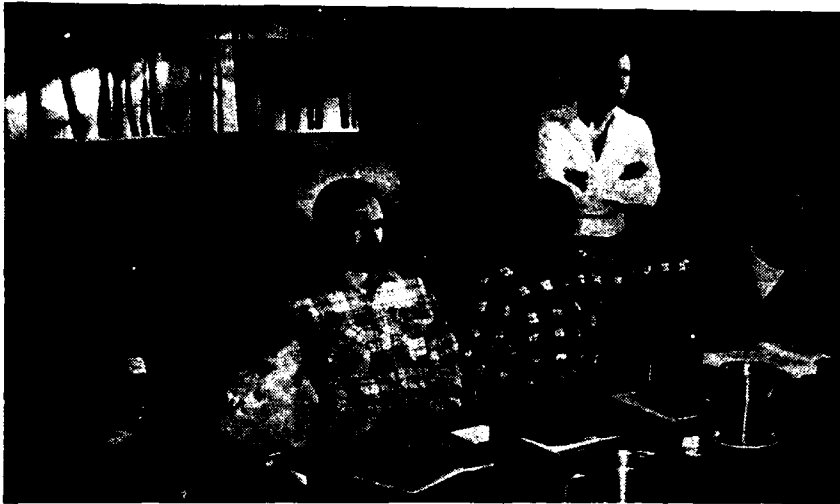
Bill Wright  
 Electronics Technology  
 & Device Laboratory  
 Beam Plasma & Display Division  
 Fort Monmouth, NJ 07703  
 201/544-5404

Karl H. Schoenbach  
 Electrical Engineering Department  
 Texas Tech University  
 P.O. 4439  
 Lubbock, TX 79409  
 806/742-3595

Santosh H. Srivastava  
 Jet Propulsion Laboratory  
 4800 Oak Grove Drive  
 Pasadena, CA 91109  
 213/354-3246

Marie Byrd  
 Workshop Secretary  
 Electrical Engineering Department  
 Texas Tech University  
 P.O. Box 4439  
 Lubbock, Texas 79409  
 806/742-3468

Peter Turchi  
 R & D Associates  
 1401 Wilson Blvd.  
 Arlington, VA 22209  
 703/522-5400



# TAMARRON

JANUARY

1982



